THE UNIVERSITY
of EDINBURGH

Cellulose as a component of plant cell walls and as a food additive in confectionery

PhD Thesis

Ninni Anniina Nuorti

The Edinburgh Cell Wall Group

The Institute of Molecular Plant Sciences

The University of Edinburgh

Submitted on 31/8/2022

The lay summary

Name of student:	Ninni Anniina Nuorti	UUN	Ss1776921
University email:	S1776921		
Degree sought:	PhD	No. of words in the main text of thesis:	47 000
Title of thesis:	Cellulose as a component of plant cell wall and as a food additive in confectionery		

This thesis aimed to study why commercially available celluloses, which were added as dietary fibre food additives to confectionery, were found to differ from each other in their 'mouthfeel' properties. As cellulose is the most abundant fibrous component of the plant cell walls, I also extended the studies to a set of samples that were isolated from various different tissue types and of pea (*Pisum sativum*) and cauliflower (*Brassica oleracea*). I showed that the commercial celluloses were relatively pure cellulose and had very few compositional differences from each other, whereas the pea and cauliflower cell walls contained all kinds of polysaccharides, proteins and lignin. I also developed two novel methods: one for measuring how charged the celluloses and cell wall isolates were, and another one for measuring how much the celluloses and plant samples could interact with molecules that surround them, and I found measurable differences between the samples in these two types of qualities.

Name of student:	Ninni Anniina Nuorti	UUN	S1776921
University email:	S1776921@ed.ac.uk		
Degree sought:	Doctorate	No. of words in the main text of thesis:	47 000
Title of thesis:	Cellulose as an architectural component of plant cell walls and as a food additive in confectionery		

Abstract

A healthy diet is rich in dietary fibre (largely indigestible polysaccharides, most of which derive from plant cell walls). Cellulose is one of the main components of plant cell walls and a major contributor to human dietary fibre intake. It is a natural component of food-plants, and can also be added during commercial preparation of foodstuffs.

This project investigates the physico-chemical properties of various commercial sources of cellulose that have been empirically found to differ in palatability, especially 'mouth feel', as additives to confectionery. The aim was to explain why these seemingly similar celluloses behave so differently as food additives. Concurrently, I performed comparable studies on plant cell walls (prepared as alcohol-insoluble residue; AIR), sourced from various plant species and tissues. Potential differences between cellulose preparations could include (a) contaminating non-cellulosic polymers, (b) degree of oxidation, and (c) accessibility of cellulosic surfaces to neighbouring solutes.

(a) Contaminating non-cellulosic polymers: I performed various studies for chemical composition – digestion with α-amylase for analysis of starch content; washing with phenol followed by $Ba(OH)_2$ hydrolysis for analysis of covalently bound proteins; assay of acetyl bromide-soluble lignin and hydrolysis with trifluoroacetic acid and H_2SO_4 (followed by thin-layer chromatography) for analysis of hemicellulose relative to cellulose content. These assays did not reveal major differences between the various commercial cellulose samples – all were relatively pure cellulose. Naturally, the AIR preparations were more diverse in chemical composition, containing all the non-cellulose polymers studied (starch, proteins, lignin, hemicelluloses and pectin).

(b) Oxidation products: I hypothesised that the commercial celluloses could have been slightly oxidised during the manufacture, introducing anionic groups. For quantifying these, I developed a novel method to study the binding of several cationic stains ($CoCl_2$, basic fuchsin, methyl violet, methyl green, malachite green, aniline blue, safranine, Janus green B, polychromic methylene blue and toluidine blue O (TB)). TB was chosen for detailed studies because it bound least to Whatman filter paper, which was used as a non-oxidised control, and well to carboxymethylcellulose, which was used as a reference sample for oxidised cellulose. Of the 'pure' celluloses, the further processed LC200 samples (LC200 in oil, LC200 spr dr, LC200 spr dr & milled) had the highest and the original LC200, Whatman filter paper and Avicel PH102 had the lowest degree of oxidation.

(c) Cellulosic surface accessibility: I developed novel methods to characterise this: (i) quantifying the adsorption of [^{3}H]cellopentaitol (relative to [^{3}H]glucose and [^{3}H]XXLGol) to the cellulose and (ii) testing its susceptibility to digestion by endocellulase. (i) Sodra A13, never-dried cellulose, Whatman filter paper and cotton wool had the highest and the AIR preparations and Curran had the lowest accessibility to [^{3}H]cellopentaitol. (ii) The microcrystalline cellulose and the LC200 processed in water (LC200 spr dr and LC200 spr dr & milled) had the highest accessibility for cellulase digestion whereas the cotton wool, Avicel PH102 and never-dried cellulose were the least accessible.

There was no single result that would point out conclusively why the commercial celluloses behaved differently as food additives and it is likely that mouth feel is the sum of several physico-chemical interactions taking place in the food matrix.

It is envisaged that the methodology and data will be beneficial to the wider field of plant cell wall research in the future, for instance the novel accessibility methods can be used in studies of polysaccharide interactions within cell walls.

Acknowledgements

Firstly, I would like to thank my supervisor Prof. Stephen C. Fry for all the dedication, encouragement and support: you have patiently instructed and guided me over the last five years to grow into the scientist I am now. It has been a great honour to work in your lab and learn from one of the best professors in the field. I am forever grateful for all the kindness you have shown me, and also for your firm critique and pruning which has helped me turn my focus on what is important and what is not. I will really miss our insightful 1-to-1 meetings and coffee break conversations.

I would also like to extend my thanks to the past and present members of the Edinburgh Cell Wall Group: Dr. Lenka Franková, Miss (soon-to-be-doctor) Marie Rapin, Dr. Chris Donohoe, Dr. Thurayya Al Hinnai, Dr. Rifat Ara Begum, Dr. Anzhou Xin, Dr. Martina Pičmanová, Dr. Anne Bulling, Dr. Michael Solvang, Dr. Klaus Herburger, Dr. Dayan Sanhueza and Miss Amy Wallace. You all made me feel so welcome when I arrived Scotland, and have also taught me so many methods and techniques in the lab.

I would like to thank MARS Inc. for the generous funding that covered all the expenses and my stipend during my studies. Thank you, Isabella, Annelie, April and Megan, also for taking time to meet with us regularly for project updates, and thanks for all the comments, suggestions and insight.

I would also like to thank my sister Viivi and mother Aila, for all the encouragement you have given me over the years. Mamma, you endeavoured to raise and support us all by yourself – as a single mom – and now all your hard work has paid off. Thank you, and congratulations.

I would also like to extend the thanks further to my extended family, and also to all my friends and 'church family' from Hillsong Edinburgh. Thank you for making Edinburgh my home.

Most and foremost I would like to thank my husband, soul mate and best friend Boby. I would have never made it without you, you are my rock and I love you so much. All your love, support and encouragement has finally got us here. Indeed, now as I am putting together and submitting this thesis, you are sitting here next to me in the middle of the night Googling how to add page numbers in a Word document, cheering me on and keeping me awake – and fuelling me up with biscuits and juice – just another example of how your love is not just words but deeds too. I can't wait to get to share the rest of my life with you and see all the adventures God puts our way. I can't think of a more appropriate way to finish these Acknowledgements than with a scripture which you will see painted in the ceiling of the McEwan Hall on my graduation day in July:

Wisdom is the principal thing, therefore get wisdom, and with all thy getting, get understanding. Exalt her and she shall bring thee to honour. ***(Proverbs 4:7 KJV)***

Declaration

I declare that I have solely composed this thesis by myself and that it has not been submitted in full or in part in any previous application for a degree. Except where I state by reference or acknowledgement, the work presented is entirely my own. One figure in this work has been published earlier in my MSc thesis, the University of Helsinki in 2017.

Table of Contents

Abbreviations

AIR	alcohol insoluble residue
Ara	arabinose
BAW	butanol/acetic acid/water
Bq	Becquerel, an unit of radioactivity
CMC	carboxymethyl cellulose
C2	cellobiose
C3	cellotriose
DNA	deoxyribonucleic acid
Dr.	doctor
E	enzyme
EPAW	ethyl acetate/pyridine/acetic acid/water
Fig.	figure
Fruc	fructose
g	unit of mass (gram) or standard gravity
Gal	galactose
GalA	galacturonic acid
Gent2	gentiobiose
Glc	glucose
HCl	hydrochloric acid
H_2SO_4	suplhuric acid
Lac	lactose
Lam4	laminaritetraose
M	molar, moles/litre
Mal	maltose
MLG	Mixed-linkage glucan
M3	maltotriose
M4	maltotetraose
Man	mannose
Mel2	melibiose

MCC	microcrystalline cellulose
m. stem	mature stem
NaB^3H_4	sodium borohydride
NaOH	sodium hydroxide
n-d	never-dried
PIR	phenol-insoluble residue
PNW	propanol/nitromethane/water
Prof	professor
RGI	rhamno-galacturonan I
Rha	rhamnose
Rib	ribose
RNA	ribonucleic acid
RO	reverse osmosis
SA	specific activity
SEM	Standard error of the mean
Soph	sophorose
Spr. dr.	spray dried
St	starch
Suc	sucrose
TB	toluidine blue
Tre	trehalose
TFA	trifluoroacetic acid
TLC	thin-layer chromatogram
U	unit, which is an unit of enzymes
VTT	Technical Research Centre of Finland (abbreviated from the Finnish name 'Valtion teknillinen tutkimuskeskus')
Xse	xylanase
Xyl	xylose
XXLGol	non-fucosylated xyloglucan octasaccharide
X2	xylobiose
X3	xylotriose

X4	xylotetraose

1 Introduction

1.1 Plant cell walls

Almost every plant cell is surrounded by a cell wall. The form, shape and support of a plant derives from its cell walls. Secondary cell walls are stiff so that the size and stance of a plant would be maintained, whereas primary walls are dynamic and allow growth. The plant cell wall defines the size of the cell which is important for instance for maintenance of turgor pressure – when the plant has enough water, the cell is turgid and it pushes against the surrounding cell wall, and the pressure contributes towards maintaining the shape of the plant (Alberts *et al*., 1989). In a wilting plant the cell does not fill the maximum space defined by the surrounding cell wall and the plant loses its stance. Although cell walls may seem very rigid, they, especially primary cell walls, are flexible and dynamic, and allow cell expansion during growth (Cosgrove and Jarvis, 2012)).

1.1.1 Composition of cell walls

The primary cell wall consists of three types of polysaccharides: cellulose, hemicelluloses and pectin. Cellulose molecules form microfibrils which function as the 'backbone' of the cell wall, and will be discussed with more detail in chapter 1.1.2 below. One model of the cell wall (Fry, 1989; Hayashi, 1989) suggests that the microfibrils are tethered by hemicelluloses and the rest of the space of the cell wall is filled by pectin. The cell wall is an aqueous environment where the pH (~4.5) is lower than inside the cell (where pH usually ~7.5 but can vary somewhat, depending on the tissue) (Martinière et al., 2018).

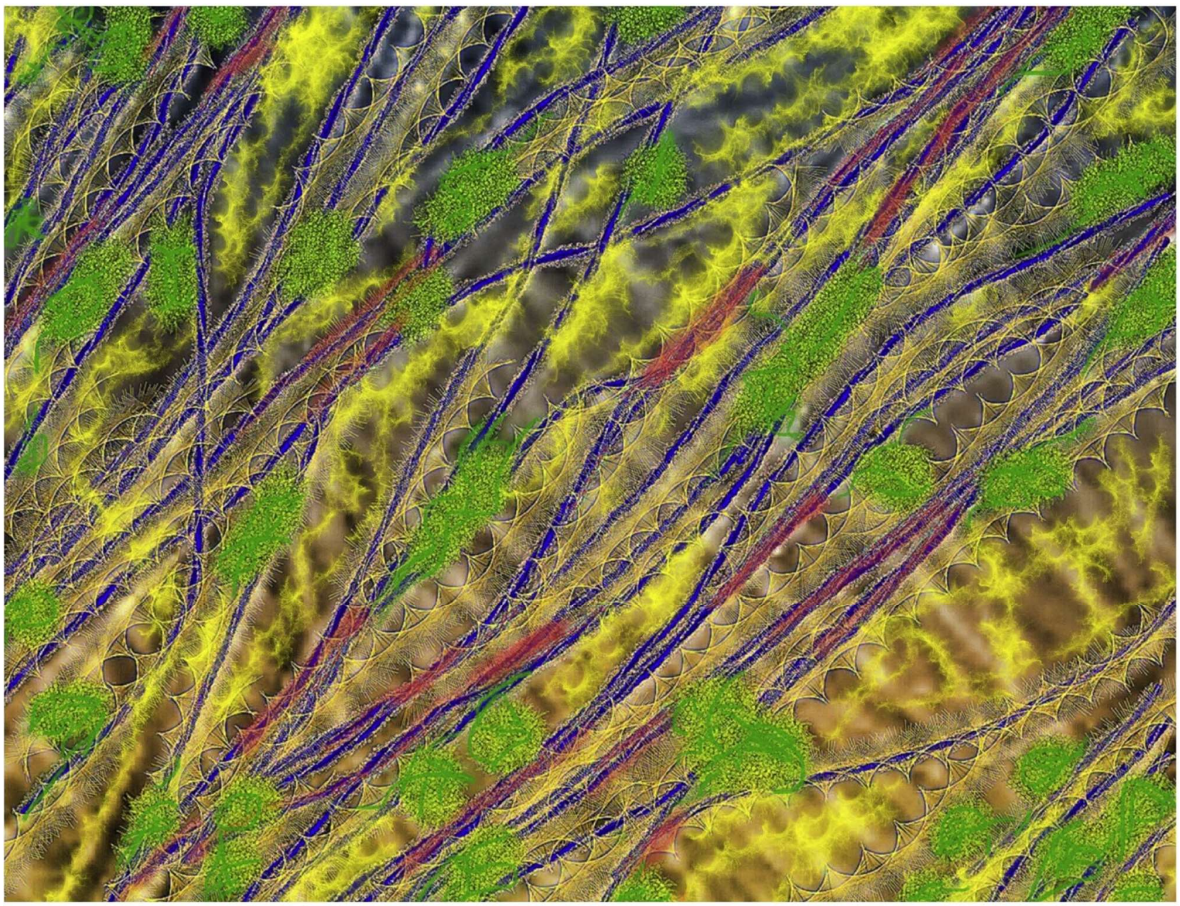

Figure 1. Artistic view of primary cell wall (from Cosgrove, 2014).

Cellulose microfibrils are shown in blue, and they are tethered by hemicelluloses (shown in green). The cell wall matrix is filled by pectin (shown in yellow). Occasionally, the cellulose microfibrils, which are close to each other, have not been covered by hemicelluloses and in those cases the microfibrils have aggregated and formed clusters of cellulose (shown in red).

Secondary cell walls typically do not have much pectin but are rich in cellulose and hemicelluloses (and sometimes also the non-polysaccharide substance, lignin). Plant cells can have several layers of secondary cell wall, especially in tissues that need to be strong (e.g. because they carry a heavy weight), such as wood tissue in tree trunks (Maaß et al., 2020). The deposition of the secondary cell wall occurs at the outside of the protoplasm (the outer surface of the plasma membrane), and as it accretes, it pushes out the primary cell wall and previous layers of the secondary wall (Maaß et al., 2020).

1.1.1.1 Pectin

Pectin forms the matrix in which the other cell wall polysaccharides are embedded. Pectin is negatively charged molecules that form cross-links in the cell wall and often need cations, such as Ca^{2+} for forming the cross-links, which is why chelating agents are used for extracting pectin (Fry, 1988; Thakur *et al*., 1997; Pelloux *et al*., 2007). Pectin includes three domains of polysaccharides: homogalacturonan, rhamnogalacturonan-I and rhamnogalacturonan-II (Thakur *et al*., 1997). Homogalacturonan is an unbranched polymer that consists D-galacturonic acid residues which are α-$1\rightarrow4$-linked (Thakur *et al*. 1997). Rhamnogalacturonan-I is a branched polymer whose backbone contains alternating galacturonic acid and rhamnose residues (Thakur *et al*., 1997). Rhamnogalacturonan-II has a galacturonic acid backbone which it is branched with complex side chains which contain many different sugar residues (Thakur *et al*., 1997). When pectin is synthesised, it is highly methylated, but in the cell wall pectin methylesterase enzymes demethylesterify pectin which makes it negatively charged (Pelloux *et al*., 2007).

In the food industry pectin is mostly used as a plant based gelling agent. For instance, many jams contain pectin which is derived from the fruits used as the main ingredients of the product, but pectin is also used as food additives to stiffen, thicken or stabilise the structure of many foods, for instance yoghurt (Everett and McLeod, 2005). Pectin, as water soluble dietary fibre, is digested in the colon by, and hence function as feed for, the gut microbiome (The European Food Safety Authority (EFSA) panel on ANS, 2017).

1.1.1.2 Hemicellulose

Hemicelluloses are polysaccharides which are not included in pectin or cellulose. They may be defined as plant cell-wall polysaccharides that hydrogen-bond to cellulose. Hemicelluloses tend to be less branched than pectin, and are usually composed of various different monosaccharides, where the backbone of the polysaccharide is composed of one type of sugar residue and the side chains can be formed from different sugars (Belgacem and Gandini, 2008). Hemicelluloses include, for instance, xylan, arabinoxylan, xyloglucan, mixed-linkage glucan and mannan (Belgacem and Gandini, 2008). Hemicelluloses are usually rather long (and hence not water extractable) and they tether cellulose microfibrils to each other via hydrogen bonds, thus helping to form net like

structures within cell walls (Cosgrove 2014). Hemicelluloses are substrates of many cell wall hydrolytic enzymes and transglycosylases (Franková & Fry, 2013) and hemicelluloses and their modifications are important for the dynamicity of cell wall.

1.1.1.3 Non-cell wall dietary fibre saccharides

Some plants store energy in shorter polymers which are oligosaccharides and therefore water extractable, for example inulin (Shoaib *et al*., 2016). Inulin, and fructo-oligosaccharides (FOS) (prepared from inulin by hydrolysis (Shoaib *et al*., 2016)), and other similar oligosaccharides, such as galacto-oligosaccharides (GOS, which are prepared from galactose enzymatically (Kuddus and Aguilar, 2022)) are novel dietary fibres. Water solubility makes them ideal dietary fibre components for many foods. They may also function as prebiotics (*i.e.* food of the gut microbes) and adding them in foods gives the foods value-added properties (Shoaib *et al*., 2016; Kuddus and Aguilar, 2022). There are several health claims food manufacturers would like to make on the water soluble oligosaccharide dietary fibres but so far they have not been approved by EU due to insufficient scientific studies published on the topic (EFSA panel on NDA, 2011a; EFSA panel on NDA, 2011b).

1.1.1.4 Lignin

In addition to polysaccharides and water, some cell walls contain lignin. Primary cell walls are mostly free from lignin (except in xylem cells and sclerenchyma), and typically secondary cell walls lignify after the cell has stopped growing, as lignin rich cell walls can no longer expand (Sixta, 2006). Lignin stiffens and hardens the cell wall, and lignin can make up to 20-30% of the dry weight of wood tissue (Hatfield and Fukushima, 2004) which explains why removing lignin from pulp is a big cost for paper industry. Lignin is hydrophobic and the synthesis of lignin makes the cell wall less aqueous – tracheids and vessel elements of xylem are waterproof (Sixta, 2006). Lignin may have a role in protecting plants from pathogens (Lee *et al*. 2019) and specific lignified tissues, such as those with a Casparian strip, can work as a physical barrier against pathogen attack (Lee *et al*. 2019) as well as entry of detrimental soil solutes.

Some plant cell walls are also impregnated with other non-polysaccharide polymers such as the polyesters cutin and suberin (Philippe *et al*., 2020).

1.1.1.5 Cell wall proteins

Plant cell walls also contain many kinds of proteins and are especially rich in extensins, which are hydroxyproline rich glycoproteins which can make a big fraction of the primary cell wall (usually 1-10% of the dry weight in dicots but up to 20% of cellular protein in sycamore culture cells) and which strengthen the cell wall by forming a crosslinked network which could influence how the cellulose microfibrils are organised (Fry, 1988; Herger *et al*., 2019). Cell walls are also rich in arabinogalactans which are arabinose- and galactose-rich glycoproteins which interlace with the pectic components of cell walls (Hozumi *et al*., 2017). Another example of non-enzymatic proteins in plant cell walls would be expansins, which bind to cellulose microfibrils and loosen the cell wall (Cosgrove, 2014; Cosgrove, 2015).

1.1.2 Dynamicity of the cell wall

In the living plant, cell walls are modified by various enzymes, such as glycosidases, endoglycanases (*e.g.* cellulase) and transglycosylases, oxidoreductases, esterases, phosphatases and proteases (Fry 1995; Gilbert, 2010). Equisetum plant cell walls even contain an enzyme, hetero-trans-β-glucanase, that can cleave and re-link different polysaccharides together – cellulose or a hemicellulose molecule (MLG) to another hemicellulose (xyloglucan) (Simmons *et al*., 2015). The modifications of cell walls can also happen via non-protein-mediated mechanisms, such as loosening of cell walls by controlled action of free hydroxyl radicals (Müller *et al*., 2009). The modifications of cell walls are important for many processes that take place during normal life cycle of plant. For instance, cell wall modifications play a major role in seed germination, elongation growth and fruit softening and ripening (Fry 1995; Gilbert, 2010).

1.2 Cellulose

Cellulose is often quantitatively the main component of cell walls and it is the most abundant organic macromolecule on earth. By definition, cellulose consists of $(1\rightarrow4)$-β-D-glucan and it is thus an unbranched and uncharged polymer (Taylor, 2018). The degree of polymerisation (DP) of cellulose varies a lot – in primary cell walls the DP is 500 – 5 000 whereas in secondary cell walls it can be up to 15 000 (Taylor, 2018). Microfibrils are straight and structurally very strong and they are sometimes compared to the steel bars in reinforced concrete as they form the skeleton of the cell wall (Cosgrove, 2014).

1.2.1 Synthesis of cellulose

Cellulose is synthesised on the outer side of the plasma membrane in 'rosette' like structures of cellulose synthase (CESA) where cellulose is extruded straight into the cell wall (Taylor, 2018; Chinga-Carrasco, 2011; Cosgrove, 2014). A number of cellulose molecules are synthesised simultaneously in the rosette and the molecules bind to each other with hydrogen bonds, forming microfibrils. Cellulose microfibril composition and diameter has been studied by myriad of techniques and research groups over the years. For a long time the cellulose microfibril was thought to have a hexagonal shape (in cross section) and microfibrils were thought consist of 36 (Cosgrove, 2014) (or even 60–70 according to Alberts *et al*., 1989), cellulose molecules (in cross-section, at any given point along the microfibril's length) because the rosette is a hexamer and each subunit consists of six CESA molecules (6×6 = 36, each CESA producing one cellulose molecule). However, many recent studies, which were reviewed by Cosgrove (2014) and Rongpipi *et al*. (2019), have challenged the 36-molecule model and suggested 24- or 18-molecule structures for the microfibril, with majority of the studies favouring the 18-molecule model. With the 18-molecule model, a dimer of CESA would form a domain (and three domains would form a rosette subunit and six subunits form a rosette), and each domain would make one cellulose molecule (Cosgrove, 2014).

As the cellulose molecules are being synthesised by the rosettes and the microfibril is being built up, the microfibril is incorporated straight into the cell wall and gets covered and tethered by hemicelluloses (Cosgrove, 2014; Taylor, 2018). As the cell wall is stiff and stationary and the microfibril is strong, straight and unyielding, the rosette will move in the plasma membrane. The direction of the movement is determined by the cortical microtubules inside the cell, and this movement in the plasma membrane is parallel to the respective microtubule; it is possible that the

part of the rosette that is inside the cell is attached to the microtubule (Alberts *et al*., 1989). As cellulose synthesis proceeds over a long period, the rosettes keep on 'circumnavigating' the cell, and the cellulose microfibrils form helical or coil like patterns around the cell in the cell wall. The orientation of the microfibrils in the cell wall define the direction the cell can grow, a bit similar to a slinky – the cell often has capacity to stretch in one direction but not in the other (Alberts *et al*., 1989). The helical structure and the direction of the microfibrils is most visible in xylem cells, which have very thick secondary cell walls (Cosgrove an Jarvis, 2012), and for instance the differentiating protoxylem cell wall has a distinct and organised coil as its secondary cell wall structure (Meents *et al*., 2018) which makes it the easiest cell type to detect in young root or shoot tissues (Fig. 2).

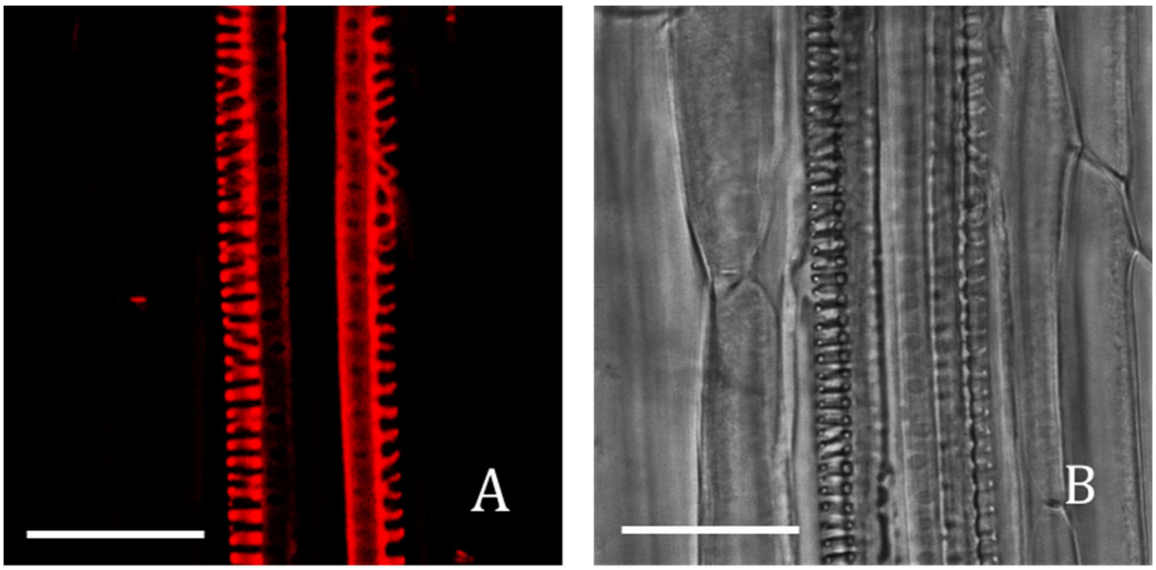

Figure 2. Confocal microscope images of protoxylem tissue in young *Arabidopsis thaliana* primary roots.

B) has been taken with visible light, whereas to A) I added propidium iodide and used the laser to get a fluorescent picture of the secondary cell walls, A) and B) have been taken from the same root at the same location. The roots used were from ecotype Col-0, 5 days post germination. Images from the author's MSc thesis, 2017, University of Helsinki. The scale bar shows 50 μm.

1.2.2 Cellulose crystal structure

The CESA enzyme makes one bond at a time, and every glucose is 180° twisted with respect to the previous one around the chain axis (Fig. 3) (Wohlert *et al.* 2021). In addition to the covalent bond, hydrogen bonds form within the molecule: between the ring oxygen and hydroxyl group of C3, and between the hydroxyl groups of C2 and C6 (Wohlert *et al.* 2021). As the cellulose molecules are

extruded by the CESA, neighbouring cellulose molecules bind to each other with hydrogen bonds between the hydroxyl groups of C3 from one cellulose molecule and C6 from another, and form a plane of glucopyranose rings (Fig. 3 and 4) (Yamane *et al*. 2006; Wohlert *et al.* 2021). When several glucopyranose ring planes are stacked on top of each other, a cellulose crystal is formed. The glucopyranose ring plane forms the (110) surface of the cellulose crystal, and the (110) surface is hydrophobic because all the carbon-bonded hydrogen atoms of the glucopyranose ring are axial (and there are no axial hydroxyl groups in glucose). The planes are held together as a stacked crystal by van der Waals forces, and because the planes are large and perfectly aligning, it is enough to keep the crystal together and make it very strong. Perpendicular to the plane of cellulose molecules is the (1-10) surface, and it is hydrophilic because all the hydroxyl groups are equatorial to glucopyranose ring of the glucose (Yamane *et al*. 2006).

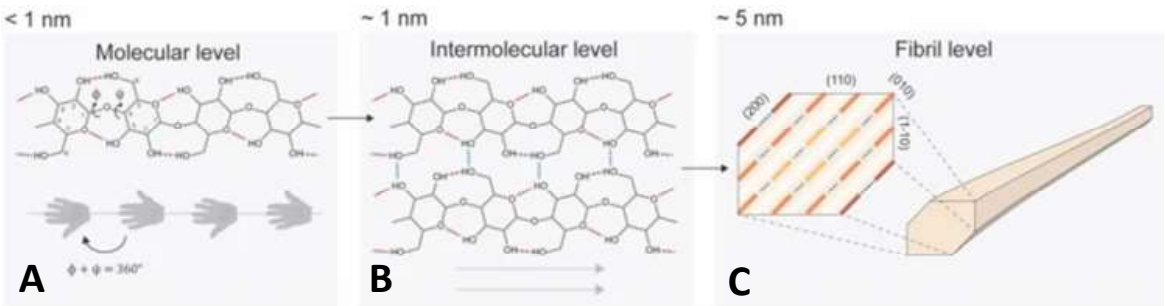

Figure 3. Schematic structure of cellulose molecule and microfibril (from Wohlert *et al.*, 2022).

(A) shows the structure of four contiguous glucose residues within a single cellulose molecule as (1→4)-β-D-glucan, (B)shows the inter- and intramolecular hydrogen bonds between two neighbouring cellulose molecules, and (C) shows the orientation of the cellulose molecules in the microfibril and the (110) and (1-10) crystal planes, where red and orange lines represent cellulose molecules that are on the microfibril surface, and yellow lines are cellulose molecules that are inside the microfibril.

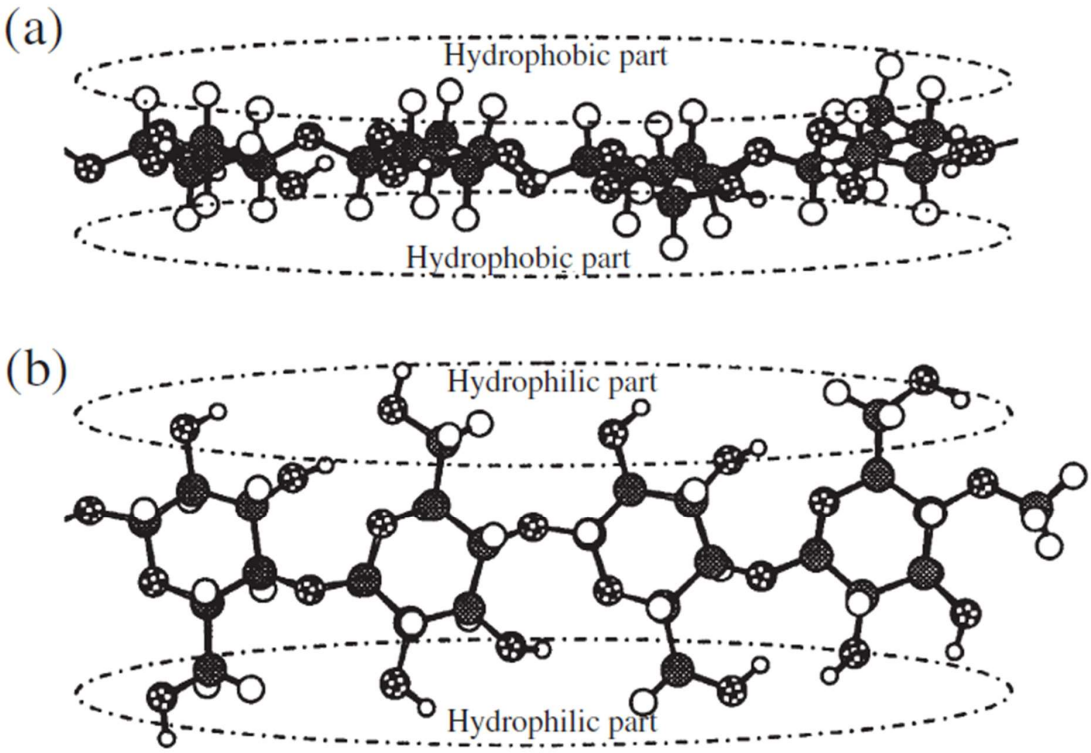

Figure 4. The orientation of cellulose molecules within the microfibril (from Yamane *et al*., 2006).

The hydrophobic (110) surface plane of the cellulose microfibril crystal in relation to a single cellulose molecule is shown in (a) and the hydrophilic (1-10) plane is shown in (b).

A microfibril consists of cellulose molecules that bind to each other with intermolecular hydrogen bonds via the hydroxyl groups that are not forming intramolecular hydrogen bonds (Wohlert *et al.* 2021). The frequency of the intermolecular hydrogen bonds in the microfibril affects the crystallinity of the cellulose – in crystalline regions the cellulose molecules are organised and densely packed and form more hydrogen bonds between the molecules within the microfibril than in amorphous regions where the cellulose molecules are spaced further away from each other (Okano and Sarko, 1985; Wohlert *et al.* 2021). My hypothesis is that some hydroxyl groups of cellulose molecules on the outer surface of the microfibril are pointing towards and forming bonds with other cellulose molecules inside of the microfibril, whereas others remain free and available to form bonds to non-cellulosic molecules that surround the microfibrils (such as hemicelluloses in the cell wall, or [^{3}Hcellopentaitol in the 3.3.1 Results – accessibility of cellulose chapter). The availability of the hydroxyl groups on the microfibril surface to form bonds with the surrounding molecules is referred to as 'accessibility of the cellulose' in this thesis.

1.2.3 Cellulose microfibrils are tethered by hemicelluloses

As soon as cellulose microfibrils are synthesised, they get covered with hemicelluloses. The hemicelluloses that cover the microfibrils not only help to bind the cell wall polysaccharides together as a net of polymers (i.e. cellulose microfibrils tethered by the hemicelluloses and matrix filled by pectin) but also help to keep the microfibrils apart from each other and spaced out in the cell wall. The orientation of microfibrils in the cell wall determinate the direction of cell expansion (Taylor, 2008).

However, there has been some shift in view, based on recent studies, on to what extent the microfibrils are covered by hemicelluloses, and there is evidence of aggregation or bundling of cellulose microfibrils on sites where the microfibrils are less covered or free from hemicelluloses (Chinga-Carrasco, 2011, Cosgrove, 2014; Cosgrove, 2015; Jarvis, 2018). Localised cellulose aggregates comprising several microfibrils can form only if the CESA rosettes are close to each other and are moving in the same direction in the cell wall at the time of the cellulose synthesis (Chinga-Carrasco, 2011). Cosgrove (2014) calls the locations where microfibrils are very close to each other or have aggregated 'biomechanical hotspots', and the 'hot spots' could be targets for expansin binding (Cosgrove, 2014; Cosgrove, 2015). Expansins might be involved in auxin-induced acid growth of the cell walls, and expansin-mediated cell-wall loosening could also introduce new binding sites for cellulases and xyloglucanases at the proximity of the 'hot spots', which could help further with cell-wall loosening (Cosgrove, 2014; Cosgrove, 2015).

1.2.4 Cellulose allomorphs

There are many cellulose allomorphs but type I is the predominant type in nature. Cellulose I_α is found in bacteria and some algae and type I_β is found in higher plants (Rongpipi *et al*., 2019). In type I cellulose microfibrils the cellulose molecules are arranged in a parallel way (with all the reducing termini of the molecules within the microfibril pointing in the same direction) (Fig. 5) (Wohlert *et al*., 2021). Cellulose II is obtained by treating cellulose I in concentrated alkali (sometimes called mercerising), and in cellulose II the cellulose molecules are arranged in antiparallel way (*i.e*. every

other cellulose molecule having the reducing terminus pointing the opposite direction) (Fig. 5) (Kolpak and Blackwell, 1975; Okano and Sarko, 1985). Existence of cellulose types III and IV has also been discussed in literature, and they would be formed by soaking cellulose I or II in ammonia or amine solutions at low temperature and by thermal treatment of cellulose III in glycerol, respectively (Wohlert *et al*., 2021). The cellulose I glucopyranose ring plane structure (introduced earlier in this chapter) is different in cellulose II – the hydrogen bonds between neighbouring cellulose molecules in the plane are formed between the hydroxyl groups of C2 and C6 in cellulose II (Kolpak and Blackwell, 1975; Wohlert *et al*., 2021), and not between C3 and C6 as in cellulose I. This structure leaves more space in the between of the molecules than in the cellulose I plane (Fig. 5), which explains why cellulose II is weaker and less stiff than cellulose I, even though cellulose II does also form crystalline structures (Wohlert *et al*., 2021).

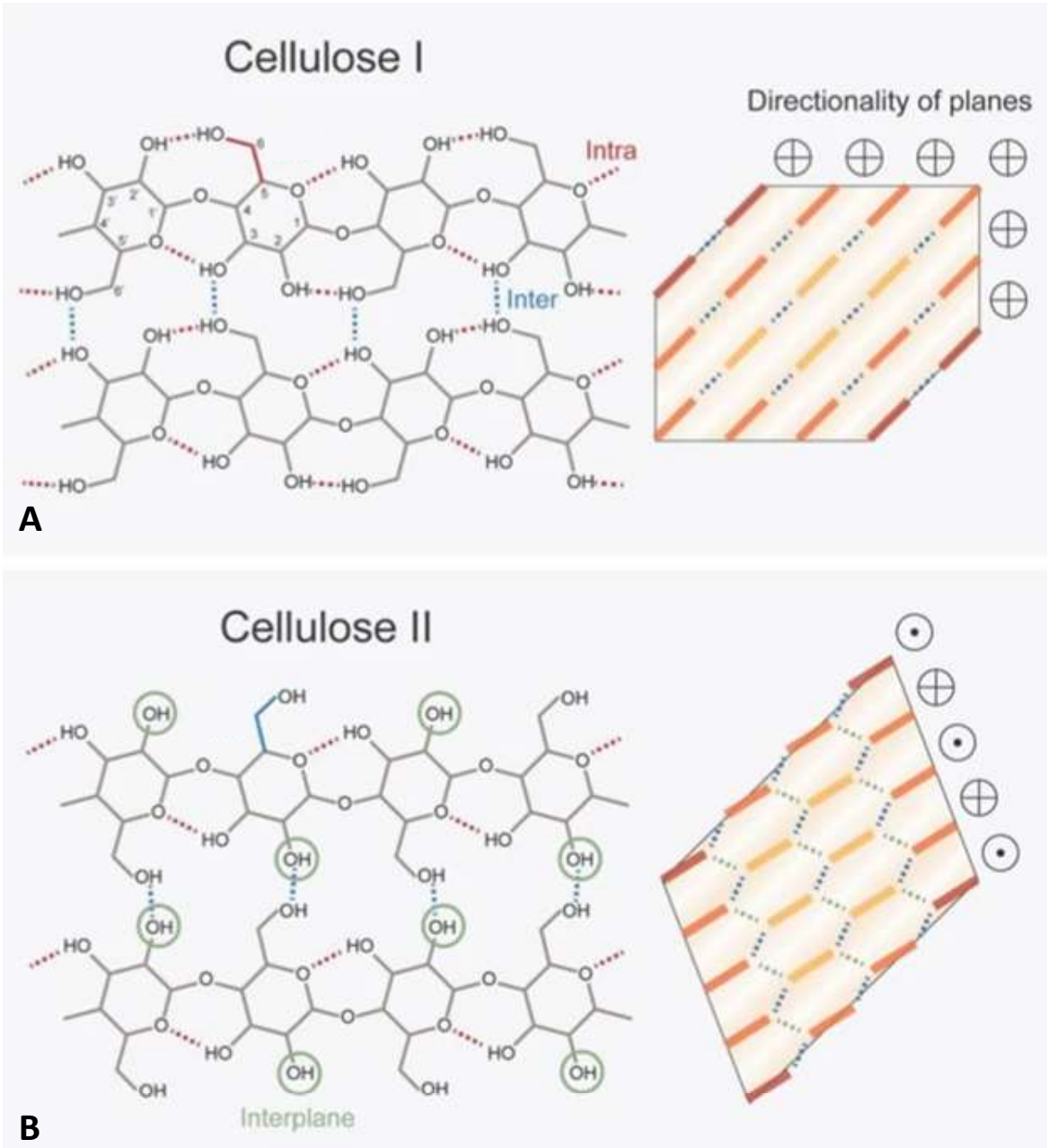

Figure 5. The orientation of cellulose molecules in cellulose I and II (from Wohlert *et al.*, 2022).

The hydrogen bonds are drawn with dotted lines, and within the cellulose molecule they are shown in red and between the molecules in blue. ⊕ and dotted circles indicate the orientation of cellulose molecules: in cellulose I the molecules are parallel (every reducing terminus pointing the same direction (A)), whereas in cellulose II the molecules are arranged in an antiparallel way (every other reducing terminus pointing the opposite direction (B)).

Sometimes one can see in the literature a classification of cellulose to α, β or γ-type. These types refer to fractions or extracts of cellulose, and Bray and Andrews (1923) described the methods for producing them: fraction β consists of cellulose that is soluble in 4.4 M NaOH at 20°C whereas type α cellulose stays insoluble. Fraction β can be separated further to cellulose types β and γ when the fraction is acidified with H_2SO_4 and diluted with water: type β cellulose precipitates and type γ stays in solution. To my opinion this classification is a bit outdated and does not really tell much about the cellulose allomorphs, and sound very similar to the fractioning of cell wall polysaccharides into hemicellulose a and b (Norris and Preese, 1923) which is still widely used in studies plant cell wall biochemistry. However, the terminology of α, β and γ-type is used in paper pulping industry (Sixta, 2016). It is worth considering that the treatment in concentrated alkali mercerises some of the cellulose from type I to type II (Roselli *et al*., 2014). Mercerising makes the cellulose swell, breaks the cellulose crystal structures and forms several intermediate Na-cellulose structures before the final cellulose II is formed (Okano and Sarko, 1985). It is possible that during the mercerisation the increased spacing between the cellulose molecules and intermediate Na-cellulose structures allows some of the cellulose molecules on the outer surface of the microfibrils to come off from the surface of the microfibrils and to be separated to the β fraction. Also, amorphous cellulose might be more extractable by the alkali treatment as highly crystalline cellulose is known to be challenging to mercerise (Okano and Sarko, 1985).

1.3 Purification and processing of cellulose

Cellulose can be purified from any plant material but most commercial manufacturers use wood as the starting material, and most pulp is produced to make paper and paper-based products (Sixta, 2006; Roselli *et al*., 2014). Although there are numerous publications for methods and improvement of methods for pulping and purification of cellulose, the exact details of the cellulose manufacturing processes are usually trade secrets. Generally speaking there are two alternative methods for processing pulp and manufacturing cellulose: the prehydrolysis Kraft (PHK) and acid sulphite (AS) methods. They differ from each other by how the polysaccharides other than cellulose degrade in the pulp: the PHK method uses alkali which results in high DP cellulose whereas AS causes acid hydrolysis of polysaccharides which results in cellulose with lower DP (Sixta, 2006; Roselli *et al*., 2014).

PHK starts with an acidic prehydrolysis step which dissolves and removes the lignin when the liquor is removed from the pulp (Sixta, 2006). The prehydrolysis liquor could be dilute sulfuric acid, when the temperate used for the reaction is 120–140°C, or just water steam at slightly higher temperatures (160–180°C) which helps the organic acids naturally occurring in the wood to hydrolyse the material. The next step is the Kraft cooking that has hot (140–175°C) and alkaline conditions. This step removes most of the remaining lignin and hemicelluloses but also causes some further degradation of cellulose. Next, the pulp goes through several steps of bleaching which oxidises any remaining lignin and makes the pulp white. The PHK pulp contains >90% α-cellulose, and the total cellulose content of PHK processed pulp is usually 94-96% (Sixta, 2006) (where the difference is presumably β and γ cellulose).

The other option for pulp processing, the AS method, uses ammonia-based spent sulphite liquor (SSL) in the first step to remove lignin (Sixta, 2006). The sulphite breaks down lignin and forms lignosulfonates which will come out of the pulp when the liquor is removed. Many value-added products can be recovered and produced from the SSL, such as vanillin, xylitol and ethanol. The remaining pulp is called the 'brown stock' and it can be purified further with hot alkali treatment or multiple steps of bleaching. The resulting 'dissolving pulp' also has an α-cellulose content >90%, with total cellulose content of 92 – 94% in the final product (Sixta, 2006).

We have not been told how the commercial celluloses used in the studies of this thesis have been processed. The cellulose manufacturing involves many steps which are done using various chemicals, and sometimes very high temperatures, and the processing could also introduce some chemical changes to cellulose, not only cleave the other polysaccharides in the pulp. For instance, the processing could oxidise cellulose. Oxidation could introduce to the cellulose some carboxylic acid groups which are negatively charged (and also aldehyde or ketone groups, which would not be charged). Therefore, I developed a novel method for detecting and quantifying negatively charged groups in cellulose (see Results, 3.2 Negatively charged groups in cellulose).

1.4 Dietary fibre

Dietary fibre consists mainly of oligo- or polysaccharides (and lignin) that are not digested in the upper gut for energy consumption by humans. As mentioned in hemicellulose chapter (§ 1.1.1.2), traditionally dietary fibre has been divided into two subgroups: soluble and insoluble fibre. Soluble fibre dissolves in water whereas insoluble fibre does not. Insoluble dietary fibres include cellulose and hemicellulose polysaccharides whereas pectin and hemicellulose oligosaccharides are classified as soluble dietary fibre. A major part of the daily dietary fibre intake of an average person is cellulose, which is why the topic of dietary fibre is related to this thesis. The terms 'soluble' and 'insoluble dietary fibre' are still occasionally used but nowadays the classification is becoming less popular as the water solubility is not always linked with the physiological role of health effects on people. It is also worth mentioning that many hemicelluloses (e.g. xyloglucan) are not extractable from the plant cell wall in water, but (once extracted in alkali) are soluble in water. Also, most pectin is not extractable in cold water. Therefore, the terms 'soluble' and 'insoluble dietary fibre' are not very informative in what comes to the solubility of the dietary fibre components.

1.4.1 The role of dietary fibre in the health of the digestive system

A major part of dietary fibre is fermented by gut microbes in the colon and caecum (Mudgil & Barak, 2013; Elleuch *et al.*, 2011; Gray *et al.*, 1993). The products of bacterial fermentation are acetate, propionate and butyrate which are classified as short-chain fatty acids (SCFA), sometimes known as volatile fatty acids (VFA) (Mudgil & Barak, 2013; Elleuch *et al.*, 2011; Eastwood, 1992; Cummings, 1981). Many soluble fibres are fermented completely, but insoluble fibre is broken down only partially (Mudgil & Barak, 2013; Elleuch *et al.*, 2011; Gray *et al.*, 1993). Gray *et al.* (1993) showed by feeding rats with primary cell walls of uniformly ^{14}C-labelled cultured spinach cells that a major part of the unfermented material was cellulose. However, since more than 80% of the cell walls were fermented in the gut, some cellulose (cellulose contributed to 21% of the ^{14}C-labelled cell wall components) must have been fermented as well (Gray *et al.*, 1993).

Consumption of dietary fibre has been shown to reduce the risk of colon cancer (EFSA panel on NDA, 2010). This could be partially explained by the flushing effect of the unfermented fibres – they catch unabsorbed solutes, which include toxic and carcinogenic compounds such as secondary bile acids and heterocyclic aromatic amines, respectively, as they pass through the colon (Harris and Ferguson, 1993). Also, dead microbes get flushed out in the process. Increased fibre consumption decreases

the passage time of the content of the large intestine which diminishes the effect of the toxic compounds on the colonic mucosa (Mudgil & Barak, 2013; Elleuch *et al.*, 2011; Eastwood 1992; Harris and Ferguson, 1993).

Most SCFAs are absorbed by colonic mucosa, which uses SCFAs, especially butyrate, as its primary energy source (Cummings, 1981, Eastwood, 1992). The reduced colon cancer risk could also be mediated by the increased anaerobic bacterial growth which enhances ammonia uptake from the colon (used for protein production by the bacteria) which, in turn, leads to lowered luminal ammonia levels (Cummings, 1981). High ammonia levels have been associated with increased occurrence of cell changes (which can develop into a cancer) in intestinal cells. Low butyrate production could be one of the factors that give rise to ulcerative colitis but at the same time ulcerative colitis could reduce butyrate production in the gut. SCFAs have an antimicrobial effect since they are known to prevent growth of pathogenic bacteria, although the low redox potential that is maintained by the anaerobic bacteria in the gut might also contribute to the suppression of growth of the pathogenic bacteria (Cummings, 1981). A low pH that is maintained by the production of SCFAs may enhance the absorption of vitamin K and magnesium as well as stimulate mucus production (Cummings, 1981).

EFSA has published an opinion on consumption of dietary fibre (EFSA panel on NDA, 2010). A recommended daily intake of 25 g/day was given based on multiple national and international studies. The studies showed that consumption of dietary fibre reduces the risk of several diseases such as colorectal cancer. It was also stated that intake higher than recommended is likely to be beneficial for health. In general, the fibre intake of most European people does not reach the recommended level (EFSA panel on NDA, 2010). In 2015, the recommended daily intake of dietary fibre in UK was set to 30 g/day by the Scientific Advisory Committee of Nutrition, but the mean daily intake of dietary fibre of an average adult is less than half the recommended level (Gressier and Frost, 2022).

Over the last decade, knowledge of the role of gut microbes in health and general well-being has boomed and become a more popular topic of discussion in non-scientific publications and media – there are frequent interviews with dieticians and medical doctors in TV, tabloids and ‘women’s magazines’ (and myriad other platforms of media) recommending people to increase the

consumption of high-fibre and plant-based foods. When combined with a reduced consumption of meat, which is widely recommended both for reasons of health and for slowing the rate of climate change, there is hope that an average consumer would be increasing the daily intake of dietary fibre. In fact, Gressier and Frost (2022) found that in the study period of six years (from 2008/2009 to 2016/2017), average consumers in the UK increased their daily dietary fibre intake by 0.09 g/year (≈0.6%/year) which is a very slow rate but a promising trend. Although Gressier's and Frost's data are already five years old, much more work is needed with the health education and outreach of the public for directing the eating habits of consumers on healthier tracks and reaching the recommended levels of consumption of dietary fibre.

1.5 Food additives

Substances that are added to food and feed in small quantities, for instance to enhance or stabilise the structure, increase the palatability or lengthen the shelf life of the product, are called food additives. All food additives are given an international identification number (INS, International Numbering System for Food Additives), and many countries and trade unions have their own numbering systems which usually follow the INS numbering system. In the European Union, the food additives are identified with E-codes.

1.5.1 Cellulose as a food additive

Cellulose is widely used as a food additive. It has uses as a stabiliser, emulsifier, thickening agent, calorie reducer and anti-caking agent (Tabara *et al*., 2014, Trache *et al*., 2016, Nsor-Atindana *et al*., 2017). It is relatively inert and tasteless. However, cellulose can have a negative effect on 'mouth feel' and thus reduce the palatability of foods. In the preliminary experiments by Mars Incorporated, cellulose that was mixed into chocolate had a grainy and dry mouth feel. On the other hand, cellulose can improve the palatability of some foods, for instance small microcrystalline cellulose particles gave rye bread a structure which was associated with freshness (Fuckerer *et al*., 2016) and Imamura and Matsushima (2013) extracted from soy sauce cellulose which suppressed unpleasant aftertastes and had molecular weights between 44900 and 47900 (DP ~300).

One of the commercial cellulose preparations studied in this project, LC200 (powdered cellulose E460ii), has been tested as a food additive in Tunisian beef sausage by Ktari *et al.* (2014). The sausages that contained cellulose were found 'juicier' by the panellists and were preferred over the non-cellulose controls. The amounts of spices and fat were kept constant between the samples and the amount of meat was reduced in the cellulose containing sausages. The authors explained the acceptance of the novel sausage by the oil- and water-binding capacities of cellulose that gave a less greasy mouth feel to the food (Ktari *et al.*, 2014).

Cellulose microfibrils consist of crystalline and amorphous regions (see § 1.2.2). In the crystalline regions, the cellulose molecules have a very organised crystalline structure bound to each other with more frequent hydrogen bonds than in the amorphous regions. The amorphous regions of cellulose interact with water and other polar solvents which can form hydrogen bonds with the free hydroxyl groups of the cellulose molecules. The crystalline structures are less 'accessible' to the surrounding solvents, especially the molecules inside the crystal. The variation of crystalline and amorphous regions, as well as the hydrophobicity of the (110) surfaces and the hydrophilicity of the (1-10) surfaces in the crystalline cellulose (Yamane *et al*. 2006), makes cellulose an emulsifier – the amorphous regions can bind the aqueous phase of the foodstuff and bring it together with the fat components, which can interact with the (110) crystalline surfaces of the cellulose microfibrils (Murray *et al.*, 2011, Nsor-Atindana *et al*., 2017).

1.5.1.1 Cellulose and cellulose derivatives permitted for food additive use in EU

Table 1. Celluloses and cellulose derivatives used as food additives internationally and in EU (sourced from EU Commission official webpage https://webgate.ec.europa.eu/foods_system/main/index.cfm on April 16th, 2021):

INS number	E number	Compound name
460	E460(i) E460(ii)	Microcrystalline cellulose Cellulose powder
461	E461	Methyl cellulose
462	E462	Ethyl cellulose
463	E463	Hydroxypropyl cellulose

464	E464	Hydroxypropyl methyl cellulose
465	E465	Ethyl methyl cellulose
466	E466	Sodium carboxymethyl cellulose
467	(not allowed in EU)	Ethyl hydroxyethyl cellulose
468	E468	Crosslinked sodium carboxymethyl cellulose
469	E469	Enzymatically hydrolysed carboxymethyl cellulose

All the celluloses and cellulose derivatives in Table 1 are ratified for food additives and are prepared from α-cellulose which has been sourced by treating pulp from fibrous plant materials (Commission regulation, 2012). By August 2022 bacterial cellulose has not yet been significantly used in EU, and its safety would need assessment by EFSA before its use could be approved for food and feed use.

1.5.1.1.1 Cellulose

E460 is given to microcrystalline cellulose (E460(i)), which is sometimes called cellulose gel, and cellulose powder (E460(ii)). The difference between these two subtypes of cellulose is that microcrystalline cellulose is highly crystalline as it has been treated with mineral acids to partially depolymerise and remove the amorphous regions whereas cellulose powder has only been mechanically disintegrated and has not undergone the mineral acid treatment (Commission regulation, 2012). The DP of E460(i) microcrystalline cellulose should be less than 400 and the particle size of both the celluloses should be bigger than 5 μm (Commission regulation, 2012). From the samples we have worked with we have noticed that microcrystalline celluloses tend to appear granular whereas cellulose powder particles seem to be more fibrous.

Native cellulose is not ionically charged and in this thesis when speaking of cellulose, I am referring to the native (unmodified) type of cellulose (E460ii). The other types of 'cellulose', listed in the paragraphs below (1.5.1.1.2 – 1.5.1.1.10), have undergone major chemical modifications and I would

regard them as ‘cellulose derivatives’ rather than ‘cellulose’, although they might be called ‘cellulose’ by the EU.

1.5.1.1.2 Methyl cellulose

Methyl cellulose (E461) has some of the hydroxyl groups etherified with methyl groups. It has to contain 25 – 33% methoxyl groups and its hydroxyethoxyl content must be under 5% (Commission regulation, 2012).

1.5.1.1.3 Ethyl cellulose

Ethyl cellulose (E462) has some of the hydroxyl groups etherified with ethyl groups. On dried basis, the ethoxyl group content must be between 44 and 50% (Commission regulation, 2012).

1.5.1.1.4 Hydroxypropyl cellulose

Most – but not more than 80.5% – of the hydroxyl groups in E463 hydroxypropyl cellulose should be etherified with hydroxypropyl groups (Commission regulation, 2012).

When the hydroxypropyl content of the cellulose is lower, it is called low-substituted hydroxypropyl cellulose (L-HPC) and the E-code for it is E463a. The molar substitution with hydroxypropyl groups of the glucose units of cellulose backbone should not exceed 0.2, whereas for E463 it is 3.5 (Commission regulation, 2012).

1.5.1.1.5 Hydroxypropyl methyl cellulose

Hydroxypropyl methyl cellulose (E464) has 19 – 30% of the hydroxyl groups etherified by methoxyl groups and 3 – 5% by hydroxypropyl groups (Commission regulation, 2012).

1.5.1.1.6 Ethyl methyl cellulose

Ethyl methyl cellulose (E465) has 3.5 – 6.5% of the hydroxyl groups etherified by methoxyl groups and 14.5 – 19.5% by ethoxyl groups. The total alkoxyl group content, should be between 13.2 and 16.9% (Commission regulation, 2012).

1.5.1.1.7 Sodium carboxymethyl cellulose

Sodium carboxymethyl cellulose (E466) has some of the hydroxyl groups etherified with carboxymethyl groups, some of which are in the sodium salt form. The molar substitution of the glucose units of cellulose backbone should be between 0.2 and 1.5 (Commission regulation, 2012). Sodium carboxymethyl cellulose is sometimes called cellulose gum.

1.5.1.1.8 Ethyl hydroxyethyl cellulose

Ethyl hydroxyethyl cellulose (EHEC) is not included in the E-numbers, although it has an INS number 467. European Commission Scientific Committee of Food (SCF) accepted the use of EHEC *quantum satis* in 1999 but European Parliament did not include EHEC in the list of food additives because of the concerns of chemical contaminants left in EHEC from its processing (European Parliament 2000a, SCF 2002). Prior to this EHEC had been used as a food additive in gluten-free breads in Sweden and Finland (European Parliament 2000b, SCF 2002). SCF gave a re-evaluated opinion in 2002 limiting the use of EHEC in gluten-free bread to 5g/kg of dry bread mixture.

1.5.1.1.9 Cross-linked sodium carboxymethyl cellulose

Cross-linked sodium carboxymethyl cellulose (E468), sometimes called cross-linked cellulose gum, is similar to sodium carboxymethyl cellulose (E466) but the cellulose backbone has been covalently cross-linked with other cellulose molecules of the same material. The same substitution regulations apply to E468 as with E466 (Commission regulation, 2012).

1.5.1.1.10 Enzymatically hydrolysed carboxymethyl cellulose

Enzymatically hydrolysed carboxymethyl cellulose (E469) is produced from sodium carboxymethyl cellulose (E466) by partial hydrolysis with *Trichoderma longibrachiatum* cellulase. The same substitution regulations apply to the hydrolysate as to the starting material E466 (Commission regulation, 2012).

1.5.1.2 The types of celluloses in our samples

All the commercial celluloses received from Mars Inc. and most of the standard celluloses are very likely to belong to the class E460 cellulose: microcrystalline cellulose. The control sample, Avicel PH102, belongs to the subgroup 'E460(i) microcrystalline cellulose' whereas all the LC200 preparations and Södra A13 are classified as E460(ii) cellulose powder.

Cellucomp's Curran® sample does not classify to any of the E460-E469 celluloses and derivatives as it is not based on pure cellulose and the material processing is not food grade. Most of the commercial celluloses are officially not food grade (LC200 celluloses might be food grade as they are sold as food additives). Whatman paper and cotton wool are almost pure cellulose but are not in powder nor microgranular form. However, they resemble E460 celluloses because they consist of (mainly) cellulose (and are not chemically modified like the cellulose derivatives). Carboxymethyl cellulose (CMC), which is used as control sample in the study of the negatively charged groups of the cellulose in chapter 1.5.1.1.7, has an E-code of E466.

1.5.2 Safety of the use of cellulose as a food additive

EFSA published in 2018 a re-evaluation on the safety of cellulose as a food additive (EFSA panel on ANS, 2018). No acceptable daily intake (ADI) value was set for cellulose since none of the studies provided showed any signs of toxicity or genotoxicity, even at the highest dosages.

1.6 Chocolate

The main ingredient of chocolate, cocoa solids (which is the cocoa powder and the cocoa fat), is sourced from cocoa beans which are fermented seeds of the cacao tree *Theobroma cacao* (Beckett, 2006; Beckett, 2017). The tree originates from central and southern America and it grows wild in the Amazon rainforest. It needs very specific growth conditions – high humidity, frequent rainfall and a warm temperature all year round – which is why it can be grown only between 20° south and 20° north of the equator in the areas that would naturally be occupied by rainforests. About 90% of world's cocoa is produced in just a few countries – Côte d'Ivoire (Ivory Coast), Ghana, Indonesia, Nigeria, Cameroon, Brazil and Ecuador (Beckett, 2006; Beckett, 2017).

The chocolate industry is facing many challenges with sourcing cocoa beans, and they include the political instability and poverty of many of the countries of origin; loss of crop due to climate change and the very specific requirements for growth conditions (which makes the cacao tree very sensitive to seasonal variation in weather); skyrocketing increase of global demand for chocolate (especially in Asian countries that are transitioning fast from developing countries to developed countries, such as China and India); and the inability to find suitable space for new cocoa tree farms because most suitable areas have already been occupied by 'cash crop' farms, such as palm oil (Beckett, 2006; Beckett, 2017). Practically the only way of increasing the global number of coca tree farms is illegal logging of the rain forest, and that is a major contributor both to climate change and to the ongoing sixth mass extinction. All the challenges combined have made many chocolate producers be more open about, pay attention to and advertise ethically sourced chocolate over the last decade.

1.6.1 Composition of chocolate

Chocolate consists of about ~50% sugar, and many people who want to eat healthily are avoiding or reducing their consumption of chocolate. There is ~30% fat in chocolate, and most of it is cocoa bean fat but milk and white chocolate also contain some fat from the milk. The fat forms the matrix in which the sugar is embedded (Beckett, 2006; Beckett, 2017). Chocolate contains 6–8% of protein, and it derives from the cocoa beans, and in case of milk and white chocolate also from milk. Chocolate liquor (which is mainly cocoa butter) contains ~10% of cellulose with derives from the cell walls of the cocoa nibs (Beckett, 2006; Beckett, 2017), but the dietary fibre content of milk chocolate

is usually only ~3%. The reason for adding cellulose to chocolate would be to reduce the proportional amount of sugar and to add dietary fibre to chocolate, which could make chocolate a healthier or 'less guilty' treat. Even if a small proportion of the sucrose were replaced with cellulose, the increase of dietary fibre content could be significant. The official EU health claim 'high fibre' could be reached if the dietary fibre content could be increased to 6 g/100g of product, or 3 g/100 kcal (retrieved on August 16th, 2022, from the European Commission official web page https://food.ec.europa.eu/safety/labelling-and-nutrition/nutrition-and-health-claims/nutrition-claims_en).

1.6.2 Processing of chocolate

Chocolate is a complex mixture and manufacturing it demands sophisticated methods (Hartel *et al.*, 2018). Cocoa beans are the seeds of the fruit of the cocoa tree, and after harvesting they undergo several processing steps before they are ready to be stored and transported to chocolate factories: the fruits are opened and the seeds are separated from the 'flesh' of the fruit, and the beans fermented, dried, cleaned and sometimes roasted already at the farm (Beckett, 2006; Beckett, 2017). All the processes done at the farm are important for the final development of the cocoa flavour and 'shelf-life' of the cocoa beans, and any mistakes in the processing would spoil the chocolate (Beckett, 2006; Beckett, 2017).

In the chocolate factory, the cocoa beans undergo numerous processes: roasting, grading, removing of shell, grinding, milling and liquefying of cocoa nib (the cotyledons inside the cocoa seed/bean), followed by separation of cocoa butter and solids (press cake) from the liquor (Beckett, 2006; Beckett, 2017). Then some of the press cake is mixed back into the cocoa butter (while the remaining press cake is converted to cocoa powder) together with the sugar, milk powder and flavourings, and the chocolate mix undergoes blending, conching and tempering before packaging (Beckett, 2006; Beckett, 2017).

While the first few steps (other than roasting) of the processing remove any impurities and unwanted parts of the cocoa beans, the final structure of the chocolate mass is determined by the grinding and milling. Usually the milling is repeated several times using different mills to reach the desired particle size: all the solid particles should be about 20 µm in size for fine and smooth

chocolate (whereas low quality chocolate has particles up to 40 µm in diameter), and therefore sucrose and milk powder are usually also milled (Beckett, 2006; Beckett, 2017).

Two of the most important steps for the development of flavour and mouth feel of the chocolate are roasting and conching (Beckett, 2006; Beckett, 2017). Roasting of the cocoa beans is very important because it brings out the flavour and aroma typical of chocolate. Many of the flavours typical of roasting are formed through Maillard reactions and especially the Amadori compounds, which were formed during the drying process, react further when heated. Also, most of the other flavour precursor compounds formed during the fermentation and drying processes do not have a detectable flavour before roasting. There are about 600 different volatile cocoa flavour components in roasted beans (Beckett, 2006; Beckett, 2017).

Conching is used to give a smooth structure and mellow taste to the final chocolate product (Beckett, 2006; Beckett, 2017). The chocolate mass is mixed in the conch for a long time – nowadays the conching takes 6-24 h but traditionally it could take up to 72 h. During the mixing the solid particles (such as sucrose and milk powder), which are added to the chocolate liquor at the beginning of conching, are fully coated with the fat matrix. During the conching, sucrose crystals pick up flavour components from the cocoa mass acting as a water-soluble carrier of the flavour. When the chocolate is eaten, the sucrose dissolves in the mouth releasing the flavour components and enhancing the taste. Another very important aspect of conching is that it allows evaporation of volatile compounds, many of which have unpleasant flavours, from chocolate making it less acidic and bitter: a major part of the acetic acid and 30% of short chain fatty acids and water are lost during the conching. The evaporation is assisted by warming of the chocolate mass which is caused by friction from the mixing. Half way through the conching, more cocoa butter is added to the conch to increase the flow and make sure all the solid particles are being coated by fat. At the end of conching, the emulsifier lecithin is added to bring the fat and sucrose firmly together and to make the liquid chocolate slightly runnier for moulding or coating (Beckett, 2006; Beckett, 2017).

1.6.3 Mouthfeel properties and the experience of eating chocolate

Chocolate is a mixture of crystalline solid particles (Beckett, 2006; Beckett, 2017). The size of the solid particles does not affect the mouthfeel in itself but the human mouth is able to detect even a

few micro meter differences in the particles which can be experienced as a 'sandy' or 'gritty' mouthfeel. Chocolate matrix is fat-based and the solidifying process of chocolate mass needs to be tightly controlled by tempering to get the fat to crystallise in the desirable polymorph. Long enough conching helps the fat to solidify slowly enough to form desirable polymorphs. Different polymorphs take different times to melt in mouth when the chocolate is eaten, and therefore it is important to regulate that all the cocoa fat has solidified in the same polymorph, as a mix of different polymorphs may give the chocolate a grainy and 'off' mouthfeel. Producing milk chocolate is more challenging since the milk fat consists of multiple different fats that, in turn, differ from the cocoa bean fat, but also the solidification and polymorphs of the milk fat influence the mouthfeel. Cocoa butter hardness (i.e. the length and degree of saturation of the fat molecules) also influences the mouthfeel, and it depends on where the cocoa beans are from – the closer to the equator the country of origin is, the harder the cocoa butter (Liendo *et al*. 1997; Beckett, 2006; Beckett, 2017). For bulk chocolate making, beans from different origins are often mixed and therefore the cocoa butter has an intermediate hardness. When producing chocolate for countries that have a warm climate, the melting point of the final chocolate product can be raised by using harder cocoa butter (Beckett, 2006; Beckett, 2017).

Sucrose that is used to sweeten the chocolate is mixed in as tiny crystalline solid particles (Beckett, 2006; Beckett, 2017; Hartel *et al.*, 2018) which dissolve only when they come to contact with saliva in mouth. Although cellulose does not dissolve when eaten, the degree of crystallinity of cellulose and the similarity in size of the particles may play a role in the mouth feel properties when added in chocolate.

In the plant cell wall the molecules surrounding the cellulose microfibrils are typically hemicelluloses that coat and tether the microfibrils forming the 'backbone' structure of the cell wall (Cosgrove, 2014). I hypothesise that in the absence of a hemicellulose coating, interactions may be formed between cellulose and other molecules as well – when eaten, for example, the commercial celluloses will come in contact with water from saliva and the binding of water to cellulose (especially the amorphous regions of cellulose microfibrils) could contribute to the 'dry mouth feel' properties observed when the cellulose containing chocolates were tested by a professional tasting panel. It was also noticed during the initial testing at the MARS chocolate factory facilities that some of the celluloses added into chocolate made the chocolate matrix clot.

1.6.4 Dietary fibre in chocolate

There are some studies published where dietary fibre has been mixed with chocolate or chocolate preparations, although none of these studies were done with pure cellulose. For instance, soluble and insoluble dietary fibre extracted from date seeds were mixed with chocolate spread (Bouaziz *et al.*, 2017) and fructooligosaccharides (FOS) and a sucrose replacer (sucralose or stevia with 97% rebaudioside A) were added with or without Goji berries to white chocolate (Morais Ferreira *et al.*, 2017). The panellists of both studies found the novel fibre-containing chocolates acceptable. Also, chocolates containing FOS are manufactured by the Belgian company Cavalier and are being sold in many EU countries.

To my knowledge, no-one is using cellulose as a food additive in commercially available chocolate yet. The commercial cellulose samples studied in this project were found in the preliminary experiments done by Mars Wrigley Inc. to differ in their properties of mixing with chocolate as well as 'mouth feel' properties.

In the chocolate matrix the cellulose microfibrils can interact with various hydrophilic (for instance sucrose, lactose and polysaccharides from cocoa press cake) and hydrophobic (such as cocoa and milk fat) molecules. The (110) cellulose microfibril crystalline surfaces, which could also have fewer free hydroxyl groups on the surface, can interact with the hydrophobic molecules whereas the amorphous regions and the (1-10) surfaces of the crystalline regions can interact with the hydrophilic molecules. The differences of how crystalline the celluloses are and how accessible the (110) and (1-10) crystalline surfaces of the commercial celluloses are to the various kind of molecules present in chocolate, saliva and/or the plant cell wall could partially explain why some of celluloses could be mixed in chocolate easily whereas the others would cause the matrix to clot. I have developed three novel methods to study the accessibility of the commercial celluloses and the cellulose-rich AIR (alcohol insoluble residue) preparations (see 3.3.1 Results – accessibility of cellulose).

1.7 Aims of the project

The foundation of this project was in the questions that were raised from the experiments of mixing cellulose into chocolate: why did some celluloses have acceptable mouthfeel properties when mixed in chocolate, whereas others had a grainy mouthfeel? Also, why did some celluloses make the chocolate matrix clot whereas others did not? What makes the celluloses different from each other?

Since cellulose is the most abundant polysaccharide in the cell wall, it was of interest to extend the studies of these questions to isolated plant cell walls (in addition to the commercial celluloses), which is why the pea and cauliflower pea AIRs were included in the experiments. Cellulose is synthesised by the cells and concurrently extruded into the cell wall, and the chemical characteristics of cellulose could derive from its purpose which is to function as the 'skeleton' of the cell wall. As discussed above, cellulose microfibrils interact with various substances, such as other polysaccharides, lignin, protein and water (and small solutes, such as salts) in the cell wall as soon as they are synthesised, and in that sense the purified commercial celluloses are in an 'unnatural' state (as they are missing the other cell wall components they usually interacts with) – and therefore it is not surprising that the celluloses made the chocolate matrix clot, for instance.

Pea and cauliflower were chosen for the studies because they both are dicots (they are rosids, but from different clades); they are widely cultivated and commercially available; and there are numerous publications made using pea and cauliflower cell walls preparations. Also, the ease of cultivation (in case of peas) and large size (in case of cauliflower) meant that I could easily grow, harvest and process enough AIR for each tissue type for conducting all the experiments performed during this study.

This project aimed to address the above questions concerning the commercial celluloses from three points of view:

a) Do the commercial celluloses differ from each other by their chemical composition?
b) Has the purification process during cellulose manufacture introduced oxidised groups (specifically, negatively charged carboxylic acid groups) into cellulose?
c) Do the celluloses differ from each other in their accessibily to surrounding molecules?

The same experiment were also performed for the plant AIRs, and the same points of view also applied for those samples. I wished to discover if the cellulose is different between tissue types in its chemical composition, oxidation and accessibility, although most of the studies of these questions were done for the AIRs as a whole (rather than for cellulose fractions that would have been isolated from the AIRs).

2 Materials and methods

2.1 Description of the samples

At the beginning of the project six commercial cellulose samples were received from Mars Inc. Additionally, alcohol-insoluble residue (AIR) of pea seedlings that were grown in dark and light conditions, pea leaves and mature (relatively woody) pea stems and cauliflower leaves, stems and florets were processed at the same time as the commercial cellulose samples. The AIR samples were named A, B, C, D, F, G and H, respectively. Whatman No.1 paper, cotton wool and Avicel PH102 were chosen for controls. The commercial cellulose samples were given numbers from 1 to 6 and the control samples from 7 to 9. Samples manufactured by Södra Skogsägarna were received after initiation of the project and the sample Sodra A13 was included in the analyses as number 10. A hard wood pulp sample, which is cellulose that had never been dried during its processing, was received from VTT Technical Research Centre of Finland as a generous donation. It was a sample derived from an old project and it had been manufactured by a commercial wood industry company in Finland but for confidentiality reasons we were not given the name of the company. The sample was named E.

Table 2. The numbering, full names and mouthfeel properties (when applicable) of the cellulose samples studied in this project. NN = Ninni Nuorti

Number/ID	Manufacturer	Sample description	Supplier/sourced from	Mouthfeel properties (determined by a professional tasting panel at Mars Inc., unless otherwise stated) and behaviour in chocolate matrix
1	(not known)	Milled microcrystalline cellulose	Commercially available, from Mars Inc.	○ 'Sandy/coarse' mouthfeel ○ Dries the mouth (absorbs saliva) ○ Worst mouthfeel from the celluloses tested

				○ Easiest to mix in chocolate
2	Vitacel	LC 200	Commercially available, from Mars Inc.	○ 'Better' and 'more acceptable' mouthfeel than with (1) MCC ○ More challenging to mix in chocolate than (1) MCC (i.e. makes melted chocolate clot easily)
3	Vitacel	MA17 LC200 M2 cellulose in sunflower oil	Commercially available, from Mars Inc.	○ Better mouthfeel properties than (2) LC200 ○ Easier to mix in chocolate than the other LC200s
4	Vitacel	E442 LC200 MIF6 spray dried	Commercially available, from Mars Inc.	○ Slightly worse mouthfeel properties than (2) LC200, but better than (1) MCC ○ Similar mixing properties in chocolate to (2) LC200
5	Vitacel	E442 LC200 MIF6 spray dried & milled	Commercially available, from Mars Inc.	○ Similar mouthfeel properties to (4) LC200 spray dried ○ Similar mixing properties in chocolate to (2) LC200
6	Cellucomp	Curran (prepared from sugar beet pulp)	Commercially available, from Mars Inc.	○ Data not available from Mars Inc. tests ○ Sugar beet fibre (for instance Fibrex by a Finnish company Reformi), used in gluten-free baking, has a strong and unpleasant taste, and the mouthfeel is like

				eating cardboard (based on author's own experience)
7	GE Healthcare Life Sciences	Whatman No 1 filter paper	Commercially available, control sample	N/A
8	Synergy Health (UK) Ltd	Cotton wool	Commercially available, control sample	N/A
9	(not known)	Avicel PH102 microcrystalline cellulose	Commercially available, control sample	N/A
10	Södra Skogsägarna	Södra A13	Commercially available, from Mars Inc.	○ The best mouthfeel from all the celluloses tested ○ Mixing properties in chocolate not known
(not included in studies)	Södra Skogsägarna	Södra A12	Commercially available, from Mars Inc.	Not as good mouthfeel as with (10) Södra A13 which is why advised by Marc Inc. not to include in the studies
(not included in studies)	Södra Skogsägarna	Södra B13	Commercially available, from Mars Inc.	Not as good mouthfeel as with (10) Södra A13 which is why advised by Mars Inc. not to include in the studies
A	NN	Young pea stems grown in light (~7 cm tall, 9-11 days after planting)	'Home-made' AIR	N/A

B	NN	Young pea stems grown in dark (~7 cm tall, 9-11 days after planting)	'Home-made' AIR	N/A
C	NN	Leaves of pea from fully grown plants that are flowering	'Home-made' AIR	N/A
D	NN	Stems (5-7 cm) of pea just above soil level of fully grown plants that do not flower anymore and have grown their fruit to full size.	'Home-made' AIR	N/A
E	(not known)	'Never-dried cellulose' Hard wood pulp	Received from VTT from Finland	N/A
F	NN	Cauliflower leaves	'Home-made' AIR	N/A
G	NN	Cauliflower stems	'Home-made' AIR	N/A
H	NN	Cauliflower florets	'Home-made' AIR	N/A

2.2 Preparation of the materials

2.2.1 Preparation of alcohol-insoluble residue (AIR)

Young pea stems grown in dark and light conditions, pea leaves of mature plant and stems of fully mature pea plants were harvested and stored frozen in -20°C until further processing.

The pea tissues were ground fine in liquid nitrogen using pestle and mortal. The materials were transferred to 50 ml Sarstedt tubes and filled to 15-ml marks. The tubes were filled to 50-ml marks with 96 % ethanol, mixed vigorously and incubated on wheel for 30 min – overnight in 20°C. The tubes were spun with 2500 g for 5 min in 20°C and the supernatants were discarded. The tubes were filled with 70% ethanol and the mixing, spinning and discarding of supernatant were repeated as before. The washes with 70% ethanol were repeated until the residues had lost their green colour and turned off-white and the discarded supernatant was clear for which typically at least five washes were needed. After the ethanol washes were finished, the alcohol-insoluble residues were either washed two to three times with water containing 0.5% chlorobutanol (when the material was used for the assaying of starch content) or dried caps off in fume hood at 20°C over 2 nights.

Cauliflowers were bought from a local supermarket and the leaves, stems and florets were separated from each other. The materials were cut smaller with a knife and homogenised in a blender adding as little as possible reverse osmosis purified (RO) water to allow sufficient flow of material in the blender. The cauliflower-water mixtures were poured to 1-l glass bottles so that the sedimenting plant materials packed to 300-ml marks. The bottles were filled to 1-l mark with more RO water and the material was mixed with magnetic stirrer for 1–2 h. The insoluble residues were drained by using cheese cloth in a Buchner funnel and returned to the same bottles. The water washes were repeated for the insoluble residues until they no longer smelt like cauliflower which took three to five washes. After that the water-insoluble residues were washed with 70 % ethanol overnight with the filtering in the between of washes as previously. The ethanol washes were repeated until the discarded supernatant came out clear which took at least five washes. The filtrated alcohol-insoluble residues were packed in plastic boxes, frozen to -80°C and dried using a freeze drier.

2.2.2 Removing oil from sample 'LC200 in sunflower oil'

LC200 in sunflower oil sample was washed with acetone until no oil remained in the sample. The washing was done by filling up the tube containing some sample with acetone, mixing the tube on wheel for 1 h – overnight, spinning down the pellet with 2000 g for 3 minutes at 20°C and discarding the supernatant. The presence of oil was checked by dipping a piece of Whatman No 3 paper into the pellet still wet with acetone and letting the paper dry. If oil was still present in the sample, there were oily spots on the paper, in which case the acetone washes were continued. If the oil had been removed sufficiently, the paper was completely dry after the acetone had evaporated. After the acetone washes were finished, the pellet was dried by leaving the tube cap off in a fume hood in 20°C overnight.

2.2.3 Defining the dry material content of the 'never-dried cellulose'

Three samples of never-dried cellulose (sample E of table 2) were dried in oven at 80°C for 26h after which the drying was continued at 120°C for further 6 h. The samples were weighed before and after drying to calculate the dry matter content which was 27.3%. The dry matter content was used for calculating the wet cellulose needed for the other analyses so that it would be comparable with the other samples by its dry weight. The oven-dried cellulose was used in lignin assay but in all the other experiments the sample E was used wet.

2.3 Chromatographic methods

2.3.1 Separation and detection of sugars on thin-layer chromatograms (TLC)

The thin-layer chromatogram (TLC) plates (Merck siliga-gel) were placed to stand in sealed glass tanks in butan-1-ol/acetic acid/water (BAW) (2:1:1), ethyl acetate/pyridine/acetic acid/water (6:3:1:1) or propanol/nitromethane/water (5:2:3) and the solvent mixture was let to ascent to the top of the plates. The plates were dried in fume hood and the chromatography was performed again with fresh solvent mixtures (unless otherwise stated).

The sugar compounds were stained by dipping the plates in thymol/H_2SO_4/ethanol (0.5g /5 ml/95 ml) after which the plates were dried, heated to 105°C for 20 min, cooled down and scanned immediately.

2.3.2 Separation and detection of amino acids on paper chromatograms (PC)

Hydrolysates of the samples were pipetted together with amino acid markers on Whatman No 20 paper on a line drawn 9 cm from the shorter edge of the paper. The paper was dried well and the edge of the paper closest to the sample loadings was placed in a glass tank on a solvent trough so that the rest of the paper was hanging over the edge of the trough. Butan-1-ol/acetic acid/water (BAW) (12:3:5) solvent mixture was poured in the trough, the tank was sealed and the solvent front was let descent for 60 h.

The paper was taken out of the tank, hanged in the fume hood and dried completely. The dry paper was dipped in 0.5% ninhydrin solution prepared in acetone, dried and heated up to 105°C for 5 min. The chromatogram was scanned in three parts and the parts were connected together using Microsoft Power Point programme.

2.4 Identification and quantification of the sample composition and removal of polymers other than cellulose

2.4.1 Assaying the starch content of samples

For dialysis, 10 ml of heat stable α-amylase (from *Bacillus amyloliquefaciens* by Sigma-Aldrich, Product A7595, CAS 9000-90-2, Batch 097K0739) was pipetted in prewetted dialysis sac with cut off value of 14 kDA. The dialysis was done against RO water containing 0.05% chlorobutanol for 48 h at 4°C. After dialysis, the volume of the solution was set to 45 ml (O'Rourke *et al.* 2015).

About 50 mg of the cellulose samples (and pea AIR sourced from 1.5–3 g of fresh material) were suspended in 5 ml (or 45 ml) of 40 mM lutidine-acetate buffer, pH 6.7, and boiled for 15 min. The

samples were cooled and 0.5 ml (or 4.5 ml) of the dialysed α-amylase were added to the samples. The samples were incubated at 60°C for 72 h and mixed by inverting regularly (O'Rourke *et al.* 2015).

For salivary α-amylase digestion, saliva, that was centrifuged at 3200 g for 15 min at 20°C in stead of dialysed commercial enzyme. The digestion was done at 37°C.

After digestion, the samples were spun down and 5 µl of the supernatants were loaded on TLC plates and separation of sugars was performed in BAW (2:1:1) as described in 'Chromatographic methods'.

2.4.2 Assaying the xylan content of samples

50 mg each of sample digested with 15 U of Megazyme M6 β-xylanase (from 'rumen micro-organism') in 5 ml of 40 mM lutidine-acetate buffer, pH 6.7, for 16 h at 20°C.

After digestion, the samples were spun down and 6 µl of each digest was loaded on the TLC. The TLCs were developed in EPAW (6:3:1:1) as described in 'Chromatographic methods'.

2.4.3 Removing other than covalently bound protein

The α-amylase digested cellulose and pea AIR samples were washed three times with RO water containing 0.5% chlorobutanol and pipetted dry. RO water was added to the tubes and the volumes were set to 1.75 ml for cellulose samples and 5 ml for pea AIR. To the cellulose samples 3.5 ml of glacial acetic acid and 8.75 ml of 80% phenol (and to the pea AIR 12 ml of glacial acetic acid and 30 ml 80% phenol) were added resulting in 2:1:1 phenol/acetic acid/water mixing ratio. The samples were incubated for 1 h at 70°C water bath and mixed regularly. After cooling down the samples were washed with RO water containing 0.5% chlorobutanol for five to seven times.

2.4.5 Hydrolysing covalently bound protein

About 10 mg of dry cellulose and AIR samples were weighed accurately in 6 ml Sarstedt tubes and 3 ml of saturated $Ba(OH)_2$ was added to the tubes. The samples were incubated in 105°C for 17 h, mixed and cooled down. The samples were titrated first to slightly alkali pH and then slowly to pH about 2.5 with 0.68 M H_2SO_4 using 10 µl of 0.47% thymol blue in 10 mM NaOH as an indicator. The supernatants were transferred to new tubes and the volumes were set to 6 ml with RO water.

About 1 ml volume of strong cation exchange resin Dowex w50x2 was packed to Polyprep columns. The resin was pretreated by washing first with plenty of 1 M ammonia and then RO water, 1 M H_2SO_4, RO water and finally 1 mM formic acid.

The suitability of the resin was first tested in triplicate with 1 kBq of [^{3}H]proline samples which were diluted to 6 ml and passed through the columns. The columns were washed first with 5 ml of RO water, then 10 ml of 10 mM formic acid and finally 4 ml of RO water. The [^{3}H]proline samples were eluted with 10 ml of 1 M ammonia after which the columns were washed with RO water, 1 M H_2SO_4, RO water and 1 mM formic acid. The washed columns were used for the next samples. Collections of 1 ml fractions were started from loading the columns and it was detected that the [^{3}H]proline was eluted straight after the first volumes of 1 M ammonia had passed through the column, in fractions 28–30.

The $Ba(OH)_2$ hydrolysed samples were passed through the column, washed and eluted similar to the [^{3}H]proline samples. Fractions 27–31 were collected and pooled together. The pooled fractions were let dry in the fume hood at 20°C caps off until they no longer smelled like ammonia after which they were cooled to -80°C and dried in the freeze dryer. The contents of the tubes were dissolved in 200 µl of RO water containing 0.5% chlorobutanol.

For identifying the amino acids freed by the hydrolysis of proteins, 70 µl of the cellulose sample fractions and 20 µl of the pea AIR fractions were loaded on paper chromatograms as described in ‘Chromatographic methods’.

2.4.6 Lignin assay

For assaying lignin, 10 mg of dry cellulose or AIR samples were weighed accurately in 2 ml Fishes glass tubes with Teflon lined screw caps. For sample E (from table 2) the oven-dried sample (see 'Defining the dry material content of the 'never-dried cellulose'') was used because water reacts with acetyl bromide.

To the tubes 1 ml acetyl bromide/acetic acid (1:3 v/v) were added and the tubes were incubated in water bath for 30 min at 70°C with mixing every 5 min. The tubes were cooled down, and 100 µl solutions were pipetted to 15 ml Sartstedt tubes containing 500 µl acetic acid and 90 µl 2M NaOH premixed. The tubes were mixed, 20 µl of 7.5M hydroxylamine-HCl was added and the tubes were mixed again. The volumes were set to 4 ml (or 8 ml in case of the positive controls) with glacial acetic acid. About 2 ml of the samples were poured in quartz cuvettes and A_{280} of the samples were measured in spectrophotometer which was zeroed against glacial acetic acid. The lignin content was calculated assuming that 10 µg/ml gives an absorbance of 0.17 (Hatfield & Fukushima, 2004; 2005).

2.4.6.1 Modified lignin assay

The assay was done similar to the Lignin assay except the samples were weighed in 2 ml Sarstedt plastic tubes, the heating was done in a heat block and and 200 µl (or 50 µl in case of positive control samples) acetylated sample was mixed with acetic acid and sodium hydroxide.

2.4.7 Acid hydrolyses

2.4.7.1 Trifluoroacetic acid (TFA) hydrolysis

From the samples from which starch and proteins had been removed, 500 µl were pipetted to 2 ml Sarstedt tubes as suspensions which contained approximately 1.8 mg of cellulose or AIR (in water) and the suspensions were mixed with 500 µl of 4 M TFA. For other analyses about 10 mg accurately weighed dry samples were mixed with 1 ml of 2 M TFA. The tubes were incubated in heat block for 1 h at 120°C and cooled down. The supernatants were pipetted to fresh tubes. The pellets were

washed with 750 µl of RO water, span down and the supernatants were transferred to the same tubes as the previous supernatants. The supernatants were dried in SpeedVac and the contents of the dry tubes were dissolved in RO water containing 0.5% chlorobutanol so that the concentration of the final solution was 56 µl/mg (of dry weight of the original sample). For TLC, 2.5–5 µl of hydrolysates were loaded on the plates and the chromatography was prepared as described in 'Separation and detection of sugars on thin-layer chromatograms (TLC)' in EPAW (6:3:1:1) solvent mixture.

For repeated TFA hydrolyses, the pellets were washed with 0.5% chlorobutanol three times and dried in a SpeedVac before repeating the hydrolysis for the same pellets. The TFA hydrolysis was repeated five times before Saeman hydrolysis of the pellets.

2.4.7.2 Saeman hydrolysis

The TFA hydrolysed pellets were dried in SpeedVac. The Saeman hydrolysis was made following the protocol described in Fry (2000). For dissolving the pellets, 72% (w/w) H_2SO_4 was added in the ratio of 20 µl/mg of sample. The dissolving was done at 20°C for one to two hours shaking the tubes gently. If the pellets did not completely dissolve in this time, more acid was gradually added. The H_2SO_4 concentrations of the solutions were diluted quickly to 3% with RO water and the tubes were incubated at 120°C for 1 h. The tubes were cooled down and 1% bromophenol blue in water was added to the tubes in the ratio of 2 µl/ml of hydrolysate. The contents of the tubes were transferred to 6 ml Sartedt tubes and saturated $Ba(OH)_2$ (0.18 M at 20°C) was added to the tubes 2.3 times the volume of the hydrolysate. The tubes were mixed on a wheel for two hours and the colour of the solutions were monitored – the supernatants should stay pale yellow but if they turned blue, 1 µl of 72% (w/w) H_2SO_4 was added to turn them yellow again. Solid $BaCO_3$ powder was added to the solutions in about 40 mg/ml ratio and the tubes were mixed on a wheel overnight after which the colour of the solutions should have been blue. The tubes were frozen, thawed, mixed and centrifuged for 15 min with 3000 g at 20°C. The supernatants were transferred to 2 ml Sarstedt tubes and 1 µl of glacial acetic acid was added to the solutions which made them turn yellow in colour. The contents of the tubes were dried in SpeedVac and dissolved in RO water to concentration of 56 µl/mg of sample.

For TLC, 0.6–3 µl of hydrolysates were loaded on the plates and the chromatography was prepared as described in 'Separation and detection of sugars on thin-layer chromatograms (TLC)' in EPAW (6:3:1:1) solvent mixture.

2.5 Studying the accessibility of the surface of cellulose microfibrils

2.5.1 Accessibility to [^{3}H]cellopentaitol

The buffer used in the experiments was 0.1 M sodium acetate buffer, pH 4.7. All the aqueous solutions used contained 0.5% chlorobutanol to prevent microbial growth. The [^{3}H]cellopentaitol stock had been prepared previously by Prof. Stephen C. Fry by reducing cellopentaose (Sigma) using NaB^3H_4. For sampling the tubes were centrifuged at 3000 g (when volume was 3 ml) or 15000 g (when volume was 0.5 ml). The samples of supernatant were taken at intervals and mixed with 900 µl of RO water and 10 ml of Perkin Elmer Optiphase HiSafe 3 aqueous-miscible scintillation liquid. The frequencies of scintillations were measured with Beckman LS500 scintillation counter twice for each vial for 2 min/measurement. After sampling the tubes were mixed by vortexing and returned on the wheel (when volume was 3 ml) or shaker (when volume was 0.5 ml).

The specific activities of the [^{3}H]cellopentaitol stocks used were 567 and 8 MBq/µmol.

The measured radioactivities of the supernatant samples from all of the four adsorption and desorption experiments were calculated related to the initial reaction volumes and how much of the radioactivity had bound to the cellulose or AIR pellets assuming that [^{3}H]cellopentaitol can only bind to cellulose and no radioactivity is lost for instance by binding to the tubes or as volatile break down products.

The desorption experiments were done for the cellulose pellets that had been incubated with [^{3}H]cellopentaitol, but no new [^{3}H]cellopentaitol was added to the solution. The reaction volume, mixing and sampling was kept the same as during adsorption step.

At the end the free solution was discarded and 3 ml of 1 M NaOH was added. The samples were boiled for 1 h, and the supernatants were neutralised with 3 ml of 2 M acetic acid, centrifuged 3200 g for 5 min at 20°C and the supernatant was assayed for radioactivity as before. Also the pellet were washed with 1% acetic acid, (6ml of wash, 3 washes), and mixed with 20 ml of the OptiPhase Hisafe 3 scintillation liquid and assayed for radioactivity.

For some experiment cellobiose or cellopentaose were used as competitor for the [^{3}H]cellopentaitol binding.

2.5.2 Accessibility to surrounding molecules of different sizes

All the aqueous solutions used contained 0.5% chlorobutanol to prevent microbial growth. The [^{3}H]cellohexaitol stock had been prepared previously by Prof. Stephen C. Fry by reducing cellohexaose (Sigma) using NaB^3H_4. [^{3}H]Glucose was commercial stock (manufacturer not known) and [^{3}H]XXLGol was prepared by Prof. Stephen C. Fry. The [^{3}H]sugars were mixed in 96% ethanol and added on cellulose. The vials were capped, shaken vigorously and incubated on a bench overnight after which the vials were opened and dried in fume hood over two night. To produce thixotropic scintillation liquid, hydrogenated castor oil was mixed with Meridian Goldstar scintillation liquid at 20°C for one month to dissolve the hydrogenated castor oil pellets in the scintillant completely. The frequencies of scintillations were measured with Beckman LS500 scintillation counter twice for each vial for 2 min for each measurement.

2.6 Studying the negatively charged groups of the samples

2.6.1 Testing of $CoCl_2$ binding to carboxymethyl cellulose

For finding a method for detecting negatively charged groups in the cellulose samples, 100 mg of Whatman No 1 paper and carboxymethyl cellulose CMC32 and CMC22 (Whatman) were washed with 10 ml of 1.2 M pyridinium acetate buffer, pH 6.5, overnight. Next the pellets were spun down, supernatants were removed and 10 ml of 10 mM pyridine 5 mM acetic acid buffer, pH 5, was added

to the tubes. The tubes were kept on wheel for at least 2 h after which the tubes were centrifuged and the washings were repeated two more times. After the last wash, the pellets were pipeted dry and 10 ml of 0, 10 or 50 mM $CoCl_2$ in the 10 mM pyridine 5 mM acetic acid buffer was added to the tubes. The samples were incubated on the mixing wheel overnight after which the pellets were washed again with the 10 mM pyridine 5 mM acetic acid buffer. The pellets were spun down, pipetted dry and cations were desorbed by adding 3 ml of 0.1 M HCl.

2.6.2 Testing the binding of the other cationic colourful substances to carboxymethyl cellulose

Cobalt chloride, aniline blue, methyl violet, basic fuchsin, polychoromic methylene blue, malachite green, Janus green B, safranine, methyl green and toluidine blue O were prepared in 10 mM pyridine 5 mM acetic acid buffer, pH 5, containing 0.5% chlorobutanol. The stains were diluted to 1 mM concentrations. About 100 mg of Whatman No 1 paper and carboxymethyl cellulose CMC32 and CMC22 (Whatman) were weighed in 15 ml Sarstedt tubes and the celluloses were washed with 10 ml of 1.2 M pyridinium acetate buffer, pH 6.5, overnight. Similar to the previous testing of $CoCl_2$ binding, the pellets were washed three times with 10 ml of 10 mM pyridine 5 mM acetic acid buffer, pH 5, but this time for at least 6 h/wash. The pellets were incubated with 5 ml of the stains overnight on the wheel after which the excess stain was washed off with the 10 mM pyridine 5 mM acetic acid buffer by repeating the washing step fifteen times. The intensities of the colours of the pellets were compared to each other visually.

2.6.3 Detecting negatively charged groups by binding of toluidine blue O

20 mg of cellulose or AIR was washed in 1.2 M pyridinium acetate buffer, pH 6.5 followed by washes 10 mM pyridinium acetate buffer, pH 5.3 similar to 'Testing of CoCl2 binding to carboxymethyl cellulose'. Then the pellets were incubated in 5 ml of 6.4 mM TB (prepared in the pH 5.3, buffer) for 16 h, followed by five washes in the pH 5.3 buffer. The TB was eluted with 5 ml of 50% formic acid and the solutions were diluted with water to be within the range 0 – 20 µM. The A_{631} was measured with standards. The experiment was performed at 20°C.

2.7 Analysis of the data

The calculations for the numerical analyses of the results were done in Microsoft Excel. To get numerical values from repeated TFA hydrolyses for Excel analysis, the intensities of the bands on the TLCs were measured using Image J programme. The figures were drawn using Microsoft Excel and Sigmaplot programmes.

For figures where error bars are shown, the error was calculated as the standard error of the mean (SEM), which was calculated by dividing the standard deviation by the square root of the sample size. Unless otherwise stated in the figure legends, the sample size consists of technical repeats.

2.8 Summary of the methods used

There is a flow chart summaring the studies done and methods used in chapter 6 Appendix.

3 Results

3.1 Composition of samples

3.1.1 Polysaccharide content

While the commercial cellulose samples should be relatively pure cellulose (as the materials have undergone several processing steps during the manufacturing), the AIRs and Curran are not. The AIRs contain all the polymers of the cell and cell wall, including polysaccharides, proteins, lignin and RNA. To study the polysaccharide content of all the samples, I digested the starch of the samples first with α-amylase, followed by removal of non-covalently bound cell wall proteins by phenol extraction (for covalently bound cell wall protein content, see chapter 3.1.2), followed by hydrolysis of cell wall polysaccharides other than cellulose, and finally hydrolysis of the remaining material (which should be mainly cellulose).

3.1.1.2 Starch content

As the AIRs were produced from fresh plant material, they contained starch. Starch works as energy store for the plant (Alberts *et al*., 1988). During the day time plants often produce starch and store it as starch grains inside the chloroplast stroma when excess energy is available for photosynthesis, and the starch is broken down and used up for growth and energy when the photosynthesis rate is slower, such as on cloudy days and during the night time. Plants often also store starch in special organs, such as tubers (for example potatoes) and seeds, and the starch gives a 'kick-start' to the growth of the next generation and is used for growing the first shoots and roots. The samples were first digested with thermo-stable α-amylase (Fig. 6, Fig. 7). The analysis of starch content was not done for the cauliflower AIRs because the cauliflower materials were ground in and washed with water several times (before washing with ethanol), and the water washing could have removed some of the starch.

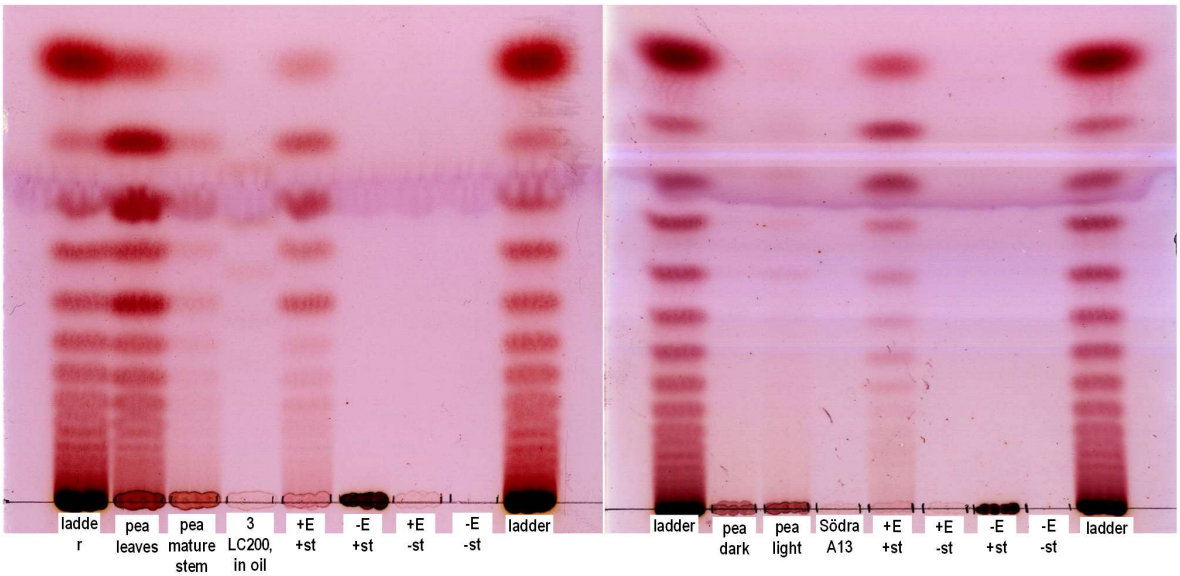

Figure 6. Amylase digestion of pea AIR and, Södra A13 and LC200 celluloses

The samples (50 mg of Södra A13 and LC200 after the oil was washed off with acetone and dried, or AIR from pea tissues that originally weighed (FW) 3-4 g (AIRs had not been dried but washed in water)) were boiled in 4.5 ml (in the case of LC200) or 45 ml (in the case of the pea AIRs) of 40 mM lutidine-acetate buffer, pH 6.7 for 15 min. After cooling, 0.1 volumes of pre-dialysed α-amylase (67 U/ml) was added and the samples were incubated at 60°C for 72 h. The samples were mixed a few times a day during the incubation. After digesting, the samples were spun down at 3200 g for 15 minutes at 20°C, and 5 μl of supernatant was loaded on a TLC alongside 2.5 μl of 1% malto-oligosaccharide ladder (prepared by Dr Sanhueza from maltodextrin), developed in BAW (2:1:1) for two ascents, and stained with thymol. For a control, 5 mg of starch with and without the enzyme were treated similarly to the LC200 sample: +E +St = enzyme and starch; +E – st = only enzyme; -E + st = only starch; -E –st = only buffer.

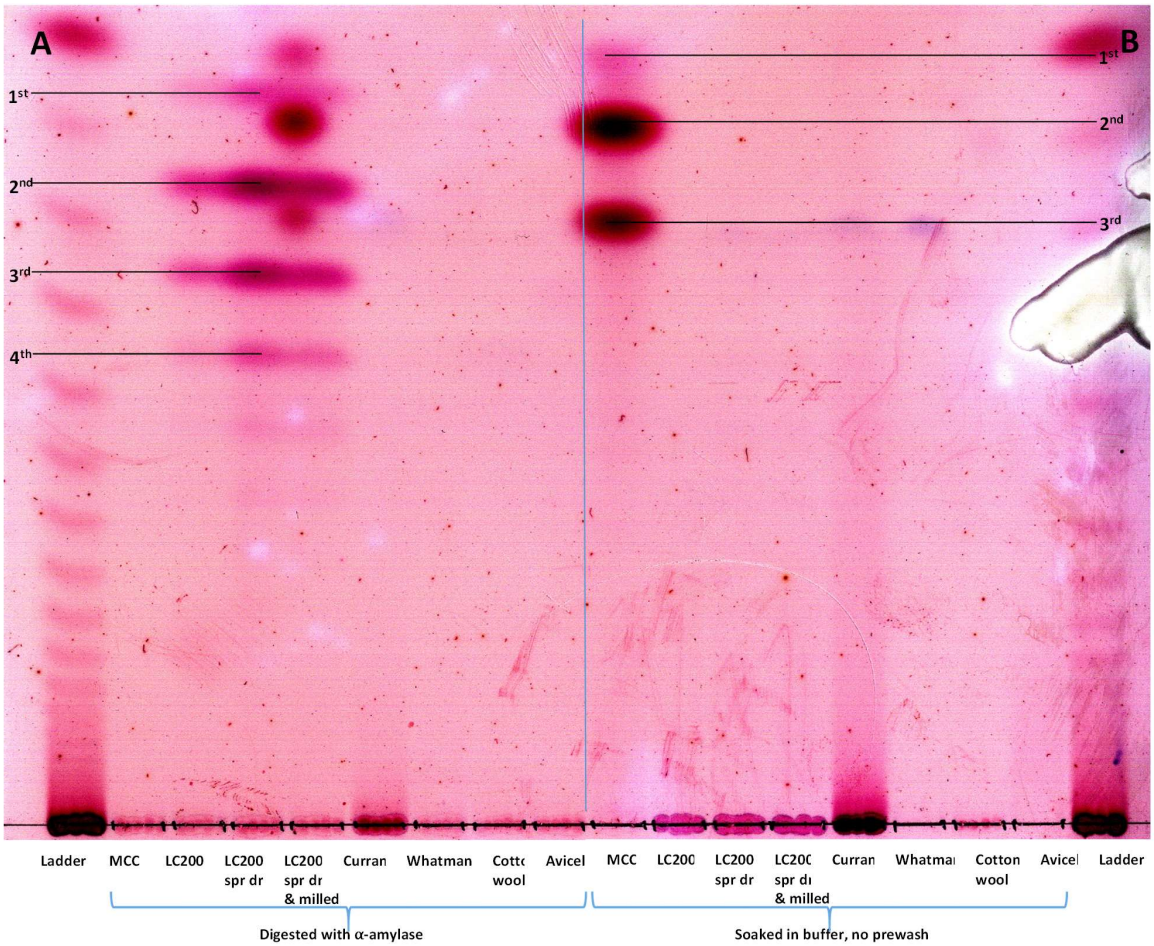

Figure 7. Amylase digestion of commercial cellulose samples.

The samples in (A) were washed in ethanol and water (similar to pea AIR). All the samples were boiled and digested similarly to the LC200 in oil in Fig. 1. For control, a second set of samples (B) were treated exactly the same as the digests (except no pre-washing) but in stead of enzyme, the lutidine buffer, pH 6.7 was added to the tubes after the boiling and cooling. The loading of samples and processing and scanning of the TLC was done as in Fig. 1.

As expected, the pea AIRs contained starch which can be seen as a pattern similar to the malto-oligosaccharide ladder (Fig. 6). There were some digestion products in the LC200 samples as well (Fig. 6 and left side of Fig. 6) but they migrated differently from the ladder, and it is possible that these digestion products are from something else than starch. Soaking the samples in buffer (Fig. 7A) did not result in the same band pattern in LC200 samples but there were some water-soluble saccharides that did not migrate from the loading origin. Also, soaking in buffer dissolved some small saccharides from the MCC sample (Fig. 7B), and the reason these bands were not visible on the left side of the TLC was that the commercial celluloses had been initially washed (similar to the AIRs) in ethanol and water before digestion with α-amylase. The Curran sample contained some water-

soluble polysaccharide other than starch because it stayed in the loading origin (Fig. 7), and it could be pectin because hemicellulose and cellulose would not dissolve in water. There were a few unexplained spots between the bands of the LC200 spray dried and milled sample but the spots are not as wide as the bands derived from the loading origin and are not present anywhere else on the plate, and it is probable that they are contaminations on the plate.

There could be also some other enzyme activity in the commercial heat-stable α-amylase. To test this theory, salivary α-amylase, which should be free from other enzymes, was used for digesting the samples (Fig. 8).

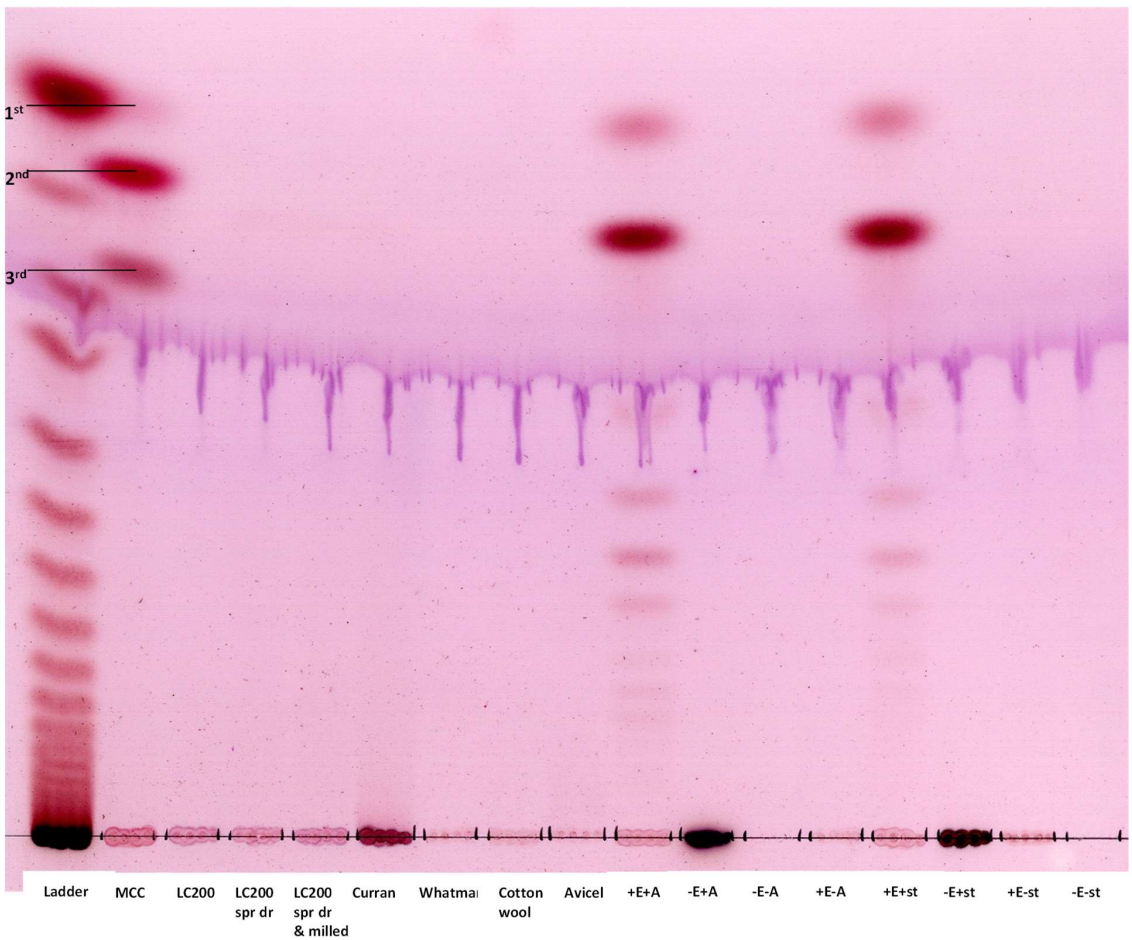

Figure 8. Salivary α-amylase digests of the commercial cellulose samples, amylopectin and starch.

The experiment was as in Fig. 6 except that salivary α-amylase was used instead and the incubation was at 37°C (instead of 60°C). The salivary enzyme was prepared by collecting saliva in a test tube and centrifuging it

at 3200 g for 15 min, and the supernatant was used as the enzyme (E). For control, starch (st) and amylopectin (A) were digested as in Fig. 6. The samples were not prewashed before digestion.

The salivary α-amylase did not digest anything in the LC200 samples, which confirms the suspicion that the commercial α-amylase could have other enzyme activities too. The unknown enzyme activity cannot be cellulase because in that case all the samples would have had digestion products in Fig. 2A. It is not likely that the bands in the LC200 samples in Fig. 2A would have been derived from pectin because the cellulose manufacturing process should break down all pectin. However, it is possible that the digestion products would be from hemicelluloses, and as cellulose is covered and tethered by hemicelluloses *in muro*, the LC200 cellulose could still contain traces of hemicelluloses. I therefore tried digesting the commercial celluloses with β-xylanase (§ 3.1.1.3; Fig. 9).

The bands in the MCC sample in Fig. 8 are similar to the ones in Fig. 2B, which is understandable because neither was washed before digestion. As the bands were migrating similar to mono- and/or disaccharides, I decided to compare their migration pattern to some authentic mono- and disaccharide markers (§ 3.1.1.4 Fig. 11 and 12).

3.1.1.3 Xylan content of the commercial celluloses

To see if the unidentified bands in Fig. 6A were derived from xylan, I digested the commercial celluloses with β-xylanase (Fig. 9).

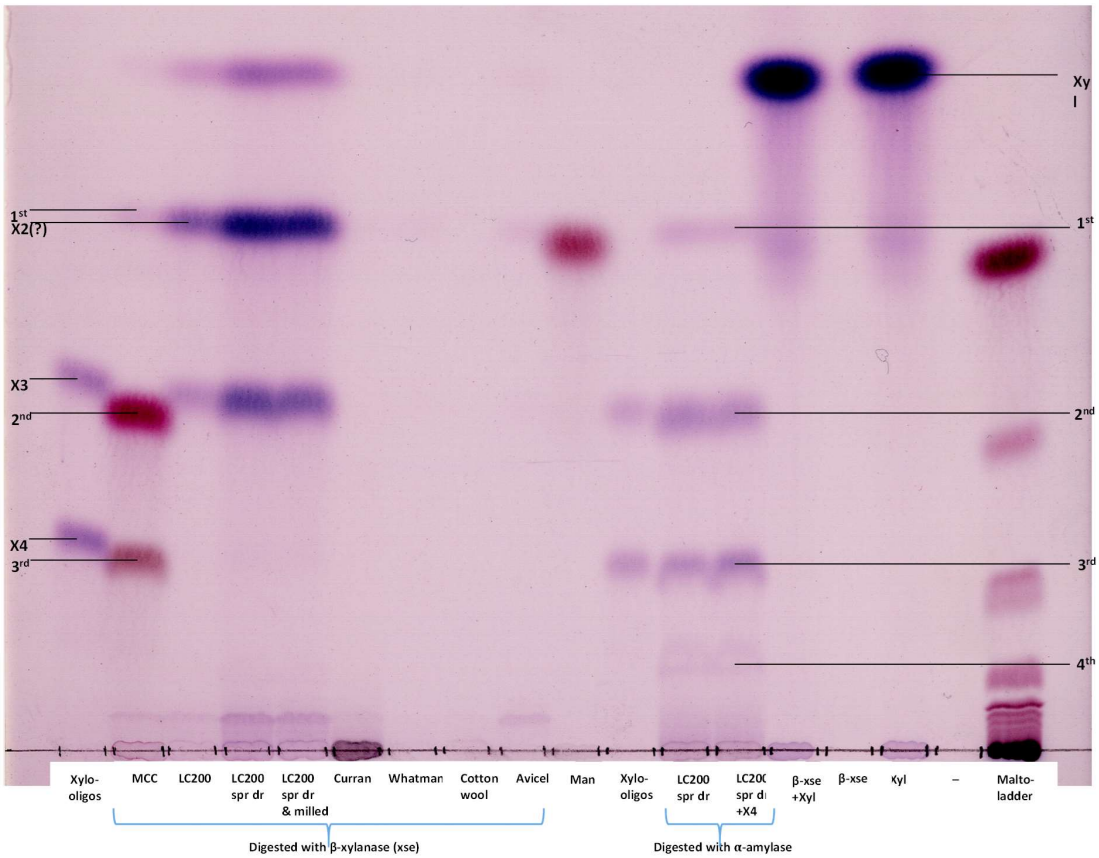

Figure 9. The β-xylanase digests of the commercial celluloses.

The commercial celluloses (50 mg each) were digested with 15 U of Megazyme M6 β-xylanase (from 'rumen micro-organism') in 5 ml of lutidine-acetate buffer, pH 6.7, for 16 h at 20°C, and 6 μl of each digest was loaded on the TLC. As markers, malto-oligo saccharide ladder ('Malto-ladder'), xylose ('Xyl'), mannose ('Man'), β-xylanase enzyme ('β-xse'), xylo-oligosaccharides ('Xylo-oligos') and some commercial α-amylase digests from Fig. 2 were loaded on the TLC. The xylo-oligosaccharides show the migration pattern of xylotriose and xylotetraose (which were purified by column chromatography by Dr L. Franková). The TLC was developed and treated as in Fig. 1 except that the solvent used was EPAW (6:3:1:1).

The β-xylanase digests of the LC200 samples migrated on the TLC similar to xylose, xylobiose and xylotriose, and the digests of the commercial α-amylase-pretreated LC200s migrated similar to xylobiose, xylotriose and xylotetraose (Fig. 9). Based on the exact migration pattern of the β-xylanase and α-amylase digests, it is probable that the commercial thermo-stable α-amylase stock contains also some xylanase activity too, and that the LC200 samples contain xylan.

The unidentified bands in MCC in Fig. 9 are presumably the same compounds as seen in Fig. 7B and 8, but they have migrated different distances in Fig. 9 because the solvent system chosen for Fig. 4

was different. From Fig. 4 one can see that unidentified saccharides of MCC migrated differently from glucose, xylose, mannose, maltose, maltotriose, xylotriose and xylotetraose, and also the colours of these bands did not match – and therefore these saccharides can be excluded from the list of candidate compounds (for identification of the compounds, see chapter 3.1.1.4 Identification of the mono- and disaccharides found in MCC).

Although the evidence of the unidentified bands being xylo-oligosaccharides in Fig. 9 is convincing, I wanted to prove further that was indeed the case. Therefore, I separated and extracted the compounds from a preparative TLC, hydrolysed them in TFA and analysed the migration patterns of the hydrolysates on TLCs using different solvent systems: BAW (4:1:1), EPAW (6:3:1:1) and PNW (5:2:3) (Fig. 10).

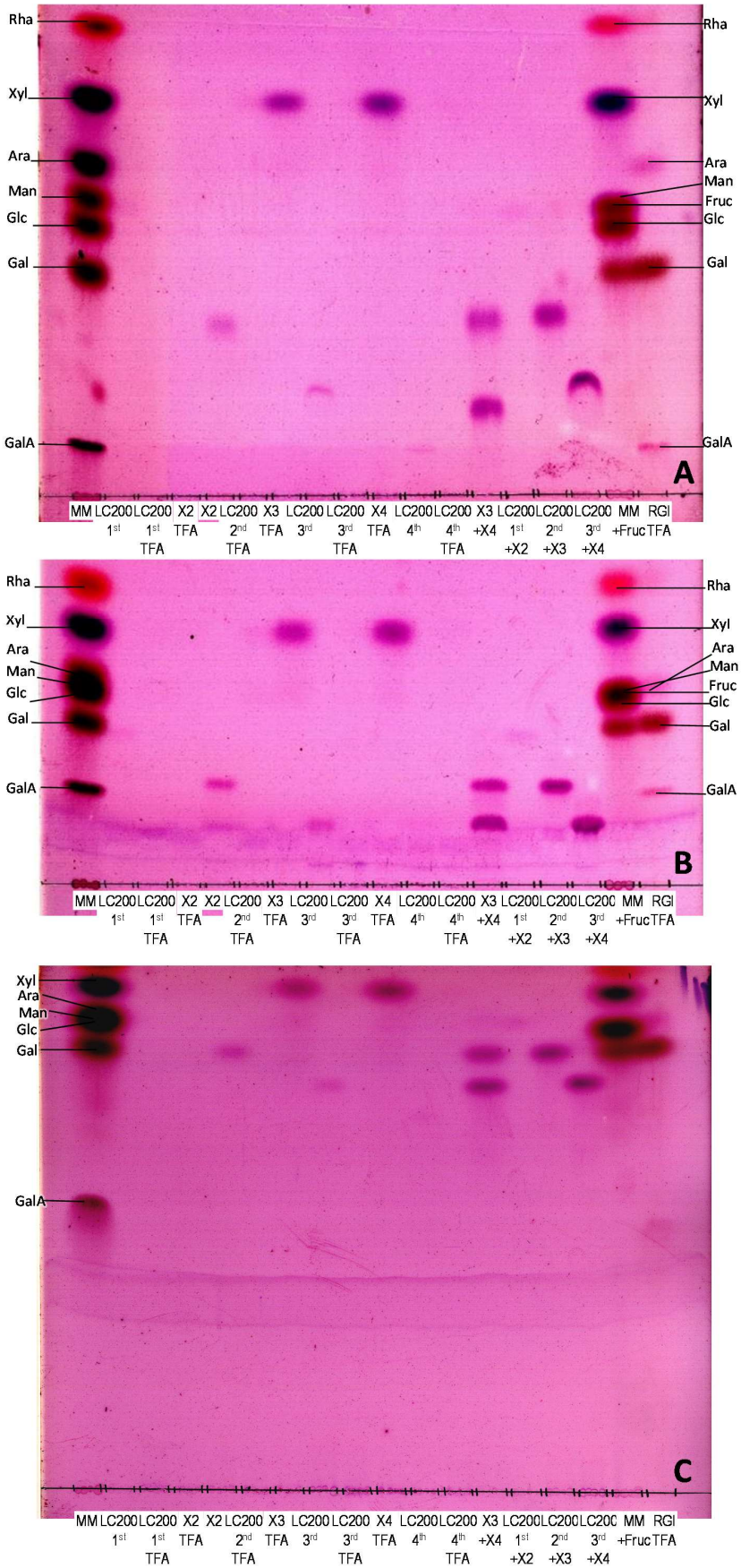
Rha
Xyl
Ara
Man
Glc
Gal
GalA
Rha
Xyl
Ara
Man
Fruc
Glc
Gal
GalA
A
MM LC200 LC200 X2 X2 LC200 X3 LC200 LC200 X4 LC200 LC200 X3 LC200 LC200 LC200 MM RGI
1st 1st TFA 2nd TFA 3rd 3rd TFA 4th 4th TFA +X4 1st +X2 2nd +X3 3rd +X4 +Fruc TFA
Rha
Xyl
Ara
Man
Glc
Gal
GalA
Rha
Xyl
Ara
Man
Fruc
Glc
Gal
GalA
B
MM LC200 LC200 X2 X2 LC200 X3 LC200 LC200 X4 LC200 LC200 X3 LC200 LC200 LC200 MM RGI
1st 1st TFA 2nd TFA 3rd 3rd TFA 4th 4th TFA +X4 1st +X2 2nd +X3 3rd +X4 +Fruc TFA
Xyl
Ara
Man
Glc
Gal
GalA
C
MM LC200 LC200 X2 X2 LC200 X3 LC200 LC200 X4 LC200 LC200 X3 LC200 LC200 LC200 MM RGI
1st 1st TFA 2nd TFA 3rd 3rd TFA 4th 4th TFA +X4 1st +X2 2nd +X3 3rd +X4 +Fruc TFA

Figure 10. TFA hydrolysates of the unidentified bands from LC200 digests.

The unidentified bands ('1st', '2nd', '3rd' and '4th') in the LC200 samples equivalent to those in Fig. 7 and 9 were isolated from a preparative TLC, hydrolysed in 2 M TFA at 120°C for 1 h, dried in a SpeedVac, redissolved in water and loaded on a TLC ('TFA' in the figure). For control, the xylo-oligosaccharide markers (X2–X4, as in Fig. 4) were included with and without the unhydrolysed samples. The marker mix ('MM') contained Rha, Xyl, Rib, Ara, Man, Gal, Glc, GalA, ± Fru (2 µg each). The TLCs were developed and treated as in Fig. 1 and 4, in EPAW (6:3:1:1) for (A), BAW (4:1:1) for (B) and PNW (5:2:3) for (C). The sugars migrated faster than expected in PNW, and Rha could not be stained but the stained part of the TLC is shown in (C).

Fig. 10 showed that the TFA hydrolysis of the unidentified compounds produced only xylose, which tells us that the compounds are solely composed of xylose. The two fastest migrating compounds ('LC200 1st' and 'LC200 2nd') are not visible on the TLCs in Fig. 10, which indicates that extraction of them (which are probably xylobiose and xylotriose) from the preparative TLC had failed. Also, the hydrolysed 2nd and unhydrolysed 3rd and 4th compounds can be seen on the TLCs, slightly more easily in Fig. 10A than 10B (but the xylose from hydrolysed 3rd and 4th compounds did not produce a spot concentrated enough to be seen). Mixing the 3rd compound with the xylotetraose marker ('LC200 3rd +x4') made the band migrate unevenly in Fig. 10A (when mixed with xylotriose the marker migrated normally in 'X3 +X4'), which indicates that there were some impurities in the extract of the unidentified compound, possibly salt. The 'RGI TFA' control sample shows monosaccharide composition of one type of pectin, but as shown in Fig. 9 and 10, the composition of the unidentified digestion products of the LC200 samples seen in Fig. 7 is solely xylose, and therefore it can be concluded that the LC200 celluloses contain xylan. The presence of a hemicellulose in the LC200 samples is further confirmed below by TFA hydrolysis in § 3.1.1.5 Hemicellulose content.

3.1.1.4 Identification of the mono- and disaccharides found in MCC

The migration of the unidentified saccharides of MCC seen if Fig. 7, 8 and 9 were compared on a TLC to several authentic sugars (rhamnose, xylose, arabinose, mannose, glucose, galactose, galacturonic acid, cellobiose, maltose, maltotriose, maltotetraose, sucrose, gentiobiose, melibiose, sophorose, laminaritetraose, trehalose and lactose), and glucose, sucrose and lactose had migration patterns close to the unidentified compounds (Fig. 11) . To see if they really matched the unidentified compounds, samples of the supernatant of the MCC (in lutidine buffer) were loaded on TLC alone and mixed in with sucrose, lactose and glucose markers (Fig. 12).

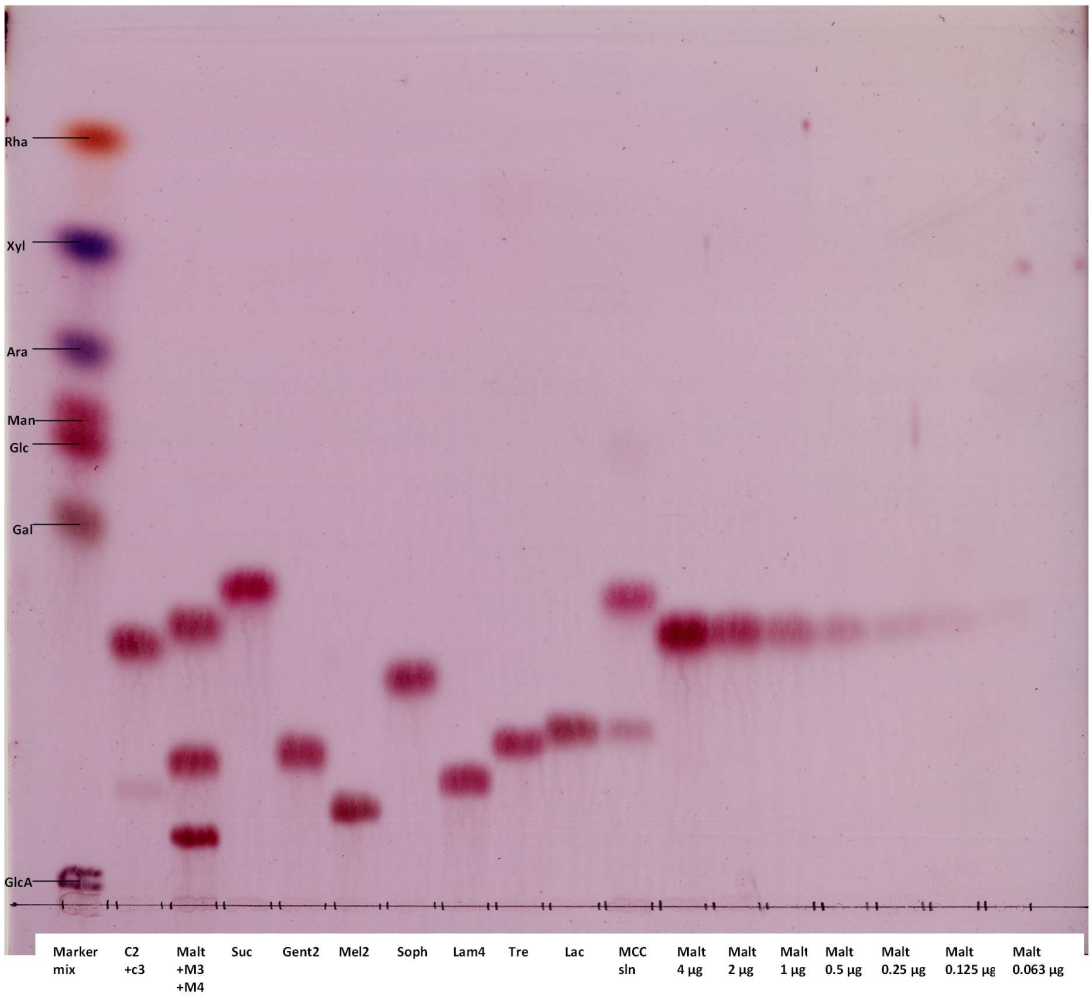

Figure 11. Unidentified compounds from microcrystalline cellulose and authentic sugar markers.

The supernatant of the MCC sample that had been soaked in lutidine-acetate buffer, pH 6.7 (as Fig. 7B), was loaded with cellobiose (C2), cellotriose (C3), maltose (Malt), maltotriose (M3), maltotetraose (M4), sucrose (Suc), gentiobiose (Gent2), melibiose (Mel2), sophorose (Soph), laminaritetraose (Lam4), trehalose (Tre) and lactose (Lac) (2 µg each) and the marker mix was also included as in Fig. 10. The TLC solvent was EPAW (as in Fig. 9).

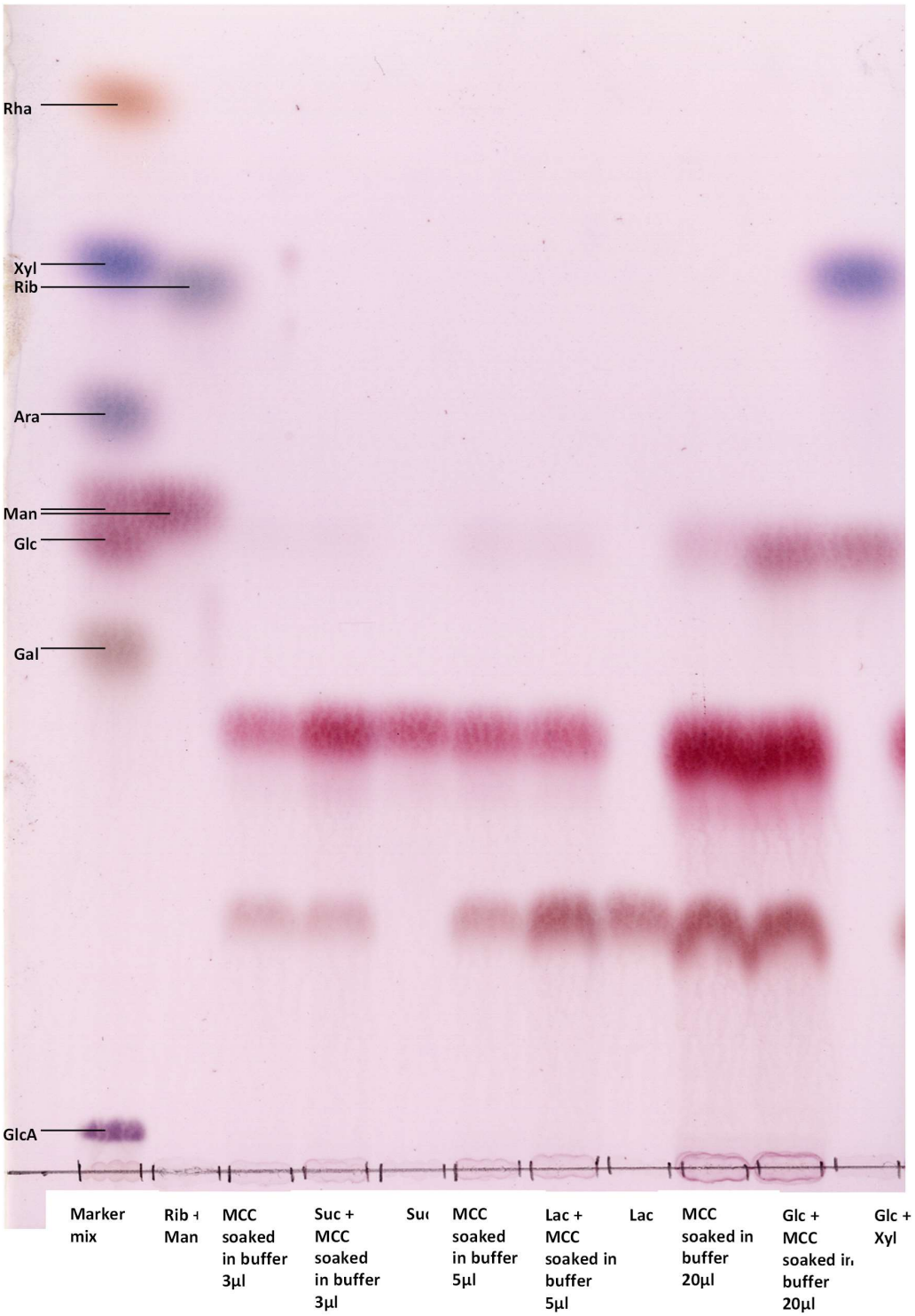

Figure 12. Contaminants of microcrystalline cellulose sample.

The supernatant of the MCC sample that had been soaked in lutidine-acetate buffer, pH 6.7 (as Fig. 7B and 11), was loaded in 3, 5 and 20 µl volumes alone and mixed in with sucrose (Suc), lactose (Lac) or glucose (Glc) (2 µg each) and the marker mix was also included as in Fig. 10. The TLC solvent was EPAW (as in Fig. 9).

The unknown compounds migrated exactly like sucrose, lactose and glucose (same distances migrated and same colours), and when MCC supernatant was mixed with the control sugars, the bands were clearly more intensively stained (Fig. 12. However, it is possible that some other sugars would migrate similarly to lactose, glucose and sucrose, and I therefore hydrolysed the sugars with enzymes and TFA and compared them to hydrolysates of the marker sugars (Fig. 13).

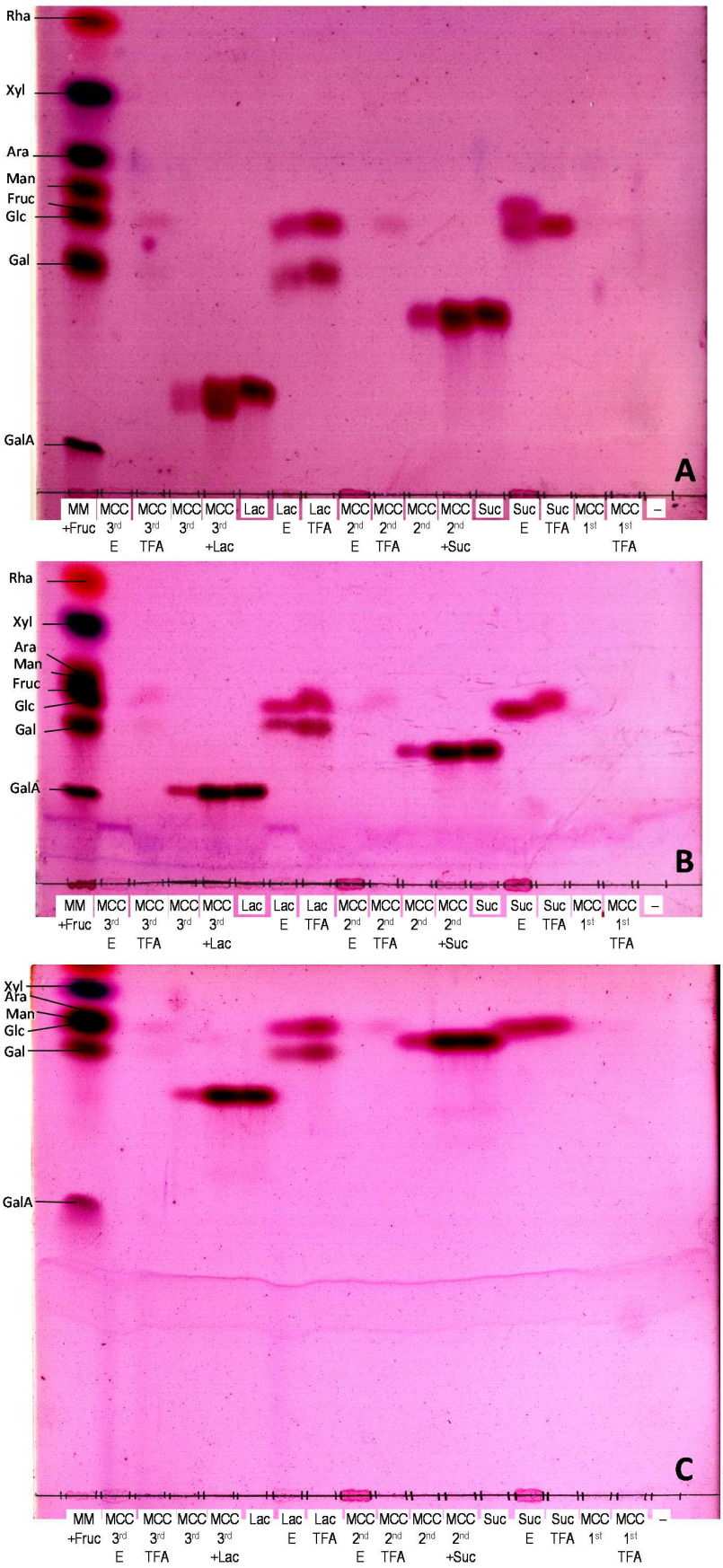
Rha
Xyl
Ara
Man
Fruc
Glc
Gal
GalA
A
MM +Fruc
MCC 3rd E
MCC 3rd TFA
MCC 3rd +Lac
Lac
Lac E
Lac TFA
MCC 2nd E
MCC 2nd TFA
MCC 2nd +Suc
Suc
Suc E
Suc TFA
MCC 1st TFA
–
Rha
Xyl
Ara
Man
Fruc
Glc
Gal
GalA
B
Xyl
Ara
Man
Glc
Gal
GalA
C

Figure 13. Hydrolysates of the unidentified compounds found in MCC.

The supernatant of MCC soaked in lutidine buffer, pH 6.7 (from Fig. 7B), fractionated as in Fig. 10. The unidentified compounds were digested ('E') in 1 ml with 4 U of invertase (from Fluka, extracted from *S. cerevisiae*) or β-galactosidase (from Megazyme), or hydrolysed in TFA as in Fig. 10. The compounds and their products were loaded with and without lactose ('+Lac') or sucrose ('+Suc') (2 µg each) and the marker mix was also included as in Fig. 10. (A) was developed with EPAW (6:3:1:1), (B) with BAW (4:1:1) and PNW (5:2:3) for (C).

The TFA hydrolysis products of the 3rd and 2nd compound ('MCC 3rd TFA' and 'MCC 2nd TFA') migrated on TLC similarly to the hydrolysates and digests of the control sugars lactose and sucrose ('Lac E', 'Lac TFA', 'Suc E' and 'Suc TFA'), forming galactose and glucose, and fructose and glucose respectively, which can be seen both in Fig. 13A and 13B. However, the enzyme digests of the unknown compounds cannot be seen on the TLCs. When the compounds are mixed with the marker sugars ('MCC 3rd +Lac' and 'MCC 2nd +Suc') in Fig. 13 (especially 13A), they form single bands that are more intense than the compounds or the control sugars alone ('MCC 3rd', 'Lac', 'MCC 2nd' and 'Suc'). The 1st compound ('MCC 1st') migrated together with glucose on both of the TLCs in Fig. 13.

To conclude from Fig. 7, 8, 9, 11, 12 and 13, the MCC sample had been contaminated with lactose, sucrose and glucose. After presenting the findings to Mars Wrigley Inc., I was informed that the MCC sample was milled further at their chocolate factory facilities and that they used the same industrial mill that is routinely used for milling milk powder (which is rich in lactose) and sucrose. In fact, the mills are usually not cleaned between milling of different ingredients in the chocolate factories, and that is one reason why all chocolate products are usually labelled with a warning 'may contain traces of nuts and milk' (even if they would not be included in the list of ingredients of the product). After this, the MCC was washed with water before using in any other experiment analysing the content of the samples.

3.1.1.5 Hemicellulose content

As seen in § 3.1.1.3 Xylan content of the commercial celluloses, the LC200 cellulose samples contained some xylan (which was accessible to β-xylanase). However, it is possible that the commercial celluloses could contain some other types of hemicelluloses too which could be studied for instance by digesting the material with different enzymes. While digesting with various enzymes could reveal which specific hemicelluloses are present in the samples (and this would be especially

interesting data to have for the AIRs), it would be time consuming. To get a general idea of the hemicellulose content of the samples, I hydrolysed the commercial celluloses and the AIRs in TFA, which should completely hydrolyse all hemicelluloses and leave the cellulose mostly intact (Fanta, *et al*., 1984; Fry, 1988) (Fig. 14).

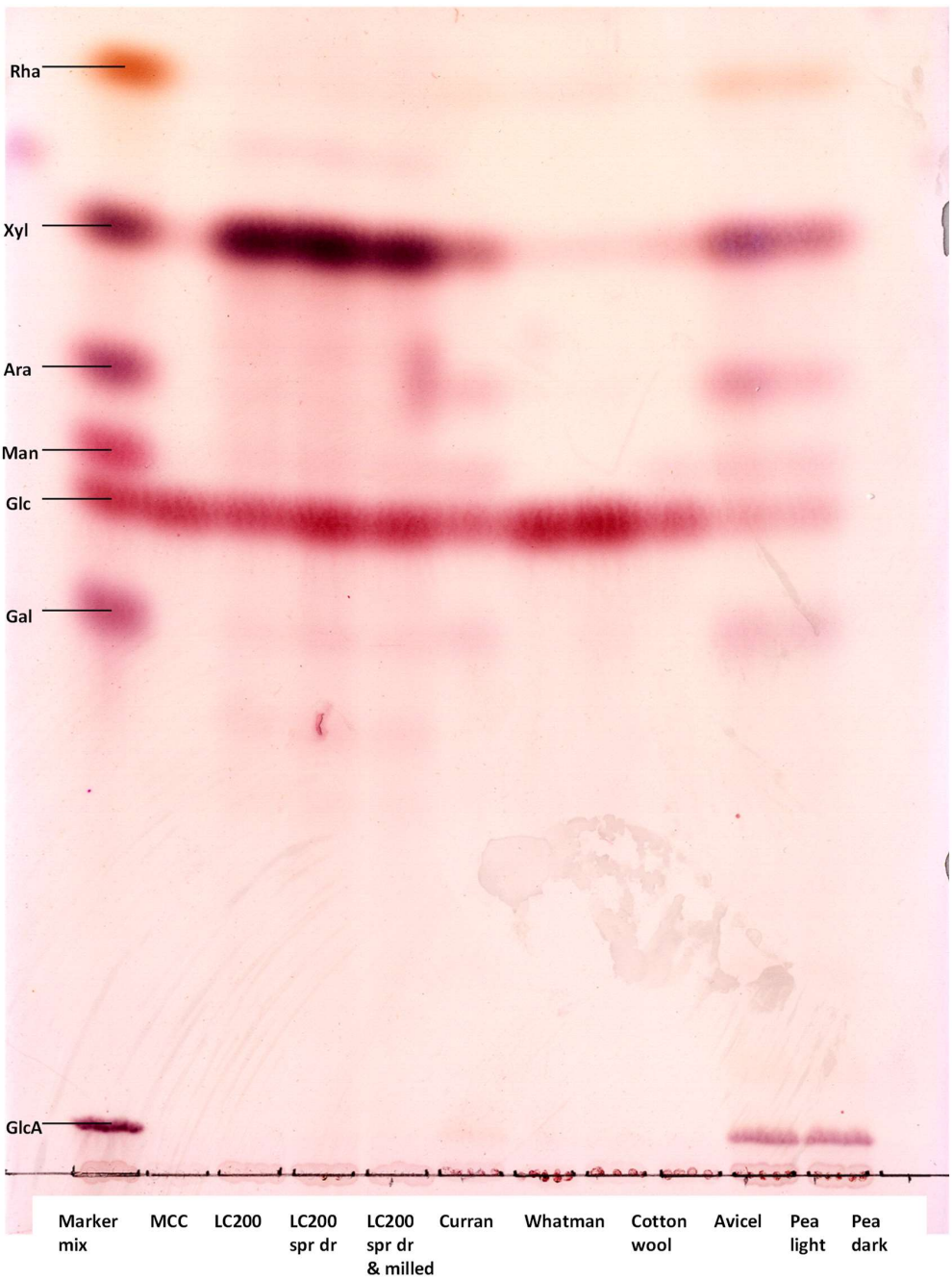

Figure 14. TFA hydrolysates of the commercial celluloses and young pea stem AIRs.

The commercial celluloses (50 mg each) and pea young stem AIRs (grown in light ('pea light') and dark ('pea dark'), fresh weight of both 2.7 g), that had gone through the removal starch with the commercial thermo-stable α-amylase digestion (see Fig. 6 and 7) and removal of non-covalently bound proteins by extraction in phenol:acetic acid:water (2:1:1) (see § 3.1.2 Covalently bound protein content), were rinsed with water (3 times with 14 ml of water containing 0.5% chlorobutanol, each washing was done on mixing wheel for 16 h). After rinsing, 1/28 of sample (equivalent to 1.8 mg) was used for the TFA hydrolysis. The samples were adjusted to 2 M TFA and hydrolysed as in Fig. 9, after which the cooled samples were centrifuged at 14 500 g for 10 min at 20°C. The supernatants were transferred to new tubes, and the pellets were rinsed twice with 0.5 ml of water (the centrifugation was repeated after each washing step), and the supernatant from each wash was added to the same tubes as the TFA. The pellets were rinsed with acetone, dried in a SpeedVac and Saeman hydrolysed (Saeman, 1945) (Fig. 13). The supernatants were also dried in SpeedVac and redissolved in 100 µl of water containing 0.5% chlorobutanol, and 3 µl of each hydrolysate (equivalent to 54 µg dry weight of polysaccharide) was analysed by TLC as in Fig. 9.

The hydrolysates of the LC200 celluloses gave mostly glucose and xylose. TFA can hydrolyse a fraction of the cellulose (Fanta *et al.,* 1984) although it should leave it mostly intact, and most of the glucose seen on the TLC in Fig. 14 could be explained by hydrolysis of cellulose, whereas some glucose could be derived from other polysaccharides. The heaviest xylose bands were in the LC200 hydrolysates, although Curran and the pea AIRs contained it too, and it is possible that in addition to xylan (see § 3.1.1.3 Xylan content of the commercial celluloses) these samples contained also xyloglucan which is also a hemicellulose. TFA hydrolysis products of xyloglucan would be glucose, xylose, galactose (and possibly fucose) (Fry, 1989), and bands of galactose can be seen in the hydrolysates of the LC200 celluloses, Curran® and pea AIRs. All the samples except for MCC, Whatman No 1 filter paper, cotton wool and Avicel PH102 hydrolysates yielded mannose, which could be derived from mannan which is also a hemicellulose that can have galactose branches (Moreira and Filho, 2008). As seen in Fig. 10, hydrolysis products of the pectic domain RG-I were rhamnose, arabinose, galactose and galacturonic acid, which can also in the hydrolysates of pea AIRs and Curran in Fig. 14, indicating that these materials contain also pectin.

To summarise, MCC, Whatman No 1 filter paper and cotton wool were 'purest' cellulose whereas the LC200s and Avicel PH102 contained traces of hemicelluloses. Curran contained traces of both hemicellulose and pectin, and the young pea stem AIRs were rich in these polysaccharides.

3.1.1.5.1 Hemicellulose could be trapped in the between of cellulose microfibril aggregates

To see if one treatment with TFA was enough to remove all the hemicellulose from the samples and to estimate what proportion of the glucose in the hydrolysate was derived from cellulose (and how much from other polysaccharides), I repeatedly hydrolysed the samples in TFA and analysed the sequential supernatants (Fig. 15).

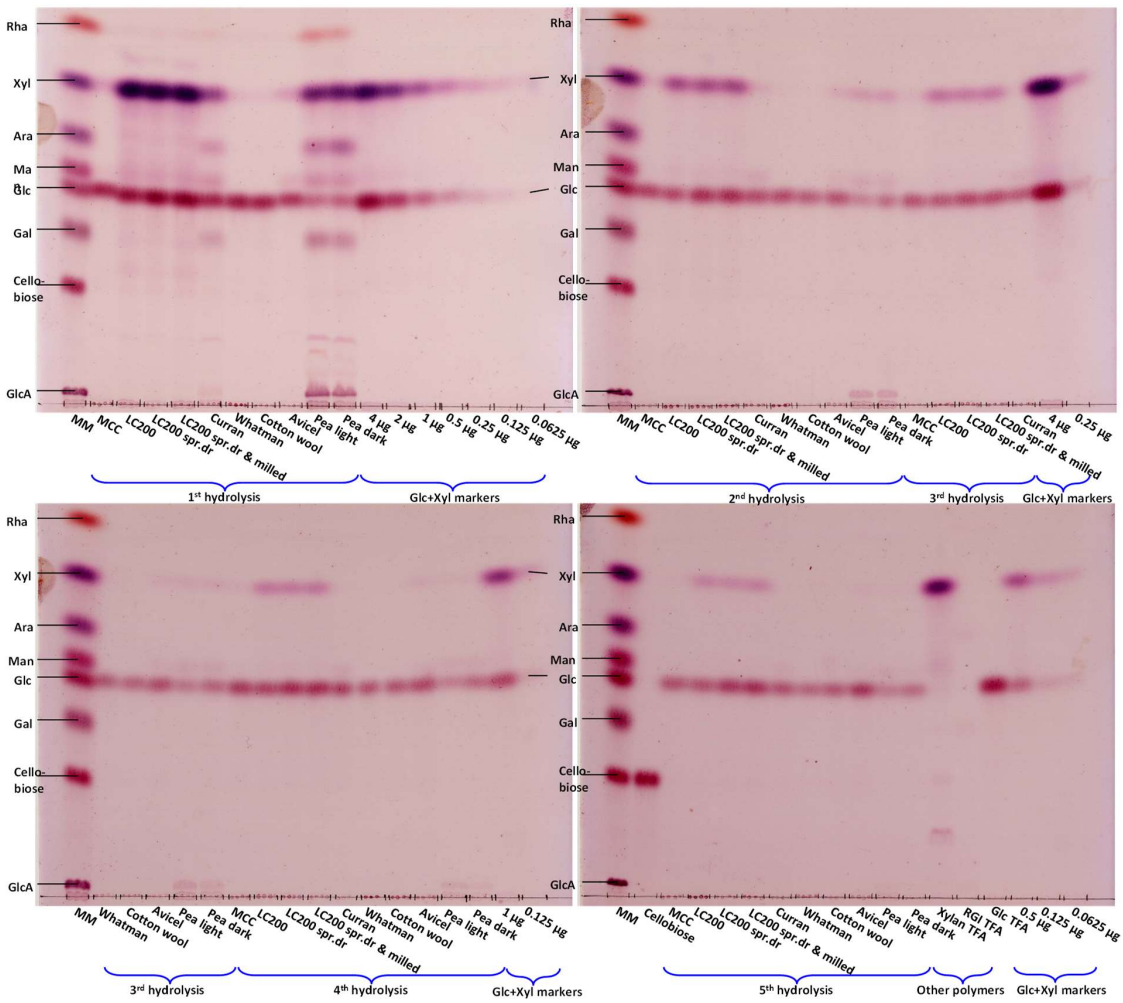

Figure 15. Repeated TFA hydrolyses of the commercial cellulose samples and the pea young stem AIRs.

From the α-amylase-treated commercial cellulose (from Fig. 7) and pea young stem AIRs (from Fig. 6), aliquots were dried in a SpeedVac and 8–10 mg of each cellulose or 3–4 mg of the pea AIR sample was hydrolysed in 1 ml of 2 M TFA as in Fig. 4. After hydrolysis, the cooled samples were centrifuged and rinsed with water as in Fig. 14 but the pellets were not rinsed with acetone nor dried. The volumes of water with the pellets were adjusted to 0.5 ml to which 0.5 ml of 4 M TFA was added (resulting in 2 M) and the samples were hydrolysed again, after which the centrifugation, washing and hydrolysis were repeated until the hydrolysis had been done five times. Also xylan, RG-I and glucose (10 mg of each) were similarly treated in TFA. All the supernatants were dried, redissolved and loaded on TLCs with marker sugars as in Fig. 14. Also, different loadings of the glucose and xylose were included. The TLC was developed and treated as in Fig. 9.

Figure 15 showed that repeating TFA hydrolysis released xylose from the LC200 samples, Curran, Avicel PH102 and the young pea stem AIRs every time, even in the fifth repeat. The xylose could derive from xylan or xyloglucan that was resistant to the TFA hydrolysis, and this idea is discussed further at the end of this chapter. The LC200 samples had the highest concentration of xylose-yielding polymer(s).

The LC200 in oil, Södra A13, pea leaf AIR, pea mature stem AIR and a new batch of young pea stem AIRs were later analysed similarly to the other samples earlier in this chapter: digestion of starch with α-amylase (for Södra A13 and pea leaf and mature stem AIRs Fig. 6 (for the new batch of pea young stem AIRs data not shown because it was identical to Fig. 6), for LC200 in oil Fig. 16) and extraction off of non-covalently cell wall bound protein by phenol:acetic acid:water, and I also hydrolysed the samples in TFA (Fig. 16 and 17) and with the Saeman method (Fig. 16, 17 and 18).

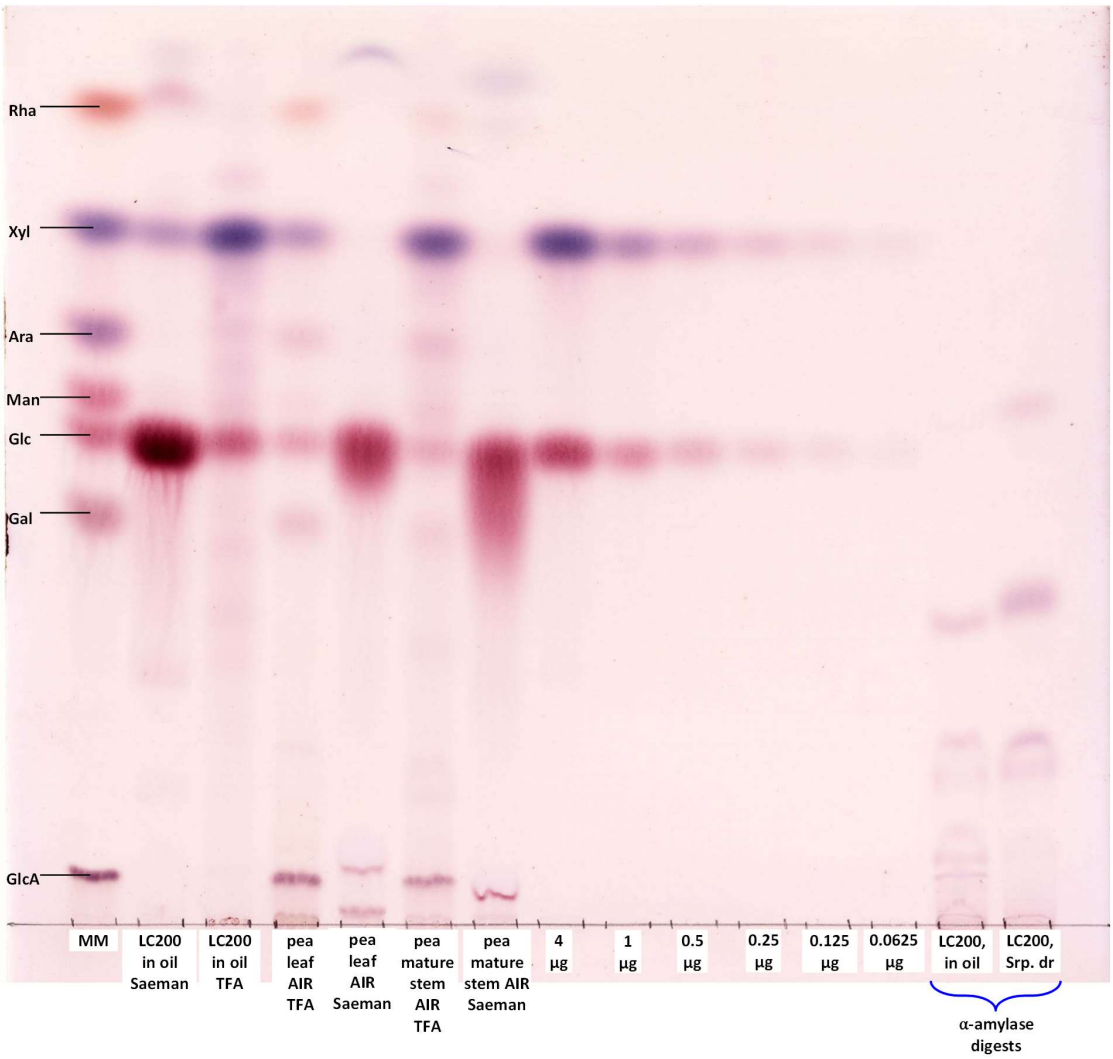

Figure 16. α-Amylase, TFA and Saeman hydrolysates of LC200 in oil, pea leaf AIR and pea mature stem AIR.

The α-amylase digestion and the TFA hydrolysis were done as in Fig. 6 and 10. Saeman hydrolysis was done on ~3.3 mg of the TFA residue. The equivalent of 50, 54 and 54 µg of polysaccharide (for amylase, TFA and Saeman products respectively) was analysed by TLC as before.

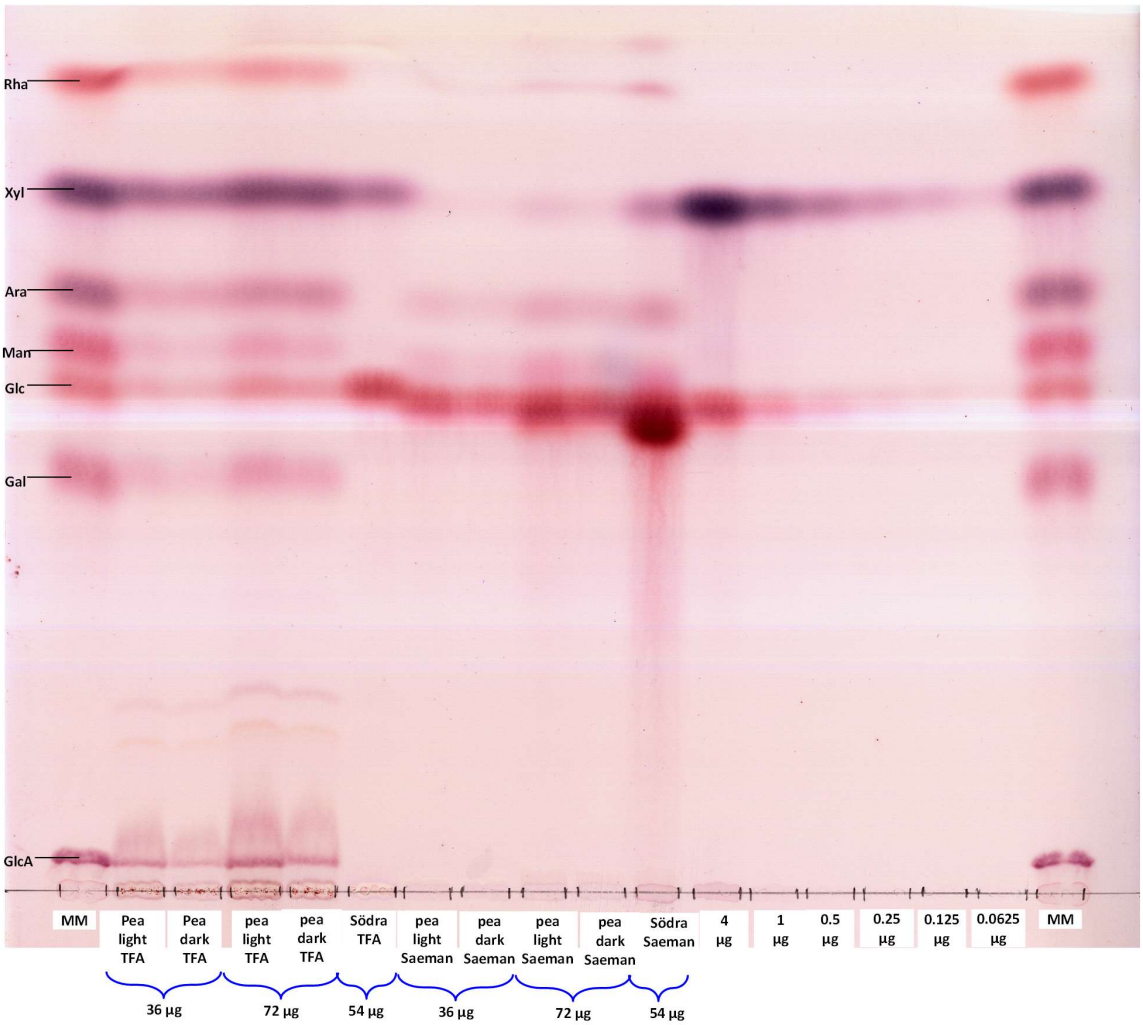

Figure 17. The TFA hydrolysates and Saeman hydrolysates of Södra A13 and the young pea stem AIRs.

The TFA hydrolysis were done as in Fig. 10 and the Saeman hydrolysis as in Fig. 16 but the equivalent of 54 (Södra A13), 36 or 72 µg of (pea AIRs) polysaccharide was analysed by TLC. Other details as before.

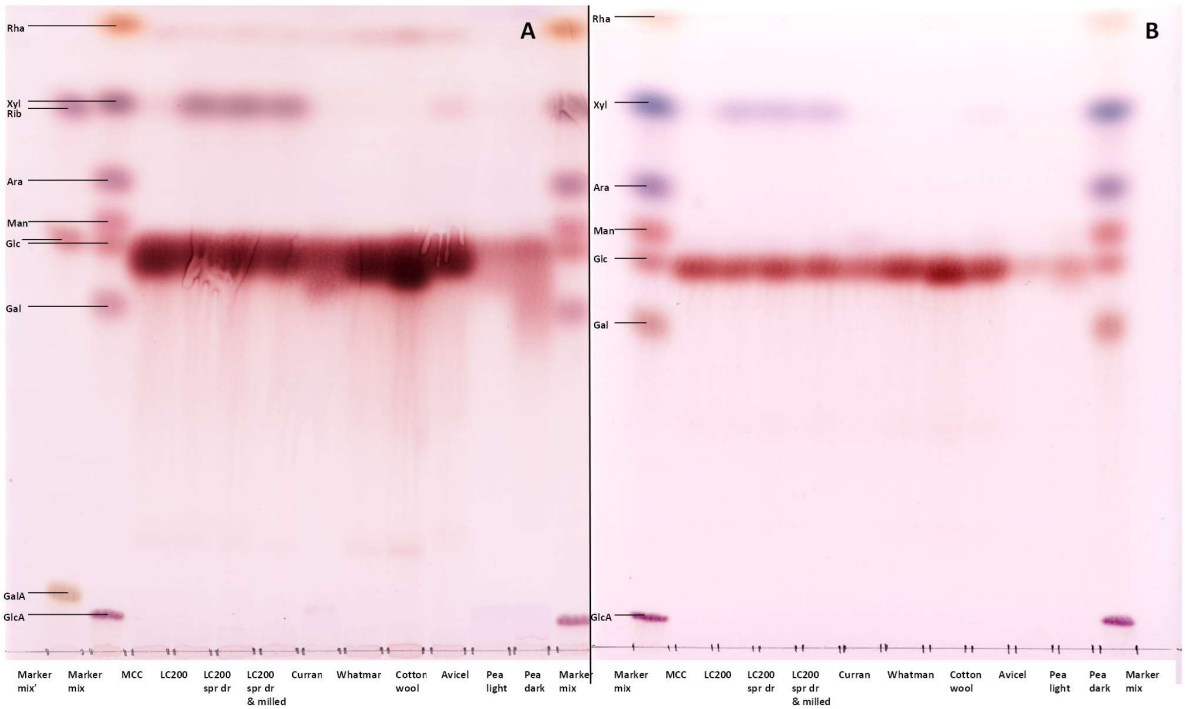

Figure 18. Saeman hydrolysates of the commercial celluloses and the young pea stem AIRs.

The Saeman hydrolysis was done and the TLC (A) loaded as in Fig. 16. For (B), the hydrolysates were diluted with water and the loadings were 20% of (A). The marker mix contained 2 μg of each sugar. TLC solvent: EPAW, 2 ascents

The α-amylase digest of LC200 processed in oil (Fig. 16) showed that also this LC200 contained xylan that was digestible by xylanase, and that the digestion products migrated on the TLC similar to the products seen in the other LC200 samples in Fig. 12. As the starting material of all the LC200 samples was the same ('LC200'), this result was not unexpected. Also the TFA hydrolysates of the LC200 in oil showed a streaked pattern similar to that of the other LC200 samples (Fig. 19), with the most concentrated band being xylose and the second most concentrated glucose (Fig. 21). Despite the smear, it is clear that the TFA hydrolysate of the LC200 in oil contained also at least arabinose, mannose and galactose (Fig. 21).

Similarly to the TFA hydrolysates of the young pea stem AIRs in Fig. 14, the new batch of the pea young stem AIRs (Fig. 17), contained rhamnose, xylose, arabinose, mannose, glucose, galactose and glucuronic acid (and possibly other unidentified saccharides), indicating that the AIRs were rich in both pectin and hemicelluloses. The pea leaf AIR and the pea mature stem AIR (Fig. 16) also contained all the same sugars as the young stem AIRs (Fig. 17) but interestingly the mature stem AIR

had a much heavier band of xylose than the leaf AIR (Fig. 16). The higher xylose content could be because the mature stem tissue has deposited thick secondary cell walls whereas the cell walls of the leaves are primary; secondary cell walls have less pectin (and more hemicellulose and lignin) than primary walls.

TFA hydrolysis of the Södra A13 cellulose showed only xylose and glucose (Fig. 17), and, similarly to the LC200 celluloses and Avicel PH102 (Fig. 14), it is clearly not pure cellulose but contains traces of hemicellulose (probably xylan).

Saeman hydrolysis, applied to the TFA pellets, showed very heavy glucose bands for all the commercial celluloses (Fig. 18A except for Fig. 16 for LC200 in oil and Fig. 17 for Södra A13). The loading of the commercial celluloses' Saeman hydrolysates in Fig. 16, 17 and 18A was proportionally the same as for the TFA hydrolysates (each loading being the products of ~50 µg of polysaccharide), indicating that the samples mainly consisted of cellulose-derived glucose. Of the commercial celluloses, LC200 (Fig. 16 and 18) and Avicel PH102 (Fig. 18) contained xylose (the LC200 especially much), even though the TFA was expected to have hydrolysed the hemicelluloses.

Even when the TFA hydrolysis was repeated five times for the same pellets, there were traces of xylose in the hydrolysates of the LC200 samples and Avicel PH102 (Fig. 15). An explanation for the TFA resistant hemicelluloses could be Cosgrove's (2014) cellulose aggregate theory: normally, hemicelluloses tether the microfibrils, but, in absence of the hemicellulose 'coating', neighbouring cellulose microfibrils may aggregate forming bigger fibre clusters (see Fig. 1 in § 1.1.1 Introduction – Composition of cell walls). On the interface of the normally hemicellulose-coated microfibrils and the non-coated (or not sufficiently coated) microfibril aggregates, some hemicelluloses could get trapped in the between of the aggregating microfibrils, and the regions of the cellulose microfibrils around the trapped hemicelluloses could physically hinder the TFA from accessing the hemicelluloses. Other publications from Cosgrove group have also reported evidence – from both computer simulations and experiments of 'wet chemistry' – supporting theory of xyloglucan being intertwined within cellulose microfibrils, and a single molecule of xyloglucan could also work as an adhesive, and hence be trapped, in the between of two cellulose microfibrils (Park and Cosgrove, 2012, Zhao *et al*., 2014). Furthermore, unpublished findings of our laboratory (Martina Pičmanová & S. C. Fry, Edinburgh Cell Wall Group) support the idea of cellulose (from *Equisetum* and *Arabidopsis*

as well as cotton wool, Whatman paper and Avicel) containing unremovable xylose, suggesting covalent incorporation of xylose/xylan/xyloglucan into cellulose chains.

However, as the TFA can hydrolyse some of the cellulose, repeating the TFA hydrolysis to the same pellets could degrade the cellulose enough to expose some of the previously trapped hemicellulose and hydrolyse it (explaining why there was xylose in the repeated hydrolysates in Fig. 15). To test if result of the xylose present in the repeated TFA hydrolysates was reproducible, I repeated the quintuplicate TFA hydrolysis for LC200 and MCC (data not shown), and the result was the same – the LC200 samples (but not MCC) contained xylose in all five hydrolysates, and the Saeman hydrolysates performed on the remaining pellets contained xylose as well.

Also, the Södra A13 Saeman hydrolysate contained xylose but also mannose and arabinose, which is interesting as mannose and arabinose were not present in the TFA hydrolysate (and TFA should have hydrolysed at least a proportion of the hemicelluloses that contained these sugars) (Fig. 17).

Overloading a TLC can make it difficult to detect any other similarly migrating compounds. From the TLC which had a lighter loading (Fig. 18B) it can be seen that Curran gave mannose, indicating that mannan could be trapped on or in the cellulose microfibrils (similarly to xylan in the LC200 samples, for example) and therefore shielded from TFA hydrolysis.

3.1.2 Phenol insoluble protein content

Plant-based protein preparations intended for human consumption often have problems with off-flavours (Mittermeier-Kleßinger *et al.*, 2021) which can be challenging when used in foods, such as plant-based meat alternatives (Kyriakopoulou *et al.*, 2021). It is possible that the commercial celluloses contain proteins which could introduce off-flavours and affect palatability when mixed into confectionery. We were also interested in seeing how much protein is left in the AIR preparations after the phenol extraction because high protein content could possibly interfere with the results of the other experiments, such as the lignin assay, since some amino acids absorb UV light at 280 nm.

To remove proteins that are not tightly bound to insoluble polysaccharides, I incubated the α-amylase-treated commercial celluloses and pea AIRs with hot phenol:acetic acid:water (2:1:1) and washed the pellets with water extensively. The remaining material (PIR; phenol-insoluble residue) was used for assaying the content of lignin, phenol-insoluble protein and polysaccharides other than cellulose.

To study phenol-insoluble proteins, I hydrolysed the pellets with hot $Ba(OH)_2$ and purified the resulting free amino acids by cation-exchange column, eluting with NH_4OH, and analysed by paper chromatography (Fig. 19 and 20).

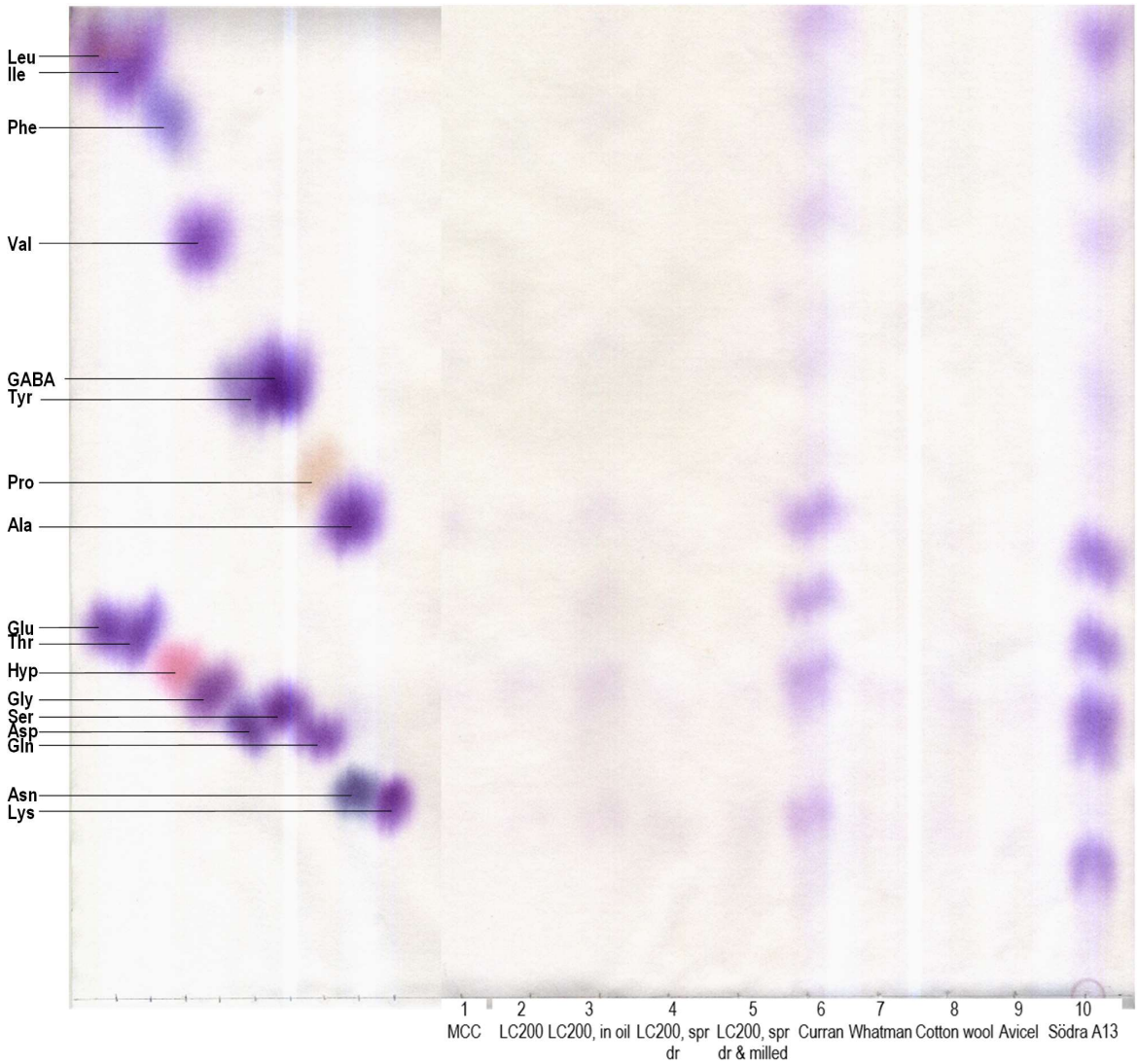

Figure 19. Paper chromatogram of alkali hydrolysates of commercial cellulose samples.

I hydrolysed the α-amylase- and phenol-pretreated samples in 200 mM $Ba(OH)_2$ at 105°C for 17 h. After cooling, I adjusted the pH of supernatants to 2.5 with H_2SO_4 using thymol blue as an indicator, and passed the hydrolysates through ~2-ml columns packed with cation exchange resin Dowex W50X2 (H^+ form) prewashed with 1 M H_2SO_4 with followed by 1 mM formic acid. Non-bound material was washed out with 10 mM formic acid followed by water and rejected, and then I eluted the amino acids with 1 M ammonia. The eluates were dried in a freeze-drier and redissolved in 200 µl of water containing 0.5% chlorobutanol, and 70 µl of the eluates were loaded on Whatman No 20 chromatography paper. The solvent BAW 12:3:5 descended the chromatogram for 60 h and the dried chromatogram was stained with ninhydrin. The chromatogram was scanned in several parts which were fitted together using PowerPoint. On the left side of the chromatogram are amino acid markers (5 µg each except for Asn, GABA, Gln, Hyp and Pro which were 12.5 µg each).

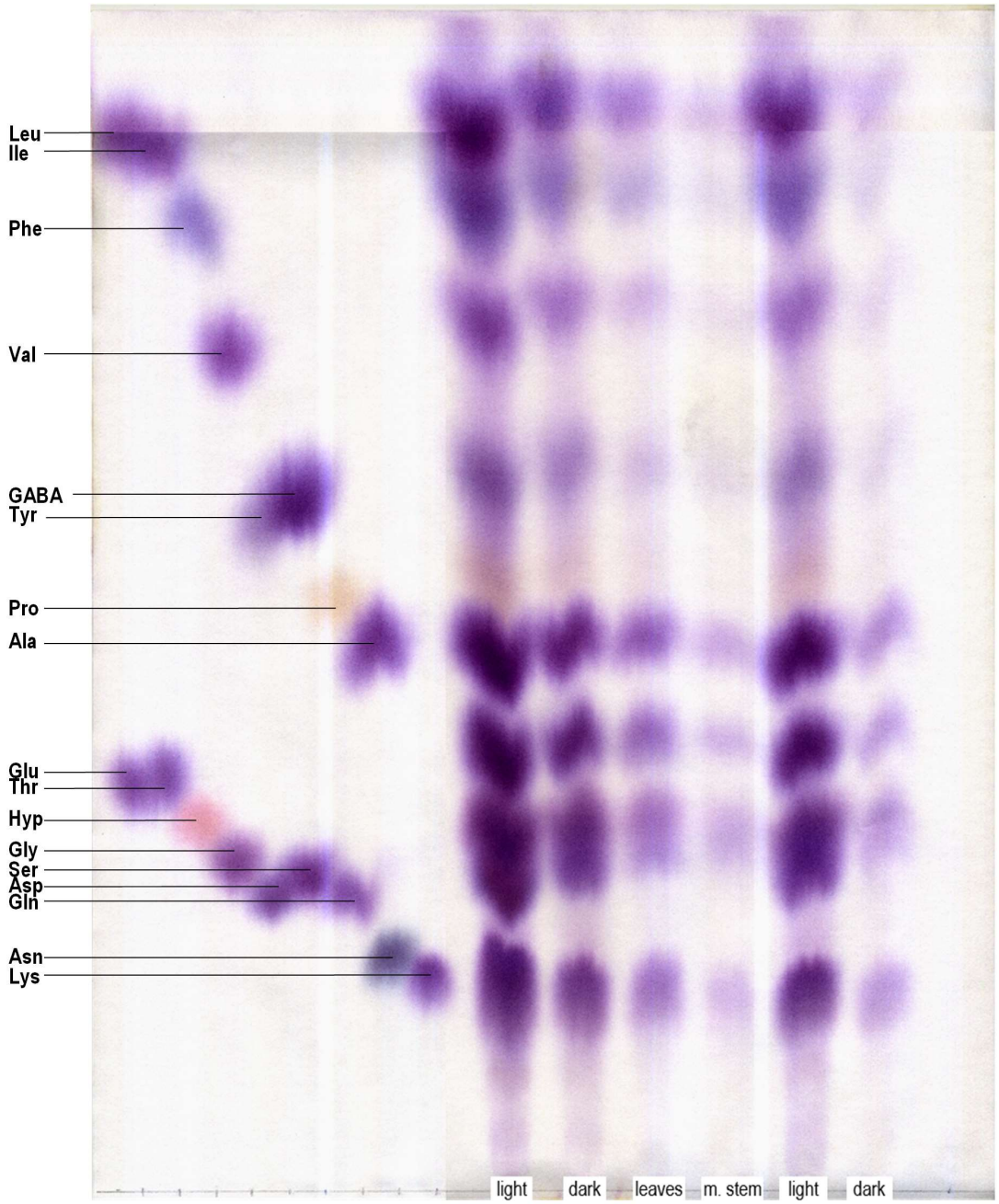

Figure 20. Paper chromatogram of alkali hydrolysates of pea PIR samples.

Description of samples: 'light' stands for young pea stems grown in the light (by the window in the laboratory); 'dark' means young pea stems grown in dark (plant pot covered with foil); 'leaves' are leaves taken from fully grown mature pea plants and 'm. stem' means the 7-cm segment of the mature pea plant primary stem which is just above the soil, excluding leaves and any branches. The 'light' and 'dark' pea PIRs in the middle of the chromatogram (grown in the winter) are from a different batch from the ones on the right side (grown in the spring). Other details as in Fig. 19, except for the loading of the eluates was 20 µl for each PIR sample.

Figure 19 shows that the commercial celluloses were relatively free from phenol-insoluble proteins and that only the Curran© and Södra A13 samples had intense spots on the chromatograms. The LC200 PIR samples had traces of amino acids, most easily detectable with the LC200 processed in oil. All the amino acids released from Curran, Södra A13 and LC200 PIR samples stained to the same shade of purple and no hydroxyproline (Hyp) and proline (Pro) (which would stain pink and yellow respectively) were detectable on the chromatogram. It can be concluded that the unpleasant mouth-feel properties of some of the commercial celluloses probably did not result from the protein content of the samples.

Based on Figure 20, the pea samples were rich in phenol-inextractable proteins, yielding most or all of the amino acids included in the markers – including the imino acids Pro and possibly Hyp, which migrated close to glutamic acid and glycine respectively and could be masked by them as Glu and Gly stained dark purple with ninhydrin. The Gly, Ser, and Asp markers migrated almost the same distances on the chromatogram, and these amino acids in the hydrolysates are not separable on the chromatogram. Acid hydrolysis converts Gln and Asn to Glu and Asp respectively, so there cannot be any Gln or Asn present in the hydrolysates. The intensity of the spots indicates that the firmly bound protein content is highest with young pea stems grown in light (within both the winter and spring grown batches) and second highest in the young stems grown in dark. The pea leaf PIR seemed to be slightly richer in proteins that the PIR from mature pea stems.

The pea PIRs were rich in firmly bound proteins as they (and the commercial celluloses) had gone through only one phenol extraction. It is possible that one phenol treatment was not sufficient to remove all the soluble proteins and that more could have been extracted if the treatment had been repeated. The cell walls contain many proteins, such as extensins which should still have been present in the PIR after the phenol extraction (Briggs & Fry, 1990), but the PIRs could still contain other (non-covalently cell wall bound) proteins which would have been extractable by a second phenol treatment. Extensins are rich in hydroxyproline (which stains yellow-pink with ninhydrin) but the PIRs were also rich in glutamic acid and glycine (which stain dark purple and) which could mask the Hyp spots on the chromatogram (Fig. 20). Qi *et al.* (1995) showed that extensins are rich in serine (Ser), lysine (Lys), valine (Val) and alanine (Ala), although Hyp was the most abundant amino acid in the fragments they had extracted. The Val, Ala and Lys spots are easily distinguishable from other amino acid markers in the Fig. 20 and all the pea PIRs contained these amino acids. Ser ran closely on the chromatogram with glycine (Gly) and aspartic acid (Asp) which makes it more difficult

to differentiate from the other amino acids in the Fig. 20. The presence of the easily detectable Lys, Val and Ala spots in the pea PIRs in Fig. 20 supports the idea that the PIRs contained extensins even though the presence of Hyp and Ser is not certain.

Based on the loading of the marker amino acids on the chromatogram, I can roughly estimate the amino acid concentrations in the hydrolysates in Fig. 20. For instance, Val runs as a clear spot, separate from the other amino acids, and is therefore convenient to choose for the estimation. The loading of the marker was 5 µg. The Val spot of the young pea stem grown in light PIR in the middle of the chromatogram in Fig. 20 is about the same intensity as the marker spot. The loading of the sample was 20 µl and the total volume of the hydrolysate was 200 µl. The PIR sample hydrolysed was initially 11 mg. Therefore the chromatogram loading was derived from 11 × 20 / 200 = 1.1 mg (= 1100 µg) of the PIR. Since this loading showed ~5 µg Val, the Val content of the PIR was ~5 / 1100 = 0.45% of its dry mass.

The Val spot of the young pea stem grown in dark has the intensity about half of the neighbouring young pea stem grown in light spot and therefore the PIR contained ~0.23 % Val. The Val spot of the pea leaves PIR is about half of the young pea stem grown in dark, giving the PIR concentration of 0.11 % Val. Respectively, the intensity of Val spot of pea mature stem PIR is half of the intensity of pea leaves PIR, giving it Val concentration of 0.06 % Val.

Concerning the other amino acids than Val, I estimate that the marker Gly, Ser and Asp (which migrated almost together) would have the same intensity when summed as the respective spot of the young pea stem grown in light PIR hydrolysate in the middle of the chromatogram in Fig. 20. Also, the Pro spots seem to have the same intensities between the young pea stem grown in light PIR hydrolydate and the marker. The GABA/Tyr spot in the PIR from young pea stems grown in light is about half of the intensity of the marker. Hydrolysis converts the Gln and Glu to Asp and Asn, respectively. However, Asn has a very different (dark grey) colour than most of the other spots, and based on the colour it is not present in the hydrolysates. The other spots in the PIR from young pea stems grown in light are roughly twice as intense as the Leu, Ile, Phe, Ala, Glu and Thr marker spots. Lys spot is approximately five times as intense as the marker. Therefore, the estimated concentrations of the amino acids in the pea PIRs would be:

Table 3. Amino acid content (%) of the pea PIR hydrolysates.

Amino acid/PIR	Young pea grown in light PIR	Young pea grown in dark PIR	Pea leaf PIR	Mature pea stem PIR
Leu	0.9	0.45	0.23	0.11
Ile	0.9	0.45	0.23	0.11
Phe	0.9	0.45	0.23	0.11
Val	0.45	0.23	0.11	0.06
GABA	0.45	0.23	0.11	0.06
Tyr	0.23	0.11	0.06	0.03
Pro	1.1	0.56	0.29	0.14
Ala	0.9	0.45	0.23	0.11
Glu	0.9	0.45	0.23	0.11
Thr	0.9	0.45	0.23	0.11
Gly	0.45	0.23	0.11	0.06
Ser	0.45	0.23	0.11	0.06
Lys	2.3	1.1	0.56	0.29
Asp	0.45	0.23	0.11	0.06
Hyp	Masked by other amino acid spots?			
Asn	Not present in hydrolysates			
Gln	Not present in hydrolysates			
Total	11.28	5.62	2.84	1.42

A rough estimate of the protein content of the young pea stem grown in light PIR is the sum of the amino acids (excluding Hyp), 11.3% (Table 3). As with Val, the intensities of the other amino acid spots of young pea stem grown in dark PIR are about half of the intensities of young pea stem grown in light PIR, the intensities of spots with the pea leaves PIR are half of the intensities of the young

pea stem grown in dark PIR and the intensities of spots with the mature pea stems PIR are half of the intensities of the pea leaves PIR. Therefore, it can be estimated that the young pea stem grown in dark PIR contained 5.6 %, pea leaves PIR 2.8% and mature pea stem PIR 1.4% proteins (Table 3).

Fig. 19 has recognisable amino acid spots only in the Curran© and Södra A13 samples – the amino acid spots of the other samples are so faint that the phenol-insoluble protein content cannot be estimated. I would estimate that the intensity of the Val spot in the Södra A13 hydrolysate is 20% of the marker, and that Curran© would be half of the intensity of Södra A13 (hence 10% of Val marker). As the loading of the commercial celluloses were 70 µl (instead of 20 µl), the Val content of Södra A13 PIR is 0.03%, and of Curran© 0.01%. As some of the amino acid spots were very faint in Fig. 19, the same ratios as in Table 3 were followed for the intensities of the spots (related to Val) (Table 4).

Table 4. Amino acid content (%) of the Curran© and Södra A13 PIR hydrolysates.

Amino acid/cellulose	Curran© PIR	Södra A13 PIR
Leu	0.05	0.03
Ile	0.05	0.03
Phe	0.05	0.03
Val	0.03	0.01
GABA	0.03	0.01
Tyr	0.01	0.006
Pro	0.08	0.04
Ala	0.05	0.03
Glu	0.05	0.03
Thr	0.05	0.03
Gly	0.03	0.01
Ser	0.03	0.01

Lys	0.1	0.06
Asp	0.03	0.01
Hyp	Not present based on colour (but could be masked by other amino acids, such as Gly)	
Asn	Not present in hydrolysates	
Gln	Not present in hydrolysates	
Total	0.64	0.34

Rough estimates of the protein content of the Curran© and Södra A13 PIRs were 0.6% and 0.3%, respectively (Table 4). The phenol-insoluble protein contents of the other commercial celluloses were too low to estimate from Fig. 19. To get the spots of the commercial celluloses other than Curran© and Södra A13 visible enough to estimate, I would probably need to hydrolyse the protein of at least 1 g of cellulose (instead of 11 mg).

3.1.3 Lignin content

In addition to polysaccharides, plant cell walls contain lignin, which is a complex polymer consisting of hydroxycinnamyl alcohols (Sixta, 2006; Hatfield and Fukushima, 2005; Lange *et al*., 2013). Lignin makes up ~one third of the chemical composition of soft wood (~quarter of hard wood), and removing lignin is a challenging and important step of the wood pulping process (Sixta, 2006). As lignin can be a major component of cell walls and traces of it might be also present in the commercial celluloses used in my work (as many of them might be made from wood pulp), I wanted to compare how much lignin was there in my samples. I studied the lignin content of the cellulose samples and AIR preparations by the acetyl bromide soluble lignin (ABSL) method modified by Hatfield and Fukushima (2004; 2005) from Johnson *et al.* (1961). The principle of the ABSL method is to dissolve the sample in 25% acetyl bromide (in glacial acetic acid) solution, acetylate the lignin when the sample is heated, hydrolyse the excess acetyl bromide with aqueous alkali (producing mainly sodium acetate and NaBr), then destroy any bromine and polybromides with hydroxylamine-HCl and to measure the absorbance of the aromatic moieties of the solubilised acetylated lignin at 280 nm, which could then be converted to lignin content with a known extinction coefficient (17 g^{-1} l cm^{-1}; Hatfield and Fukushima (2004; 2005)). Other widely used methods for assaying lignin are acid detergent, Klason and permanganate methods but acetyl bromide soluble lignin gave Hatfield and Fukushima (2004) results that were about an average of the range of all methods tested.

3.1.3.1 Testing the suitability of ABSL method with the commercial celluloses and the AIR samples

First, I tested the suitability of the method for my samples – the commercial celluloses should be relatively free from lignin after the manufacturing processes and therefore the method chosen would need to be able to detect low concentrations of lignin. The samples were mixed with the acetyl bromide reagent in glass vials capped with Teflon lined caps and heated in 70°C water bath for approximately 30 min, as described by Hatfield and Fukushima (2004; 2005). The calculated lignin contents of the samples are shown in Figure 21.

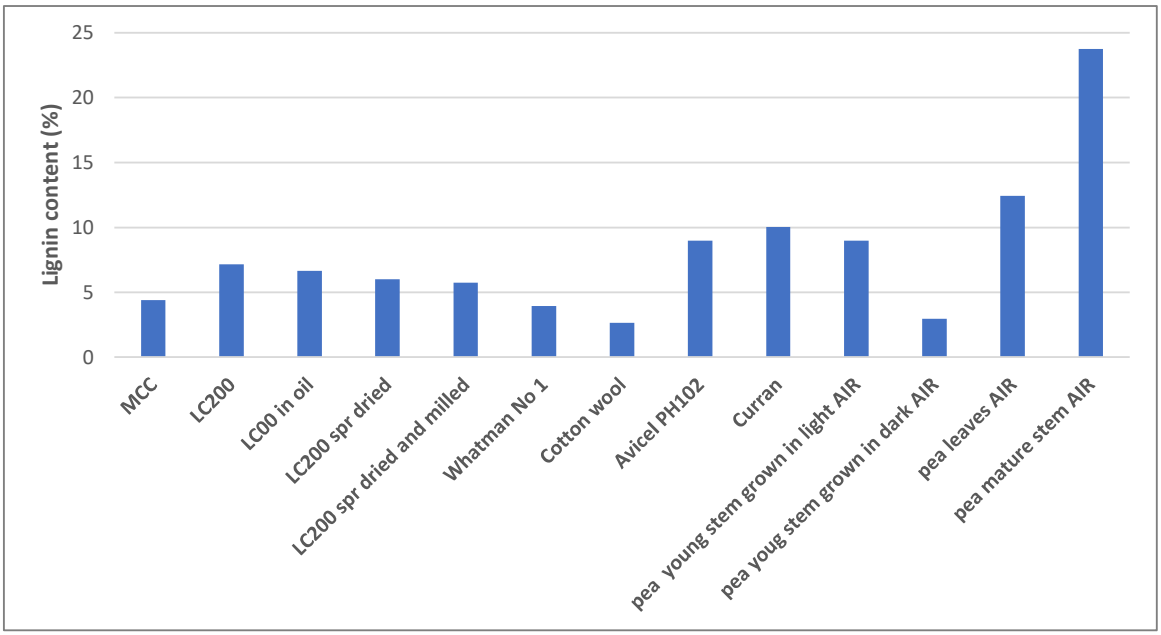

Figure 21. Lignin content of some of the commercial celluloses and AIR preparations.

The lignin content was assayed using the acetyl bromide method (ABSL) (Hatfield and Fukushima, 2004), using 17 g^{-1} l cm^{-1} as the extinction coefficient (average from various plant materials; Hatfield and Fukushima (2004). Samples were in hot acetyl bromide for approximately 30 min. The spectrophotometer was blanked against a no-cellulose control, N = 1.

The data suggest that this method was able to detect some lignin-like material in the commercial cellulose samples and that there were differences between the samples. Also, Curran® and the AIR samples (except for AIR from young pea stems grown in dark) contained more lignin-like compounds than the commercial celluloses (Fig. 21).

Next I tested how the ABSL method would perform with reference samples that are pure lignin or related components (Fig. 22). The 30-min duration for which the samples were in hot acetyl bromide was more precisely controlled than in Fig. 21.

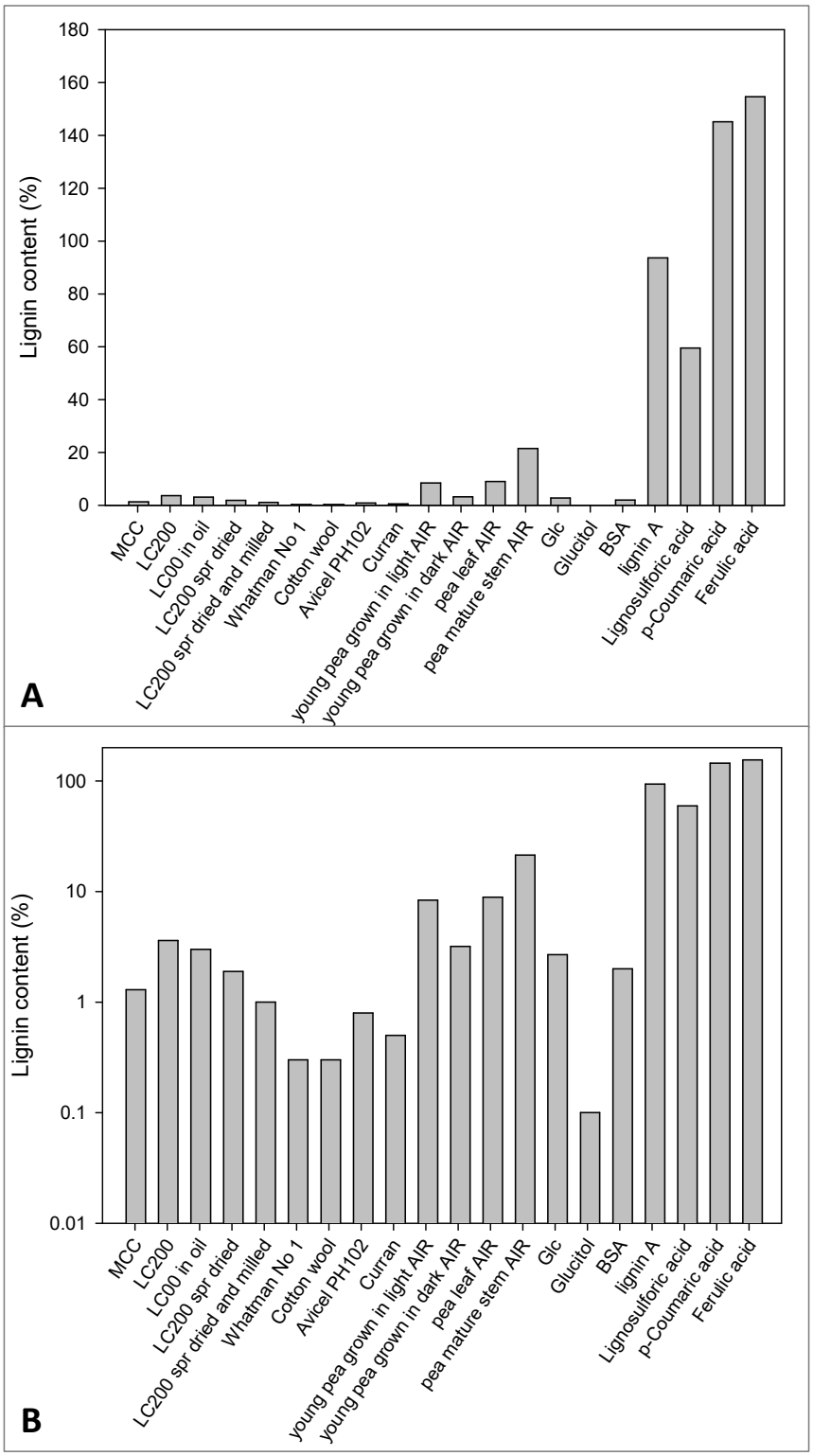

Figure 22. Lignin content of some of the commercial celluloses, AIR preparations and standards.

The assay was done as in Fig. 21 but samples were in hot acetyl bromide for exactly 30 min. (A) and (B) show the same data on different scales; in (B), the y-axis is in log scale.

The lignin contents of the samples in Fig. 22 are generally lower than in Fig. 21, and as the incubation time in Fig. 21 was more variable, Fig. 22 is more reliable. The content of lignin-like compounds in the pea AIRs varied a lot between the tissue types, and the lignin-like compound content of young pea stems grown in light AIR and pea leaf AIR was ~9%, whereas the young pea stems grown in dark AIR had ~5% and pea mature stem AIR ~21% lignin-like compounds (Fig. 22). The commercial celluloses had less (but measurable) lignin-like material, and the LC200 cellulose was the highest in lignin (~3.5%) (Fig. 22). Interestingly Curran® had a lignin content lower than MCC, the LC200 celluloses and Avicel PH102 which is unexpected as Curran® is not composed of solely cellulose (Curran® is rich in pectin and hemicellulose as shown in § 3.1.1 Polysaccharide content) (Fig. 22). The commercial celluloses had undergone various treatments that should have removed most lignin, whereas Curran® had not. Therefore, I would have expected Curran® to contain more lignin than most of the commercial celluloses, which is not the case in Fig. 22.

Our in-house control 'lignin A' (Kraft-Eucalin) gave a lignin content close to 100%, whereas the lignosulphonic acid gave only ~60% lignin content (Fig. 22). Lignosulphonates, which are removed from wood by sulphite pulping, contain 0.4 – 0.7 sulphonate groups per phenylpropane unit (Sixta, 2006), but also Kraft lignin, usually has 70–75% of its hydroxyl groups sulphonated (Lange *et al*., 2013). According to the manufacturer (Aldrich) of the lignosulphonic acid, it is a desulphonated sodium salt that contains 2% (w/w) sulphur and 9% (w/w) sodium, and Ye *et al*. (2017) showed that desulphonation of lignosulphonic acid by alkali hydrolysis reduces the sulphur content of lignosulphonate by 60%. The molecular formula of lignosulphonic acid is $C_{20}H_{26}O_{10}S_2$ (PubChem website, retrieved on August 26th, 2022, https://pubchem.ncbi.nlm.nih.gov/compound/Lignosulfonic-acid), which is ~490 Da, and the proportion of sulphonate groups $(SO_3H)_2$, which is ~164 Da, is therefore ~34% (w/w) of the polymer. The remaining sulphonate groups in the desulphonated lignosulponic acid could explain why the measured lignin content was less than 100%. Furthermore, the

differences in the ‘lignin content’ of the control lignin samples could be explained by their degree of sulphonation.

Lignin consists of hydroxycinnamyl alcohols (*p*-coumaryl alcohol, coniferyl alcohol and sinapyl alcohol) (Sixta, 2006; Lange *et al*., 2013), and the ferulic and *p*-coumaric acids, which were used as control samples, are aromatic carboxylic acids that structurally resemble these compounds and gave over estimated 'lignin contents' (Fig. 22). The difference in 'lignin content' of the lignin controls and the ferulic and *p*-coumaric acid (Fig. 22) could also be explained by the degree of sulphonation of the lignin standards (and the lack of sulphonates in pure ferulic and p-coumaric acid). The bovine serum albumin (BSA), a protein, did not dissolve in the acetyl bromide solution and formed an orange clump at the bottom of the vial. If any proteins did dissolve from the clump, they contributed little to A_{280} measurement. Glucose gave detectable interference with the A_{280} measurement whereas glucitol did not, and this is relevant because cellulose consists of glucose residues, which are non-reducing, like glucitol; free glucose is a reducing sugar and its aldehyde groups are likely to be highly reactive. Indeed, glucose turned black in the presence of acetyl bromide, whereas cellulose did not. The lignin, ferulic and *p*-coumaric acid samples also produced black solutions during the heating (although the lignin powders were dark brown to start with). Also, Curran® and AIR preparations had gained a slight caramel colour after the heating step. All the other samples remained colourless during the assay. The colour of the solution of the Curran® and AIR samples could indicate that some polysaccharide (probably pectin because it is the most acid-labile cell wall polysaccharide and these samples were the only ones containing traces of pectin in § 3.1.1 Polysaccharide content) was partially depolymerised during the acetylation step.

Later-received samples (Södra A13, never-dried cellulose, young pea stem AIR...) were assayed for lignin in a separate experiment alongside more standards (Fig. 23). The never-dried cellulose was dried in the oven (as in § 2.2.3 Materials and methods – Defining the dry material content of the 'never-dried cellulose') before assaying for lignin because acetyl bromide reacts strongly with water.

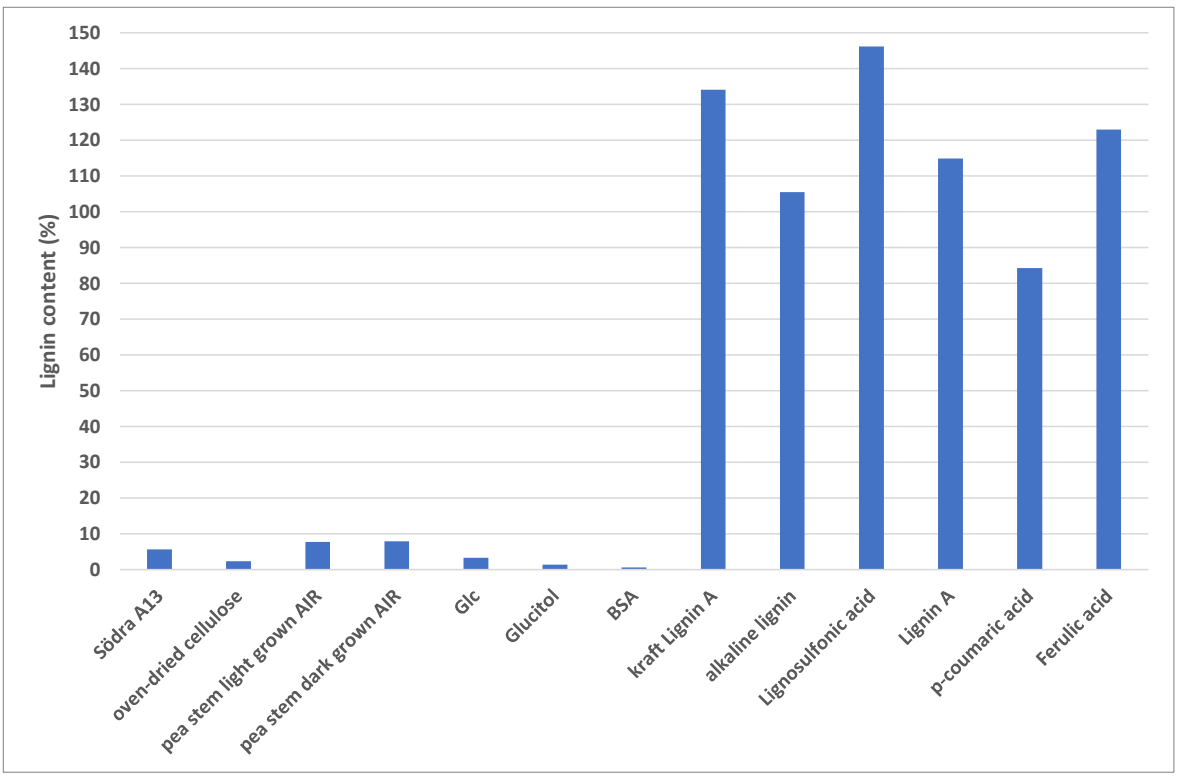

Figure 23. Lignin content of Södra A13, never-dried cellulose and young pea stem AIR preparations alongside various phenolic standards.

The experiment was done as in Fig. 22, other details as in Fig. 21. The Kraft lignin A was eucalyptus lignin 'Eucalin' from a Spanish company, ENCE. The other 'lignin A' was produced by TheraPharm. The lignosulphonic acid (desulphonated sodium salt, 471046-100G) and alkali lignin (370959-100G) were from Aldrich.

The AIR preparations from the new batch of young pea stems grown in light and dark were not as different from each other as in the previous batch (compare Fig 21 and 22 to Fig 23). The Södra A13 and oven-dried (previously 'never-dried') cellulose had low lignin content (Fig 23). During the heating step the oven-dried cellulose and pea AIRs had gained a caramel colour but the Södra A13 stayed colourless, and it is possible that the never-dried cellulose contains some unidentified non-cellulose contaminants.

Out of the 'pure' lignin samples, lignin A and alkali lignin had measured lignin contents closest to 100% when assayed by ABSL method (Fig. 23). The 'A' in lignin A probably refers to 'fraction A' (i.e. when the lignin was extracted off from the Kraft cooking liquor) – usually the processing of pulp involves several processing steps (Sixta, 2006), and separating lignin from the cooking liquor tends to demand multiple steps which divides lignin into fractions (Lange *et al*., 2013). As described previously, all the lignin samples were dark brown as dry powders and gave black solutions during the heating step.

The foregoing preliminary tests on the cellulose samples and AIR preparations using the ABSL method showed that lignin content can be reliably measured, even in samples that were relatively low in lignin (commercial celluloses). Therefore, I used the ABSL method for measuring the lignin content from all the cellulose samples and AIR preparations with suitable controls. For getting statistically significant results, I assayed the samples in quadruplicate (Fig. 24). The results are discussed together with Fig. 25 below.

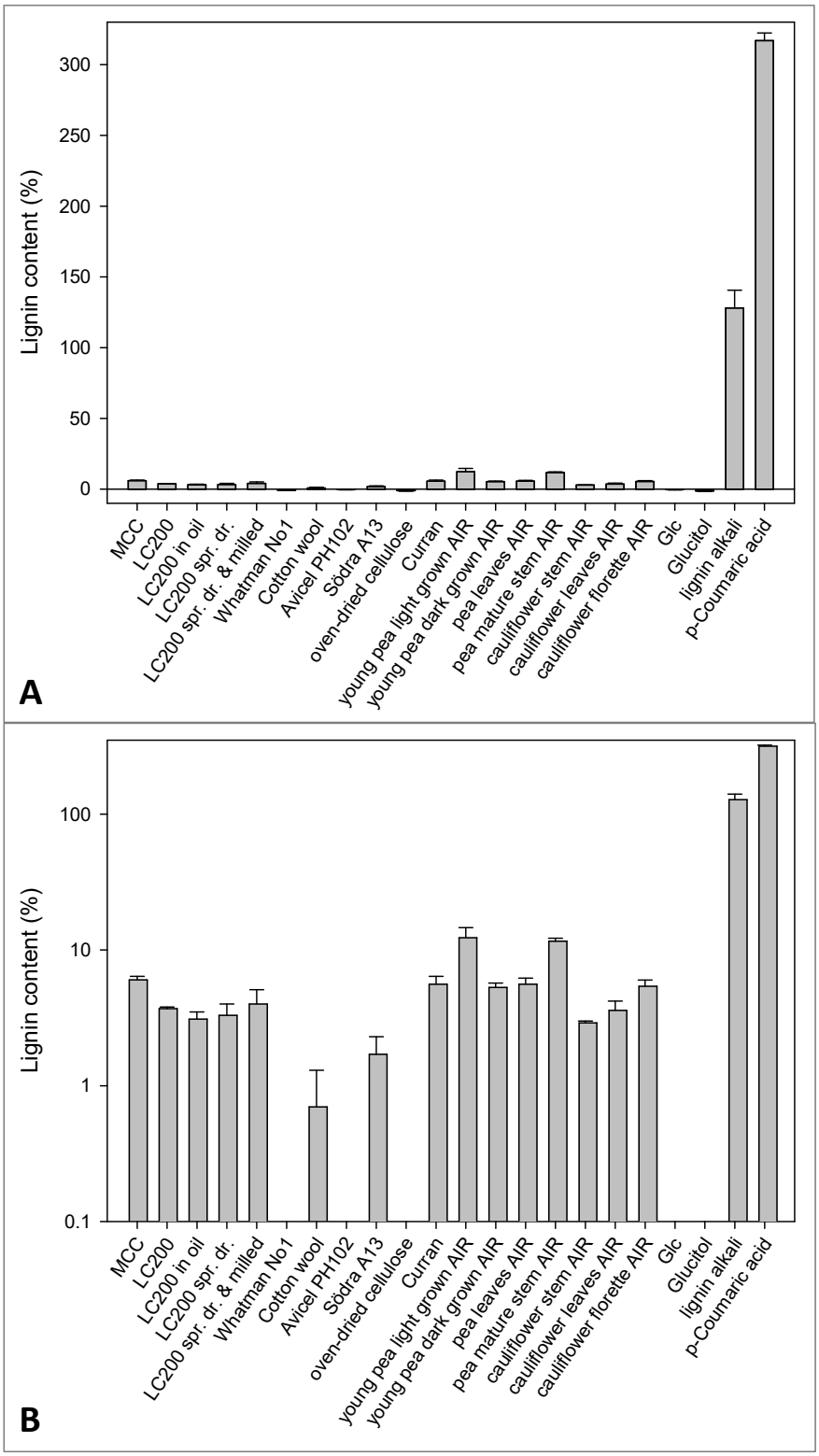

Figure 24. Lignin content of the commercial cellulose samples, AIR preparations and standards, measured in quadruplicate.

The experiment was done as in Fig. 21 and 22. (A) and (B) show the same data on different scales; in (B), the y-axis is in log scale. The 'oven-dried' cellulose was prepared by drying 1 g of previously 'never-dried' cellulose in oven at 80°C for 26 h, and then at 120°C for 72h. Error bars represent standard error of the mean (SEM), N = 4 (technical repeats).

3.1.3.2 Determining the lignin content with modified ABSL method

Heating the samples in glass vials in a water bath is laborious as the vials need to be wiped dry carefully after heating because condensed water can react with the acetyl bromide. Therefore, I tested doing the heating in 2-ml Sarstedt screw-capped plastic tubes in a heat block. Also, for decreasing the error bars with the 'pure cellulose' samples, I used a fourfold concentration of acetylated sample for measuring the A_{280}. For statistically reliable results, I again assayed the samples in quadruplicate (Figure 25).

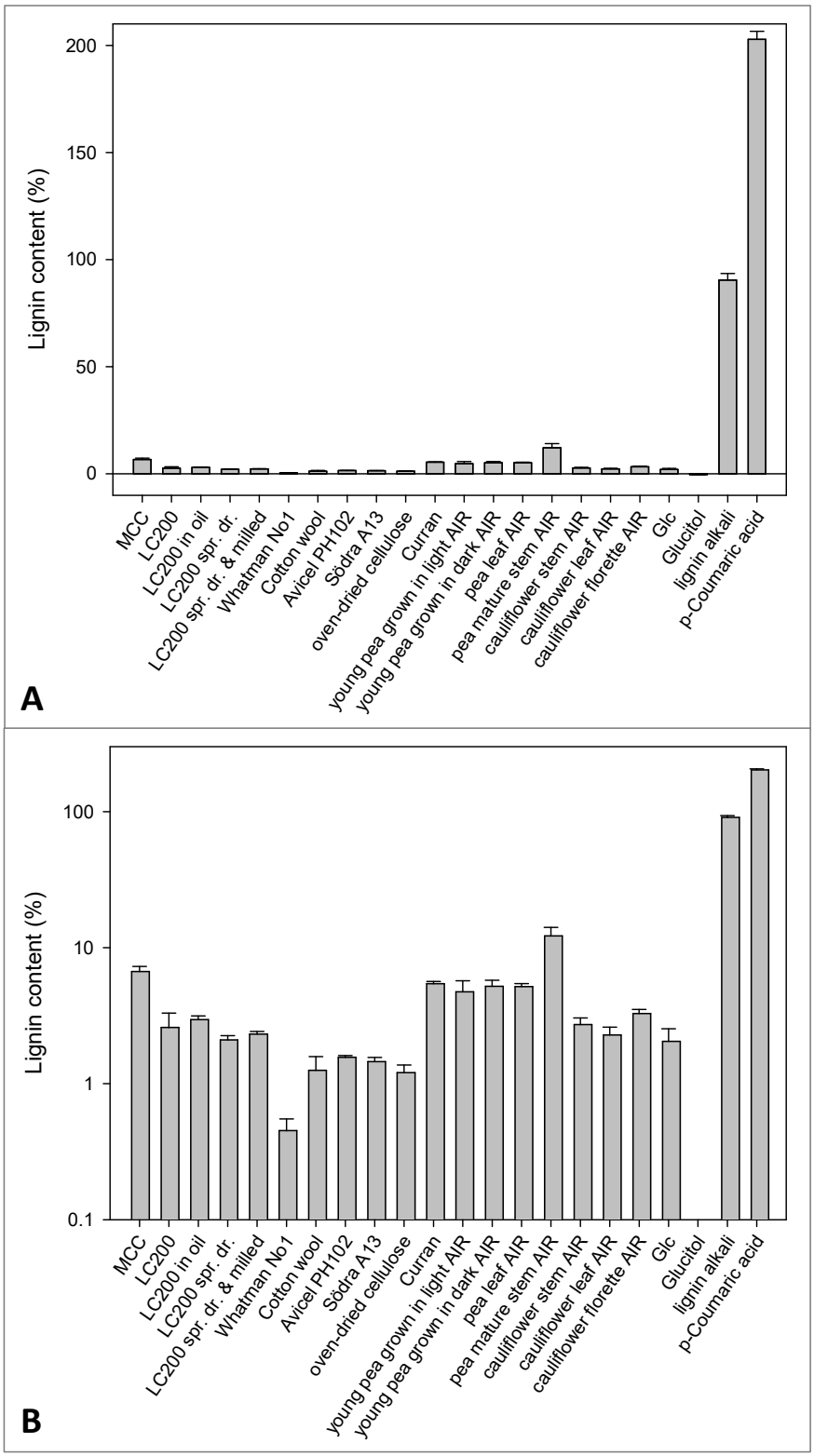

Figure 25. Lignin content of the cellulose samples, AIR preparations and control samples, measured with a modified ABSL method.

The experiment was done as in Fig. 21 and 22 but the samples were heated in a heat block instead of a water bath and a fourfold concentration of acetylated sample was used for measurements of the commercial celluloses, Curran® and the AIRs. (A) and (B) show the same data on different scales; in (B), the y-axis is in log scale. Error bars represent SEM, N = 4 (technical repeats).

The final and most trustworthy data on lignin are in Fig. 24 and 25, as the data of previous figures were gained during practising and optimising the method. The alkali lignin standard, as expected, had a lignin content close to 100% (Fig. 24 and 25). The AIR from young pea stem grown in light had higher content of lignin-like compounds than the AIR from young pea stems grown in dark in Fig. 24B (but not in Fig. 5), which was in line with the previous data (Fig. 21 and 22). In Fig. 25 all the pea AIRs contained similar amounts of lignin-like compounds except for the mature pea stem AIR which was twice as high in lignin (as expected since mature stems have secondary cell walls which contain much more lignin than the primary cell walls which predominate in young stems and the leaves). All the cauliflower AIRs were lower in lignin-like compounds than the pea AIRs (Fig. 24 and 25). Curran® had a content of lignin-like compounds higher than most commercial celluloses in figures 21 and 24 and 25 but not in figure 22B which suggests an error in Fig. 22B. The differences in the lignin contents between the LC200 samples are not statistically significant (Fig. 24 and 25). A few samples gave slightly negative values when the spectrophotometer was blanked against a no-cellulose sample (Fig. 24B). MCC had a higher 'lignin' content than the other commercial celluloses (Fig. 24 and 25).

To conclude, the ABSL method was suitable for assessing our commercial celluloses and AIR preparations for even trace lignin content, and, after optimising the method, I gained reproducible and statistically validated results from the measurements. The mature pea stem AIR was the highest in lignin (~12%), followed by the other pea AIRs (~5%) (where the young pea stem grown in light AIR contained more lignin-like compounds than the dark grown one in Fig. 24) (Fig. 24 and 25). The MCC cellulose had 'lignin-like compound' content (~6–7%) highest of the commercial celluloses, and it was similar to that of Curran® (~5.5%) (Fig. 24 and 25). The lignin-like compound content of the cauliflower AIRs was ~3–5% (Fig. 24 and 25). The LC200 contained ~2–4 % of lignin-like compounds whereas the other commercial celluloses contained <1.5% lignin-like compounds (Fig. 24 and 25). Thus all the cellulose samples used in this work contained measurable traces of lignin — different proportions in different stocks, which will be discussed (§ 4.1.5) in relation to the different stocks' performance in confectionery applications.

3.2 Negatively charged groups in cellulose or AIR

The commercial celluloses described in § 2.1 could have been manufactured with different methods as they were produced by several different companies. It is possible that some of the processing methods can oxidise cellulose. Oxidation could introduce to cellulose carboxyl groups which are acidic and therefore have negative charges which could contribute to the differing properties of 'mouth feel' or mixing into the chocolate matrix. The negatively charged groups could affect the mouthfeel because they can bind and interact with positively charged substances such as salivary proteins, and negatively charged cellulose derivatives (such as carboxymethyl cellulose) can even be used as a chromatographic cation exchange resin to remove positively charged molecules from a solution.

3.2.1 Preliminary qualitative tests of coloured cation binding and desorption

3.2.1.1 Cobalt (II) ion binding and desorption

For detecting possible negative charges in the celluloses and plant AIR samples, I initially tested the binding of a coloured cation, Co^{2+}, to two types of carboxymethyl cellulose (by Whatman, fibrous CMC22 and granular CMC32) and Whatman No 1 filter paper as model substrates, respectively with and without many negative charges. The 'concentration' of negative charges of the carboxymethyl celluloses had been defined by the manufacturer (0.6 meq/g for CMC22 and 1.0 meq/g for CMC32) and therefore they were used as negatively charged 'model' substrates, whereas the filter paper, used as a non-charged control, has very few, if any, negative charges and is similar to untreated cellulose (such as cotton wool).

Filter paper and carboxymethyl celluloses were washed with concentrated then dilute buffer, then incubated with $CoCl_2$ solutions in dilute buffer overnight. The pellets were again washed with the buffer and the cations were desorbed with dilute HCl (Fig. 26).

Before the HCl treatment, the filter paper pellets where white whereas the carboxymethyl celluloses were pink (Fig. 26) Promisingly, the CMC32 cellulose was more intensely pink than the CMC22 cellulose which was expected as CMC32 carries more charged groups per gram (Fig. 26A). However, after unbinding the cations with HCl the supernatants were barely coloured and difficult to quantify accurately (Fig. 26B).

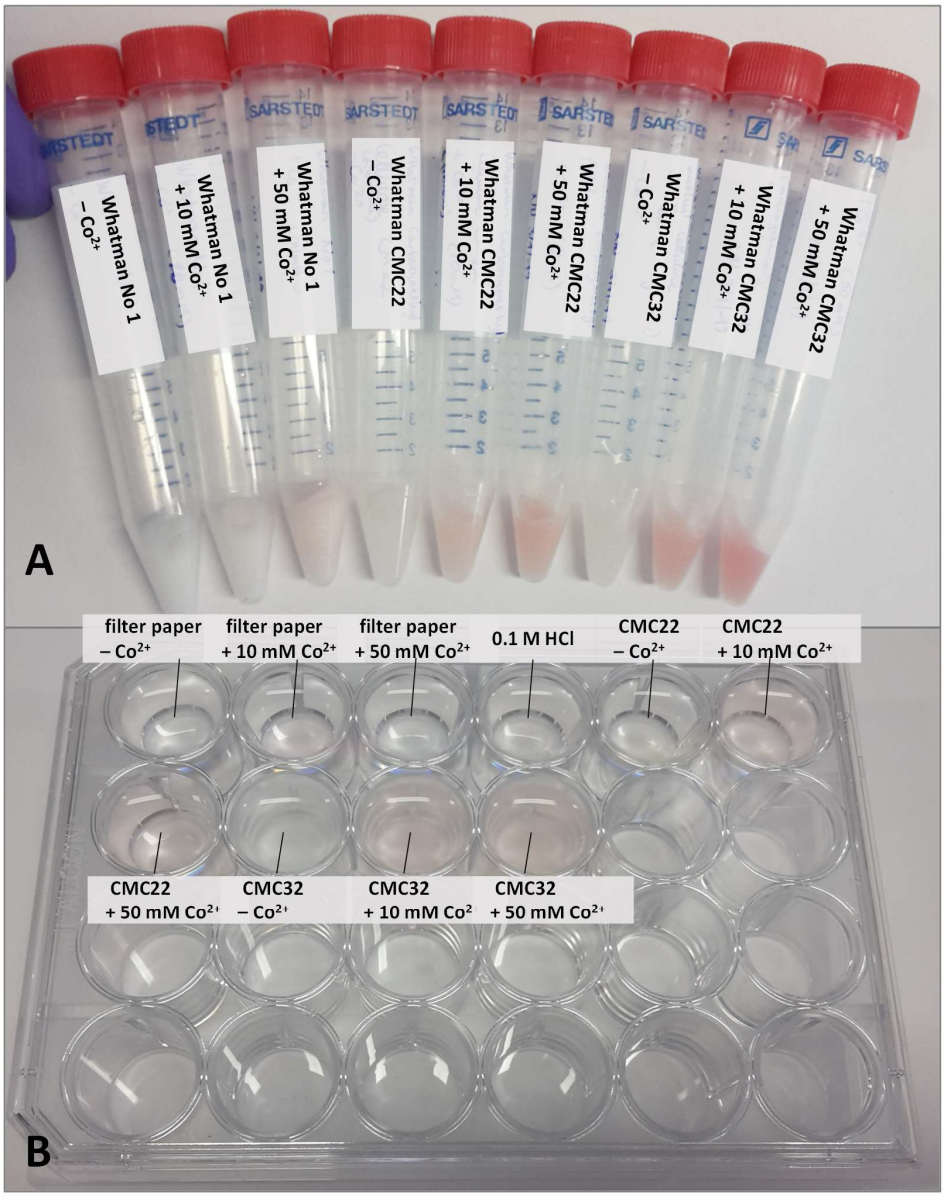

Figure 26. Binding of Co^{2+} to Whatman filter paper and carboxymethyl cellulose.

Whatman No. 1 filter paper and Whatman carboxymethyl cellulose CMC22 and Whatman CMC32 (100 mg of each) were washed with 10 ml of 1.23 M pyridinium acetate, pH 6.5 buffer for 16 h at 20°C on a mixing wheel. Next the pellets were washed three times with 10 ml of 10 mM pyridinium acetate buffer, pH 5, for at least 2h/wash, and incubated with 10 ml of 0, 10 or 50 mM $CoCl_2$ in the pH 5.3 buffer for 16 h at 20°C. The pellets were again washed with the buffer and photographed (A) after which any remaining Co^{2+} was desorbed with 3 ml of 0.1 M HCl and the free solutions were transferred to 24-well polypropylene plate (B).

3.2.1.2 Binding and desorption of histological stains

To find more intensely coloured cations for detecting negative charges, several histological stains were tested. The CMC and filter paper celluloses were treated the same way as with $CoCl_2$ except that 1 mM solutions of basic fuchsin, methyl violet, methyl green, malachite green, aniline blue, safranine, Janus green B, polychromic methylene blue and toluidine blue O were used instead of $CoCl_2$ (Fig. 27). All stains other than malachite green (Fig. 27F) and aniline blue (Fig. 27B) left the CMC pellets very intensely stained. The supernatants from the CMC samples treated with basic fuchsin (Fig. 27C), methyl violet (Fig. 27D) and methyl green (Fig. 27E) were clearly coloured even after several washes in pH 5 buffer, indicating that their elution was very gradual, so they were omitted from the candidates of suitable stains. Out of the remaining stains, toluidine blue O (Fig. 27I) had the biggest contrast between the non-charged cellulose and negatively charged cellulose derivatives, as it left the filter paper pellet almost white, and it was selected for further studies.

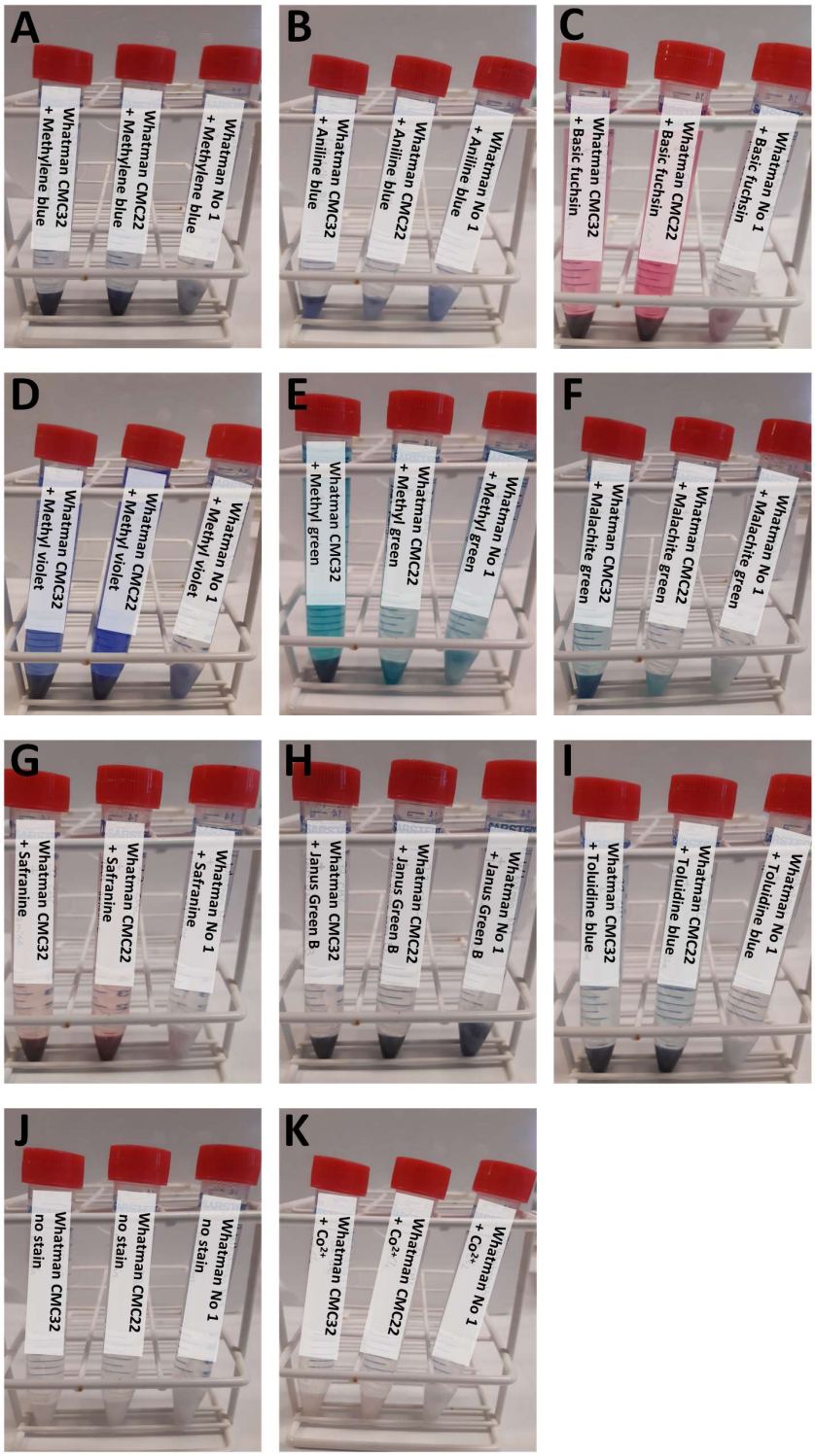

Figure 27. Binding of various histological stains to Whatman filter paper and carboxymethyl cellulose.

Details as in Fig. 26A except for 1 mM polychromic methylene blue (A), aniline blue (B), basic fuchsin (C), methyl violet (D), methyl green (E), malachite green (F), safranine (G), Janus green B (H), toluidine blue O (I) or $CoCl_2$ (K) was used instead of (0, 10 or 50 mM) $CoCl_2$. As a control, buffer with no stain (J) was included.

For eluting toluidine blue O (TB) from the dilute buffer-washed cellulose pellets, 90% formic acid, formic acid:ethanol:water (1:1:1 by vol.), and 96% ethanol were tested (Fig. 28A). Neat formic acid eluted the stain most readily (Fig. 28A). Therefore, a concentration series of formic acid (diluted with water) was tested: 1% formic acid was found to unbind some stain, although complete desorption was achieved when the concentration was 50% or higher (Fig. 28B).

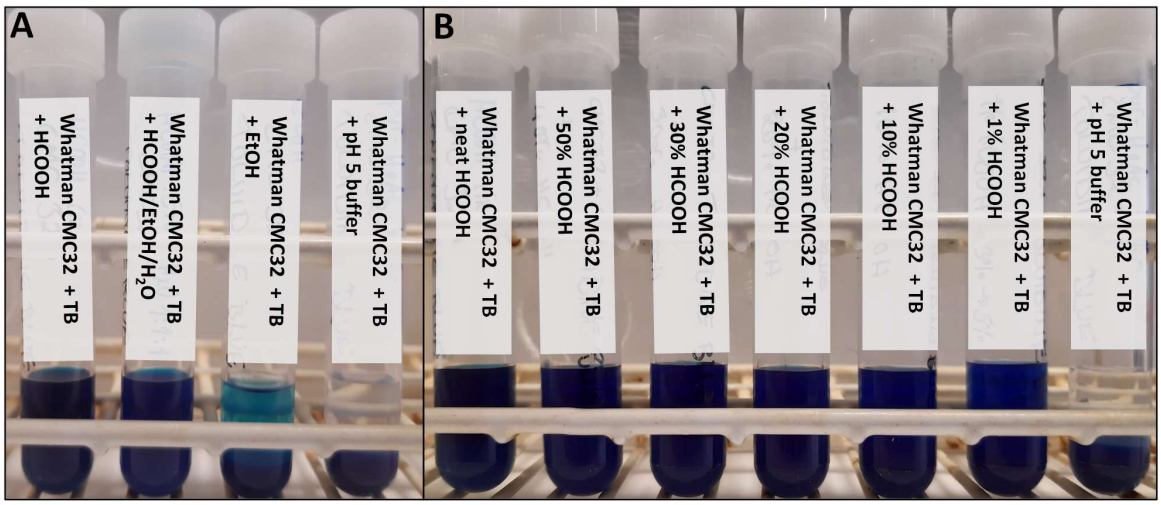

Figure 28. Desorption of toluidine blue O from carboxymethyl cellulose with different solvents.

Details for binding of stain as in Fig. 27I and desorption of stain as in Fig. 26B, except for the solution used was either 90% formic acid, formic acid/ethanol/water (1/1/1 by vol.) or 96% ethanol (A), or a concentration series (90%, 50%, 30%, 20%, 10% or 1%) of formic acid (B). As a non-desorbing control, 10 mM pyridinium acetate, pH 5.3 was used (A and B). TB = toluidine blue O.

3.2.1.3 Quantitative tests of toluidine blue O binding and desorption

3.2.1.3.1 Defining the constants for the toluidine blue O binding assay

To see how much TB stain the CMC32 could bind, a concentration series of the stain was tested on the CMC pellets (Fig. 29B). CMC bound all the stain from all the solutions except for the 6.4 mM concentration where the solution stayed very slightly blue (Fig. 29B). Similar results were gained when 90 mg of CMC32 was incubated with series of volumes (1–32 ml) of 1 mM stain solution (same amount of substance, n, of TB as with the concentration series experiment) – the biggest volume was left slightly blue (Fig. 29A). To make sure the celluloses would be provided with excess stain, the pellets sizes were reduced to 20 mg for the further experiments.

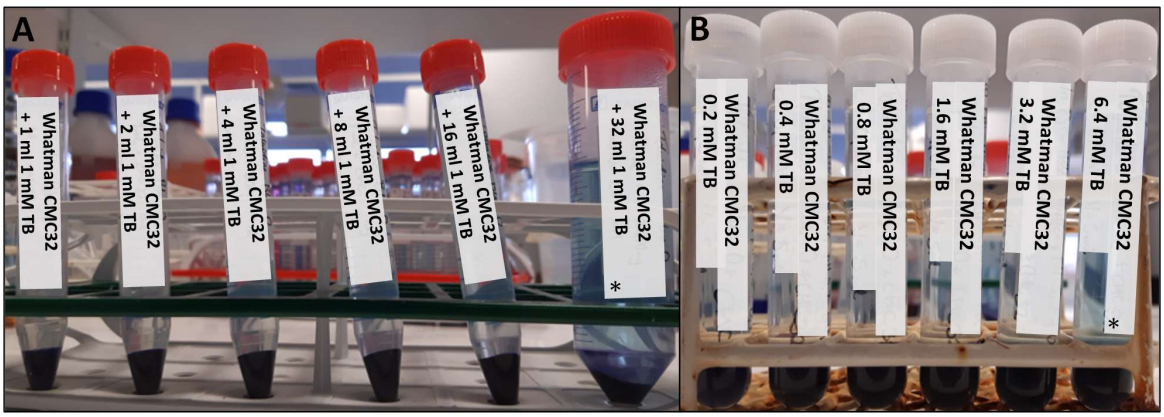

Figure 29. Testing the effect of volume and concentration on the binding of TB to CMC32.

The technical details are as in Fig. 27I except for a range of volumes (1, 2, 4, 8, 16 or 32 ml) of 1 mM TB (A) or a range of concentrations of stain (0.2, 0.4, 0.8, 1.6, 3.2 or 6.4 mM, each 5 ml) (B) were used. Also, the TB solution was not removed from the tubes (and the cellulose was not washed with buffer) when the pictures were taken. The amount of substance, n, of TB fed to the CMC (90 mg each) was the same between the respective tubes in (A) and (B), (i.e. 1 ml of 1 mM TB and 5 ml of 0.2 mM TB). The free solution in tubes marked with * is visibly blue. TB = toluidine blue O.

The absorption spectra of 0, 10 and 20 µM toluidine blue O were measured and the absorption maximum was at 631 nm (Fig. 30). Adsorption of a dilution series of the TB stain was measured and the correlation of A_{631} and concentration was linear between 0 and 20 µM (Fig. 31).

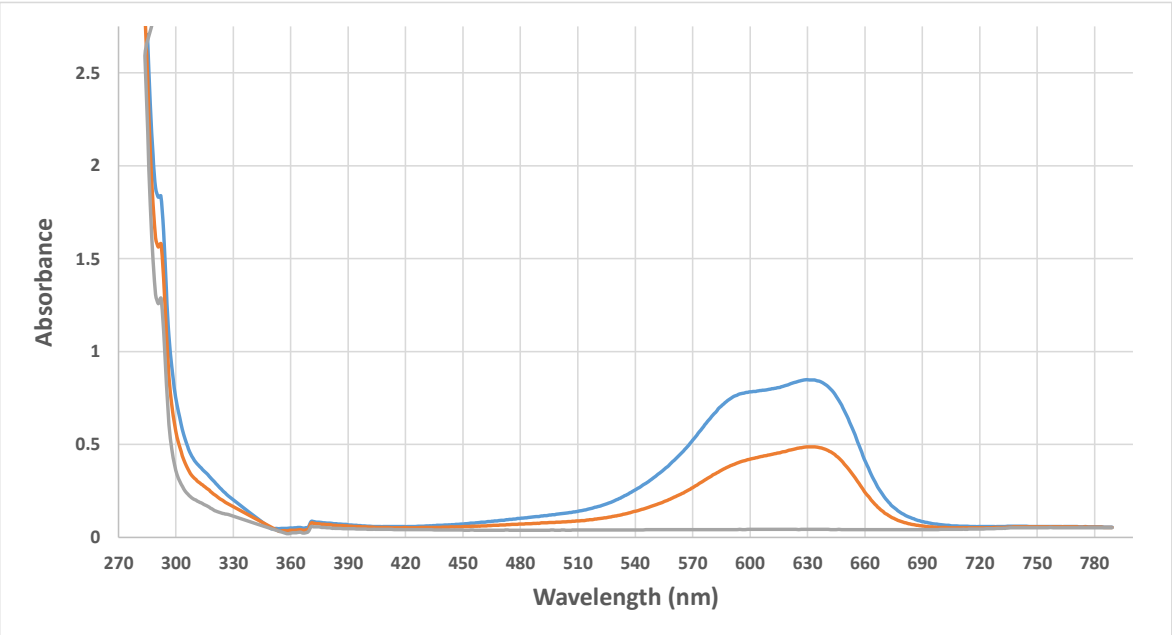

Figure 30. Absorption spectra of toluidine blue O at 0, 10 and 20 µM concentrations.

The absorption spectra were measured with a Perkin Elmer Victor X3 plate reader from a 24-well polypropylene plate. The TB solutions were prepared in the 10 mM pyridinium acetate buffer, pH 5.3. The A_{max} is at 631 nm.

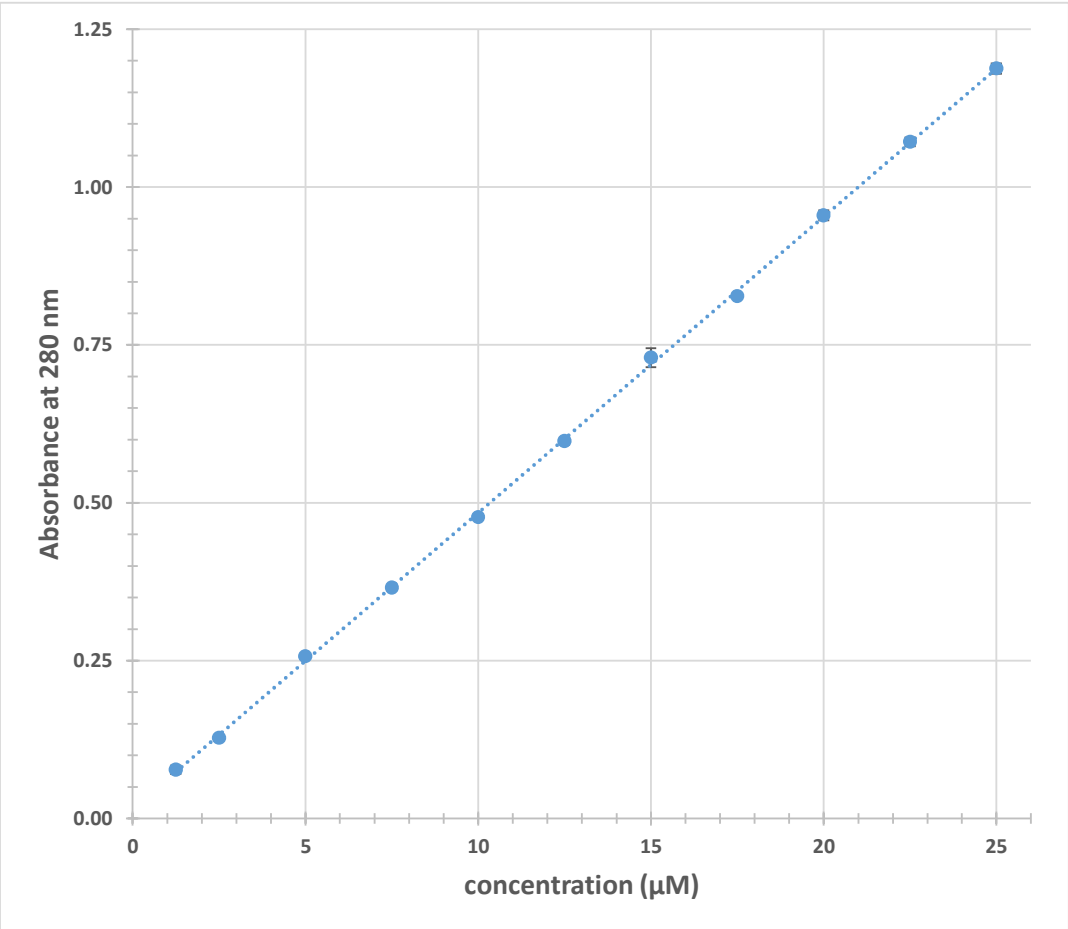

Figure 31. The standard curve of toluidine blue O.

A dilution series of the TB was prepared in triplicate in 10 mM pyridinium acetate buffer, pH 5.3 buffer and the A_{631} was measured with a Cecil 8000 spectrophotometer in polystyrene cuvettes. The correlation of A_{631} and concentration is linear between 0 and at least 20 µM.

Toluidine blue O is known to be a metachromatic dye, and the absorption maximum shifts when it forms dimers or trimers instead of monomers (D'Ilario and Martinelli, 2006). The measured spectrum with a single peak at 631 nm is typical of the monomeric dye and it can be assumed that the stain behaves as monomers in these experiments. The metachromasy of TB is discussed further in § 4.2 Discussion chapter.

3.2.2 Measuring the negatively charged group content of the commercial celluloses and AIRs

For assaying negative groups in all of the cellulose samples, 20-mg samples were washed with the concentrated buffer, followed by three washes in the dilute buffer, after which the pellets were incubated with 5 ml of 6.4 mM TB. The pellets were washed five times with the dilute buffer, and then elution of stain was done with 5 ml of 50% formic acid. Before measuring the absorbance, the eluates were diluted to be within the range 0 – 20 µM and the A_{631} was measured (Fig 32 A). To show that the results were reproducible, the whole procedure was repeated (Fig. 32B), and the averages of these are shown in Fig 33.

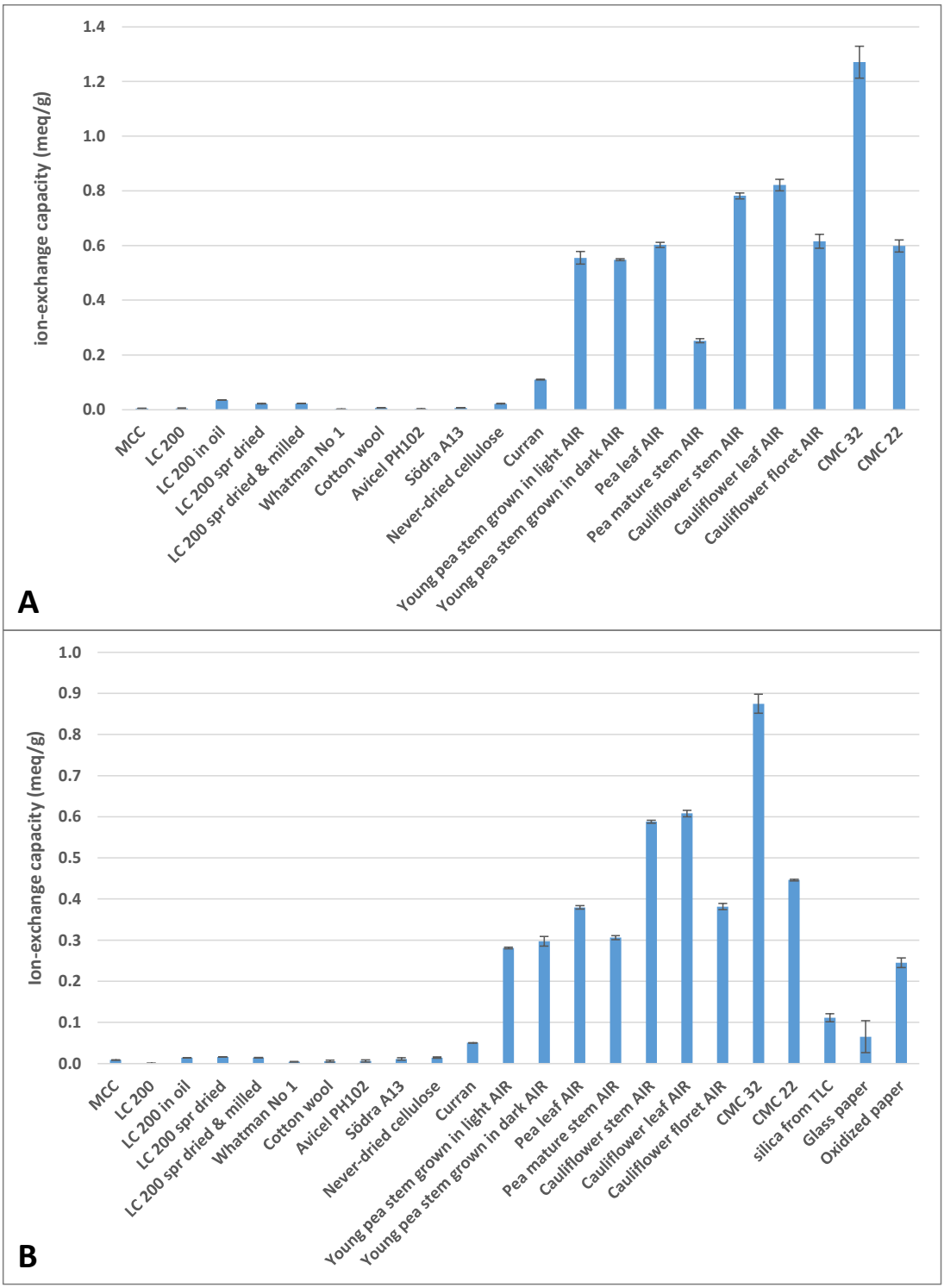

Figure 32. Observed negatively charged groups in the commercial celluloses and AIRs.

The commercial cellulose and AIR pellets (20 mg each) were washed with 5 ml of 1.23 M pyridinium acetate, pH 6.5, buffer at 20°C for 16 h on a mixing wheel, followed by three washes in 5 ml of 10 mM pyridinium acetate, pH 5.3, buffer (2 h for of each wash). Then the pellets were incubated in 5 ml of 6.4 mM TB (prepared in the pH 5.3,

buffer) for 16 h, followed by five washes in the pH 5.3 buffer. The TB was eluted with 5 ml of 50% formic acid and the solutions were diluted with water to be within the range 0 – 20 μM. The A_{631} was measured with standards as in Fig. 31. The results were calculated as millimoles of negatively charged groups per 1 g of dry weight of cellulose (i.e., meq/g) assuming the sample consists solely of cellulose. (A) and (B) show the data of the first (A) and second (B) repeat of the experiment. The error bars show SEM, N = 3 (technical repeats).

The results of Fig. 32 are discussed together with the results of Fig. 33 below.

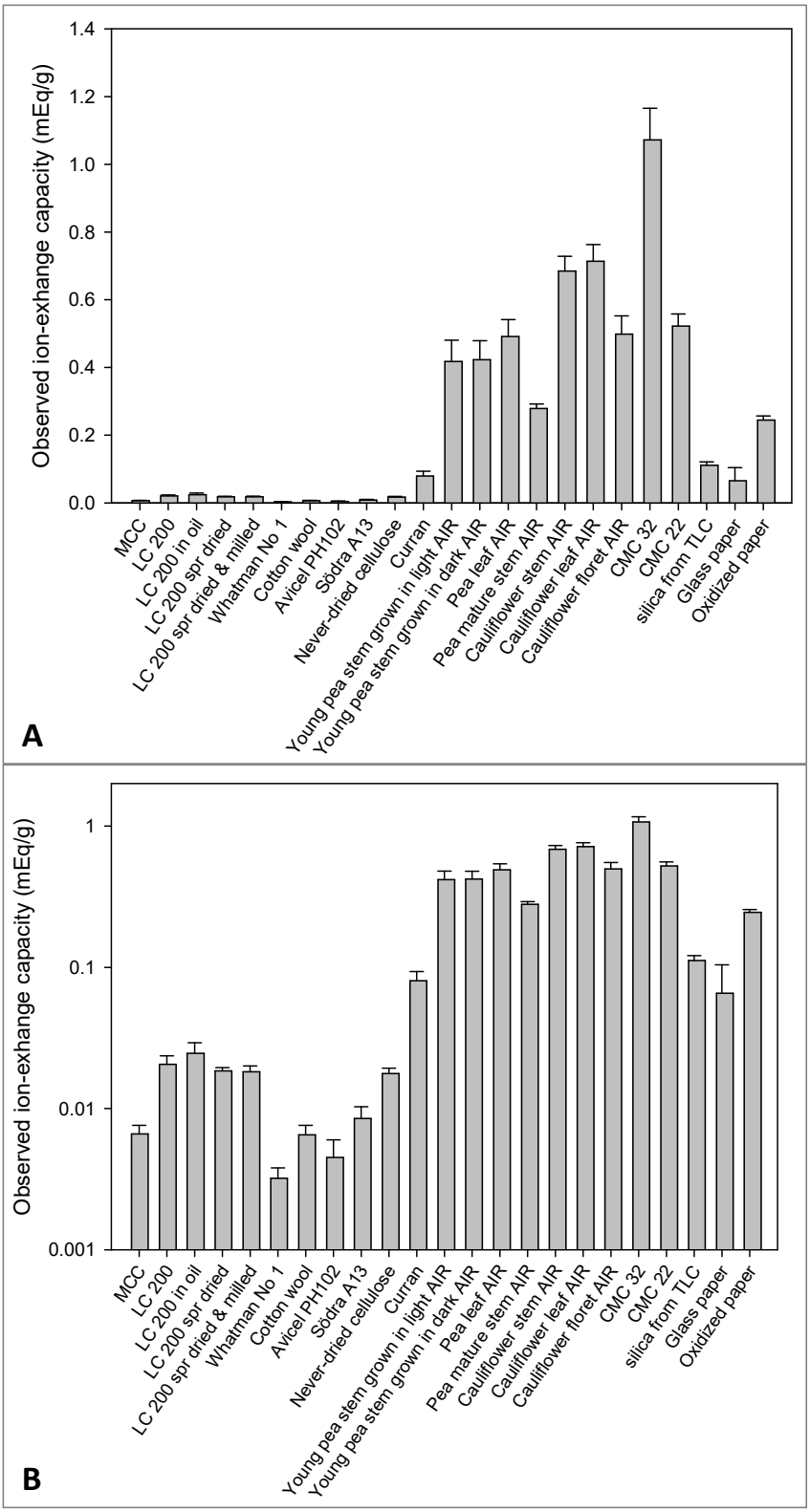

Figure 33. Observed negatively charged groups in the commercial celluloses and AIRs (average from Fig. 22A and 22B).

Figure shows average calculated from 32A and 32B. (A) and (B) show the same data on different scales; in (B), the y-axis is in log scale. The error bars show SEM, N = 6 (3 technical repeats, and 2 biological repeats). The oxidized paper was made from Whatman filter paper by Mr. C. Donohoe using TEMPO oxidation method.

The AIRs, which are rich in negatively charged polymers such as pectin, proteins and RNA, bound more stain than the commercial celluloses (Fig. 32 and 33). Curran, which is known not to be pure cellulose, bound more TB than the commercial celluloses (Fig. 32 and 33) which have previously been shown to have little if any other contaminating polysaccharides (§ 3.1.1. Results - Polysaccharide content). The mature pea stem AIR bound less stain than the other pea tissues tested in Fig. 32 but in Fig. 33 the mature pea AIR bound TB as much as the young pea stem AIRs did. The reason why the mature pea stem AIR bound less TB than the pea leaf AIR could be explained by the mature stem tissue containing secondary cell walls which have less pectin (and respectively more lignin) than the primary cell walls of the pea leaf AIR. The cauliflower floret AIR contained less negatively charged groups than the cauliflower leaf and stem AIRs (Fig. 32 and 33).

The (relatively pure) commercial celluloses had very low concentrations of negatively charged groups compared with the AIRs (Fig. 32 and 33). The model substrates for negatively charged cellulose, CMC22 and CMC32, were very rich in negative charges and the CMC32 was the most negatively charged material studied (Fig. 32 and 33). The LC200 samples which were processed further from the original LC200 were much more negatively charged than the original LC200 (Fig. 32 and 33), which suggests that some of the Glc residues of the cellulose could have been oxidised (for example to GlcA) during the further processing at VTT. The NaOCl/TEMPO-oxidised paper (Fig. 33) contained 4% of negatively charged 'Glc' residues, possibly GlcA, which confirms that it is possible to oxidise some of the Glc residues of cellulose by chemical treatment.

3.3 Studying the accessibility of cellulose to surrounding molecules

This chapter aimed to develop a method that could be used to compare how available, in other words accessible, the cellulose is in the samples. Inaccessible surfaces could be covered by hemicelluloses, for instance, but accessible surfaces would be bare and could interact neighbouring molecules, e.g. soluble carbohydrates. Also, the thickness of the microfibrils (i.e. thick microfibrils have proportionally less surface area than thin microfibrils) or crystallinity of the cellulose could affect how much cellulose can interact with its neighbouring molecules. For convenience, [^{3}H]cellopentaitol, was used as an easily detectable, quantifiable and water-soluble model for polysaccharides that could bind to 'accessible' cellulose. The accessibilities of the cellulose microfibrils to surrounding molecules were studied in several experiments where [^{3}H]cellopentaitol was allowed to adsorb to cellulose from free solution followed by experiments where the [^{3}H]cellopentaitol was desorbed from cellulose to free solution.

3.3.1 Accessibility of cellulose to [^{3}H]cellopentaitol

3.3.1.1 Different binding affinities of the celluloses

In the first adsorption–desorption experiment (Fig. 34–37), 90 mg of each commercial cellulose or AIR preparation, listed in 'Materials and Methods', was mixed with 3 ml of pH 4.7 buffer and 830 Bq carrier-free of [^{3}H]cellopentaitol (making 0.49 nM oligosaccharide). The tubes were mixed constantly on a wheel at 20°C. At intervals, samples of the supernatant were assayed for remaining soluble radioactivity.

The celluloses that adsorbed most [^{3}H]cellopentaitol in the initial 1000-h adsorption phase of the experiment were Södra A13, never-dried cellulose, Whatman filter paper and cotton wool (Fig. 36A). Even in these cases, approximately one third of the available radioactivity stayed in solution. Although the starting material for all four 'LC200' celluloses was the same, the adsorption rate and total adsorption of [^{3}H]cellopentaitol varied between the samples (Fig. 34A). The adsorption rate and total adsorption of [^{3}H]cellopentaitol were the lowest with Avicel PH 102, MCC and Curran® (Fig. 37A). The young pea stem AIRs had lower adsorption rate and approximately one third lower total

adsorption of [^{3}H]cellopentaitol than the pea leaf AIR and mature pea stem AIR (Fig. 35A). The adsorption of [^{3}H]cellopentaitol was initially rapid (fastest during the first hour) and by 3 h the adsorption reached a plateau. However, some further adsorption seemed to happen between 32 and 172 h, after which the adsorption reached the final plateau (Fig. 34–37A).

After 1000 h, the cellulose was rinsed with the buffer and resuspended in 3 ml of fresh, non-radioactive buffer to see if any of the bound [^{3}H]cellopentaitol could be desorbed from the cellulose. The sampling and assaying for re-solubilised radioactivity was as in the previous step.

The [^{3}H]cellopentaitol binding to cellulose seemed to be almost permanent – once it had bound to cellulose most of it did not desorb into free solution (Fig. 33–37B). During the 1000 h of the desorption step, the Whatman filter paper, never-dried cellulose and Södra A13 desorbed least (5, 7 and 10%, respectively), and Avicel PH102 desorbed most (36%) of the initially bound [^{3}H]cellopentaitol. The rest of the commercial celluloses desorbed 15–21% of the initially bound [^{3}H]cellopentaitol. Curran® and the AIRs from young pea stem grown in light and dark desorbed ~25%, and pea leaf AIR and pea mature stem AIR desorbed 17% and 13%, respectively, of the initially bound [^{3}H]cellopentaitol. The desorption rate seemed to be constant throughout the step (as the curves in Fig. 34–37B are ~ linear; more easily seen if plotted on a linear time axis).

To test if any additional [^{3}H]cellopentaitol could be desorbed by competitive binding of concentrated cellobiose to cellulose, the cellulose left from the previous desorption step was resuspended in 3 ml of fresh, non-radioactive buffer containing 400 mM cellobiose and the sampling and assaying for solubilised radioactivity was repeated as before. The idea was that cellobiose would bind on the cellulose surfaces and its binding would compete with the binding of [^{3}H]cellopentaitol which would force the [^{3}H]cellopentaitol to desorb (as the cellobiose concentration was $\sim 8.2 \times 10^8$ times higher than of the [^{3}H]cellopentaitol).

Even the addition of cellobiose to make 400 mM, as potential competitor, did not desorb most of the [^{3}H]cellopentaitol that had been bound previously (Fig. 34C–37C). From the [^{3}H]cellopentaitol that was still left in the cellulose at the end of the previous desorption step, the only some desorbed over the 221 h the celluloses were incubated in 400 mM cellobiose. Avicel PH102 desorbed most,

again (by 24%), and Södra A13 (12%) and never-dried cellulose (15%) desorbed least [^{3}H]cellopentaitol. The rest of the commercial celluloses desorbed 16–22%, and Curran and pea AIRs desorbed 17–21% of [^{3}H]cellopentaitol. As with the previous desorption step, the desorption rate in 400 mM cellobiose was ~ constant (Fig. 34–37C).

Next, the pellets were boiled with 3 ml of 1 M sodium hydroxide. At this alkali concentration, all remaining oligosaccharide was expected to be solubilised from cellulose without degradation – Herburger *et al.* (2020) showed that reductively tritiated oligosaccharides are stable in 6 M NaOH (which is much more concentrated solution than I used) at 100 °C and that cellulose I does not convert to cellulose II in NaOH concentrations lower than 3 M. The neutralized supernatants were assayed for solubilised radioactivity as before. Finally, the wet cellulose was washed with pH 4.7 buffer and assayed for any remaining adsorbed radioactivity.

Boiling the celluloses and AIRs in 1 M sodium hydroxide was expected to completely remove the [^{3}H]cellopentaitol from cellulose and did indeed release some of the radioactivity into solution (right-hand side of Fig. 34C–37C), yet some radioactivity was still detected in the final pellets (listed in legends of Fig. 34–37). However, if one summed the radioactivities of the final pellets and what was desorbed (by buffer, cellobiose and NaOH), it would exceeded the initially added ^{3}H (Fig. 34A–37A compared to Fig. 34B,C– 37B,C and radioactivities of the pellets, listed in Fig. 34–37 legends) and it is therefore possible that the measurements of radioactivities in the wet pellets were overestimated.

The first experiment taught us that the celluloses and AIRs do differ from each other in their ability to bind [^{3}H]cellopentaitol. What was also evident was that [^{3}H]cellopentaitol binding affinity to cellulose was high and that [^{3}H]cellopentaitol bound to cellulose is difficult to desorb. However, it is peculiar that all of the [^{3}H]cellopentaitol available in the free solution does not bind to the cellulose although the cellulose would probably have a huge excess of available binding sites, and that the binding stops around 200 h. Also, the shape of the binding curves were approximately double hyperbolic (Fig. 34–37A) which indicates that the binding of [^{3}H]cellopentaitol to cellulose might happen in two phases. These questions, in addition to having a need to repeat the experiment to

test reproducibility, led to the next experiment where a competitor for the initial binding of [^{3}H]cellopentaitol was included.

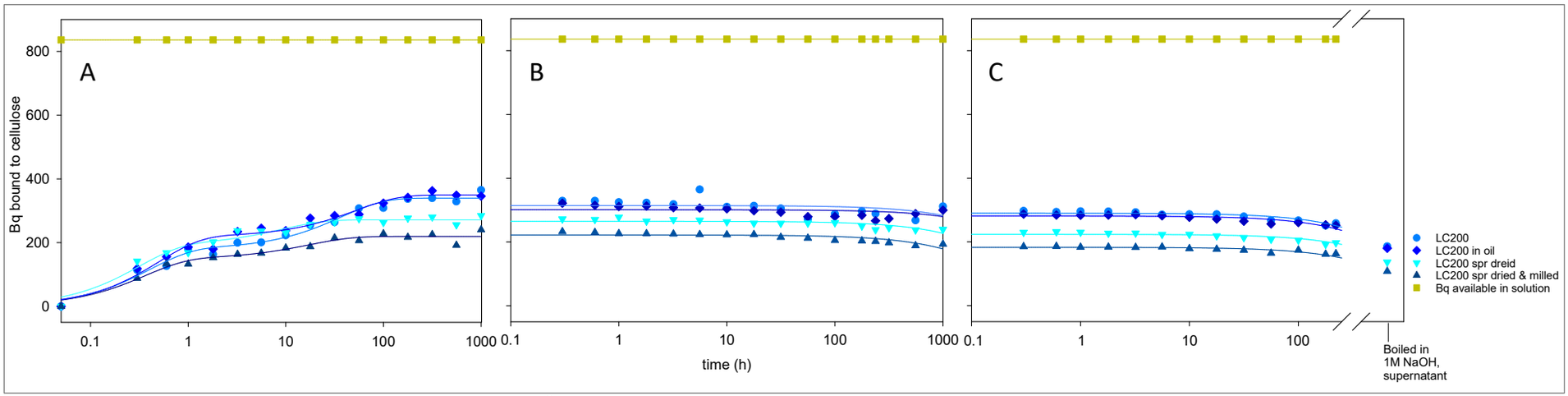

Figure 34. Adsorption and desorption of carrier-free [^{3}H]cellopentaitol to/from (LC200) cellulose samples from/to free solution.

Cellulose samples (90 mg each, N=1) were incubated in 3 ml of 105 mM sodium acetate buffer, pH 4.7, containing 0.5% chlorobutanol. At the adsorption step (A), 830 Bq of [^{3}H]cellopentaitol (specific activity (SA) 567 MBq/µmol, which results in 0.49 nM pentasaccharide) was added to the buffer. The tubes were incubated at 20°C on a mixing wheel. At intervals, the tubes were centrifuged at 3200g for 1 min and 100-µl samples were taken from the supernatants after which the tubes were returned to the wheel. The sampled supernatants were mixed with 900 µl of water and 10 ml of Perkin Elmer Optiphase Hisafe 3 aqueous miscible scintillation liquid and assayed for radioactivity. The figure was drawn as the [^{3}H]cellopentaitol missing from free solution has bound to the cellulose. After finishing the adsorption step, the remaining supernatants and pellets were transferred to Polyprep columns. The remaining supernatants were let through the column and discarded, and the pellets were washed by letting 10 ml of reverse-osmosis water containing 0.5% chlorobutanol flow through the columns.

For the desorption step (B), 3 ml of fresh buffer was added to the capped columns and the columns were incubated on the wheel. The sampling was done by collecting some supernatant, out of which 100-µl samples were taken for scintillation counting and the remaining drops of supernatant were returned into the columns. Some of the celluloses tended to make the sampling from the columns very challenging by blocking the flow of the supernatant, and after ten samplings the remaining pellets and supernatants were transferred to test tubes and from this forward the sampling was done as during step A. The figure was drawn as the [^{3}H]cellopentaitol bound in A was the starting point and the radioactivity detected during desorption step was reduced from it. At the end of B the remaining supernatants were discarded and a further 3 ml of buffer containing 400 mM cellobiose was added (C). The tubes were incubated on a wheel and sampled as in A. At the end of C, the remaining supernatants were discarded. The pellets were boiled in 3 ml of 1 M NaOH and then adjusted to pH ~4.7 by addition of 3 ml of 2 M acetic acid. For assaying the radioactivity of the solution, 1 ml of solution was mixed with 10 ml of scintillant. The pellets were washed three times with 6 ml of 1% acetic acid (duration of washes: first wash, 1 h; second wash, 3 h; third wash, 16 h) after which the free solution was pipetted off. The (wet) pellets were also mixed with the scintillant and assayed for radioactivity. The radioactivity measured in the pellets were: LC200, 152 Bq; LC200 in oil, 123 Bq; LC200 spr dr, 143 Bq; and LC200 spr dr & milled, 73 Bq.

The ‘theoretical max’ shows how much [^{3}H]cellopentaitol was available for binding in the tube at the beginning of A. Spr dr = spray dried. The smooth curves in A were created with SigmaPlot’s regression wizard: exponential rise to maximum, double, 4 parameter; according to the equation: $f = a\left(1 - e^{(-bx)}\right) + c\left(1 - e^{(-dx)}\right)$, where *a*, *b*, *c* and *d* are constants. The curves in B and C were drawn with: exponential decay, single, 2 parameter; according to the equation: $f = ae^{(-bx)}$, where *a* and *b* are constants.

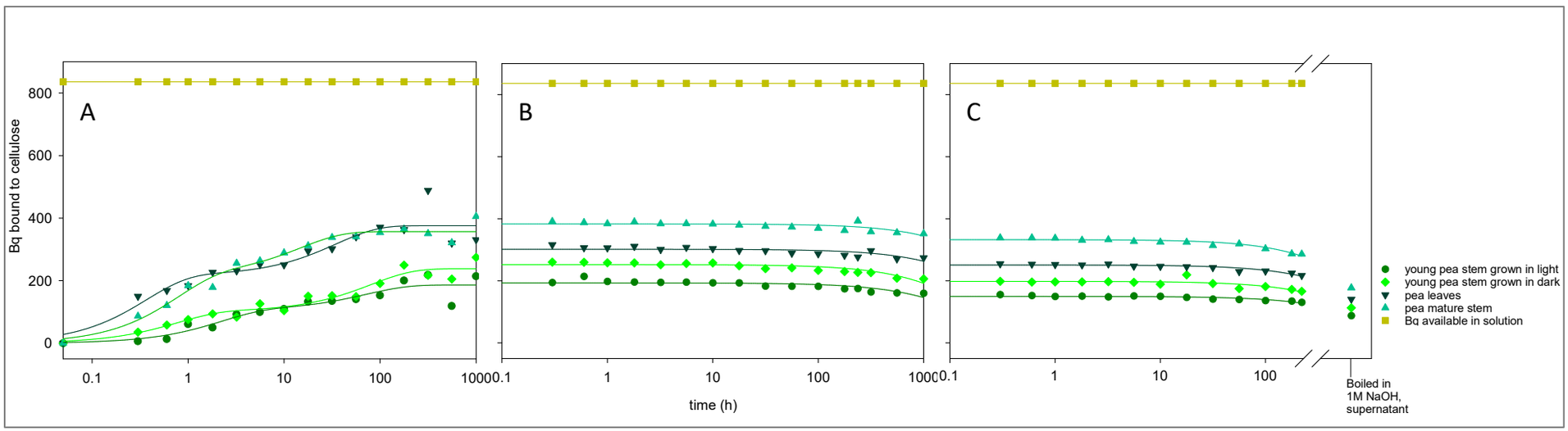

Figure 35. Adsorption and desorption of carrier-free [^{3}H]cellopentaitol to/from pea AIR samples from/to free solution.

Technical details as in Fig. 34 except for the samples were AIR. The radioactivity measured in the pellets at the end of C were: mature pea stem AIR, 30 Bq; pea leaves AIR, 49 Bq; (young) pea stem grown in dark, 54 Bq; and (young) pea stem grown in light, 55 Bq.

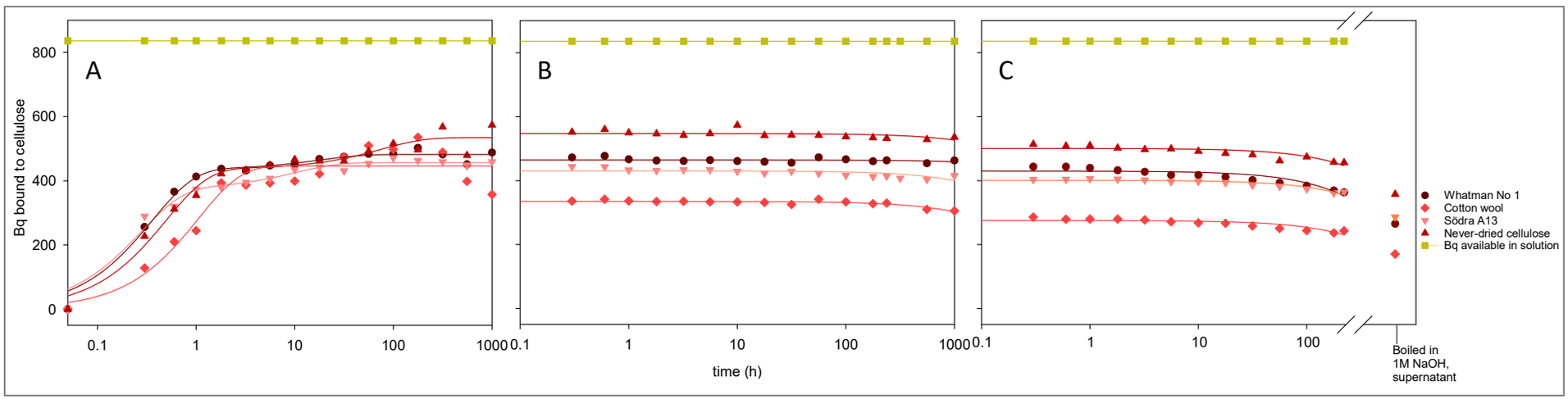

Figure 36. Adsorption and desorption of carrier-free [^{3}H]cellopentaitol to/from cellulose samples (the best adsorbers) from/to free solution.

Technical details as in Fig. 34, except for cotton wool in A was drawn with: exponential rise to maximum, single, 2 parameter, according to the equation: $f = a\left(1 - e^{(-bx)}\right)$, where *a* and *b* are constants, which was done so that the curve would not turn down after reaching the plateau. The radioactivity measured in the samples at the end of C were: never-dried cellulose, 217 Bq; Whatman No1 filter paper, 261 Bq; Södra A13, 229 Bq; and cotton wool, 107 Bq.

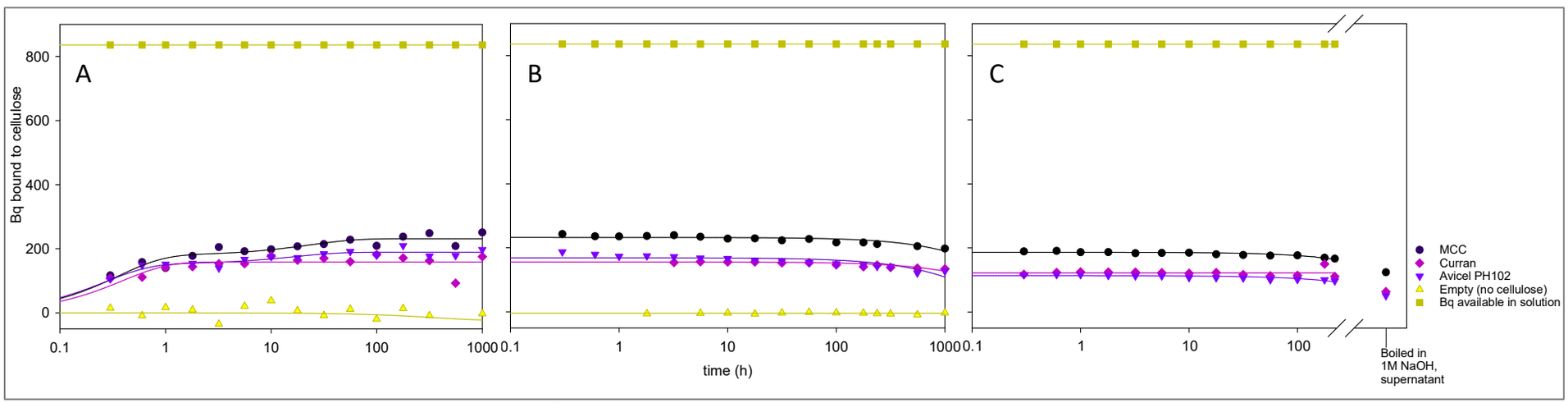

Figure 37. Adsorption and desorption of carrier-free [^{3}H]cellopentaitol to/from cellulose samples (the poorest adsorbers) from/to free solution.

Technical details as in Fig. 34. The radioactivity measured in the samples at the end of C were: MCC, 38 Bq; Curran by Cellucomp, 53 Bq; and Avicel PH102, 38 Bq.

3.3.1.2 Adsorption of [^{3}H]cellopentaitol to cellulose when competed by cellobiose

It is likely that the celluloses in the first experiment had many more accessible binding sites than [^{3}H]cellopentaitol molecules that could bind to them (each sample had 1.47 pmol of pentasaccharide and 5.6×10^8 pmol of Glc units in the cellulose giving a ratio of 1: 3.8×10^8), yet all the [^{3}H]cellopentaitol did not bind to the cellulose from the free solution. Also, the double hyperbolic shape of the adsorption curves indicated that the binding of [^{3}H]cellopentaitol to cellulose might be complex and happen in two phases. To study further the [^{3}H]cellopentaitol binding kinetics to cellulose, I wanted to find an affordable competitor that could bind on the available cellulose surfaces and study the adsorption of [^{3}H]cellopentaitol in that situation. The second experiment (Figs. 38–42), carried out to explore this, was similar to that described in 3.3.1.1 but with and without 50 mM cellobiose as a competitor for the binding of [^{3}H]cellopentaitol during the initial 1000-h adsorption phase. The desorption steps and boiling in NaOH were similar to the first experiment. After the NaOH treatment the pellets were washed with buffer and hydrolysed in TFA.

The adsorption of [^{3}H]cellopentaitol to cellulose/AIR pellets was noticeably competed by 50 mM cellobiose in LC200, Whatman No1 filter paper, cotton wool and never-dried cellulose (Fig. 38). Interestingly 50 mM cellobiose concentration inhibited the [^{3}H]cellopentaitol binding to Whatman filter paper by about one third whereas previously we had seen the [^{3}H]cellopentaitol binding half at this cellobiose concentration (Fry, unpublished). With Södra A13, pea leaves AIR, pea mature stem AIR, cauliflower stem AIR and cauliflower leaves AIR the cellobiose containing sample seems to reach the same level of adsorption of [^{3}H]cellopentaitol as the respective cellobiose-free samples at the end of the incubation time. In other words the cellobiose slowed down the binding of [^{3}H]cellopentaitol but did not prevent it.

Similar to the first experiment (Fig. 34–37), [^{3}H]cellopentaitol was most adsorbed by never-dried cellulose, Whatman No1 filter paper, Södra A13 and cotton wool (Fig. 38). Slightly more than half of the radioactivity available was bound by these celluloses during the adsorption step. The almost horizontal lines in the figures of the desorption steps (Fig. 39 and 40) indicate that the [^{3}H]cellopentaitol stayed bound to the cellulose, similar to the results of the first experiment (Fig. 34–37). However, a closer look shows that with most celluloses and AIRs about 25–50 % of the [^{3}H]cellopentaitol that had initially adsorbed to the pellets was desorbed during the first and second desorption steps (sum of grey and orange bars in Fig. 41 and 42). Boiling in NaOH released some more of the [^{3}H]cellopentaitol to free solution (yellow bars in Fig. 41 and 42). Even hydrolysing in TFA (blue bars in Fig. 41 and 42), which usually hydrolyses oligosaccharides to

monomers, did not release all the ^{3}H from the pellets (green bars in Fig. 41 and 42) which confirms further that the binding affinity of [^{3}H]cellopentaitol to the cellulose microfibril surface was very high.

Clearly 50 mM cellobiose is not ideal inhibitor for [^{3}H]cellopentaitol binding, although it does slow down and in some cases reduce the extent of binding of [^{3}H]cellopentaitol to cellulose. The binding curves were still double hyperbolic by shape which indicates that cellobiose does not change how the [^{3}H]cellopentaitol binds to the cellulose, which is possibly in two phases. The next experiment was necessary in order to find a better competitor for [^{3}H]cellopentaitol binding.

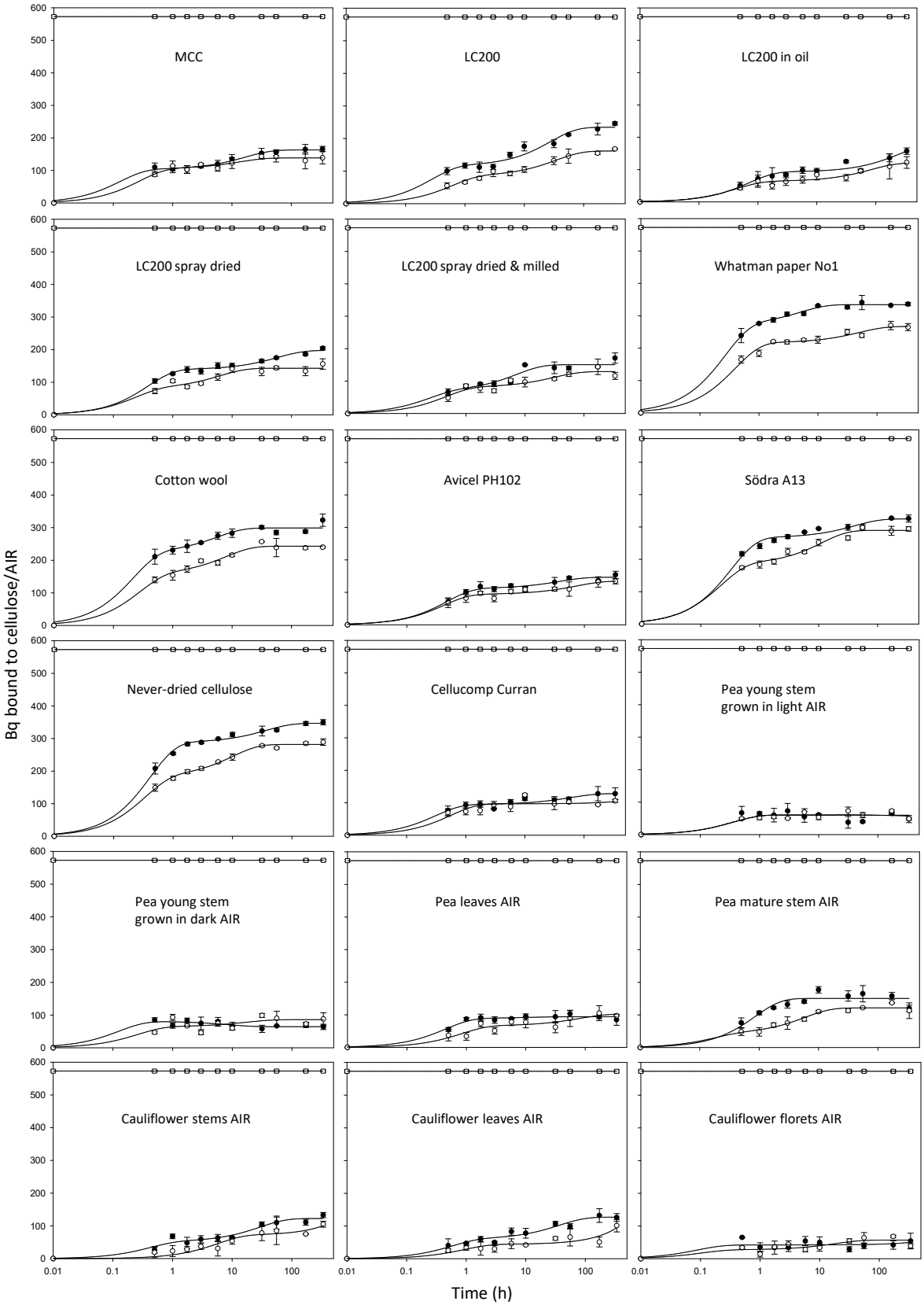
MCC
LC200
LC200 in oil
LC200 spray dried
LC200 spray dried & milled
Whatman paper No1
Cotton wool
Avicel PH102
Södra A13
Never-dried cellulose
Cellucomp Curran
Pea young stem grown in light AIR
Pea young stem grown in dark AIR
Pea leaves AIR
Pea mature stem AIR
Cauliflower stems AIR
Cauliflower leaves AIR
Cauliflower florets AIR
Bq bound to cellulose/AIR
Time (h)
0
100
200
300
400
500
600
0.01
0.1
1
10
100

Figure 38. Adsorption of [^{3}H]cellopentaitol to cellulose and AIR with and without cellobiose as a competitor of binding.

Technical details were similar to those Fig. 34A but with 580 Bq of [^{3}H]cellopentaitol (making 0.34 nM pentasaccharide) per sample. There were two sets of samples – one set with 50 mM cellobiose(○) and one without (●). Open squares show how much radioactivity was available for binding at time 0. The error bars show SEM, N=3 (technical repeats). The smooth curves were created with SigmaPlot's regression wizard: exponential rise to maximum, double, 4 parameter; according to the same equation as in Fig. 1: $f = a\left(1 - e^{(-bx)}\right) + c\left(1 - e^{(-dx)}\right)$, where *a*, *b*, *c* and *d* are constants.

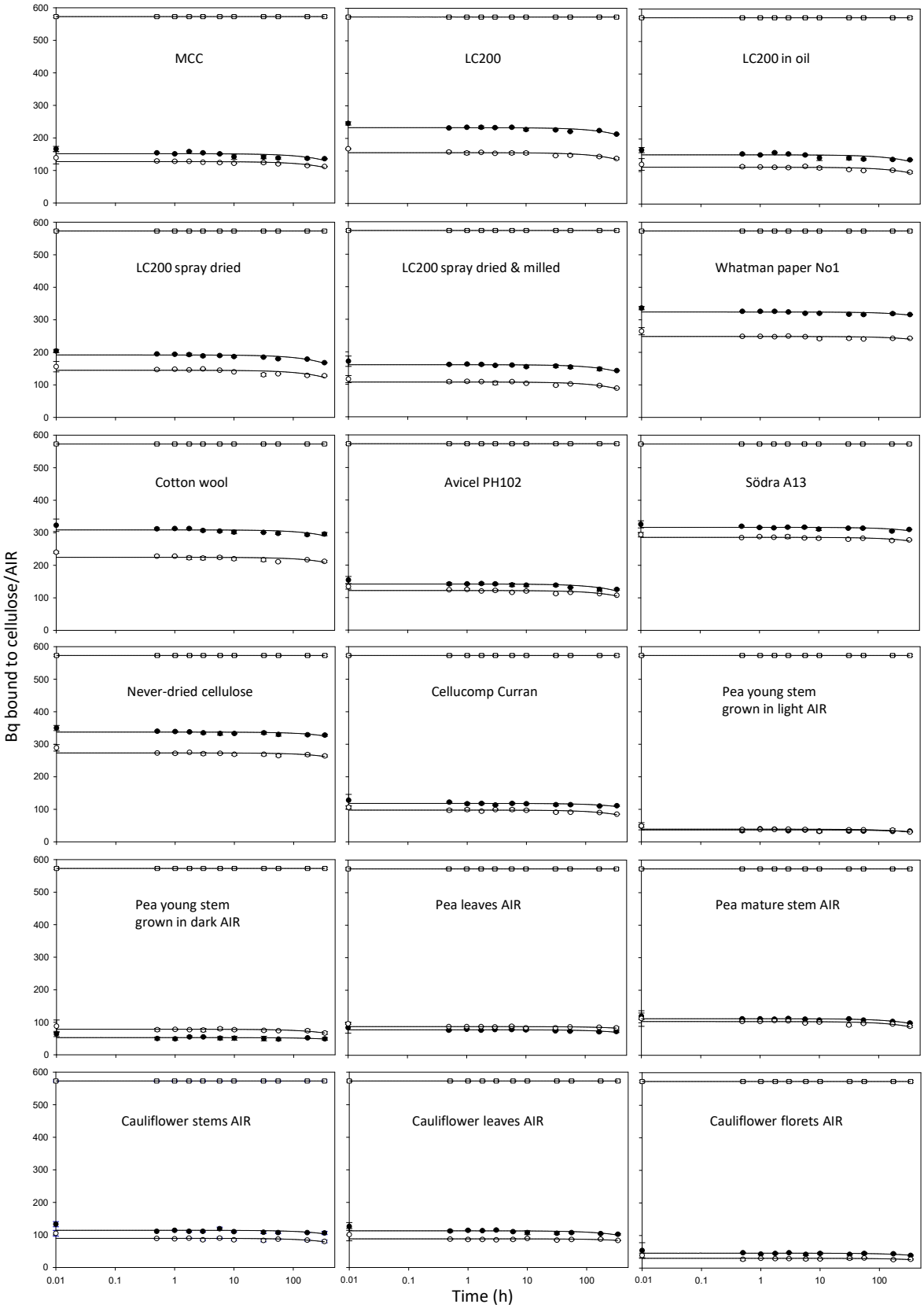
MCC
LC200
LC200 in oil
LC200 spray dried
LC200 spray dried & milled
Whatman paper No1
Cotton wool
Avicel PH102
Södra A13
Never-dried cellulose
Cellucomp Curran
Pea young stem
grown in light AIR
Pea young stem
grown in dark AIR
Pea leaves AIR
Pea mature stem AIR
Cauliflower stems AIR
Cauliflower leaves AIR
Cauliflower florets AIR
Bq bound to cellulose/AIR
Time (h)
0
100
200
300
400
500
600
0.01
0.1
1
10
100

Figure 39. Desorption of [^{3}H]cellopentaitol from cellulose and AIR to free solution.

Technical details as in Fig. 34B and 38, except for the samples were kept in tubes (not PolyPrep columns). The celluloses from the adsorption step (Fig. 38) were washed with buffer (three times with 3 ml for 30 min each) and fresh buffer was added (all lacking cellobiose). (○), With 50 mM cellobiose during adsorption; (●), without.

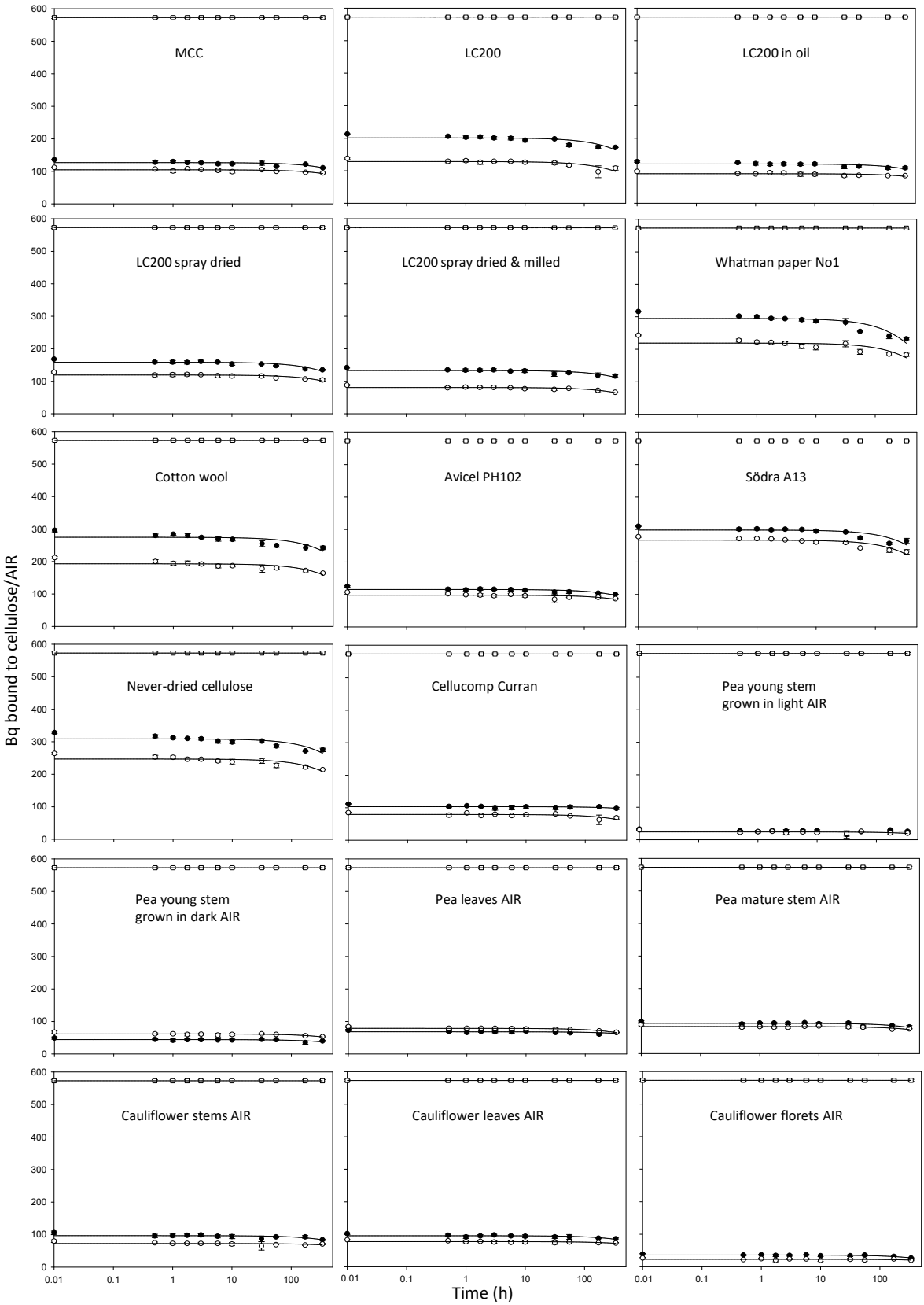

Figure 40. Desorption of [^{3}H]cellopentaitol from cellulose and AIR by competitive binding of 400 mM

cellobiose.

Technical details were as in Fig. 34C and 38 and 39.

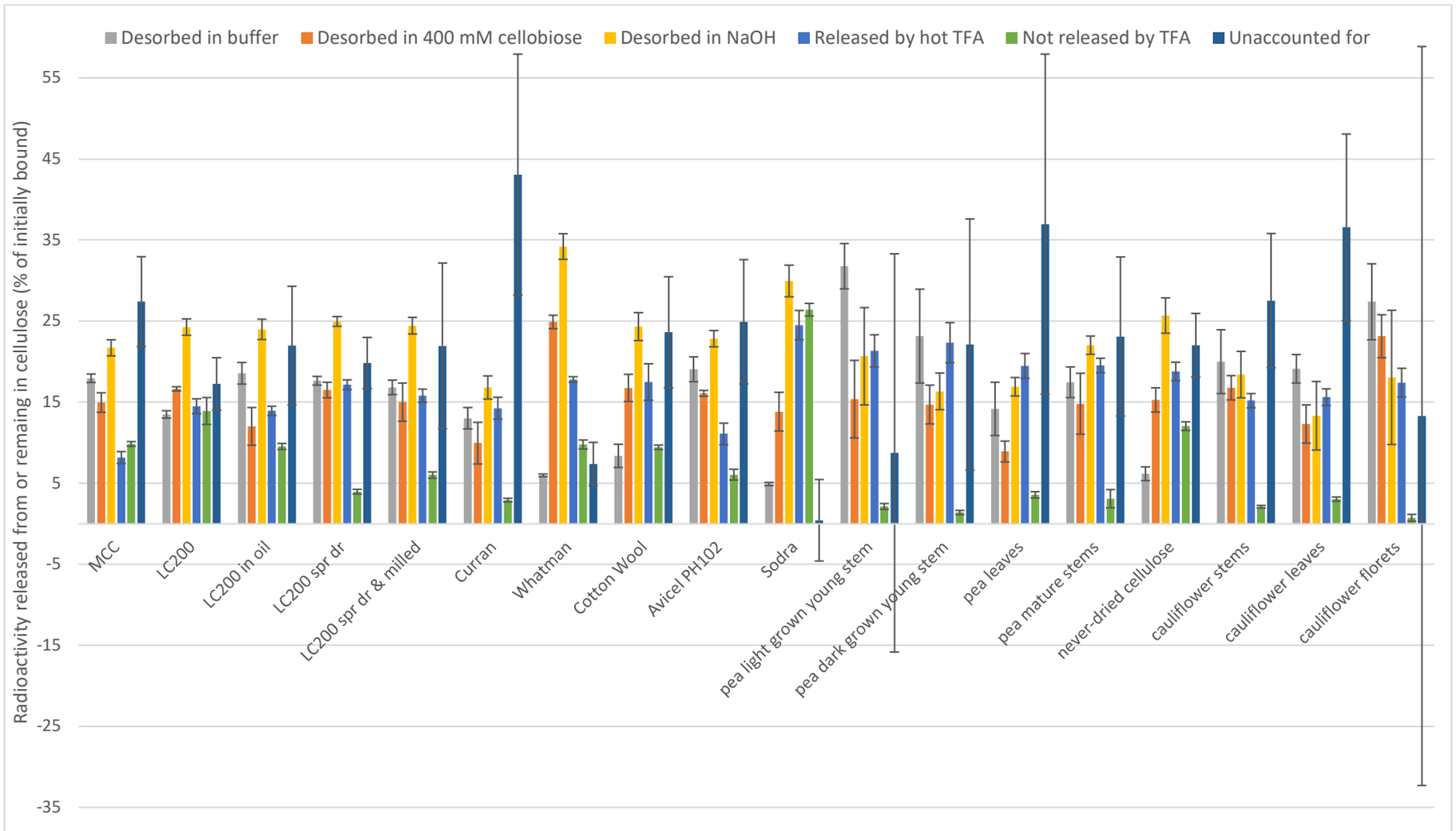

Figure 41. [^{3}H]Cellopentaitol desorbed from or remaining in pellets that did not have cellobiose during adsorption step.

All values are related to what adsorbed to the cellulose (Fig. 38) and desorption in buffer and desorption in 400 mM cellobiose are from Fig. 39 and 40, respectively. The error bars show SEM (N = 3, technical repeats) and the error bars of the 'unaccounted for' columns are sums of the errors of the whole experiment.

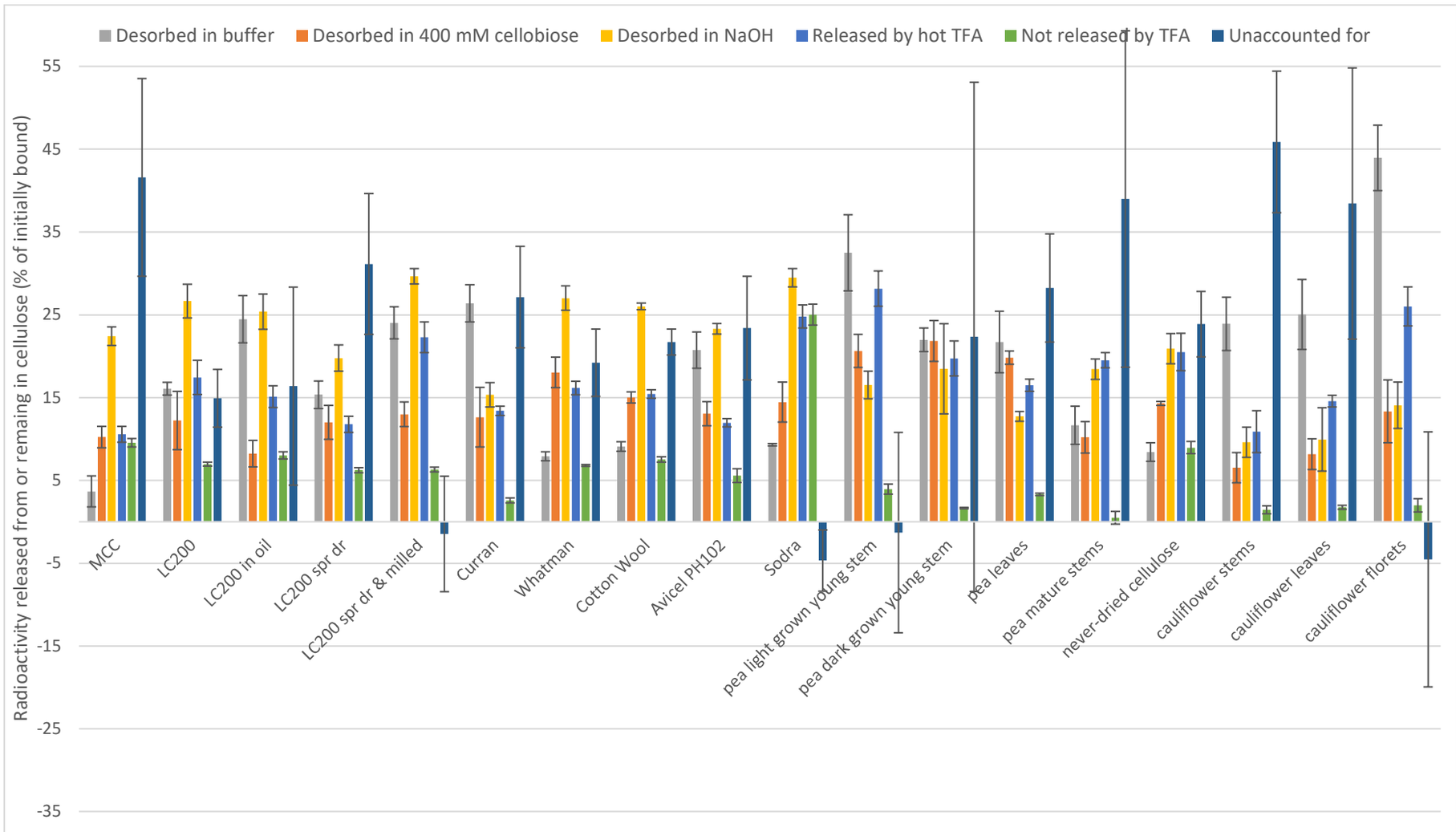

Figure 42. [^{3}H]Cellopentaitol desorbed from or remaining in pellets that had had 50 mM cellobiose during adsorption step.

Details as in Fig. 41 except for the initial adsorption of [^{3}H]cellopentaitol was competed by 50 mM cellobiose.

3.3.1.3 Binding of [^{3}H]cellopentaitol to filter paper when competed by the binding of cellopentaose

Using cellobiose as a competitor for [^{3}H]cellopentaitol binding was not ideal – cellobiose did not have the same binding affinity to cellulose as [^{3}H]cellopentaitol did because it was much shorter (disaccharide versus pentasaccharide) and thus formed fewer hydrogen bonds with cellulose and any bonding was extremely short-lived. Cellopentaose is likely to be a much better competitor for [^{3}H]cellopentaitol binding because it is the same length as [^{3}H]cellopentaitol and assumedly has very similar binding affinity to cellulose. To find a cellopentaose concentration where [^{3}H]cellopentaitol adsorption would be noticeably competed but not completely prevented, the third experiment (Figs. 43-45) was done using only Whatman filter paper as cellulose sample. The adsorption of 580 Bq of [^{3}H]cellopentaitol (SA of 8 MBq/µmol, resulting in 0.145 µM final concentration) to 15-mg paper pieces was competed with non-radioactive cellopentaose (0–3200 µM, each concentration in triplicate) in 0.5 ml of buffer. At intervals, samples were assayed for remaining soluble ^{3}H (Fig. 43).

"The adsorption phase" showed that when the binding of [^{3}H]cellopentaitol was not competed by cellopentaose, about two thirds of the radioactivity was adsorbed by the cellulose ('no cellopentaose' versus 'theoretical max' in Fig. 43) which was in line with the results of the first experiment (Fig. 34–37). The adsorption of [^{3}H]cellopentaitol was approximately halved when the cellopentaose concentration was 25 µM (Fig. 43) and this concentration of cellopentaose was chosen for the fourth experiment.

Although in the sample with 3200 µM cellopentaose there was much more cellopentaose than [^{3}H]cellopentaitol (73 pmol [^{3}H]cellopentaitol vs 1.6×10^6 pmol cellopentaose (and considering that not all of the molecules in the [^{3}H]cellopentaitol stock were labelled), <0.005% of pentasaccharide of the experiment was [^{3}H]cellopentaitol), still a clearly measurable 68 Bq of [^{3}H]cellopentaitol was adsorbed by cellulose (Fig. 43). Assuming cellopentaose and [^{3}H]cellopentaitol bind to cellulose with the same affinity, 68 Bq (which is about 8 pmol or 12% of the available [^{3}H]cellopentaitol in the solution) [^{3}H]cellopentaitol adsorption would mean 1.9×10^5 pmol pentasaccharide was adsorbed to cellulose. There was 15 mg of cellulose which is $9.3\text{x}10^7$ pmol Glc units which would mean that 0.2% of the Glc units in cellulose had bound a pentasaccharide – and here it is also worth mentioning that each pentasaccharide is likely bound to more than one Glc unit in the cellulose because the binding affinity is high (which must mean that several hydrogen bonds have formed), as pointed out

previously. Also all the Glc units would not be on the cellulose microfibril's outer surface and capable of interacting with the pentasaccharides because they would be in the middle of the microfibril and completely covered by other cellulose molecules. Therefore it would be justified to assume that all, or at least nearly all, the binding sites of the cellulose would be saturated by the pentasaccharides in the '3200 µM sample'. On the other hand, the '0 µM cellopentaose' sample bound 370 Bq which is 46 pmol [^{3}H]cellopentaitol which in relation to Glc units of cellulose is 0.00005% which is only a fraction when compared to the sample with 3200 µM cellopentaose. This further underlines the question why some of the [^{3}H]cellopentaitol never gets bound from the free solution by the cellulose (Fig. 34–37A, 38 and 43). To study if it was possible for more pentasaccharide to be adsorbed to cellulose from the free solutions, new 'binding sites' were provided by adding new paper. After the last sampling time, the paper was removed and new 7.5-mg pieces were added to the remaining 250 µl solution to test if the remaining radioactivity could be adsorbed from the free solution. Samples were assayed for soluble radioactivity after a further 0.5 and 20 h (Fig. 44).

Further adsorption of [^{3}H]cellopentaitol from old supernatants to new pieces of paper was detected at cellopentaose concentrations 3–50 µM (Fig. 44) but not significantly when the concentrations were lower. This suggests that the remaining radioactivity in free solution might not be [^{3}H]cellopentaitol but something else that co-migrates with cellopentaose and cellopentaitol on TLC plates in BAW 2:1:1 solvent system which was used for purification and quality control checking of the compound prior to the experiments. Also, when the cellopentaose concentration was higher than 100 µM (Fig. 44), no significant [^{3}H]cellopentaitol adsorption was detected from the free solution to the paper. This suggest that high concentrations of cellopentaose efficiently compete with the binding of [^{3}H]cellopentaitol to the cellulose.

When the papers that were first incubated with [^{3}H]cellopentaitol with and without cellopentaose (Fig. 43) were put to new tubes that contained fresh buffer free from cello-oligosaccharides, only a small fraction of the [^{3}H]cellopentaitol desorbed (Fig. 45). This is in line with the previous observations made of the [^{3}H]cellopentaitol desorption. Interestingly, the [^{3}H]cellopentaitol desorption seemed to be almost constant (20–40 Bq out of the originally available 580 Bq) no matter what the original cellopentaose concentration during the adsorption had been (Fig. 45). This is especially interesting because as calculated above, the sample with 3200 µM cellopentaose had adsorbed much more pentasaccharide than the sample that had no cellopentaose. If it is assumed that the binding affinity of cellopentaose is similar to that of [^{3}H]cellopentaitol, it would make sense

that the amount of pentasaccharide that desorbs would be proportional to the amount of pentasaccharide that adsorbed in the first place rather than being almost a constant as measured (Fig. 45).

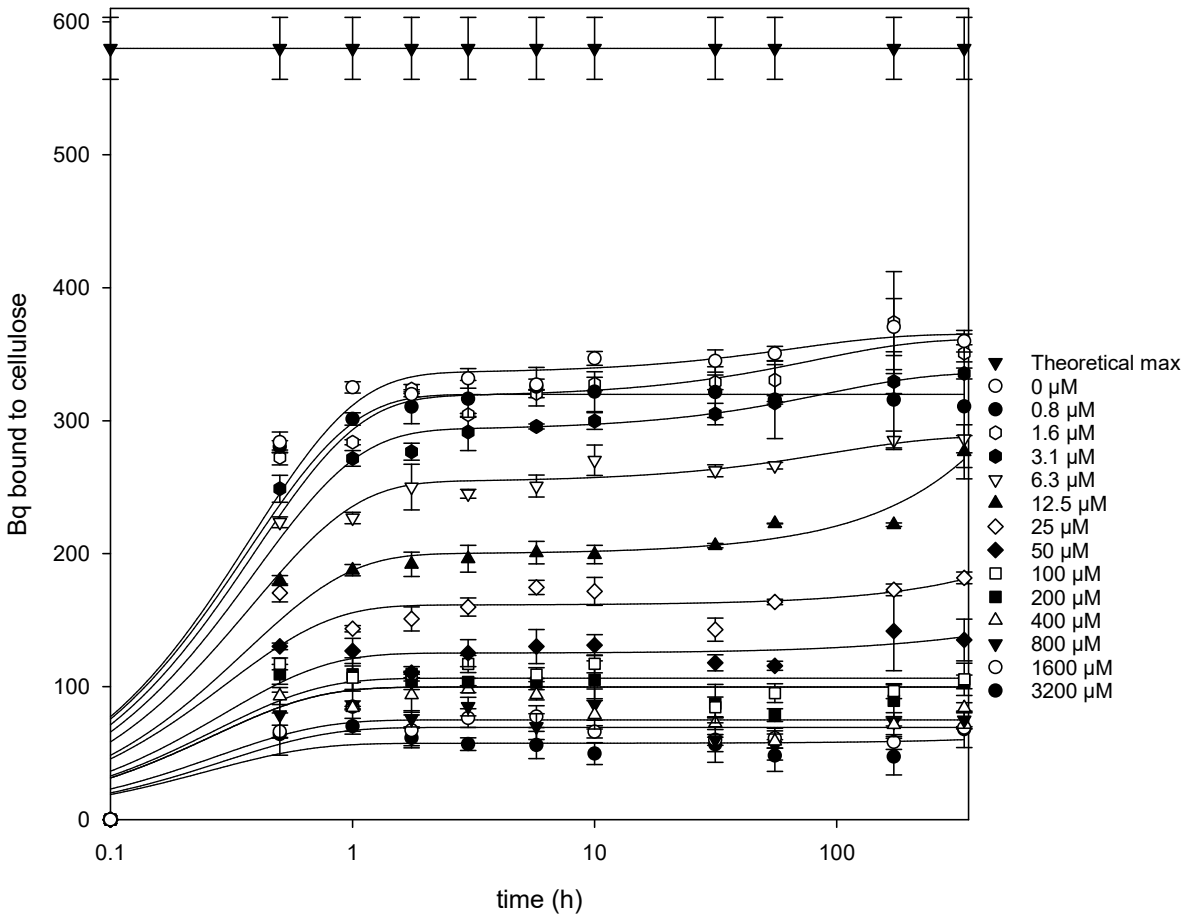

Figure 43. Adsorption of [^{3}H]cellopentaitol to cellulose (Whatman No 1 filter paper) when competed by a concentration range of cellopentaose.

Technical details as in Fig. 34A and 38 except for a range of concentrations (0–3200 µM) of cellopentaose was used instead of cellobiose. The [^{3}H]cellopentaitol was from a new batch which had a SA of 8 MBq/µmol, resulting in 0.25 µM final concentration. The paper pieces were 15 mg each and the volume 0.5 ml (giving the same weight:volume ratio (30 mg/ml) as in the previous experiments). The samples taken from the free supernatants were 20 µl each which were mixed with 980 µl of water and 10 ml of scintillant. The tubes were mixed on a shaker instead of a wheel to prevent the paper pieces from breaking. The error bars show SEM, N=3 (technical repeats). The smooth curves were created with SigmaPlot's regression wizard: exponential rise to maximum, double, 4 parameter; according to the equation: $f = a\left(1 - e^{(-bx)}\right) + c\left(1 - e^{(-dx)}\right)$, except for 0.8 µM, 100 µM, 200 µM, 800 µM and 1600 µM cellopentaose, which were drawn with: exponential rise to maximum, single, 2 parameter, according to the equation: $f = a\left(1 - e^{(-bx)}\right)$, which was done to avoid the curve from turning down after reaching the plateau.

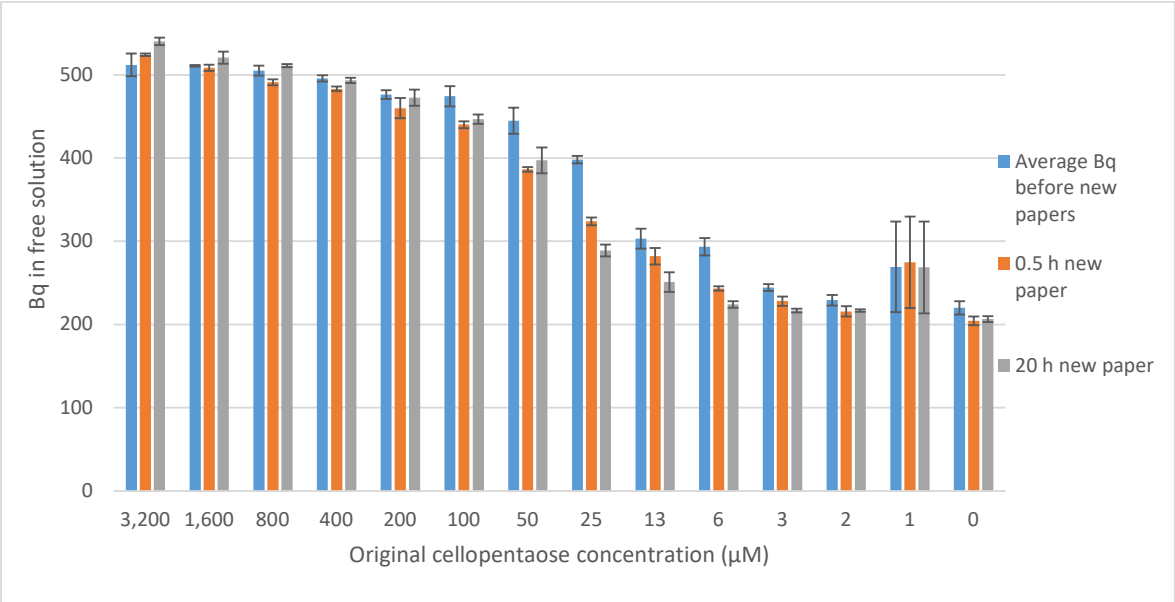

Figure 44. Adsorption of [^{3}H]cellopentaitol to new pieces of cellulosic paper.

New pieces of Whatman No1 filter paper (7.5 mg each) were added to the remaining supernatants from Fig. 43 (250 µl each). The tubes were incubated on a shaker and the supernatant was sampled at 0.5 h and 20 h as in Fig. 43.

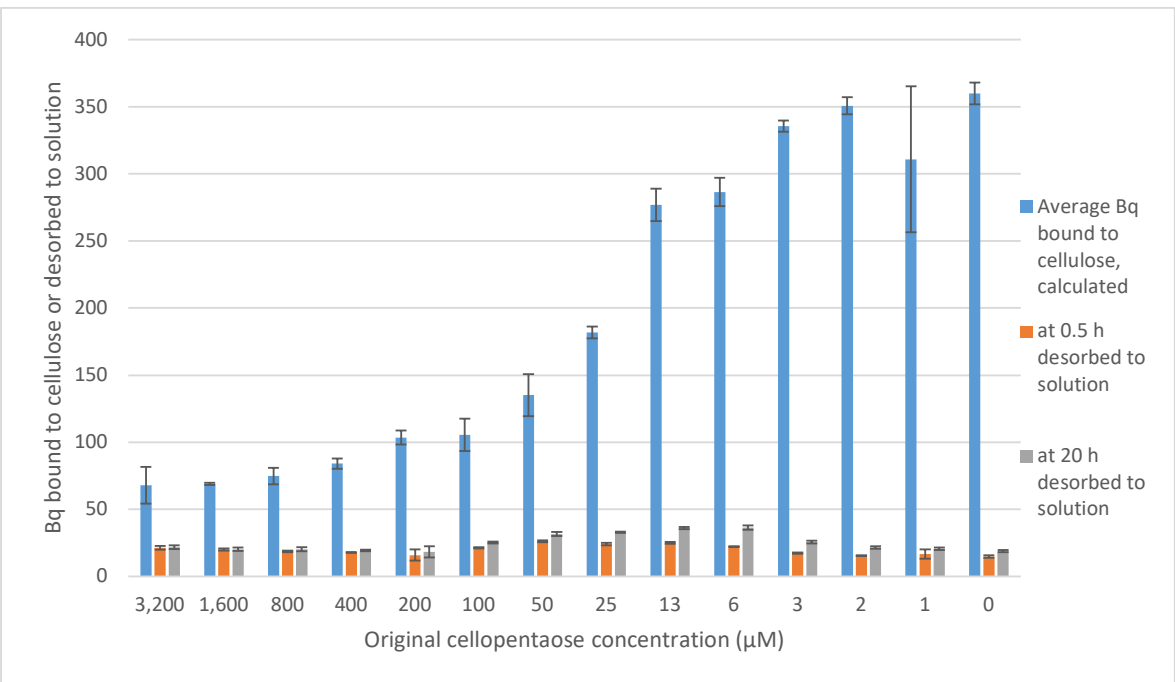

Figure 45. Desorption of [^{3}H]cellopentaitol from paper to free solution.

The paper pieces from Fig. 43 were put to new tubes containing buffer that did not contain cellopentaose. The supernatants were sampled at 0.5 h and 20 h as in Fig. 43 and 44.

3.3.1.4 Binding of [^{3}H]cellopentaitol to different celluloses and AIRs when competed by the binding of 25 µM cellopentaose

Based on 3.3.1.3, 25 µM cellopentaose was chosen for use in the fourth experiment in order to study the pentasaccharide adsorption to all the cellulose and AIR samples when the oligosaccharide was provided in excess which, in turn, could work as an indicator for accessibilities of the celluloses. The adsorption of 500 Bq of [^{3}H]cellopentaitol (SA 8 MBq/µmol, resulting in 0.125 µM concentration) when competed by 25 µM cellopentaose to 15 mg of the cellulose and AIR in 0.5 ml of buffer (i.e. 12.56 nmol pentasaccharide + 93,000 nmol cellulosic Glc residues, which applies when assuming the sample is pure cellulose which, however, is not the case with Curran® and AIRs) was observed (Fig. 46–50).

In this experiment most [^{3}H]cellopentaitol was adsorbed by Södra A13, never-dried cellulose, Whatman No1 filter paper and cotton wool (Fig. 49) which is in line with the results of the previous experiments (Fig. 34A–37A and Fig. 38). However, also MCC and Avicel PH102 celluloses adsorbed a lot of [^{3}H]cellopentaitol (24% and 22%, respectively) (Fig. 50) which was unexpected based on Fig. 37A and 38. Although the [^{3}H]cellopentaitol used in the third (Fig. 43) and fourth (Fig. 46–50) experiment was from a different batch than in the previous experiments (Fig. 34–38), the observation of some of the [^{3}H]cellopentaitol never binding to cellulose stayed the same. In the third experiment 25 µM cellopentaose concentration was shown to halve the [^{3}H]cellopentaitol binding (Fig. 43) which explains why only 52% of the [^{3}H]cellopentaitol was bound by the best binder, Södra A13, in the fourth experiment (Fig 49).

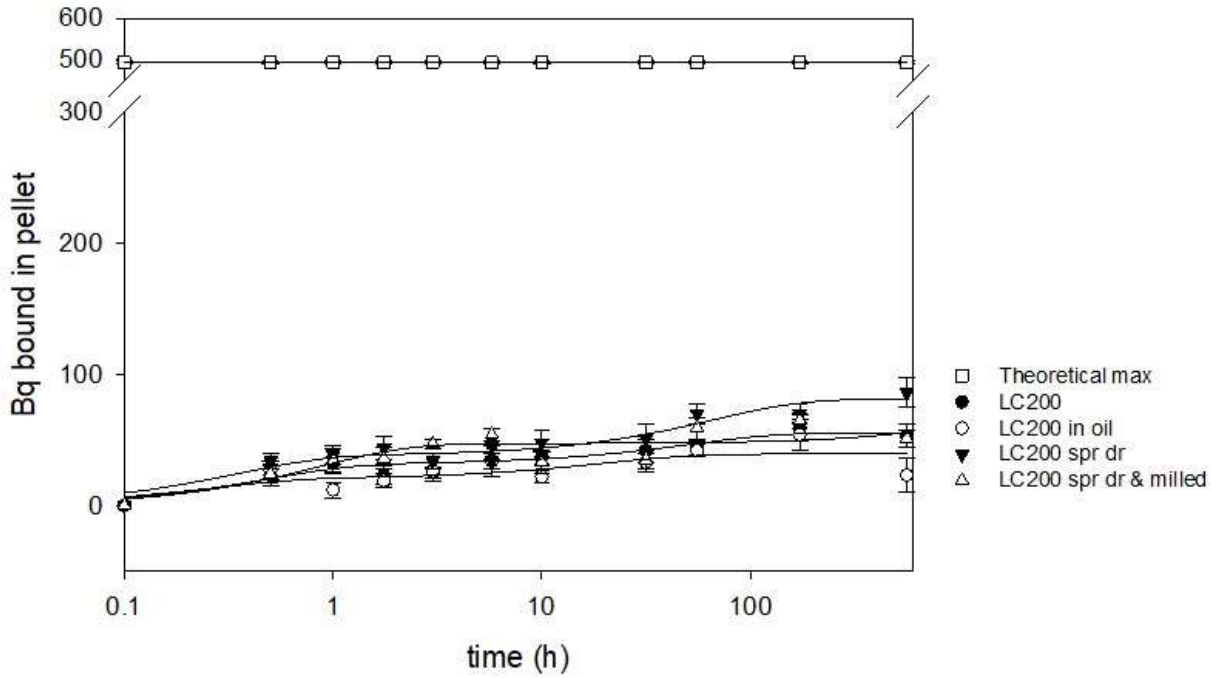

Figure 46. Adsorption of [^{3}H]cellopentaitol to LC200 celluloses when competed by 25 μM cellopentaose.

Technical details as in Fig. 43 except that each sample was incubated in buffer with 500 Bq (making 0.125 μM) of [^{3}H]cellopentaitol and 25 μM cellopentaose. The shaking of the tubes and the sampling were as in Fig. 43 but this time all the tubes other than Whatman paper and the 'no cellulose' controls were centrifuged at 15000 g for 7 min before the supernatant samples were taken. After sampling the cellulose samples were resuspended by vortex and returned to the shaker. . The error bars show SEM, N=3 (technical repeats). The smooth curves were created with SigmaPlot's regression wizard: exponential rise to maximum, double, 4 parameter; according to the equation: $f = a\left(1 - e^{(-b\ )}\right) + c\left(1 - e^{(-dx)}\right)$.

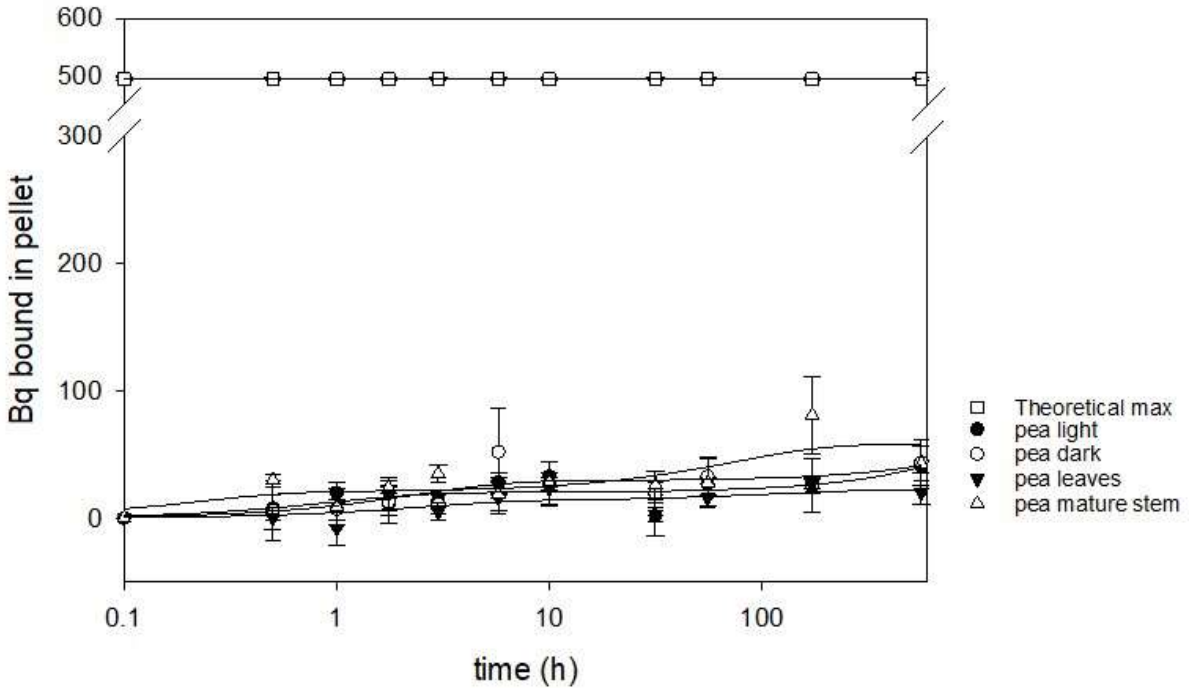

Figure 47. Adsorption of [^{3}H]cellopentaitol to pea AIRs when competed by 25 µM cellopentaose.

Technical details as in Fig. 46.

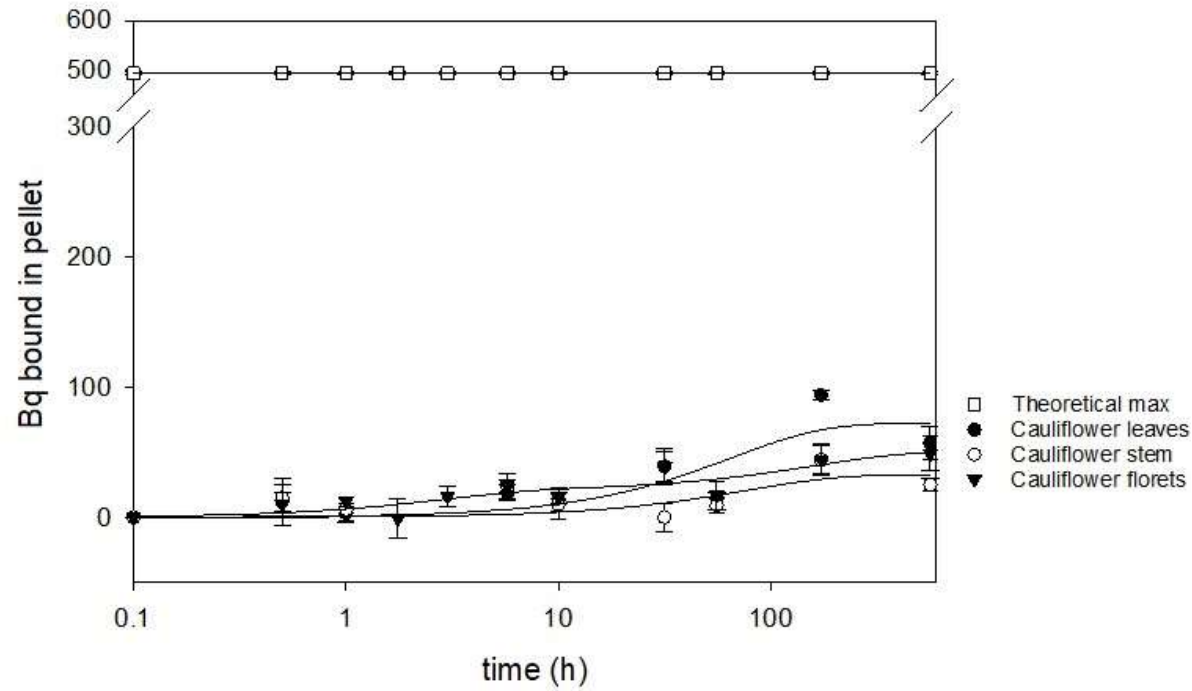

Figure 48. Adsorption of [^{3}H]cellopentaitol to cauliflower AIRs when competed by 25 μM cellopentaose.

Technical details as in Fig. 46.

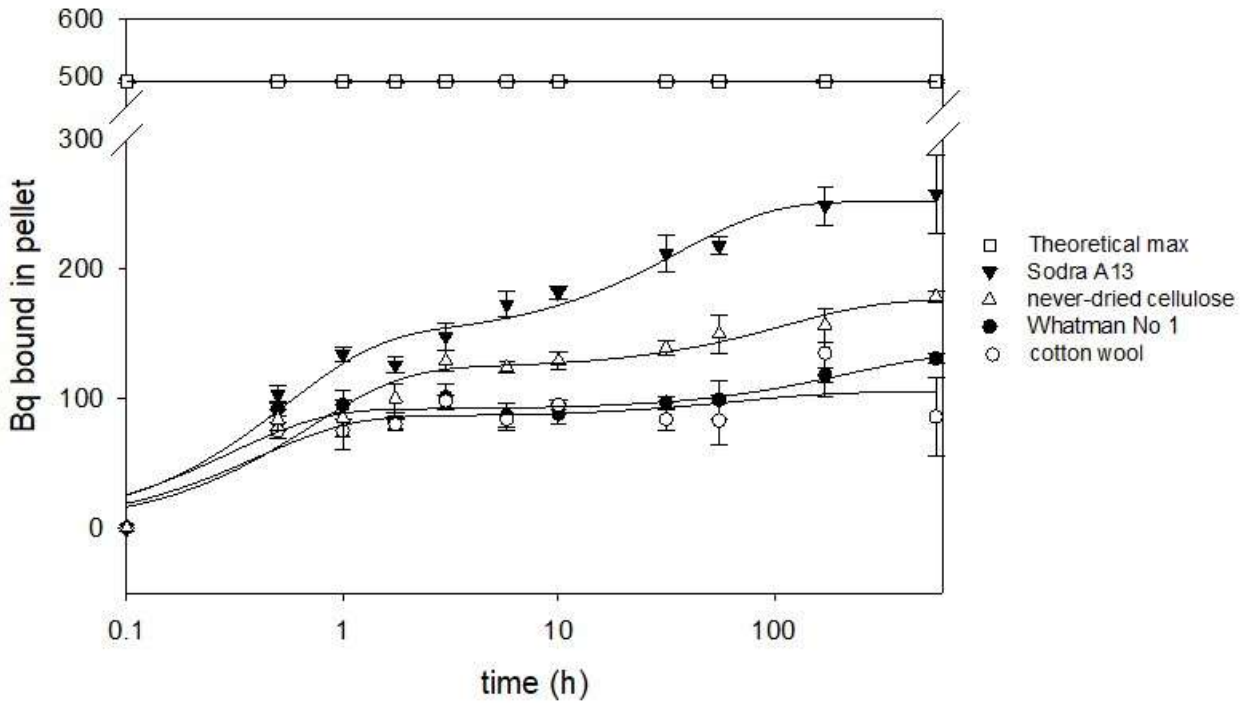

Figure 49. Adsorption of [^{3}H]cellopentaitol to cellulose (the best adsorbers) when competed by 25 μM cellopentaose.

Technical details as in Fig. 46.

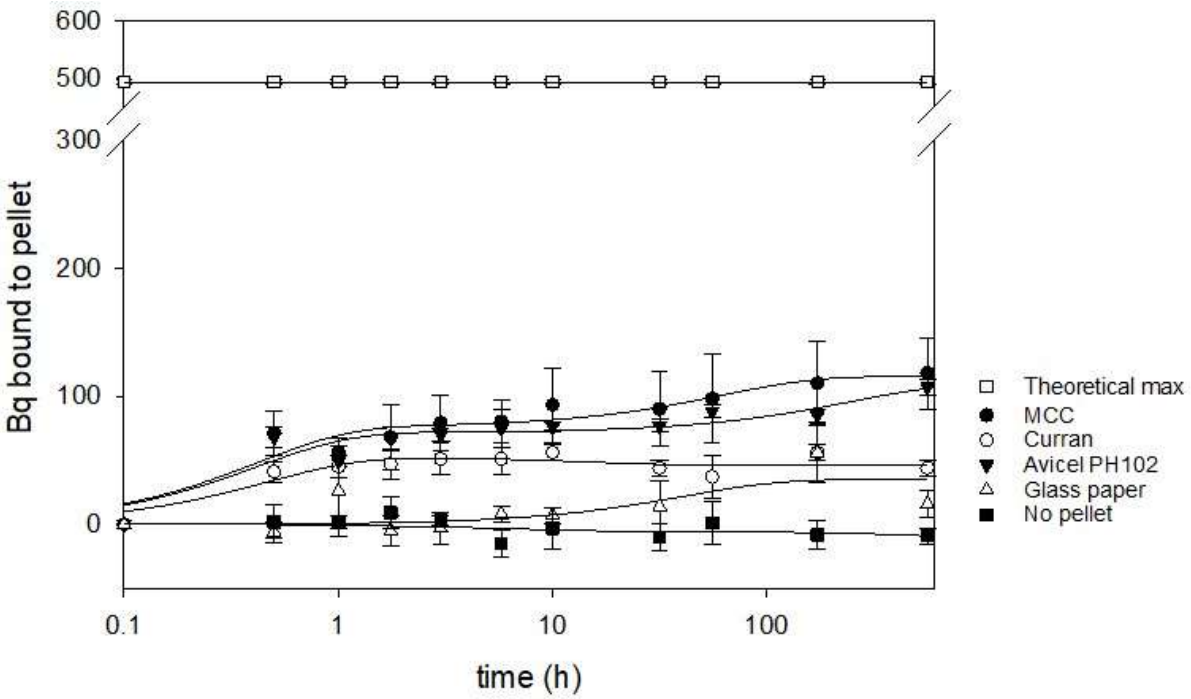

Figure 50. Adsorption of [^{3}H]cellopentaitol to cellulose (the poorest adsorbers) when competed by 25 µM cellopentaose.

Technical details as in Fig. 46.

When I put the constants *a*, *b*, *c* and *d* (given by Sigmaplot's regression wizard) in the equation used for drawing the smooth curves in Fig. 46–50 and set the time to 1,000,000 hours (effectively 'infinity'), I could estimate the final maximum adsorption, i.e. when the plateau has been reached, and these values were comparable to the last data point collected at 560 h. The comparison showed that MCC, LC200, LC200 spray dried, Whatman filter paper, Avicel PH102, Södra A13, never-dried cellulose, Curran, pea leaf AIR, cauliflower stem AIR and cauliflower floret AIR had reached the plateau by 560 h, whereas LC200 processed in oil, LC200 spray dried & milled, cotton wool, young pea stems grown in light AIR, young pea stems grown in dark AIR, mature pea stem AIR and cauliflower leaf AIR had not yet reached the plateau by the end of the adsorption experiment. For all the samples the adsorption at 1,000,000 h was used in Fig. 51 except for LC200 pray dried & milled and the young pea stem AIRs to which the equation gave impossibly high (in the magnitude of 10 000 – 16 000 Bq) adsorptions at 1,000,000 h, and for these samples adsorption at 560 h was used instead. (I would assume the equation is not ideal for these three samples because the data did not really approximate the equation used).

Fig. 51 compares the first and fourth experiments to indicate the relative cellopentaose effect as an inhibitor of [^{3}H]cellopentaitol binding. (Cauliflower AIRs could not be compared because they did not exist when the first experiment was done). Cellopentaose had the biggest competitor effect with LC200, LC200 processed in oil and the pea AIRs (especially with pea leaf AIR). The relative difference between cellopentaose-competed and cellopentaose-free adsorptions was smallest in Avicel PH102 and Södra A13 samples which is very interesting because Södra A13 adsorbed most [^{3}H]cellopentaitol throughout the experiments whereas Avicel PH102 was usually among of the poorest adsorbers out of the commercial celluloses (Fig. 34–37A, 38 and 36–51).

The level of adsorption in second experiment was different from the first experiment in the cases of LC200 processed in oil, cotton wool, never-dried cellulose and all the pea AIRs; in all the other samples (when a comparison is possible) the [^{3}H]cellopentaitol adsorption stayed proportionally the same in the first and second experiment (Fig. 51). The young pea stem AIRs had much lower levels of [^{3}H]cellopentaitol adsorption in the second experiment when compared to the first one, and the adsorption of [^{3}H]cellopentaitol when competed by binding of cellopentaose is almost the same as the adsorption of the second, competitor-free, experiment (which is also the case with the cauliflower floret AIR) (Fig. 51).

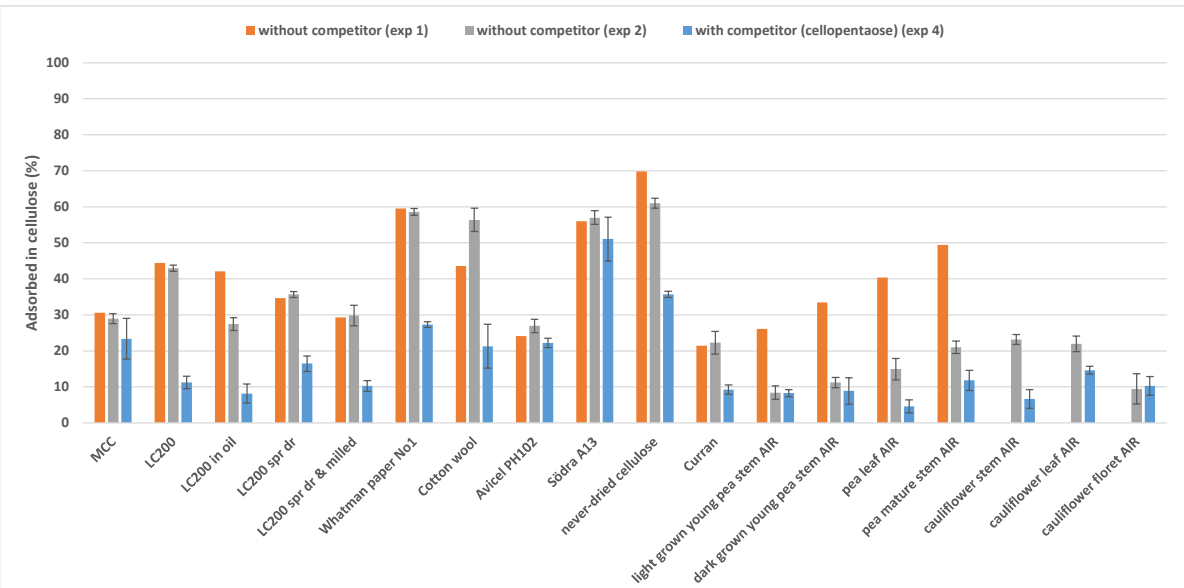

Figure 51. Proportion of [^{3}H]cellopentaitol adsorbed to cellulose and AIR during the first, second and fourth experiment.

The bars show how much of [^{3}H]cellopentaitol was adsorbed to cellulose and AIR samples in relation to what was available in the free solution (Fig. 34–37A, 38 and 46–50). Orange bars show the adsorption recorded at 1,000 h in the first experiment (Fig. 1–4A) which was done without inhibitor/competitor, grey bars at 560 h of the second experiment (without inhibitor) (Fig. 38), and blue bars at infinite time (1,000,000 h, except LC200 spr dr & milled and the young pea stem AIRs which show at 560 h) (Fig. 46–50) which was done with cellopentaose as an inhibitor. The infinite time was done by inserting the values of constants *a, b, c* and *d* (defined by Sigmaplot's regression wizard) in the equation $f = a\left(1 - e^{(-bx)}\right) + c\left(1 - e^{(-dx)}\right)$ used for drawing the smooth curves of Fig. 46–50 to ensure the adsorption had reached a plateau. The error bars show the standard error as % (please note there were no error bars (no multiple samples) in the first experiment), N=3. Spr dr = spray dried, exp = experiment.

Throughout all experiments on accessibility of cellulose to [^{3}H]cellopentaitol, the pea mature stem AIR was the best adsorber from the category of pea AIR samples (Fig. 35, 38 and 47), followed by the pea leaf AIR (Fig.35 and 38) and then the young pea stem AIRs which did not behave differently though they had been grown in different conditions (light versus dark in Fig. 35, 38 and 47). That could be explained by the presence of secondary cell walls in mature stem and leaf samples, and mature stems having a woody structure and therefore having the biggest proportion of cellulose in its cell walls (primary cell walls consist of 15–40% cellulose whereas secondary walls contain 40–90% cellulose (Fry, 1988; Cosgrove and Jarvis, 2012; Timell, 1967)). With cauliflower samples the leaf and stem AIRs adsorbed slightly more [^{3}H]cellopentaitol than the floret AIR in Fig. 38 but in Fig. 48 the leaf AIR was the best adsorber. Overall, the pea and cauliflower AIRs (Fig. 35, 38, 47, 48 and 51) and Cellucomp's Curran® (Fig. 37, 38, 50 and 51) adsorbed least [^{3}H]cellopentaitol throughout the experiments (excluding pea mature stem AIR and pea leaf AIR in the first experiment) which could be because they were not pure cellulose. Also, the cellulose in the AIRs could have been completely covered (i.e. occupied and not available to bind [^{3}H]cellopentaitol) by other cell wall polymers such as hemicelluloses and pectins. It would be interesting to test whether, if I used a larger mass of Curran® and the AIRs (bringing the amount of cellulose in the samples to the constant of 90 mg), the total adsorption of [^{3}H]cellopentaitol would increase. Another option for further experiments would be to hydrolyse or digest off the other cell wall polymers from the AIRs, so that only the cellulose fraction would remain, and then test if the cellulose fractions form various tissue types would differ in their [^{3}H]cellopentaitol accessibility.

All the LC200 samples adsorbed [^{3}H]cellopentaitol similarly to each other (Fig. 34, 38, 46 and 51) which was usually about half of what the best adsorbers (Fig. 34, 38, 49 and 51) did. In the first two experiments (Fig. 34, 38 and 61) out of the group of LC200 samples, the original LC200 adsorbed most [^{3}H]cellopentaitol but in the last experiment it was the second best adsorber (Fig. 46 and 51).

None of the other LC200 samples behaved as consistently throughout the experiments – for instance, in the first experiment LC200 processed in oil adsorbed almost as much [^{3}H]cellopentaitol as LC200 (Fig. 34 and 51) but in the last experiment it was the poorest adsorber (Fig. 46 and 51). This tells us that further processing (whether it was in oil or water) or milling did not change the accessibility of the cellulose dramatically. Even the milled sample would still have a large excess of available binding sites for the [^{3}H]cellopentaitol. The majority of the binding sites would not be destroyed by the further processing or milling but on the other hand no new binding sites seemed to be introduced by the increase of the surface area.

Throughout the experiments the best adsorbers were never-dried cellulose, Södra A13, Whatman No 1 filter paper and cotton wool (Fig. 36, 38, 49 and 51), usually in this order except that Södra A13 was clearly the best adsorber in the last experiment (Fig. 49 and 51). Even the best adsorbers could not adsorb all the pentasaccharide from the free solution, and in every experiment at least one third of it remained in the solution (Fig. 36, 38, 49 and 51). When new cellulose was offered to the remaining unbound [^{3}H]cellopentaitol, only a small fraction of the pentasaccharide could adsorb from the solution (Fig. 44) which underlines the doubt that the [^{3}H]cellopentaitol purified and quality checked by TLC could contain an impurity which could be a tritiated molecule that migrates on TLC together with [^{3}H]cellopentaitol but is unable to bind to the cellulose.

MCC and Avicel were among the poorest adsorbers out of commercial celluloses in the first two experiments (Fig. 37, 38 and 51) but surprisingly adsorbed more [^{3}H]cellopentaitol in the presence of non-radioactive cellopentaose, reaching almost same adsorption level as cotton wool (Fig. 51 and 50 versus 49).

The first three experiments showed that once [^{3}H]cellopentaitol binds to the cellulose, it does not resolubilise easily (Fig. 34–37, 39, 40 and 45). Only small fractions of it can be removed from cellulose by soaking in buffer for 1000 hours or in buffer containing concentrated cellobiose (Fig. 34–37, 39–42 and 45), boiling in alkali or hydrolysing with TFA (Fig. 41 and 42), and even a combination of these methods still left detectable radioactivity in the cellulose pellets (Fig. 34–37, 41 and 42), indicating that [^{3}H]cellopentaitol binds so strongly to the cellulose microfibril that it actually becomes part of it.

The ability of the [^{3}H]cellopentaitol to irreversibly integrate into cellulose microfibrils supports the theory that in cell walls, just after synthesis, some regions in cellulose microfibrils couple with neighbouring microfibrils (instead of hemicelluloses that may usually cover and tether the microfibrils; Fry, 1989) forming a cluster of cellulosic microfibrils hydrogen bound to each other (Chinga-Carrasco, 2011; Jarvis, 2018). Cellulose fibres formed from several microfibrils can form only if the cellulose synthase complexes are close to each other and are moving in the same direction in the cell wall at the time of the cellulose synthesis (Chinga-Carrasco, 2011). The cellulose fibres have a bigger diameter than a microfibril (Chinga-Carrasco, 2011 and Jarvis, 2018). Especially conifer and bamboo wood have aggregated microfibrils (Jarvis, 2018) and since we do not know the source for most of the commercial celluloses, it seems plausible that these aggregates would be present in the commercial cellulose samples and that the differences in the accessibilities could be partially explained by cellulose microfibril fibres having a greater diameter and thus smaller surface-to-volume ratio. Cotton wool microfibrils have a greater diameter than microfibrils sourced from most plants (Jarvis, 2018) which makes it interesting that cotton wool has an ability to adsorb so much [^{3}H]cellopentaitol.

3.3.2 Results - accessibility to cellulase

In Section 3.3.1 I discussed the accessibility of cellulose to cellopentaitol and other oligosaccharides. However, cellulose would also be in contact with various other substances when incorporated in cell walls, mixed into chocolate or in contact with saliva. The other substances could be much larger than the oligosaccharides studied, such as proteins, including enzymes. If the enzymes are able to bind to the cellulose, such binding could be easier to amorphous than crystalline regions of cellulose and therefore the accessibility to highly crystalline cellulose could differ from the accessibility to more amorphous cellulose preparations. For studying the accessibility of the celluloses to a relevant enzyme, I assayed their digestibility by endo-cellulase.

3.3.2.1 Method development for cellulase digestion

For exploring the suitability of the method, I tested the digestion of 150-mg pieces of Whatman No 1 filter paper. Buffer-washed paper was treated with a cellulase preparation (that does not digest xyloglucan) in buffer on a mixing wheel, and the solubilised carbohydrate was anthrone-assayed at intervals by reference to a dilution series of glucose standards.

The standard curve (Fig. 52) shows that a hexose concentration of 50 µg/ml gave A_{620} ~ 1 in the anthrone assay and that the curve was approximately linear for concentrations lower than this. The error bars were acceptably small. For analysis of the cellulase digests it was decided to dilute the supernatants to soluble sugar concentrations less than 50 µg/ml.

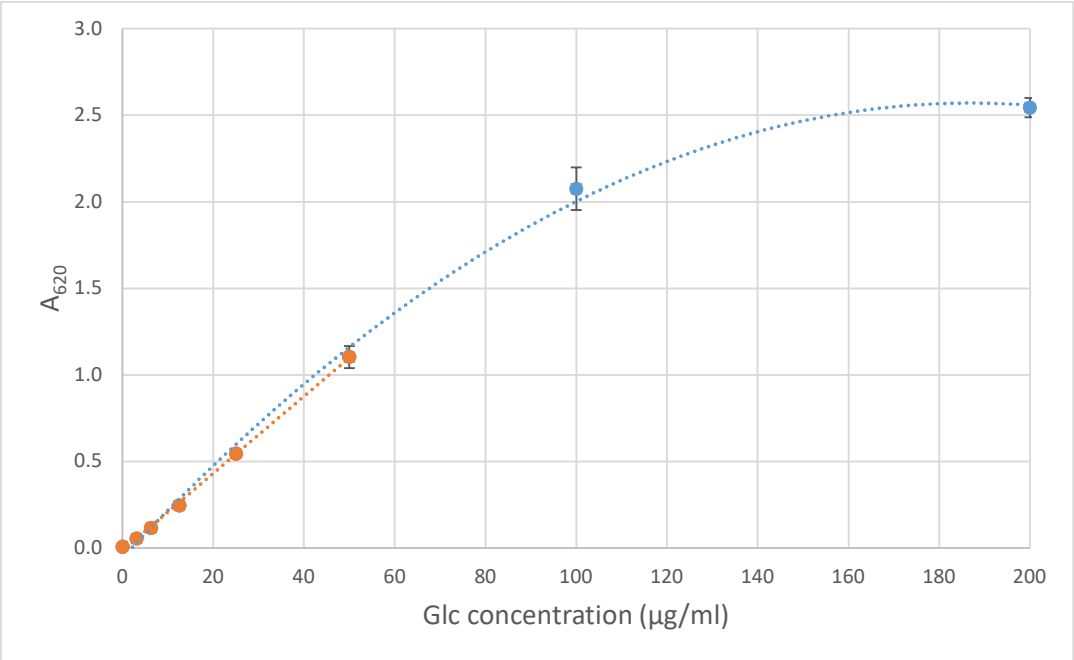

Figure 52. Standard curve for hexoses in free solution.

A dilution series of glucose was assayed by the anthrone method by mixing 1 ml of 0.2% (w/w) anthrone dissolved in concentrated sulphuric acid with 0.5 ml of glucose solution, heating to 100°C for 5 min and reading A_{620} after cooling down. N for each concentration was 3 (technical repeats) and the error bars show SEM. The blue curve was drawn with all samples analysed, the orange curve shows the range of samples where the correlation was approximately linear.

The digestion of Whatman filter paper (Fig. 53) was initially rapid, but started slowing down after about 6 h. The occasional large error bars were possibly due to the pellet being disturbed during pipetting or some contaminating lint in the test tubes and do not affect the trend. For reference, complete hydrolysis of the cellulose (150 mg / 6 ml) to glucose would give a soluble hexose concentration of 27,800 µg/ml in Fig. 53, so the digestion was ~0.7% complete by 200 h, which shows that only a fraction of the cellulose had been hydrolysed. It is likely that cellulase had digested the most accessible parts of cellulose, such as amorphous cellulose, by 200 h but most of the microfibrils of the crystalline cellulose were still intact. A 3-h digestion time was chosen for the future experiments as the reaction had definitely not plateaued.

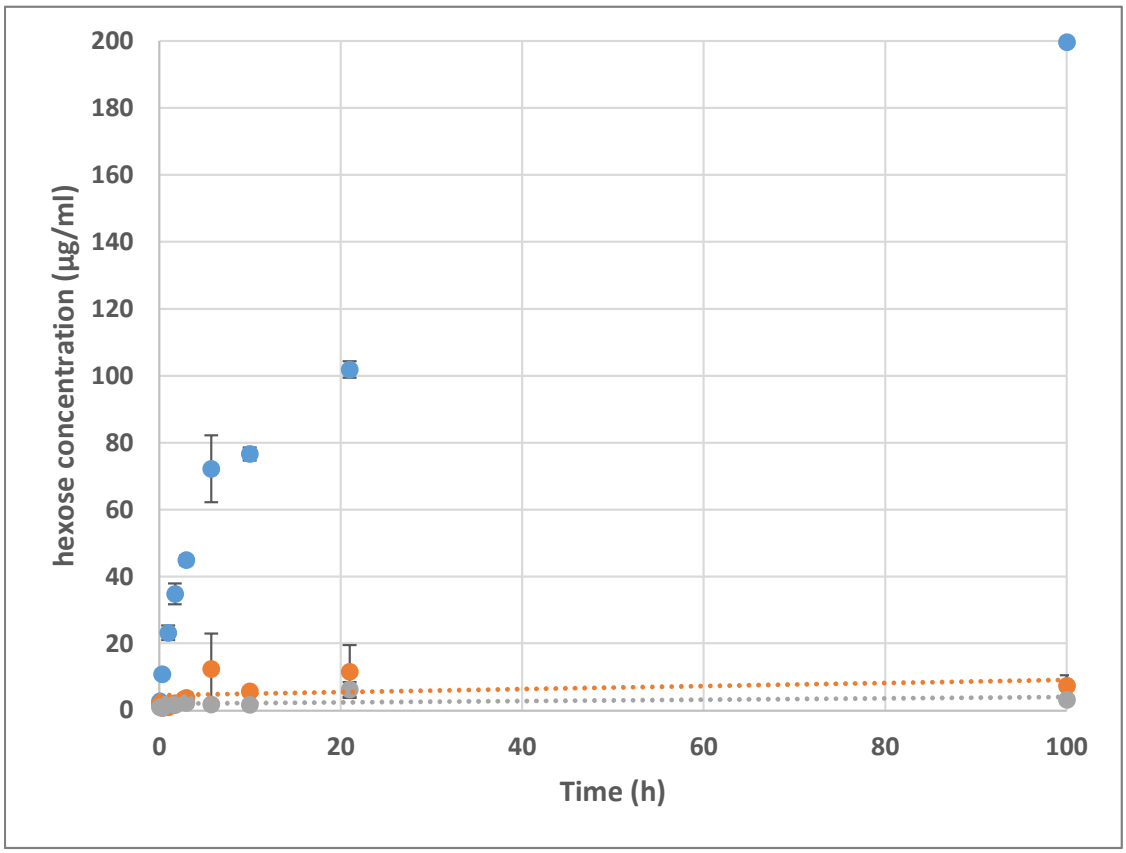

Figure 53. Cellulase digestion of Whatman No 1 filter paper over time.

Whatman filter paper pieces (150 mg), which had been prewashed in buffer (PAW 1:1:98 (v/v) containing 0.5% chlorobutanol, three washes, each in 6 ml of buffer for 16 h), were digested in 6 ml buffer with 3 U of endo-cellulase from *A. niger* (blue dots) or incubated without enzyme (orange dots); grey dots represent enzyme without paper. The incubations were done at 20°C on a mixing wheel. At times, the tubes were centrifuged at 2500 g for 5 min and 0.5 ml samples of the free solution were taken and analysed by the anthrone method (along with glucose standards as in Fig. 52). When needed, the digests were diluted with buffer to hexose concentration below 50 µg/ml. N for each sample was 3 (technical repeats) and error bars show SEM.

3.3.2.2 Digestion of AIRs and commercial celluloses

For studying the accessibility of all the cellulose and AIR samples to cellulase, I digested 40 mg with 0.8 U of cellulase in 1.6 ml of buffer for 3 h and assayed the soluble digestion products by the anthrone method (Fig. 54).

The least accessible commercial celluloses were the cotton wool, never-dried cellulose and Avicel PH102, and the most accessible samples were Curran, LC200 that had been processed in water and

spray dried (LC200 spr dr), and the same sample after further milling (LC200 spr dr & milled). The accessibilities of Whatman No 1 filter paper and Södra A13 cellulose were about the average of all the commercial cellulose samples. Although cotton wool was the least accessible substrate for cellulase, it was still digestible because its average soluble hexose yield was statistically different from the background (cotton wool versus 'enzyme only' in Fig. 54, confirmed by a t-test, p=0.015).

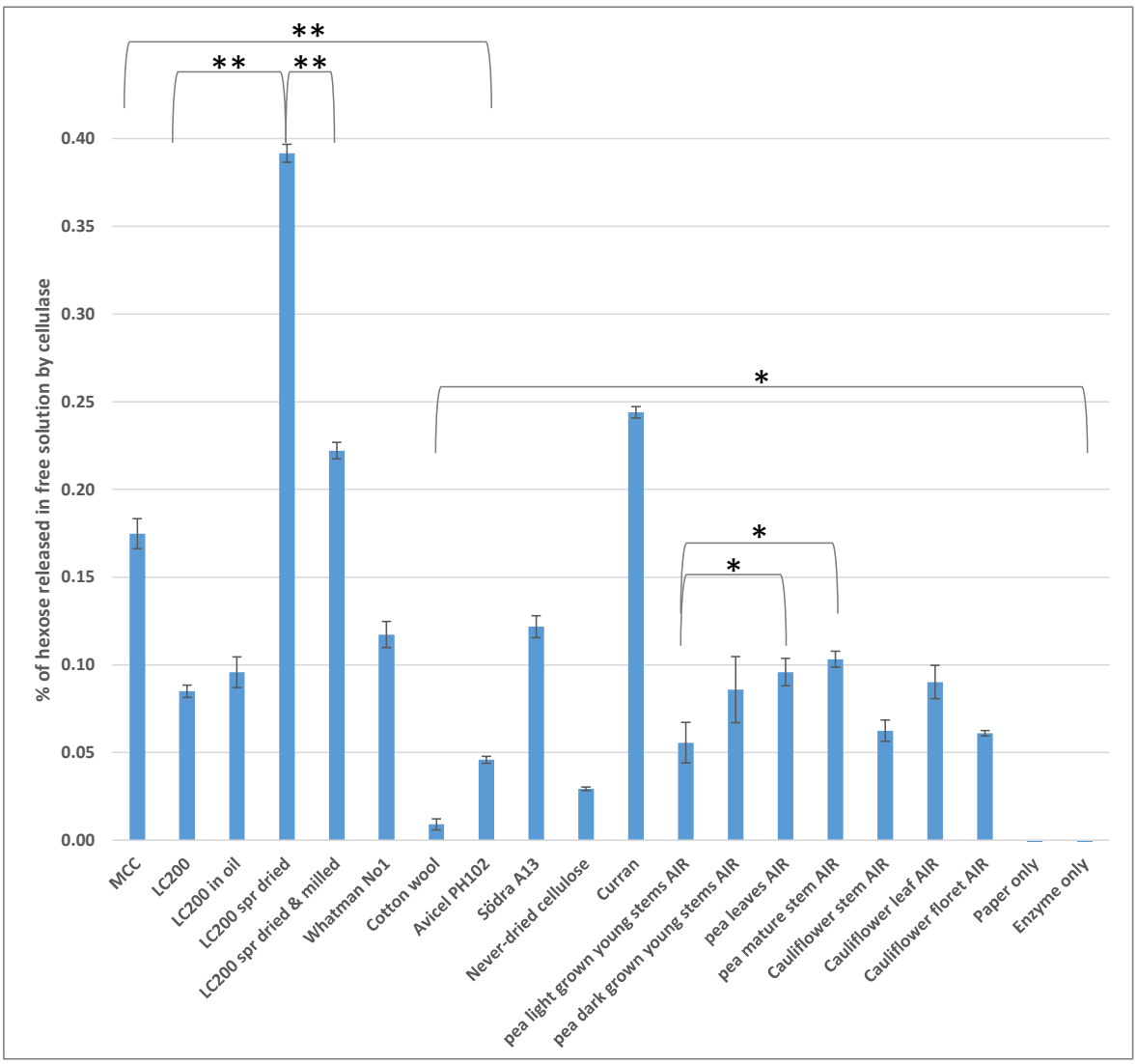

Figure 54. Hexose release from AIRs and commercial celluloses into free solution after 3 h digestion with cellulase.

Prewashed samples (40 mg DW; washing done as in Fig. 2) were digested with 0.8 U of enzyme in 1.6 ml of buffer (PAW 1:1:98 (v/v)) at 20°C on a mixing wheel. At 3 h the tubes were centrifuged as in Fig. 2 and 0.5 ml of the digest was anthrone assayed (after dilution if necessary). The calculations assume that the whole 40-mg of

sample consists of hexose residues only, such as pure cellulose. N for each sample was 3 (i.e., three separate 40-mg cellulose samples were digested, technical repeats) and error bars show SEM. For paired samples marked with a bracket and start there was a statistical difference (* for p≤0.05 and **p≤0.01).

Both the cotton wool and never-dried cellulose are very fluffy and they occupy a large volume in a test tube. The particle sizes of these celluloses are large and the reason they stand out from the other celluloses could be that they have not been processed to fine powders or pulp like the other celluloses and therefore they could have less surface area and fewer binding sites available for the cellulase.

However, Fan *et a*l. (1980) showed that crystallinity is a more important variable for cellulose digestibility and digestion rate than surface area. Crystallinity, which is discussed further in § 4.3 Discussion, could explain why some celluloses are less accessible to cellulase than most of the other celluloses – it is more difficult for cellulase to bind to tightly packed crystalline surfaces. However, our other microcrystalline cellulose (MCC in Fig. 54) is much more accessible to cellulase than Avicel (significant difference confirmed by a t-test, p=0.005), which was unexpected.

There was a lot of variation between the accessibilities of the four LC200 samples (Fig. 54). Processing of the LC200 in oil did not change the accessibility (LC200 versus LC200 in oil, p=0.33) but processing in water and spray-drying strongly increased the accessibility (LC200 versus LC200 spr dried, difference confirmed by a t-test, p<0.01). However, when the spray-dried LC200 was milled further the accessibility was significantly reduced ("LC200 spr dried" versus "LC200 spr dried & milled", difference confirmed by a t-test, p=0.00002).

Of the samples known to contain abundant non-cellulosic polymers, Curran® had the highest accessibility, which could be because it had undergone various oxidising treatments during its manufacture whereas the AIR samples had not. The differences of the accessibilities of the pea AIR samples are small (Fig. 54) and not statistically significant (confirmed by t-tests) between: young stems grown in light versus dark (p=0.26), young stems grown in dark versus mature stems (p=0.46), young stems grown in dark versus leaves (p=0.66), and leaves versus mature stems (p=0.47). But there is a statistically significant difference between young stems grown in light versus mature stems (p=0.032), and between young stems grown in light versus leaves (p=0.045) (Fig. 54).

With cauliflower AIR, no samples were statistically different from each other: leaves versus florets ($p=0.094$), stems versus florets ($p=0.86$), and stems versus leaves ($p=0.090$). Pea mature stem AIR was statistically different from cauliflower stem AIR ($p=0.006$) (Fig. 54) but both the light and dark grown young pea stem AIRs were not statistically different from cauliflower stem AIR ($p=0.64$ and $p=0.36$, respectively). Also, there was no statistical difference between leaf AIRs from cauliflowers and peas ($p=0.67$).

It is likely that most AIRs are only ~15–40% cellulose, as they consist of mainly primary cell walls (Cosgrove and Jarvis, 2012), but the mature pea stem AIR could contain more cellulose as it has secondary cell walls [40-90% cellulose (Fry, 1988); for example, secondary cell walls in wood tissue contain 40-50% cellulose (Timell, 1967)], and therefore when digesting 40 mg of AIR I was actually digesting only ~10 mg cellulose. Also, the cellulose microfibrils of the AIR samples are covered by tethering hemicelluloses which could act as a physical barrier between the cellulose surfaces and cellulase enzymes, and therefore bigger differences in accessibilities could be detected if the celluloses of the AIR samples were first freed from pectins and hemicelluloses.

3.3.3 Results - accessibility of cellulose to small molecules

In the previous section (§ 3.3.1) the surface accessibility of cellulose was studied by binding of [^{3}H]cellopentaitol. The pentasaccharide molecule presumably binds on the cellulose microfibril surface, and is assumed to stay on the outside, coating it. Other sugars (exemplified in the present section by a xyloglucan oligosaccharide (XXLGol) and free glucose) do not have any appreciable affinity for cellulose surfaces but may enter the interior of the cellulose (micro)fibrils. This section investigates differences between cellulose samples in their penetrability to such molecules (with the surface-binding Cell$_5$-ol as a control). The basic rationale of the method was to apply ^{3}H-labelled sugars to cellulose (pure or present in AIR) and monitor the detectability of the known quantity of added ^{3}H by liquid scintillation-counting. If the ^{3}H permeates the cellulose, it will be partially shielded from the scintillation fluid and thus detected with a lower counting efficiency.

3.3.3.1 Testing how much solvent is needed for wetting cellulose

In order to find a suitable solvent that could bring the 3H-labelled sugars into contact with the cellulose, I tested how cellulose behaves when made wet with water, ethanol or acetone and dried. Mixing with water made the cellulose clump whereas acetone and ethanol formed pastes with cellulose. When the solvents were allowed to evaporate off from uncapped tubes in a fume hood, water-treated cellulose became hard and lumpy but ethanol- and acetone-treated celluloses stayed as fluffy as they were before the wetting and these solvents were therefore preferred.

The celluloses and AIRs are very different from each other in their initial fluffiness. For instance, a gram of cotton wool takes a much bigger space in a test tube than a gram of microcrystalline cellulose (MCC), which is a fine powder. For determining how much solvent I would need to make the celluloses moist, 100 mg (DW) cellulose was wetted with 96% ethanol, 50 µl at a time, until a paste-like consistency was reached – I wanted to make the cellulose wet enough so the sugars dissolved in the solvent could come in contact with all the 100 mg of cellulose but not too wet to avoid the cellulose pellet from sitting in a puddle of solvent. The volumes needed for making the celluloses into a wet paste are listed in Table 5 which was used for wetting the celluloses in 3.3.3.3 Effect on scintillation counting efficiency when drying [3H]sugars on/in celluloses and AIRs.

Table 5. Ethanol (96%) needed for making 100 mg (DW) of cellulose and AIR preparations into a paste that could be subsequently treated with [^{3}H]sugars.

Sample ID	Cellulose or AIR name	Volume of EtOH needed for making a 100-mg of cellulose or AIR into a moist paste (µl)
1	Microcrystalline cellulose	200
2	LC200	400
3	LC200 in oil	400
4	LC200 spray dried	150
5	LC200 spray dried and milled	200
6	Curran® by Cellucomp	150
7	Whatman No 1 filter paper	100
8	Cotton wool	1200
9	Avicel PH102	250
10	Södra A13	500
A	Young pea stem grown in light AIR	1200
B	Young pea stem grown in dark AIR	1400
C	Pea leaves AIR	1000
D	Pea mature stem AIR	400
E	Never-dried cellulose (wet)	850
F	Cauliflower stems AIR	1200
G	Cauliflower leaves AIR	1200
H	Cauliflower florets AIR	1200
GP	Glass paper, Whatman, GF A	100

3.3.3.2 Solubility of [^{3}H]cellohexaitol in acetone and ethanol

Next I tested the solubility of [^{3}H]cellohexaitol in ethanol and acetone. The cello-oligosaccharides are water soluble and mixing them with concentrated ethanol or acetone could make them precipitate.

If the cellohexaitol was not in solution, it would not properly come in contact with the cellulose when mixed with the pellet to form a paste. For testing the solubility, 100 Bq of [^{3}H]cellohexaitol dissolved in 20 µl water was mixed with 980 µl of 50 – 100% acetone or ethanol, and 250-µl samples of the solution were taken after 1-h and overnight incubations at 20°C. During the incubation, the samples were not mixed and any precipitate was allowed to sediment without centrifugation. For a control, water was used instead of acetone or ethanol. The supernatant samples were assayed for radioactivity (Fig. 55).

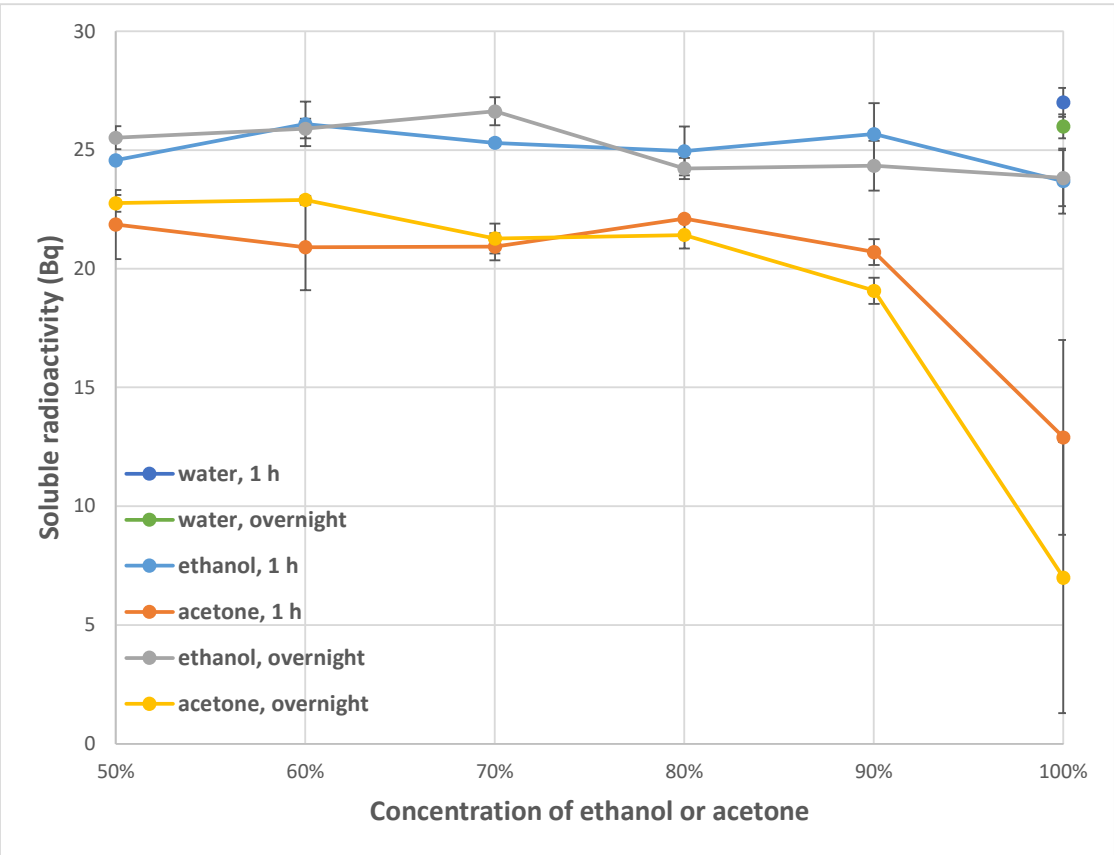

Figure 55. Solubility of [^{3}H]cellohexaitol in different concentrations of acetone and ethanol.

To test if acetone or ethanol precipitates [^{3}H]cellohexaitol, 100 Bq of [^{3}H]cellohexaitol dissolved in 20 µl water was mixed with 980 µl of 50 – 100% acetone or ethanol and incubated on the bench without mixing at 20°C for 1 h and overnight. For sampling, 250 µl of solution was taken (from as close as possible to the surface) without disturbing the possible sediment. The supernatants were assayed for radioactivity. For a control, water was used instead of acetone or ethanol, and 'water, 1 h' and 'water, overnight' show the radioactivity when all the [^{3}H]cellohexaitol stays soluble (arbitrarily plotted at concentration "100%"). Error bars show SEM, N = 3 (technical repeats).

Fig. 55 shows that some [^{3}H]cellohexaitol precipitated when acetone concentrations were ≥90%. [^{3}H]Cellohexaitol did not precipitate in concentrated ethanol (no significant difference between 50% and 100% ethanol according to a T-test, p=0.58 for 1 h and p=0.28 for overnight incubated samples). Therefore, 96% ethanol was chosen for wetting the celluloses and AIRs in the following experiment.

3.3.3.3 Effect on scintillation counting efficiency when drying [^{3}H]sugars on/in celluloses and AIRs

To test how penetrable the celluloses were for molecules that vary by size, I mixed 100 mg of each type of cellulose and AIR with 1 kBq of [^{3}H]cellohexaitol, [^{3}H]glucose or [^{3}H]XXLGol in 96% ethanol in the volumes which are listed in Table 5. The idea was that penetrable celluloses could trap and 'hide' the tritiated molecules (especially the smallest molecules) from scintillation counting whereas the largest molecules and those with an affinity for the cellulosic surface would stay on the surface and could be more efficiently detected by the scintillation counter. Tritium was chosen because it could be hidden more easily than ^{14}C (which has about 7.5 times higher decay energy). The moist samples were incubated overnight after which they were dried and mixed with thixotropic scintillation fluid. The viscous scintillation fluid prevented the cellulose from sedimenting to the bottom of the vials during scintillation counting.

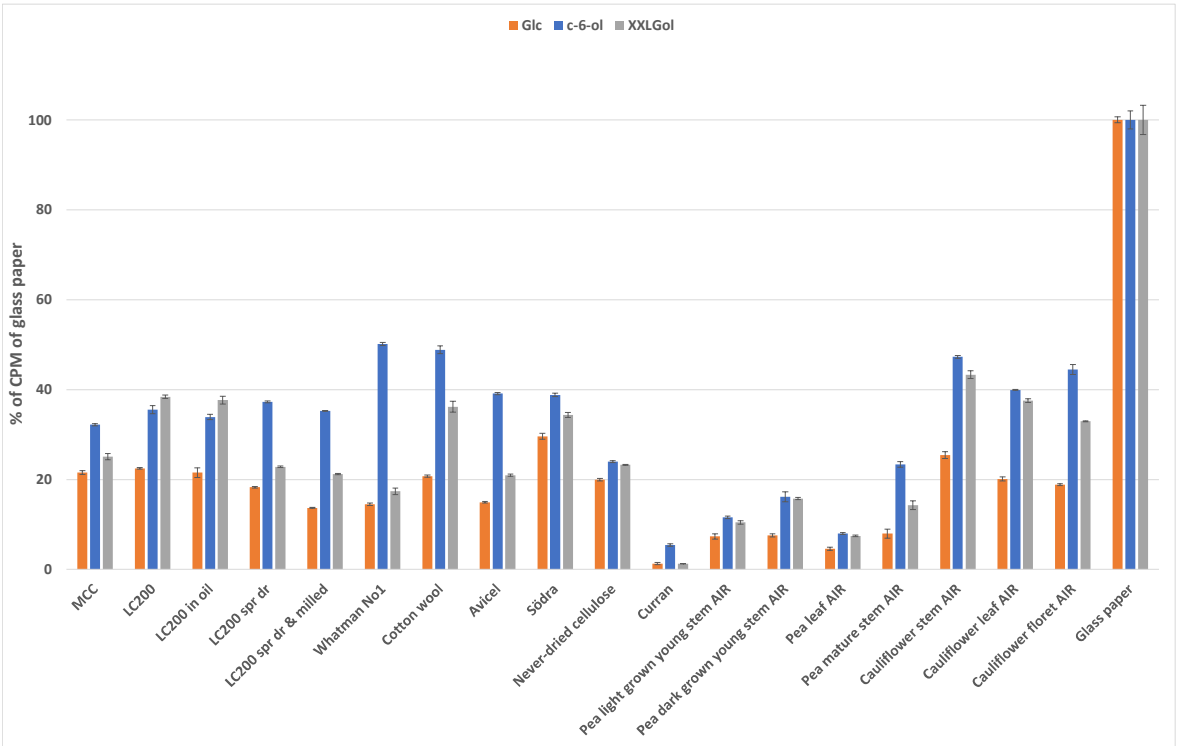

Figure 56. Scintillation counting efficiency of [^{3}H]glucose, [^{3}H]cellohexaitol and [^{3}H]XXLGol dried on (or in) cellulose or AIR.

[3H]Glucose, [3H]cellohexaitol and [3H]XXLGol in 96% ethanol were applied to 100-mg cellulose and AIR samples. The [^{3}H]saccharides were first dried in a SpeedVac and redissolved in 20 µl of water after which they were mixed in 96% ethanol (volumes of which are listed in Table 1). The solutions were added to dry celluloses and AIRs, mixed well and the vials were left to stand on the bench tightly capped at 20°C overnight. The next day the caps were removed and the ethanol was allowed to evaporate off in the fume hood for two days. The samples were mixed with 10 ml of thixotropic scintillation liquid (prepared by dissolving 10 g of hydrogenated castor oil pellets in a litre of Gold Star scintillation liquid) and the vials were assayed for radioactivity. The measured scintillations (CPM = 'counts per minute') are expressed as a % of what was measured with the glass paper samples (glass paper does not quench the measurements, unlike the cellulose and AIR samples). For controls, samples of the [^{3}H]saccharide solutions were mixed with water and aqueous miscible scintillation liquid (Optiphase Hisafe 3), and assayed for radioactivity. The measured activities in the aqueous samples were: [^{3}H]glucose, 800 Bq (1400 CPM); [^{3}H]cellohexaitol, 1000 Bq (1800 CPM); and [^{3}H]XXLGol, 1500 Bq (2500 CPM). Error bars show SEM, N=3 (technical repeats). C-6-ol = cellohexaitol

All samples in Fig. 56 contain the same amount of [^{3}H]saccharides (800 Bq of [^{3}H]glucose, 1000 Bq of [^{3}H]cellohexaitol or 1500 Bq of [^{3}H]XXLGol) but the measured radioactivity may vary owing to differences in counting efficiencies. The counting efficiency on glass paper is maximal because the fibres are made of glass (which does not quench the scintillations) and therefore the measurements from the celluloses and AIRs could be compared with those on glass paper. As expected, the smallest of the sugars, [^{3}H]glucose, had a lower counting efficiency on cellulose than the other two sugars

tested (Fig. 56). This suggests that [^{3}H]glucose can penetrate the cellulose or AIR easiest, as expected in view of its low molecular weight and lack of surface binding affinity for cellulose. The octasaccharide [^{3}H]XXLGol was the second most concealed in the cellulose or AIR except with LC200 and LC200 processed in oil (Fig. 56). [^{3}H]Cellohexaitol has a high binding affinity to cellulose, as shown in experiments with cellopentaose and [^{3}H]cellopentaitol (see § 3.3.1), whereas [^{3}H]XXLGol presumably does not (as XXXGol, which is very similar to XXLGol, washes away from cellulose easily (Herburger *et al*., 2020)). It is likely that some of the [^{3}H]cellohexaitol was coating the cellulose microfibrils, where it could be efficiently detected by the scintillation counter. Especially Whatman filer paper and cotton wool seemed to bind well [^{3}H]cellohexaitol on the cellulose (rather than hide it in the cellulose) because they had CPM 50% that of the glass paper (Fig. 56). Also, [^{3}H]XXLGol was evidently able to get concealed by the cellulose or AIR better than [^{3}H]cellohexaitol and almost as well [^{3}H]glucose (Fig. 56), in microcrystalline cellulose, LC200 spray dried, Whatman No 1 filter paper, never-dried cellulose, Curran®, and AIR from young light-grown pea stems and pea leaves (Fig. 56). Surprisingly, the counting efficiency was similar between [^{3}H]XXLGol and [^{3}H]cellohexaitol with LC200, LC200 processed in oil, Södra A13, never-dried cellulose, young pea stem (grown in light and dark) AIRs, pea leaf AIR, cauliflower stem AIR and cauliflower leaf AIR. With these samples the penetrability to cellulose was equally good between [^{3}H]XXLGol and [^{3}H]cellohexaitol.

However, the counting efficiencies of the ^{3}H-sugar samples were not truly comparable to each other because some of the cellulose suspensions had more quenching, measured by the scintillation counter, (and therefore lower counting efficiency) than the others (Fig. 57A).

3.3.3.4 Equalising the counting efficiencies of all samples by adding *p*-coumaric acid

The counting efficiency of a radiochemical that is soluble in scintillation fluid can be determined from an 'H-number' (measured by the scintillation counter) with the help of a calibration curve. The H# will be raised (indicating increased quenching, thus diminished counting efficiency) by the presence of coloured or UV-absorbing substances dissolved in the sample/scintillant mixture. This type of quenching (of material in solution) is unrelated to the shielding being sought in the present work to test for the ability of ^{3}H-sugars to 'hide' within cellulose fibres. Nevertheless, quenching due to contaminating solutes will decrease counts and thus give the impression of shielding within the cellulose fibres. Therefore, I attempted to equalise the H# of all samples so that any remaining differences between samples could be reliably ascribed to 'hiding' within cellulose fibres.

The calibration curves for our counters were produced by Dr Rachel C. Smith of this laboratory. The H-numbers varied a lot between the samples (Fig. 57A), especially between the celluloses, Curran® and the pea AIR preparations, suggesting that some substances that were leached out of Curran® and AIR samples by the scintillation fluid can interfere with the measurements. This is a problem because the interference affects the counting efficiency and therefore differences in the celluloses' capabilities for 'hiding' the tritiated molecules could be partially due to lower counting efficiencies, not the penetrability of the surface of the cellulose. To get around this problem I purposefully lowered the counting efficiencies of some of the samples (those with an H# lower than that of the Curran® suspensions) by adding 200–300 µl of 10% *p*-coumaric acid dissolved in acetone (exact amounts adjusted for each sample based on the original H-number (Fig. 57A) and the finding that addition of 2.7 µl of *p*-coumaric acid solution increases by one unit the H-number). This procedure was applied to the samples with low H-numbers (all the commercial celluloses, cauliflower AIRs and glass paper (Fig. 57A)), thus adjusting the quenching to the same level as the Curran® sample (Fig. 57B). The original H-numbers of pea AIRs were higher than that of Curran® so no *p*-coumaric acid was added to them. The samples were then re-assayed for radioactivity (Fig. 58).

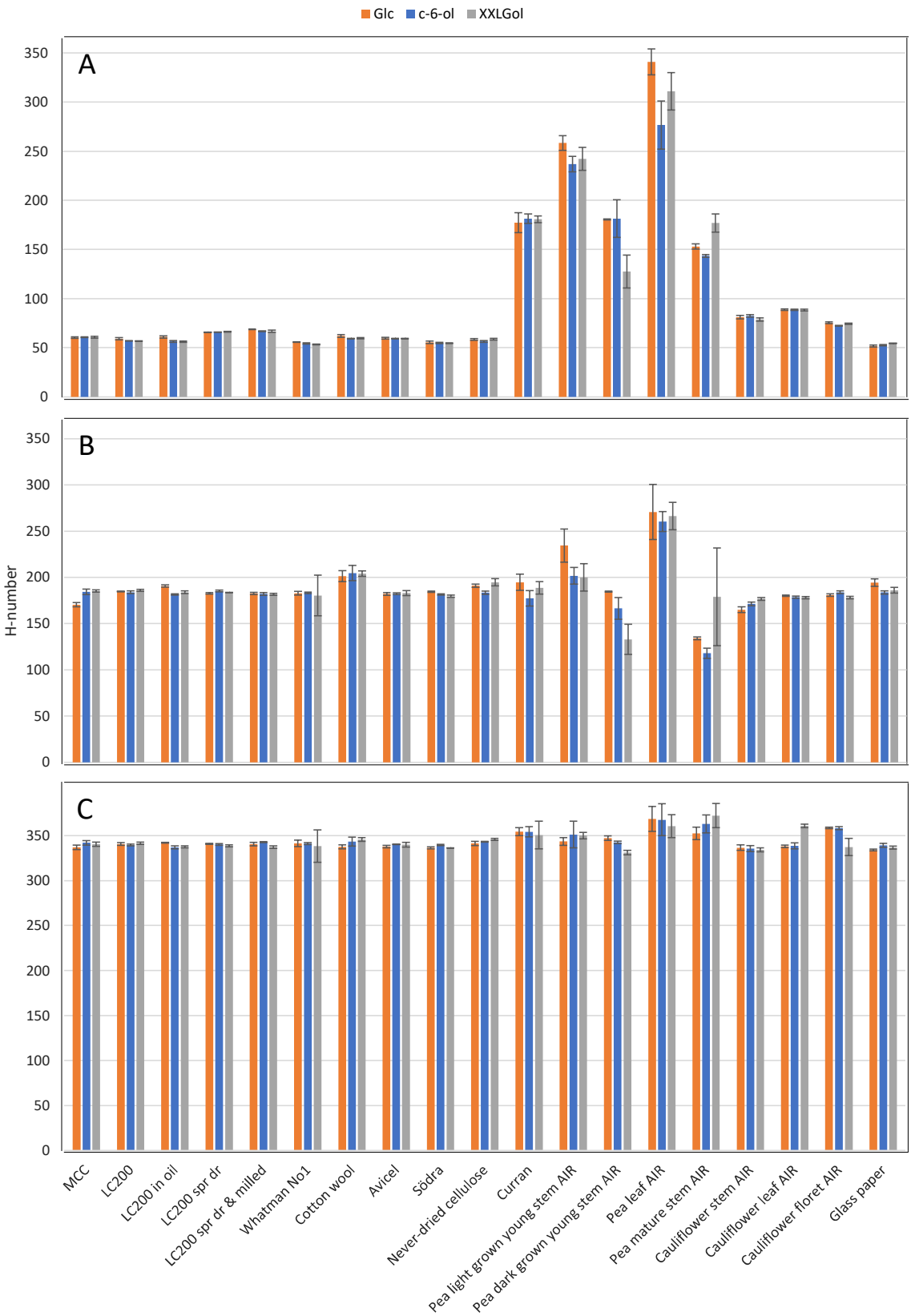
Glc
c-6-ol
XXLGol
A
B
C
H-number
0
50
100
150
200
250
300
350
MCC
LC200
LC200 in oil
LC200 spr dr
LC200 spr dr & milled
Whatman No1
Cotton wool
Avicel
Södra
Never-dried cellulose
Curran
Pea light grown young stem AIR
Pea dark grown young stem AIR
Pea leaf AIR
Pea mature stem AIR
Cauliflower stem AIR
Cauliflower leaf AIR
Cauliflower floret AIR
Glass paper

Figure 57. H-numbers before and after adjustments

The H-numbers, which indicate counting efficiency of ^{3}H-labelled compounds in solution, were measured by the scintillation counter (A). To make the low-H# samples comparable to Curran®, their H-numbers were adjusted to ~180 by adding 10% *p*-coumaric acid, dissolved in acetone (B). Finally, to make all the samples comparable to each other, the H-numbers were adjusted to ~350 by adding more 10% *p*-coumaric acid, making sure every sample contained at least some *p*-coumaric acid (C). The amount of *p*-coumaric acid added was calculated based on the original H-numbers (A) and finding that 2.7 µl of the solution increases the H-number by one unit (which was determined by adding gradually *p*-coumaric acid solution to the viscous scintillant and measuring the increase in H-number after every addition, resulting in a linear correlation). Error bars show SEM, N=3 (technical repeats).

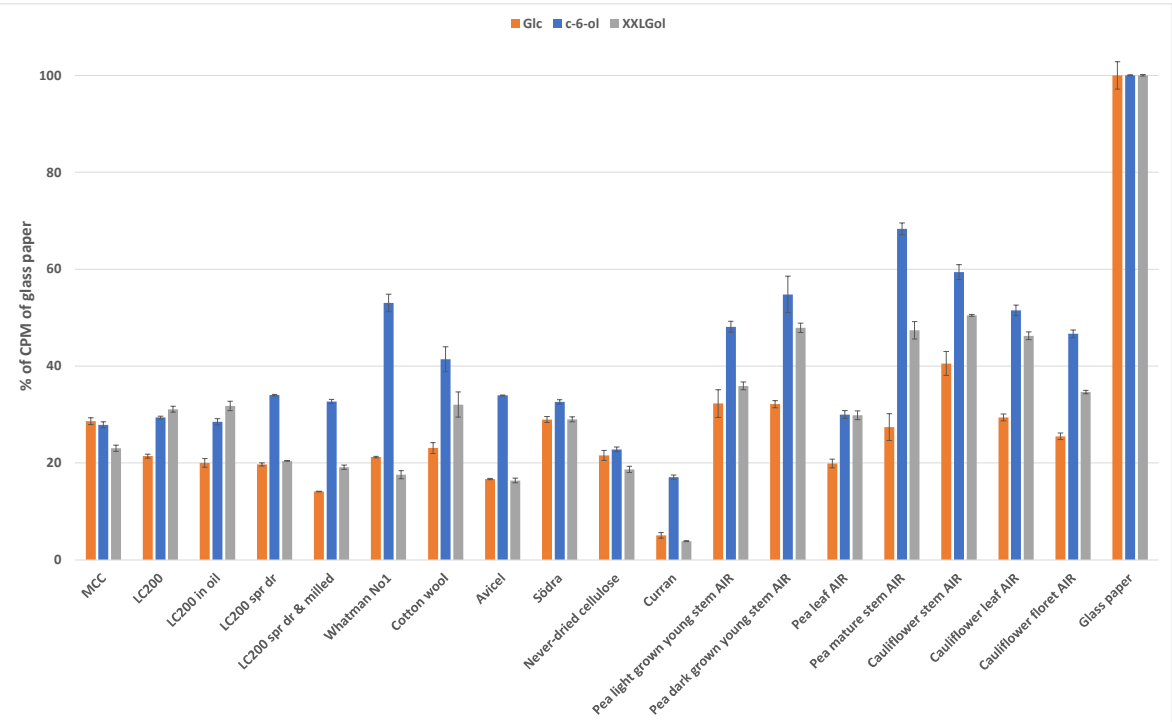

Figure 58. Scintillation-counts of [^{3}H]glucose, [^{3}H]cellohexaitol and [^{3}H]XXLGol dried on cellulose or AIR surface, after equalising most H-numbers with *p*-coumaric acid.

The H-numbers of the low-H# samples (commercial celluloses, cauliflower AIRs and glass paper) were adjusted to ~180, as described in Fig. 57B, after which the samples were assayed for radioactivity. The scintillations measured are expressed relative (%) to glass paper as in Fig. 56. Error bars show SEM, N=3 (technical repeats). Note that the following samples still had H# values exceeding Curran®: young pea stem grown in light AIR and pea leaf AIR.

Even after the adjustment of most of the H-numbers to the same level as the Curran® sample (Fig. 3B), the Curran® sample still had the least detected scintillations (Fig. 58), although I do not know why it was so different from the other samples studied.

After the adjustment with *p*-coumaric acid, the cauliflower AIRs generally gave higher cpm values than the pure celluloses (Fig. 58), whereas before addition of *p*-coumaric acid the scintillations in the cauliflower AIRs were approximately as detectable as in the pure celluloses (Fig. 56). The pea AIRs originally hid the [^{3}H]sugars better than pure celluloses and cauliflower AIRs in Fig. 56 but after the adjustment of H-numbers the pea and cauliflower AIRs hid the scintillations equally well, and the commercial celluloses were generally better at hiding the [^{3}H]sugars than the AIRs (Fig. 58).

However, all of the samples were still not fully comparable to each other as the cotton wool, light grown young pea stem AIR and the pea leaf AIR had H-numbers higher, and the dark grown young pea stem AIR and the mature pea stem AIR had H-numbers lower, than to what the other samples were adjusted to (Fig. 57B). Therefore, I added more *p*-coumaric acid to the previously adjusted samples and to the pea AIR samples so that all the samples would contain at least some *p*-coumaric acid added and have similar H-numbers (Fig. 57C). The samples were assayed for radioactivity again (Fig. 59).

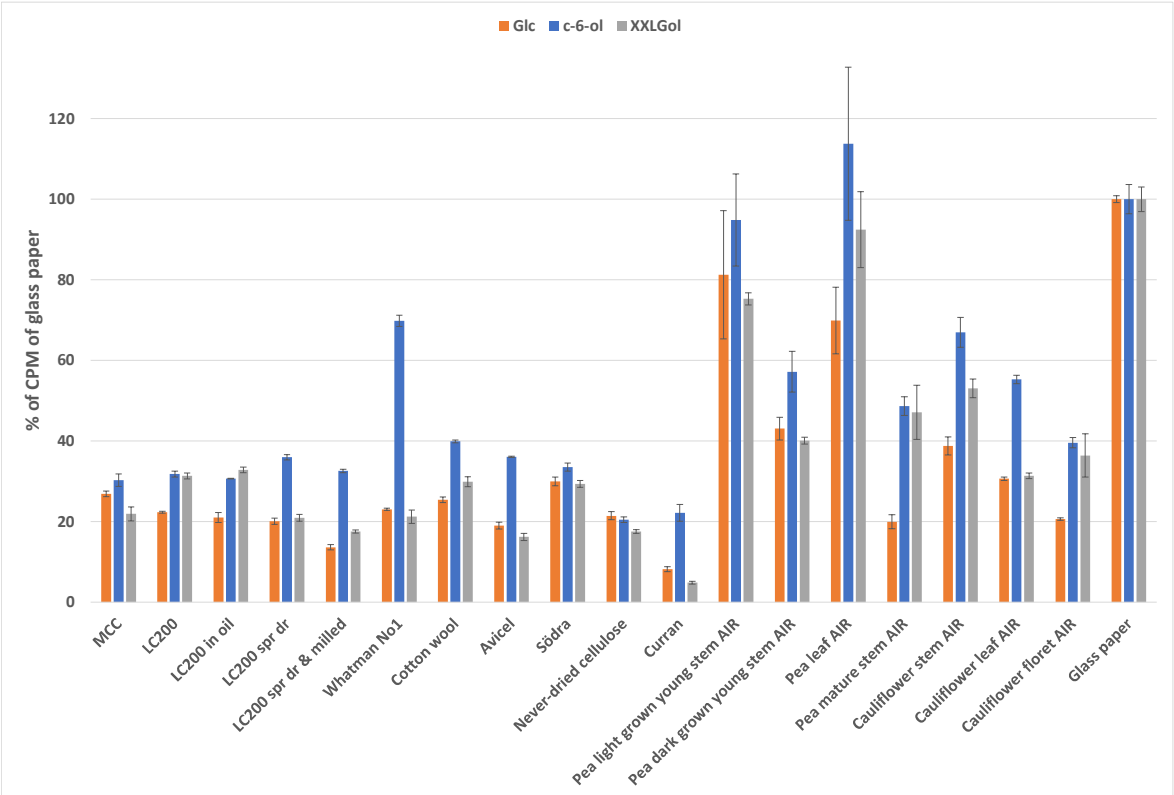

Figure 59. Scintillation-counts of [^{3}H]glucose, [^{3}H]cellohexaitol and [^{3}H]XXLGol dried on/in cellulose or AIR, after equalising the H# for all samples by adding *p*-coumaric acid.

More *p*-coumaric acid was added to the samples from Fig. 58, ~equalising the H-numbers at ~340 of the samples (Fig. 57C). Measured scintillations are expressed relative (%) to glass paper as in Fig. 56 and 58. Error bars show SEM, N=3 (technical repeats).

After the final addition of *p*-coumaric acid, Curran® was still hiding the scintillations from [^{3}H]glucose and [^{3}H]XXLGol more than any other sample (Fig. 59). This is surprising because in the [^{3}H]cellopentaitol experiments Curran® was a poor absorber, and may be due to the oxidative treatments (Curran is treated with sodium hypochlorite and hydrogen peroxide) done during the manufacturing ? [^{3}H]Cellohexaitol was hidden most by Curran® and never-dried cellulose (Fig. 59) when compared to the other celluloses and AIRs. About 70% of the [^{3}H]cellohexaitol dried on Whatman filter paper was detectable when related to the glass paper measurements, implying that [^{3}H]cellohexaitol was indeed largely confined to the outer surface of the fibres (thus maximally exposed to scintillation fluid) rather than permeating them and becoming shielded from the scintillant. Surprisingly, the [^{3}H]cellohexaitol dried on AIRs derived from the young pea stems grown in light and pea leaves was as detectable as from the glass paper sample (Fig. 59) – however, the standard errors of these samples were rather large. Interestingly, the never-dried and Södra celluloses had similar detectabilities between all of the three [^{3}H]sugars tested (Fig. 58 and 59) suggesting their surfaces were less selective for the size of the sugars that can penetrable fibres.

With all the other samples [^{3}H]glucose was hidden most and [^{3}H]cellohexaitol least (except for LC200, LC200 processed in oil and pea mature stem AIR which had similar scintillation detection efficiencies for both [^{3}H]XXLGol and [^{3}H]cellohexaitol) (Fig. 59).

The detected scintillations relative to glass paper were more comparable and informative in Fig. 59 than in Fig. 56 and 58 because the samples in Fig. 59 have similar H-numbers. However, it is good to keep in mind that H-number is a number calculated by the scintillation counter's program based on an estimation the efficiency of the measurement of the sample the scintillation counter is measuring at that moment and that the estimation can vary. For instance, the H-numbers of the pea AIRs should in theory be the same in Fig. 57A and 57B because no *p*-coumaric acid had been added to the pea AIR samples at that point, but the measurements did not turn out the same (for instance, pea leaf AIR treated with [^{3}H]glucose had H-number of ~340 in Fig. 57A and ~270 in Fig. 57B). One could argue that this could be due to the samples being older in Fig. 57B than in 57A and more compounds could have come into contact or dissolved into the solvents of the scintillation liquid but in practice the measurements of H-number can vary even if one measures the same sample again just a few minutes later (data not shown), and the variations in H-numbers are bigger if the H-numbers are big and if the material is coloured (as is, for example, with the pea AIRs which are yellowish brown and Curran® which is brown in colour). This observation is supported by the big error bars of pea AIRs and Curran® in Fig. 57, especially in Fig. 57C where I had tried to balance out the variation between samples by adding an individually tailored amount of *p*-coumaric acid to each sample.

The key findings were that [^{3}H]cellohexaitol was 'the most accessible' compound to the scintillation counting because its scintillations were the easiest to detect (except for with Södra A13 and never-dried cellulose which had very similar accessibilities for all of the compounds) (Fig. 59). The other two sugars tested were either as accessible (with LC200 spray dried, Whatman No1 and cauliflower leaf AIR), or [^{3}H]XXLGol was more accessible for scintillation counting (the rest of the samples).

The key findings suggest, as I pointed out earlier in chapter 3.3.3.3, that [^{3}H]cellohexaitol has a high binding affinity to the cellulose surface and it presumably sits on the microfibril coating it and is therefore relatively easy for the scintillation counter to detect. Furthermore, the penetrability of the surface is unsmooth enough to hide the other two molecules, [^{3}H]glucose and [^{3}H]XXLGol (which differ by their size but not by their affinity to bind to cellulose), more than [^{3}H]cellohexaitol. It is also

possible that glucose, as a small molecule, can penetrate the cellulose microfibril. However, with some samples, [^{3}H]glucose and [^{3}H]XXLGol were hidden equally well (or almost) whereas with other samples [^{3}H]XXLGol was clearly more excluded from the fibres (thus accessible to scintillation counting) than [^{3}H]glucose. This suggests that with the samples where the [^{3}H]glucose and [^{3}H]XXLGol were hidden equally well the surface could be very penetrable and it would not make a difference whether it is concealing a small ([^{3}H]glucose) or a many times bigger ([^{3}H]XXLGol) molecule. Accordingly, with the samples that showed [^{3}H]XXLGol being more accessible, the surface could be less penetrable and it could hide a small molecule ([^{3}H]glucose) easily but [^{3}H]XXLGol would be too big to be hidden, leaving it on the surface where it can be detected.

3.3.3.5 Recovering the cellulose from the scintillation liquid for use in the desorption experiment

When the tritiated sugars were added to the celluloses in a minimal volume of ethanol, it is possible that some of the [^{3}H]sugar molecules did not have a chance to permeate the fibres. For instance, we know from chapter 3.3.1 that [^{3}H]cellopentaitol, which presumably behaves very similarly to [^{3}H]cellohexaitol, binds on the cellulose permanently in aqueous conditions over time (although the binding is fastest over the first hour). However, the present conditions were not similar to those earlier experiments because:

- the solvent used in the present experiments contained only very little water (90% ethanol), which might induce hydrogen bonding to cellulose surface;
- the celluloses were not freely suspended in the solvent but had just barely enough ethanol to make the [^{3}H]sugars come in contact with the celluloses and AIRs;
- the samples were not constantly mixed;
- and the incubation lasted only ~16 h (instead of hundreds of hours).

Therefore, it would be interesting to study if the differences in penetrability seen in Fig. 56, 58 and 59 derived from the [^{3}H]sugars sitting on the surface of the cellulose and being hidden by the penetrability of cellulose, or if the celluloses and AIRs had absorbed some of the [^{3}H]sugars (especially glucose). In order to conduct further studies with the material, I had to wash off the scintillation liquid (containing hydrogenated castor oil and *p*-coumaric acid) off the cellulosic samples (because the scintillant and oil would not mix with water). I washed the scintillation liquid off from the celluloses and AIRs with acetone:diethyl ether (1:1) (not expected to be a good solvent for sugars) and assayed the washings for radioactivity (Fig. 60).

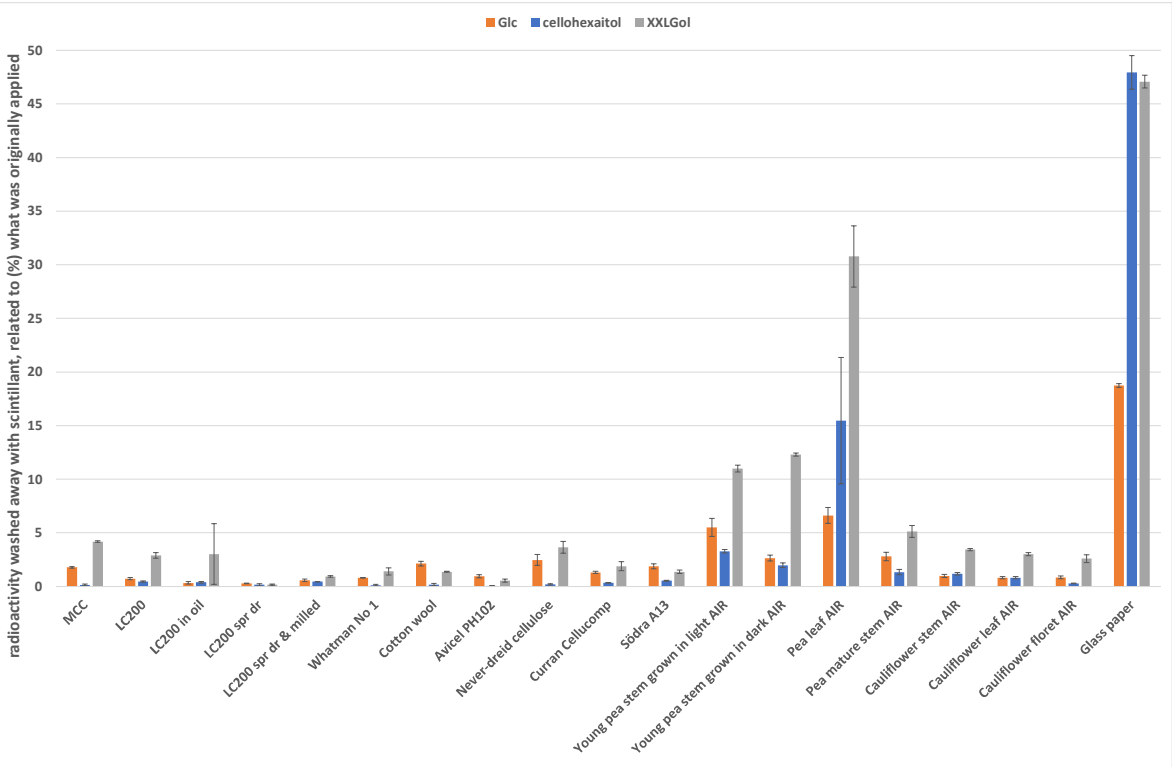

Figure 60. [^{3}H]Glc, [^{3}H]cellohexaitol and [^{3}H]XXLGol washed off from the cellulose, when scintillation liquid was removed using acetone:diethyl ether (1:1)

The cellulose and AIR, which were mixed with the scintillation liquid (from Fig. 59), were transferred from the scintillation vials into 15-ml test tubes using acetone:diethyl ether (1:1). The tubes were centrifuged for 10 min at 2000 g and the supernatants were transferred to fresh scintillation vials. The pellets were washed again with acetone:diethyl ether (1:1), and the supernatants were collected to the same vials. The acetone and ether were allowed to evaporate from the uncapped vials in fume hood overnight after which the remaining scintillation liquids were assayed for radioactivity. The radioactivity measured (Bq calculated from non-aq. scintillations, corrected by reference to the H#) was calculated related (%) to what was originally added (Bq calculated from aq. scintillations, water control sample in the legend of Fig. 56). Error bars show SEM, N=3 (technical repeats).

Surprisingly, almost half of the [^{3}H]XXLGol and [^{3}H]cellohexaitol and a fifth of [^{3}H]glucose had come off from the glass paper into the scintillant fluid (Fig. 60). This was surprising because scintillation fluid, acetone and ether are not expected to be good solvents for sugars. The scintillation liquid, acetone and ether had washed off a third of the [^{3}H]XXLGol and a sixth of the [^{3}H]cellohexaitol from the pea leaf AIR (Fig. 60). About 11 – 12% of [^{3}H]XXLGol from the young pea stem AIRs was washed off into the scintillant fluid (Fig. 60). Less than 5% of the [^{3}H]sugars were washed off from the rest of the samples (Fig. 60).

Acetone:diethyl ether did not remove the hydrogenated castor oil and most of the *p*-coumaric acid from the cellulose pellets (or at least there was a thick layer of white oily subtance, similar in colour to the solid hydrogenated castor oil flaxes I had dissolved in the scintillant, and a separate layer of pale orange liquid that was similar in colour to the p-coumaric acid when it was dissolved in acetone, whereas and the scintillation liquid is almost colourless and transparent). Therefore, I washed the cellulose and AIR pellets with toluene 15 times, allowing the tubes to mix overnight on wheel between every wash, to remove the solid hydrogenated castor oil layer from the cellulose pellets. At the end, I washed the pellets with acetone to remove any remaining toluene (which is volatile but evaporates slowly when compared to acetone) from the pellets and left the pellets to dry in fume hood over two nights. After this the cellulose and AIR pellets were dry and fluffy (and free from scintillation liquid and the white and orange layers of liquid seen earlier) and looked as they did when the [^{3}H]sugars were dried on them in chapter 3.3.3.3. The binding of the [^{3}H]sugars on the cellulose and AIR could next be studied in a new experiment that has aqueous conditions (which would have been incompatible with the cellulosic material if the scintillation liquid, oil and *p*-coumaric acid had not been removed first).

3.3.3.6 Estimating the strength of binding by desorbing the [^{3}H]sugars from cellulose and AIR to water

When the [^{3}H]sugars were added to the cellulose and AIR pellets (in ethanol in chapter 3.3.3.3), it is likely that some of the sugar molecules (especially [^{3}H]cellopentaitol) adsorbed to the cellulose (i.e. bound permanently and tightly, as described with [^{3}H]cellopentaitol's binding to cellulose from water in chapter 3.3.1) whereas others were just in contact with the cellulose without being bound to it. To study to what extent the [^{3}H]sugars had bound to the cellulose, I added aqueous buffer to the cellulose and AIR pellets and assayed the free solution for radioactivity after 15 min and 20 h incubations (Figs. 61–63).

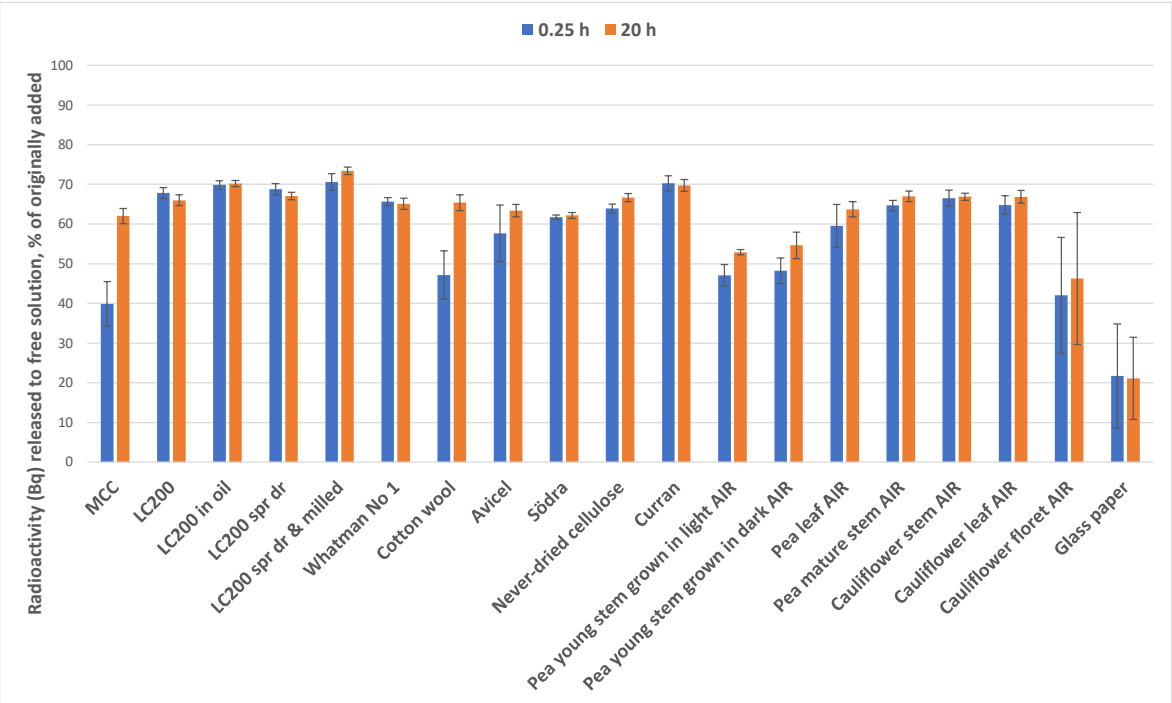

Figure 61. [^{3}H]Glucose desorbed from the cellulose and AIR to free solution after 15 min and 20 h.

The cellulose pellets from Fig. 60 were washed with toluene (15 times, each wash overnight) and acetone (once) and dried, after which the pellets were mixed with 105 mM acetate (Na^+) buffer, pH 4.7. The samples were incubated on a wheel at 20°C. At 15 min and 20 h, the samples were centrifuged at 2000 g for 10 min and 100 µl of the free solution was sampled and mixed with 400 µl of water and 5 ml of OptiPhase Hisafe 3 scintillation liquid. The radioactivity measured (Bq) from free solution was calculated related to what was originally added (values of which are listed in the legend of Fig. 56). Error bars show SEM, N=3 (technical repeats).

With most of the celluloses and AIRs, almost all the [^{3}H]glucose that can desorb had desorbed from the pellet even after only 15 min of mixing but MCC and cotton wool released significantly more [^{3}H]glucose into solution after 20 h incubation (Fig. 61). This suggests that small molecules such as glucose are not trapped and can wash out as easily as it can penetrate. In contrast with most of the celluloses tested, cotton wool has a very fluffy structure that absorbs liquids very well and it is possible that 15 min is just not enough to desorb everything from such a complex structure. On the other hand, microcrystalline cellulose is a fine powder and it does not absorb liquids in such quantities (as seen in Table 5). Perhaps MCC could have somehow different structure that can resist releasing the internalised glucose into aqueous solution for longer.

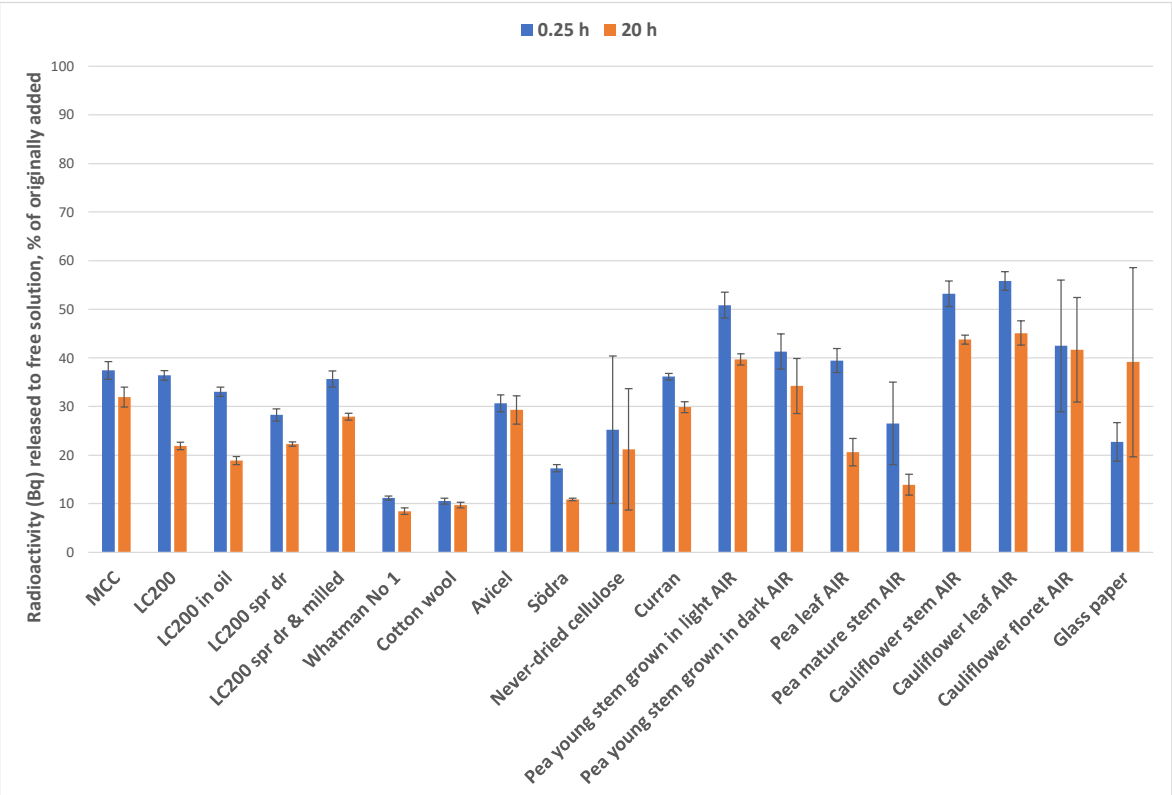

Figure 62. [^{3}H]Cellohexaitol desorbed from the cellulose and AIR to free solution after 15 min and 20 h.

Technical details as in Fig. 7. Error bars show SEM, N=3 (technical repeats).

The radioactivity eluted into free solution from the [^{3}H]cellohexaitol samples (Fig. 62) was much lower than from [^{3}H]glucose (Fig. 61) or [^{3}H]XXGol (Fig. 63) samples. As mentioned earlier, cello-oligosaccharides have high binding affinity to cellulose and it is likely that some of the [^{3}H]cellohexaitol molecules had firmly hydrogen-bonded to the cellulose surfaces before the ethanol was evaporated off. This hypothesis is supported also by the fact that the radioactivity eluted from Whatman No 1 filter paper, cotton wool and Avicel samples are almost the same between 15 min and 20 h time points (Fig. 62) – all the [^{3}H]cellohexaitol had been bound on the cellulose before 15 min had passed in aqueous solution, and the binding had probably happened before the ethanol had been evaporated off. Never-dried cellulose and cauliflower floret AIR had standard errors so big that no clear conclusions could be made from the data (Fig. 62). The amounts of eluted [^{3}H]cellohexaitol were lowest with Whatman No 1 filter paper, cotton wool and Södra A13 (Fig. 62), which is not surprising because these samples were also among the best binders of [^{3}H]cellopentaitol in chapter 3.3.1, but interestingly the amount of [^{3}H]cellohexaitol eluted from pea mature stem AIR was almost as low as with Södra A13. All the other samples, excluding glass paper, had a clear trend of

eluting more [^{3}H]cellohexaitol after 15 min than 20 h of incubation (Fig. 62). Probably the [^{3}H]cellohexaitol that had not initially bound firmly to the cellulose surface from ethanol, was desorbed in water first but in time bound back on the cellulose.

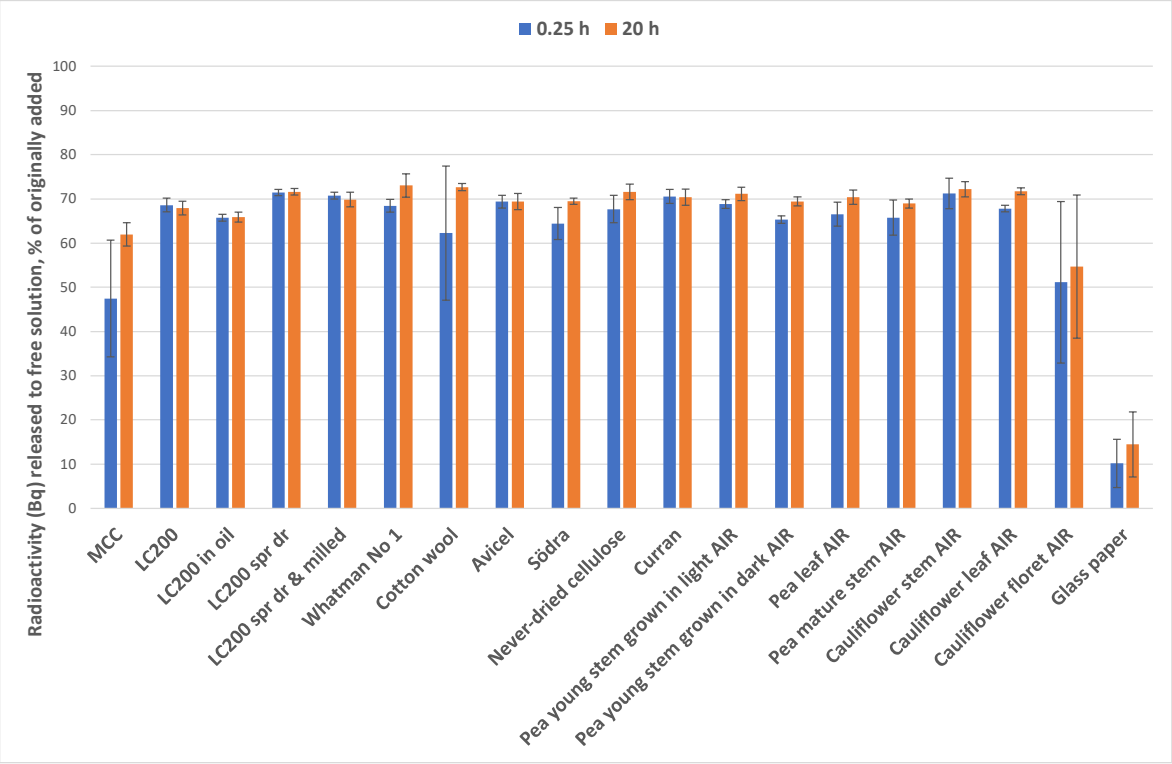

Figure 63. [^{3}H]XXLGol desorbed from the cellulose and AIR to free solution after 15 min and 20 h.

Technical details as in Fig. 61. Error bars show SEM, N=3 (technical repeats).

As with [^{3}H]glucose (Fig. 61), most of [^{3}H]XXLGol that can desorb had desorbed from the samples already after 15 min of incubation (Fig. 63).

Even though a lot of the [^{3}H]XXLGol was released from the pellets of AIRs from young pea stems grown in light and dark (~12% each) and pea leaves (~30%) when the scintillant was washed off (Fig. 60), there were no clear differences in water-desorbed [^{3}H]XXLGol levels between these samples and the others.

Glass paper is not made of cellulose but of very fine glass fibres that have no affinity for any of the sugars tested. That could explain why so much of the radiolabelled sugars were washed off from glass paper surface in the scintillation fluid–acetone–ether solvent mixture (Fig. 60) even though the sugars are not soluble in these solvents. It is also possible that some of the sugars were washed from the samples when the cellulose and AIR pellets were washed repeatedly in toluene followed by a wash in acetone (the solutions were discarded without measuring their radioactivity) which, when summed with the observations made from Fig. 60, could partially explain why the eluted radioactivity never reached 100% of what was initially added in Fig. 61, 62 and 63.

The results of these accessibility experiments showed, that the celluloses and AIRs differ from each other in how well small molecules can penetrate them. [^{3}H]Cellohexaitol could bind to the cellulose surface whereas the [^{3}H]Glc and [^{3}H]XXLGol, which did not have binding affinity, could penetrate the cellulose. The attachment of [^{3}H]cellohexaitol to the cellulose was not as firm in concentrated ethanol as of [^{3}H]cellopentaitol in aqueous solution, and when water was added to the cellulose containing [^{3}H]cellohexaitol, the loosely bound [^{3}H]cellohexaitol first desorbed from the cellulose and bound back again (this time probably as permanently as [^{3}H]cellopentaitol in the other experiments).

Any variation in penetrability could derive from the altering crystalline and amorphous regions in the microfibrils and the presence of other cell wall matrix polymers that coat (or even penetrate) the cellulose microfibrils (especially in AIR preparations that contain all the cell wall polymers, not only cellulose).

For instance, when the commercial celluloses were mixed in chocolate and given to a professional tasting panel for evaluation (during the initial testing by Mars Wrigley), some of celluloses were described to have ‘sandy’ and dry ‘mouthfeel’. The coarseness could influence how the cellulose surface interacts with – or in other words is accessible to – small molecules surrounding it, and in the case of the celluloses with ‘sandy’ mouthfeel, the cellulose could absorb saliva from the mouth.

4 Discussion

At the end of introduction chapter I asked three research questions which were used to build up this thesis. The questions were asking if the commercial celluloses and plant cell-wall preparations (AIRs) differ from each other in their:

a) chemical composition (including non-cellulosic contaminants)
b) degree of oxidation (introducing carboxylic acid groups)
c) accessibility to surrounding molecules.

In this thesis, I have aimed to answer these questions, and I have shown data gained from many experiments to support my answers, as discussed in this chapter.

4.1 Do the celluloses differ from each other by their chemical composition?

I studied the composition of the commercial celluloses and the AIRs for starch, phenol-insoluble protein, lignin, hemicellulose and cellulose. Although the plant cell walls also would contain in addition to these polymers a significant proportion of pectin and phenol-extractable proteins, the phenol-soluble proteins were not studied and presence of pectin was only estimated from the TFA hydrolysates since the focus of this project was on cellulose both in the commercial celluloses and the cellulosic preparations (AIRs).

4.1.1 Pectin

Pectin is the easiest polysaccharide to remove from the plant cell wall preparations, and is extractable with chelating agents (Fry, 1988; Thakur *et al*., 1997; Pelloux *et al*., 2007). It would be unusual to have pectin present in the commercial celluloses, at least in quantities bigger than traces. Also, in the cell wall, cellulose microfibrils are thought to interact with and bind to hemicelluloses, while pectin fills the remaining space in the wall matrix around

the network formed by cellulose microfibrils (the 'skeleton' of the wall that gives it the strength and support) and hemicelluloses (which tether the cellulose microfibrils and thus bind them into the network) (Fry, 1989; Hayashi, 1989; Cosgrove 2014); pectin itself is not definitively established to bind to cellulose. Having said that, Curran® and pea AIRs did have clearly detectable pectic hydrolysis products. Cotton wool showed very faint spot of galactose and possibly rhamnose which are typical for pectin hydrolysates, and cotton fibres are reported to contain 0.9% pectin (Kozłowski, 2012), and it is likely that the cotton wool has not gone through the same purification processes as the other commercial celluloses have during manufacturing.

4.1.2 Phenol-inextractable protein

The cellulose manufacturing process contains several steps which usually involve cooking of pulp in high temperatures with alkali or sulphites, followed by bleaching (Sixta, 2006), and it is likely that such chemical treatments would remove most protein from the pulp. Therefore I decided to study the protein content of the commercial celluloses and AIRs after phenol extraction (which leaves only firmly ('covalently') cell wall-bound protein in the samples). The proteins which are firmly bound to cell wall include extensins.

As briefly discussed in 3.1.2 Phenol insoluble protein content, the pea PIRs were rich in protein and might have contained extensins even though presence of Hyp and Ser could not be confirmed. From the commercial celluloses, only Södra A13 contained detectable protein. Also Curran® was rich in 'covalently bound' protein, but not as rich as the pea AIRs. In addition to extensins, the PIRs probably contain expansins. They are proteins that are associated with cell wall expansion and growth. Cosgrove (2014; 2015) discussed the role of expansins, and studies he reviewed had shown that they might bind to hemicellulose and cellulose (and maybe even pectin) and contribute to the breaking of crosslinks between different polysaccharides in the cell wall. He also speculated that the formation of cellulose microfibril aggregates (Jarvis and Cosgrove 2012; Cosgrove 2014; Cosgrove 2015), where microfibrils have bound together in absence of (sufficient) hemicellulose coating, could be

partially controlled by expansins. Cosgrove (1998) suggested a cell wall model where expansins would temporarily break the hydrogen bonds between cellulose microfibrils and other (hemicellulose) polysaccharides that tether the cellulose, and thus allow the cell wall to expand (creep) when there is tension. After the cellulose and hemicellulose had slid relative one another, the hydrogen bonds between the microfibril and hemicelluloses would form again (Cosgrove 1998).

Estimation of the protein content of the pea AIRs and commercial celluloses was an order-of magnitude estimate, based on comparing the intensity of the marker spot valine visually to the spots in the hydrolysates; there was only one loading of each maker spot on the chromatograms. It should also be noted that I was missing five common amino acids from the markers (arginine, histidine, cysteine, methionine and tryptophan), and it is likely that they would have been present (though quantitatively minor constituents) in the hydrolysates as well. More trustworthy methods for quantifying the amino acid content would have been to load a dilution series of markers (and to include all the common amino acids in the markers) and analyse scans of the chromatograms digitally against the intensity of the spots compared to the hydrolysate spots (ImageJ, for instance, could be appropriate for this). Also, with several amino acids, there was incomplete resolution on the chromatogram. The amino acids that migrated together could have been separated if several different solvent systems were tested and the chromatograms compared to each other. For better-resolution separation and precise quantification, HPLC (high-performance liquid chromatography) could have been used. However, a semiquantitative result was enough for the purposes of this thesis.

The pea leaf PIR seemed to be slightly richer in proteins that the PIR from mature pea stems, which could be an interesting result for the food and feed industry: usually pea pods and seeds are the only parts of the (mature) plants that are utilised, but also the leaves of pea plants are rich in protein and could be used as well. Although young pea shoots, which were the richest PIRs studied in protein, are also grown for salads and other similar applications, growing them is usually done in green houses or vertical farms, and these

facilities take a lot of electricity to maintain. However, pea plants are mostly grown on fields (to produce pea seeds), and pea leaves would be a readily available ingredient for foods or a source for plant-based protein extracts. Considering that the phenol and water soluble proteins have been removed from the pea leaf PIR, untreated pea leaves would probably have a much higher protein content that what can be concluded from the hydrolysates. Although studying the total leaf protein would have been interesting for food industry's point of view, studying phenol-insoluble proteins can tell us more about proteins that might interact with cellulose in the cell wall (such as extension and expansin).

It can be concluded that the unpleasant mouth-feel properties of some of the commercial celluloses probably did not result from the protein content of the samples. When mixed in chocolate, Södra A13 had the least unpleasant mouthfeel although it had the highest phenol-insoluble protein content. There were no detectable differences in phenol-insoluble protein content between the microcrystalline cellulose and most of the LC200 samples, and yet the microcrystalline cellulose had the worst mouthfeel properties. However, when compared to Curran® or pea AIRs, the commercial celluloses were relatively free from (firmly cell wall bound) protein, and it is possible that a high protein content (as high as Curran's®) does have a negative effect on the palatability (because we know from personal communication with the manufacturer that Curran® is not yet suitable as a food additive. It is also known that sugar beet pulp fibre Fibrex®, which is used in gluten-free baking and as dietary fibre supplement, and which produced by Oriola Finland Oy Consumer Health, has a very strong and unpleasant taste, and a coarse and chewy mouthfeel).

4.1.3 Starch

The starch content of pea AIRs was high, and it was highest in the young pea stem grown in light AIR, and the lowest in the mature pea stem AIR. The AIRs were produced from fresh plant material and it was expected that they would contain starch because the plants were photosynthesising (and storing energy as starch) when they were harvested and frozen in the liquid nitrogen. Even the young pea stems grown in dark contained a lot of starch,

where it must derive from sugar released from starch stored in the pea seed. The commercial celluloses did not contain measurable starch, probably because the pulping process and cellulose manufacturing includes hydrolysing treatments done at high temperatures (Sixta, 2006) which solubilise and hydrolyse starch.

4.1.4 Hemicellulose

The pea AIRs were rich in hemicelluloses, which was expected, as the hemicelluloses had not been removed from the material prior to TFA hydrolysis. Most of the commercial celluloses contained some hemicellulose (either a trace, such as cotton wool and Avicel, or in bigger quantities such as the LC200s). The presence of hemicellulose in MCC and Whatman paper was not clear because the heavy xylose spots in the LC200s and the pea AIRs left a streak across the TLC plate, and faint xylose spots could have been masked by it. To get around this problem I would in future work prepare a separate TLC for the MCC and Whatman filter paper hydrolysates, increase the loading to at least 5-fold, reduce the loading of the markers, and increase the separation on the plate between neighbouring hydrolysate loadings. The Saeman hydrolysate of Södra A13 contained xylose but also mannose and arabinose, which is interesting as mannose and arabinose were not present in the TFA hydrolysate. TFA would have been expected to hydrolyse at least a proportion of the hemicelluloses that contained these sugars. In future, it would be of interest to repeat the hydrolyses of the Södra A13 to see if this is a reproducible result.

The xylanase activity found in the commercial thermo-stable α-amylase shows that commercial enzyme preparations sometimes lack purity. It is also possible that the same enzyme has several different activities in one molecule or complex. For instance, *Equisetum* HTG can catalyse transglycosylation with several different donor substrates (xyloglucan, cellulose or mixed linkage glucan), and thus has three different enzyme activities in one (Simmons *et al*. 2015). However, it seems unlikely that an exo-acting α-glucosidase would also possess endo-acting b-xylosidase activity. The solution to the problem of unwanted xylanase activity in the commercial α-amylase was to use the salivary enzyme which has

only α-amylase activity (Boehlke *et al*. 2015). The β-xylanase digests showed that at least some of the hemicellulose in the LC200 and Avicel PH102 samples was xylan, and that there was no detectable xylan in the MCC, Whatman paper and cotton wool.

The β-xylanase hydrolysis products and the TFA hydrolysis products of the LC200 celluloses matched perfectly the migration patterns of xylo-oligosaccharides in several different TLC solvent mixtures. The quintuplicate TFA hydrolysis of the commercial celluloses and the pea AIRs showed that some xylose is released from the pellet every time the material is hydrolysed, even though it had been hydrolysed before. These data support the theory that hemicelluloses not only tether the surface of the cellulose microfibrils but also are incorporated into the microfibrils (Martina Pičmanová & S. C. Fry, Edinburgh Cell Wall Group, unpublished) or trapped between two aggregating microfibrils (Park and Cosgrove, 2012; Jarvis and Cosgrove, 2012; Zhao *et al*., 2014; Cosgrove, 2014), and perhaps it would be time to update the Fry (1989) and Hayashi (1989) cell wall model with these more complex cellulose–hemicellulose interactions.

Correlations between the mouthfeel properties and hemicellulose content are not straightforward. Södra A13, which had the best mouthfeel, appeared to contain hemicellulose. The LC200s had a high hemicellulose content and they had the second-best mouthfeel properties. Avicel, which had a palatable mouthfeel in Tunisian beef sausage, might behave differently if mixed into chocolate instead (although the sausage and chocolate both have a high fat content) (Ktari *et al*., 2014). MCC had the lowest hemicellulose content but also the worst mouthfeel properties, and it is therefore possible that having a trace of hemicellulose in the cellulose preparation can help with the mouthfeel properties. The reason behind this could be that the tethering hemicelluloses could help to bring the other components of the chocolate matrix into contact with the cellulose – similar to the hemicelluloses tethering the cellulose microfibrils in the cell wall and allowing other hemicelluloses, protein and pectins to come into close contact with the microfibrils. This might not happen as easily without the hemicelluloses because pectin, for instance, has a negative charge and cellulose is uncharged.

4.1.5 Lignin

Many of the results of the lignin content were discussed already in the results chapter, so the discussion here is brief. The results of the lignin assays showed that lignin content can be reliably measured using the ABSL method, even in samples that were relatively low in lignin (the commercial celluloses). I gained reproducible and statistically validated results from the measurements, and all the cellulose samples used in this work contained measurable traces of lignin.

MCC had a surprisingly high 'lignin' content, possibly because MCC was contaminated with sucrose, glucose and lactose (from the milling at MARS facilities), and perhaps the high reading could partially be explained by the free glucose in sample (as glucose turned black during acetylation with acetyl bromide). Also, it is possible that the never-dried cellulose contains some unidentified non-cellulosic contaminants (because it gained a caramel colour during acetylation), but these contaminants remain unidentified.

Sulphonated lignins were used as a standard, and its variable degree of sulphonation could explain why some commercial lignins did not add up to 100% in the ASBL assay.

The acetylation products of commercial cellulose samples of the last repeat of lignin content assay were slightly cloudy after heating in the heat block, and the cloudiness could have disturbed the absorbance measurements. For further experiments I would suggest a short centrifugation for the hydrolysates after cooling.

There seemed to be a correlation between high lignin content of commercial cellulose preparations and a bad mouthfeel. As stated before, the mouthfeel properties of MCC were the worst and of Södra A13 the best, and LC200s were between these two in their

mouthfeel. The lignin content was highest in MCC and lowest in Södra A13; the lignin content of the LC200s was mid-range. Curran® had much higher lignin content that the 'pure' commercial celluloses, and also unpalatable properties as a food ingredient.

4.2 Is cellulose oxidised?

In the results chapter (§ 3.2) I showed that the TB method I developed could be used to detect negative charges in both the commercial celluloses and AIRs. The method was well suited for detecting the fine differences in charges between the samples, and the results were reproducible and quantifiable. The most interesting difference was detected in the LC200s, which had evidently increased ten-fold in negative charges during the further processing at VTT. The report I have seen about what was done for the celluloses at VTT said that they were milled either in oil or water, and then spray-dried the samples (if milled in water). Therefore, we can assume that the milling processes probably introduced the negative charges to the cellulose.

Oxidation can introduce carboxylic acid groups into cellulose but also ketone and aldehyde groups. However, an acidic group would seem likely to have a bigger influence on the food-additive properties of cellulose than uncharged ketone and aldehyde groups, and therefore I decided to develop a method for detecting of the carboxylic acid groups in the cellulose. Another student of our research group, Christian Donohoe, developed a method for assaying cellulosic ketone and aldehyde groups using a Schiff's base method, which could in the future be applied in my work, to provide more information about the oxidation of cellulose.

As pectin is also negatively charged, the toluidine blue method I developed was well suited for measuring the net charge of the total cell wall polymers, and it could have many applications in studies of the cell wall polysaccharides. In fact, it would be interesting to test further the TB method and see if it could be applied for studying other AIR samples too, e.g. for monitoring changes in pectin content (and charge) during fruit ripening. When pectin is

newly synthesised, it is highly methyl-esterified, but in the cell wall pectin methylesterase enzymes demethylesterify pectin which makes it more negatively charged (Pelloux *et al*., 2007). Therefore, there should be a measurable difference in the TB binding to the pectin of the AIRs made from fruits that differ from each other in ripeness.

Also, it could be also interesting to use this method to estimate the anion content of different cell wall polysaccharides by extracting one by one polysaccharides other than cellulose from various AIR materials and monitoring the decrease in the negatively charged group contents of remaining materials. Ideally, after all the extractions, one would be left with only cellulose and any negative groups still observed would indicate how oxidized the cellulose is *in muro* and whether there are differences between the celluloses sourced from different plant materials.

The TB method could also be used to study whether various drying methods can introduce negative charges to cellulose.

To date (August 31st, 2022), I have not found any published studies of TB binding to cellulose. Toluidine blue is a metachromatic dye (Bergeron and Singer, 1958), which means it forms aggregates in concentrated solutions and as a solid. Hanh *et al*. (2016) studied the binding of TB to sulphonated polysaccharides (fucoidan and dextran sulphates). Their data showed that TB binds to the sulphate groups of fucoidan and dextran, and therefore the type of the polysaccharide itself (whether it is fucoidan or dextran) is not important. Their titration data also suggested that TB might first bind to the sulphite groups as a monomer but, at high TB concentration, some of the excess dye could bind to the TB molecules that had already been bound by the sulphites, and thus aggregates could be formed. D'Ilario and Martinelli (2006) showed that metachromatic dyes can form three types of aggregates and Matassa et al. (2007) took the aggregate hypothesis a step further by showing that as a solid, TB forms large, double-helical aggregates. However, the shape of the absorption spectra of TB monomer and aggregates were quite different from each other (D'Ilario and Martinelli, 2006), and the shape of their monomer spectrum was very similar to the one I

had measured in Fig. 30 (§ 3.2.), whereas the dimeric form of TB has two peaks (at 640 and 580 nm) (D'Ilario and Martinelli, 2006). Whether TB is in its monomeric or aggregated form in an aqueous solution depends on its concentration (D'Ilario and Martinelli, 2006). Because of the shape of the absorption spectrum which I observed and the low concentration of the TB solutions, I can assume TB to have been in its monomeric form in my experiments.

There was no obvious correlation between the quantity of negative charges and mouthfeel as Södra A13 was as charged as MCC. LC200 was in between these in mouthfeel range, but was more charged after processing at VTT. I do not know if there was any preference which LC200 had the best mouthfeel and which had the worst. However, Curran® contained many times more charges than the processed LC200s, and it is possible that such a big difference in the charge could contribute to the difference in palatability as a food additive.

4.3 Do the celluloses differ from each other in their accessibilities?

Perhaps the most interesting part of my thesis has been to study the accessibility of the celluloses to added molecules. The accessibility was studied in various experiments, which aimed to give a picture of how much the celluloses and AIRs can interact with their surroundings.

4.3.1 Accessibility to cellulase

Most of the cellulose was not digested in the preliminary test with Whatman paper (even though the digestion time was as long as 200 h), and the digestion rate was quite slow if compared to Agarwal *et al*. (2013) who showed that the extent of enzymatic hydrolysis of cellulose over 72 h correlates with the crystallinity of cellulose, and the more crystalline a cellulose preparation is the less it is hydrolysed by the enzyme. Agarwal *et al*. (2013) hydrolysed 40% of the cellulose over 72 h reaction but they used less cellulose and a bigger volume (0.5 g / 50 ml) for the digestion and the enzymes were a mixture of two cellulases

from Novozymes: Novozyme 188 (15 U) and Cellucast 1.5 L (15 U), whereas proportionally the same numbers for my experiment were 1.24 g / 50 ml and 25 U, respectively.

Chen *et al*. (2007) and Calvimontes *et al.* (2009) showed that digestibility depends on crystallinity, particle size and the total area of cellulose, and whether the cellulose is type I or II. According to Ioelovich (2009), Avicel PH102 is microcrystalline cellulose that consists of 78% crystalline and 22% amorphous regions (which was high when compared with the other celluloses he studied – for instance Kraft and sulphite pulp celluloses were 65% and 63% crystalline, respectively, and cotton cellulose was 71% crystalline). According to Klem *et al*. (2005), cotton wool linter microfibrils are 56–65% crystalline and dissolving pulp 43–56% crystalline. Agarwal *et al*. (2013) showed that crystallinity of Whatman CC31 cellulose powder was 80%. There seem to be no published records of crystallinity of Whatman filter paper *per se* but it has been used as a control sample in studies of crystallinity of other celluloses. Tawalbeh *et al*. (2021) published SFG spectroscopic, attenuated total reflectance–Fourier transform infrared (ATR-FTIR) spectroscopic and X-ray diffraction measurements of Avicel and Whatman filter paper celluloses, and Whatman filter paper had higher and sharper crystalline peaks than Avicel cellulose. Alonso-Lerma *et al*. (2020) showed that Whatman filter paper had an X-ray diffraction pattern very similar (same shape and size of peaks) to the nanocelluloses that were produced from the filter paper using endoglucanase or acid hydrolysis, and the crystallinity of the nanocelluloses was 85–88% and 80%, respectively. If the findings of Tawalbeh *et al*. (2021), Alonso-Lerma *et al*. (2020), Agarwal *et al*. (2013) and Ioelovich (2009) are put together, we can conclude that Whatman filter paper is highly crystalline, probably ≥80%. There appear to be no publications on the crystallinity of the LC200 celluloses. The never-dried cellulose could be similar to the wood pulp crystallinity reported by Klem *et al*. (2005) and Ioelovich (2009). Milling reduces the crystallinity of cellulose. Agarwal *et al*., (2013) showed that ball milling Whatman CC31 cellulose powder reduces its crystallinity, and the longer the sample is milled, the less crystalline it becomes (unmilled sample was 80% crystalline, 2.5 min decreased it to 61%, 5 min to 46%, 10 min to 33%, 15 min to 31% and by 1 h no detectable crystallinity (by FT-Raman method) was left). Agarwal *et al*. (2013) also showed that lignin slows enzymatic

hydrolysis. Hassan and Mansour (2017) made the same conclusion of lignin hindering cellulose digestion when they digested cellulose and pulp samples with microbial cultures.

MCC was digested more than Avicel PH102, which was unexpected based on their crystallinity. We do not know the crystallinity of our MCC; it could be as crystalline as Avicel. Also, the particle sizes in MCC and Avicel are unknown – we know that Mars tried to mill MCC further in the chocolate factory, so it is possible that MCC has more surface area than the other celluloses. Processing in water and spray-drying strongly increased the accessibility of LC200, which was interesting; it can be speculated that the negative charges detected in the processed LC200 samples could also influence the digestibility. However, when the spray-dried LC200 was milled further, the accessibility was significantly reduced, which was the opposite result to what I was expecting. There was no clear correlation between cellulase accessibility and mouthfeel properties.

4.3.2 Accessibility to [^{3}H]cellopentaitol

I discussed in the accessibility of cellulose to [^{3}H]cellopentaitol in the results chapter quite extensively, so the discussion here is brief. I developed a novel method for studying the accessibility of the cellulose molecules, and the differences in accessibility were accurately measurable and reproducible. Cellopentaitol was used as a water-soluble model of cellulose molecule, and the binding of [^{3}H]cellopentaitol to the celluloses was proven to be almost permanent, which indicates how strongly the cellulose molecules are bound to each other in the cellulose microfibril.

One surprising aspect of these experiments was that some of the [^{3}H]cellopentaitol never bound to the cellulose from the free solution, even though there would be many more available binding sites on the cellulose available. Even when new pieces of filter paper were added to the old supernatants, not much more of the remaining soluble [^{3}H]cellopentaitol was adsorbed from the solution. An explanation to this could be that all the

[^{3}H]cellopentaitol remaining in solution was not all [^{3}H]cellopentaitol. Also, the [^{3}H]cellopentaitol desorption seemed to be almost constant no matter how much [^{3}H]cellopentaitol or cellopentaose the cellulose had adsorbed, and this was most clearly seen in the second to last experiment, in which Whatman paper that had been incubated in 3200 µM cellopentaose had adsorbed much more pentasaccharide than the sample that had no cellopentaose. If it is assumed that the binding affinity of cellopentaose is similar to that of [^{3}H]cellopentaitol (as seems likely), it would make sense that the amount of pentasaccharide that desorbs would be proportional to the amount of pentasaccharide that had adsorbed in the first place rather than being almost a constant as measured. These questions leave a lot room for further studies. An example of further studies could be adsorbing tritiated hemicellulose to different celluloses, and the advantage of that would be that it would resemble the situation of the cell wall better, where the microfibrils are mostly coated by hemicelluloses.

Throughout the experiments, the never-dried cellulose, Södra A13, Whatman filter paper and cotton wool were the best adsorbers of [^{3}H]cellopentaitol. MCC and Avicel were among the poorest adsorbers out of commercial celluloses in the first two experiments but surprisingly adsorbed more [^{3}H]cellopentaitol in the presence of non-radioactive cellopentaose, reaching almost same adsorption level as cotton wool. As stated with the cellulase accessibility, the thickness of the microfibrils, surface area or crystallinity of the cellulose could affect how much cellulose can interact with its neighbouring molecules, although milling of spray-dried LC200 did not change its accessibility to [^{3}H]cellopentaitol even though it was less crystalline. Also if the cellulose is already coated by other polymers, such as hemicelluloses, the cellulose cannot bind as much [^{3}H]cellopentaitol because its binding sites have already been occupied. It is also worth considering that that most AIRs are likely to be only ~15–40% cellulose (Cosgrove and Jarvis, 2012), but the mature pea stem AIR could contain 40-50% cellulose (Fry, 1988; Timell, 1967).

There seemed to be a correlation between the mouthfeel properties and the accessibility of the cellulose to [^{3}H]cellopentaitol. Södra A13 was the most accessible cellulose, and it had

the best mouthfeel properties. LC200s were about an average in their accessibilities and also in their mouthfeel properties. MCC was usually among the poorest adsorbers of [^{3}H]cellopentaitol but it also had a bad mouthfeel. It would be very interesting to repeat the [^{3}H]cellopentaitol experiments with more celluloses that could be tested with professional panels for mouthfeel and try to make the mouthfeel property a quantifiable quality.

4.3.3 Accessibility to saccharides of different sizes

This accessibility study highlighted the observation made during the [^{3}H]cellopentaitol experiments that cello-oligosaccharides have a high binding affinity to cellulose, and [^{3}H]XXLGol and [^{3}H]glucose did not bind to cellulose with the same affinity or permanence. [^{3}H]XXLGol (DP 8) is slightly bigger than [^{3}H]cellohexaitol (DP 6), but often [^{3}H]cellohexaitol was more easily detected (less 'shielded' by the cellulose) than [^{3}H]XXLGol or [^{3}H]Glc. [^{3}H]XXLGol is hemicellulose-derived oligosaccharide, and comparing [^{3}H]XXLGol and [^{3}H]cellohexaitol binding to cellulose gave information about the affinity with which cellulose molecules bind each other inside the cellulose microfibril when compared to the affinity that hemicelluloses tether the cellulose microfibrils. The smaller binding affinity of hemicelluloses to cellulose makes it possible for the cell wall to be dynamic and allow the cell to grow, as described by Cosgrove (1998) in his cell wall model. The weaker binding between tethering hemicelluloses and cellulose allows expansins to temporarily break the hydrogen bonds and to enable cell wall expansion (creeping), and then forming of the bonds again.

When the celluloses were wetted with water, they formed clumps which was both frustrating and interesting. This raised the question, however, of whether 'clumpability' could be a measure to study the mouthfeel? Some of the celluloses and AIRs formed hard clumps as soon as they came in contact with water, and some of these clumps became very hard and impossible to break after drying. Although chocolate is fat-based, cocoa liquor does contain some residual water and the cellulose could clump in the matrix. When chocolate is cooked in the conch, many volatile compounds evaporate, and water must

evaporate too, which could make the clumped cellulose hard and thus contribute to the 'sandy' mouthfeel. Alternatively, if the cellulose managed to stay dispersed in the chocolate, in the mouth it does come in contact with water and it could absorb saliva and form clumps, both of which could contribute to dry or 'sandy' mouthfeel. Another interesting approach to rationalising the observed differences in mouthfeel could be how much the different celluloses can absorb liquid, as there were very large differences in this quality when the cellulose pastes were prepared.

5 References

Agarwal, U.A.P., Zhu, J.Y. and Ralph, S.A. (2013). Enzymatic hydrolysis of loblolly pine: effects of cellulose crystallinity and delignification. Holzforschung, 67, 371-377.

Alonso-Lerma, B., Barandiaran, L., Ugarte, L. (2020). High performance crystalline nanocellulose using an ancestral endoglucanase. Communications Materials, 1, 57

Bergeron J. and Singer M. (1958). Metachromacy: An experimental and theoretical reevaluation. The Journal of Biophysical and Biochemical Cytology, 4, 433-457

Boehlke C., Zierau O. and Hannig C. (2015). Salivary amylase – The enzyme of unspecialized euryphagous animals. Archives of Oral Biology, 60, 1162-1176.

Bouaziz MA, Abbes F, Mokni A, Blecker C, Attia H, Besbes S (2017). The addition effect of Tunisian date seed fibers on the quality of chocolate spreads. Journal of Texture Studies, 48: 143-150

Bray M.W. and Andrews T.M. (1923). An improved method for the determination of alpha-, beta-, and gamma-cellulose. Industrial and engineering chemistry, 15, 377-378

Briggs K. J., & Fry S. C. (1990). Solubilization of covalently bound extensin from capsicum cell walls. Plant Physiology, 92, 197-204.

Cassie A.B. and Baxter S. (1944). Wettability of porous surfaces. Transactions of the Faraday Society, 1944,40, 546-551.

Calvimontes A., Stamm M. and Dutschk V. (2009). Effect of cellulase enzyme on cellulose nano-topology. Tenside Surfactants Detergents, 46, 368-372.

Chem C., Duan C., Li J., Liu Y., Ma X., Zheng L., Stavik J. and Ni Y. (2016). Cellulose (dissolve pulp) manufacturing processes and properties: a-mini-review. Bioresources, 11, 5553-5564.

Chen Y., J. Stipanovic A.J., Winter W.T.,Wilson D.B. and Kim Y-J. (2007) Effect of digestion by pure cellulases on crystallinity and average chain length for bacterial and microcrystalline celluloses. Cellulose, 14, 283–293.

Chinga-Carrasco G. (2011). Cellulose fibres, nanofibrils and microfibrils: The morphological sequence of MFC components from a plant physiology and fibre technology point of view. Nanoscale research letters, 6, 417

Cogrove D.J. (2014). Re-constructing our models of cellulose and primary cell wall assembly. Current opinion in plant biology, 22, 122-131.

Cosgrove D.J. (2015). Plant expansins: diversity and interactions with plant cell walls. Current opinion in plant biology, 25, 162-172.

Cosgrove D.J. and Jarvis M.C. (2012). Comparative structure and biomechanics of plant primary and secondary cell walls. Frontiers in plant science, 3, 204

Cummings JH. (1981) Dietary fibre. British Medical Bulletin, 37, 65-70.

D'Ilario L. and Martinelli A. (2006). Toluidine blue: aggregation properties and structural aspects. Modelling and Simulation in Materials Science and Engineering, 14, 581–595

Eastwood MA. (1992). The physiological effect of dietary fiber: an update. Annual Review of Nutrition, 12, 19-35.

EFSA panel on dietetic products, nutrition and allergies (NDA) (2010). Scientific opinion on dietary reference values for carbohydrates and dietary fibre. EFSA journal, 8, 1462

EFSA panel on dietetic products, nutrition and allergies (NDA) (2011). Scientific opinion on the substantiation of health claims to galacto-oligosaccharides (GOS) and reduction of gastro-intestinal discomfort (ID 763) and decreasing potentially pathogenic microorganisms (ID 765) pursuant to article 13(1) of regulation (EC) No 1924/2006. EFSA journal, 9, 2060.

EFSA panel on food additives and nutrition sources added to food (ANS) (2017). Re-evaluation of pectin (E440i) and amidated pectin (E440ii) as food additives. EFSA journal, 15, 4866.

EFSA panel on food additives and nutrition sources added to food (ANS) (2018). Re-evaluation of celluloses E460(i), E460(ii), E461, E462, E463, E464, E465, E466, E468 and E469 as food additives. EFSA journal, 16, 5047.

Elleuch M., Bedigian D., Roiseux O., Besbes S., Blecker C. and Attia H. (2011). Dietary fiber and fiber-rich by-products of food processing: characterization, technological functionality and commercial applications: a review. Food Chemistry, 124, 411–421.

Everett D.W. and McLeod R.E. (2004). Interaction of polysaccharide stabilisers with casein aggregates in stirred skim-milk yoghurt. International Dairy Journal, 15, 1175–1183

Fan L.T., Lee Y.-H. and Beardmore D.H. (1980). Mechanism of the enzymatic hydrolysis of cellulose: effects of major structural features of cellulose on enzymatic hydrolysis. Biotechnology and Bioengineering, 12, 177- 199.

Fanta G.F., Abbot T.P., Herman A.I., Burr R.C. and Doane W.M. (1984). Hydrolysis of wheat straw hemicellulose with trifluoroacetic acid. Fermentation of xylose with *Pachysole tannophilus*. Biotechnology and bioengineering, 26, 1122-1125

Franková L. and Fry S.C. (2013). Biochemistry and physiological roles of enzymes that 'cut and paste' plant cell-wall polysaccharides. Journal of Experimental Botany, 64, 3519–3550.

Fry S.C. (1989). Structure and functions of xyloglucan. Journal of experimental botany, 40, 1-11.

Fry S.C. (1995) Polysaccharide-modifying enzymes in the plant cell wall. Annual Review of Plant Physiology and Plant Molecular Biology, 46, 497-520.

Fuckerer K, Hensel O, Schmitt JJ (2016). Rye bread fortified with cellulose and its acceptance by elderlies in nursing homes and young adults. Journal of Food Studies, 5: 1-11.

Fukushima RS, Hatfield RD. (2004). Comparison of the acetyl bromide spectrophotometric method with other analytical lignin methods for determining lignin concentration in forage samples. Journal of Agricultural and Food Chemistry, 52, 3713-3720.

Gehmayr V., Potthast A. and Sixta H. (2012). Reactivity of dissolving pulp modified by TEMPO-mediated oxidation. Cellulose, 19, 1125-1134.

Gilbert H.J. (2010). The biochemistry and structural biology of plant cell wall deconstruction, Plant Physiology, 153, 444–455.

Gottschalk R.G., Hoch H. and Stidworthy G.H. (1962). Beta radiation self adsorption of precipitates collected on filter paper. Clinical chemistry, 8, 318-332.

Gray DF, Fry SF, Eastwood MA (1993). Uniformly 14C- labelled plant cell walls: production, analysis and behaviour in rat gastrointestinal tract. British journal Of Nutrition, 69: 177-188.

Gressier M, Frost G. (2022). Minor changes in fibre intake in the UK population between 2008/2009 and 2016/2017. European Journal of Clinical Nutrition, 76, 322-327.

Hahn T., Kai Muffler K., and Ulber R. (2016) Isothermal microcalorimetric studies of toluidine blue O/sulfated polysaccharides interactions. Journal of Thermal Analysis and Calorimetry 123:2291–2296

Harris PJ, Ferguson LR. (1993). Dietary fibre: its composition and role in protection against colorectal cancer. Mutation Research, 290, 97-110.

Hassan R.R.A. and Mansour M.M.A. (2017). A Microscopic study of paper decayed by *Trichoderma harzianum* and *Paecilomyces variotii*. Journal of Polymers and the Environment, 26, 2698–2707.

Hatfield, R.D., & Fukushima, R.S. (2005). Can lignin be accurately measured. Crop Science, 45, 832-839.

Hayashi, T. (1989) Xyloglucans in the primary cell wall. Annual Review of Plant Physiology and Plant Molecular Biology, 40, 139-168.Herburger et al. 2020

Herger A., Dünser K., Kleine-Vehn J. and Ringli C. (2019). Leucine-rich repeat extensin proteins and their role in cell wall sensing, Current Biology, 29, R851-R858.

Hozumi A., Bera S., Fujiwara D., Obayashi T., Yokoyama R., Nishitani K. and Aoki K. (2017). Arabinogalactan proteins accumulate in the cell walls of searching hyphae of the stem parasitic plants, *Cuscuta campestris* and *Cuscuta japonica*, Plant and Cell Physiology, 58, 1868–1877.

Ioelovich M. (2009). Accessibility and crystallinity of cellulose. BioResources, 4, 1168-1177.

Imamura M and Matsushima K (2013). Suppression of umami aftertaste by polysaccharides in soy sauce. Journal of Food Science, 78: C1136-C1143.

Jarvis M.C. (2018). Structure of native cellulose microfibrils, the starting point for nanocellulose manufacture. Philosophical Transactions of the Royal Society A, 376, 20170045.

Klem D., Heublein B., Fink H.P. and Bohn A. (2005) Cellulose: fascinating biopolymer and sustainable raw material. Angewandte Chemie International Edition, 44, 3358-3393.

Kolpak FJ, Blackwell J. (1975) Deformation of Cotton and Bacterial Cellulose Microfibrils. Textile Research Journal, 45, 568-572.

Ktari N, Smaoui S, Trabelsi I, Nasri M and Ben Salah R (2014). Chemical composition, techno-functional and sensory properties and effects of three dietary fibers on the quality characteristics of Tunisian beef sausage. Meat Science, 96, 521-525.

Kyriakopoulou, K., Keppler, J. K., & van der Goot, A. J. (2021). Functionality of ingredients and additives in plant-based meat analogues. Foods, 10, 600.

Lange H., Silvia D. And Claudia C. (2013). Oxidative upgrade of lignin – recent routes reviewed. European Polymer Journal, 49, 1151-1173.

Lee M.H., Jeon H.S., Kim S.H., Chung J.H., Roppolo D., Lee H.J., Cho H.J., Tobimatsu Y., Ralph J. and Park O.K. (2019). Lignin-based barrier restricts pathogens to the infection site and confers resistance in plants. The EMBO Journal, 38, e101948

Liendo R., Padilla F.P. and Quintana A. (1997). Characterization of cocoa butter extracted from Criollo cultivars of Theobroma cacao L.. Food Research International, 30, 727-731.

Maaß M.-C., Saleh S., Militz, H. and Volkert C.A. (2020). The structurel origins of wood cell wall toughness. Adv. Mater., 32, 1907693.

Matassa R., Sadun C., D'Ilario L., Martinelli A., and Caminiti R. (2007). Supramolecular organization of toluidine blue dye in solid amorphous phases. J. Phys. Chem. B, 111, 1994-1999.

Martinière A., Gibrat R., Sentenac H., Dumont X., Gaillard I. and Paris N. (2018) Uncovering pH at both sides of the root plasma membrane interface using noninvasive imaging. PNAS, 115, 6488-6493

Meents MJ, Watanabe Y, Samuels AL (2018). The cell biology of secondary cell wall biosynthesis. Annals of Botany, 121, 1107-1125.

Mittermeier-Kleßinger, V. K., Hofmann T., & Dawid, C. (2021). Mitigating off-flavors of plant-based proteins. Journal of Agricultural and Food Chemistry, 69, 9202-9207.

Morais Ferreira JM, Azavedo BM, Luccas V, Bolini HM (2017). Sensory profile and consumer acceptability of prebiotic white chocolate with sucrose substitutes and the addition of goji berry (Lycium barbarum). Journal of Food Sciences, 82:818-824.

Moreira L.R., Filho E.X. (2008). An overview of mannan structure and mannan-degrading enzyme systems. Appl Microbiol Biotechnol. 79, 165-78.

Mudgil D, Barak S. (2013). Composition, properties and health benefits of indigestible carbohydrate polymers as dietary fiber: a review. International Journal for Biological Macromolecules, 61, 1-6.

Müller K., Linkies A., Vreeburg R.A.M., Fry S.C., Krieger-Liszkay A. and Leubner-Metzger G. (2009) In-vivo cell wall loosening by hydroxyl radicals during cress (*Lepidium sativum* L.) seed germination and elongation growth. Plant Physiology, 150, 1855–1865.

Murray BS, Durga K, de Groot PWN, Kakoulli A, Stoyanov SD (2011). Preparation and characterization of the foam-stabilizing properties of cellulose – ethyl cellulose complexes for use in foods. The Journal of Agricultural and Food Chemistry, 59: 13227-13288.

Norris F.W. and Preece I.A. (1930). Studies on hemicelluloses: the hemicelluloses of wheat bran. The Biochemical journal, 24, 59-66.

Nsor-Atindana J, Chen M, Goff DH, Zhong F, Sharif HR, Li Y (2017). Functionality and nutritional aspects of microcrystalline cellulose in foods. Carbohydrate polymers, 172: 159-174.

Okano T. and Sarko A. (1985). Mercerization of cellulose. II. alkali-cellulose intermediates and a possible mercerization mechanism. Journal of applied polymer science, 30, 325-332.

O'Rourke C., Gregson T., Murray L, Sadler I.H. and Fry S.C. (2015). Sugar composition of the pectic polysaccharides of charophytes, the closest algal relatives of land-plants: presence of 3-O-methyl-D-galactose residues. Annals of Botany 116, 225–236.

Park Y.B. and Cosgrove D.J. (2012). A revised architecture of primary cell walls based on biomechanical changes induced by substrate-specific endoglucanases. Plant Physiology, 158, 1933-1943.

Pelloux J., Rustérucci C., Mellerowicz E.J. (2007). New insights into pectin methylesterase structure and function. Trends in Plant Science, 12, 267-277.

Philippe G., Sørensen I., Jiao C., Sun X., Fei Z., Domozych D.S. and Rose J.C.K., (2020) Cutin and suberin: assembly and origins of specialized lipidic cell wall scaffolds. Current Opinion in Plant Biology, 55, 11-20.

Qi X., Behrens N. X., West P. R., & Mort A. J. (1995). Solubilization and partial characterization of extensin fragments from cell walls of cotton suspension cultures. Plant Physiology, 108, 1691-1 701

Rongpipi, S., Ye, D., Gomez, E. D., & Gomez, E. W. (2019, March 1). Progress and opportunities in the characterization of cellulose – an important regulator of cell wall growth and mechanics. Frontiers in Plant Science. Frontiers Media S.A. https://doi.org/10.3389/fpls.2018.01894

Roland, W. S. U., Pouvreau L., Curran J., van de Velde F., & de Kok P. M. T. (2016). Flavor aspects of pulse ingredients. Cereal Chemistry, 94, 58–65.

Saeman J.F. (1945). Kinetics of wood saccharification — hydrolysis of cellulose and decomposition of sugars in dilute acid at high temperature. Ind. Eng. Chem. 37, 43–52

Sicard-Roselli, C., Brun, E., Gilles, M., Baldacchino, G., Kelsey, C., McQuaid, H., Polin, C., Wardlow, N. and Currell, F. (2014). A new mechanism for hydroxyl radical production in irradiated nanoparticle solutions. Small, 10, 3338-3346.

Simmons, T.J., Mohler, K.E., Holland, C., Goubet, F., Franková, L., Houston, D.R., Hudson, A.D., Meulewaeter, F. and Fry, S.C. (2015). Hetero-trans-β-glucanase, an enzyme unique to *Equisetum* plants, functionalises cellulose. Plant Journal 83: 753-769.

Shoaib M., Shehzad A., Omar M., Rakha A., Raza H., Sharif H.R., Shakeel A., Ansari A. and Niazi S. (2016). Inulin: properties, health benefits and food applications. Carbohydrate Polymers, 147, 444-454.

Tabara A, Yamane C, Seguchi M (2012). Low calorie bread baked with charred cellulose granules and wheat flour to eliminate toxic xanthene food dye in the alimentary canal. Bioscience, Biotechnology and Biochemistry, 76: 2173-2180.

Tawalbeh M., Rajangam A.S., Salameh T., Al-Othman A. and Alkasrawi M. (2021) Characterization of paper mill sludge as a renewable feedstock for sustainable hydrogen and biofuels production. International Journal of Hydrogen Energy, 46, 4761-4775.

Taylor N.G. (2018). Cellulose biosynthesis and deposition in higher plants. New Phytologist, 178, 239-252.

Thakur B.R., Singh R.K. and Handa A.K. (1997). Chemistry and uses of pectin — a review. Critical Reviews in Food Science and Nutrition, 37, 47-73.

Timell T.E. (1967). Recent progress in the chemistry of wood hemicelluloses. Wood Science and Technology, 1, 45-70.

Trache D, Hussin MH, Chuin CTH, Sabar S, Fazita NMR, Taiwo OFA, Hassan TM, Haafiz MMK (2016). Microcrystalline cellulose: Isolation, characterization and bio-composites application – A review. International Journal of Biological Macromolecules, 93: 789-804.

Wohlert M, Benselfelt T, Wågberg L, Furó I, Berglund LA, Wohlert J (2021). Cellulose and the role of hydrogen bonds: not in charge of everything. Cellulose 29, 1–23.

Yamane C, Aoyagi T, Ago M, Sato K, Okajima K, Takahashi T (2006) Two different surface properties of regenerated cellulose due to structural anisotropy. Polymer Journal, 38, 819–826

Ye, H., Zhang, Y., and Yu, Z. (2017). "Effect of desulfonation of lignosulfonate on the properties of poly(lactic acid)/lignin composites," BioRes. 12(3), 4810-4829.

Zhao Z., Crespi V.H., Kubicki J.D., Cosgrove D.J. and Zhong L. (2014) Molecular dynamics simulation study of xyloglucan adsorption on cellulose surfaces: effects of surface hydrophobicity and side-chain variation. Cellulose, 21. 1025-1039.

Books:

Alberts B., Bray D., Lewis J., Raff M., Roberts K. and Watson J.D. (1988). The molecular biology of the cell, 2nd edition, Garland publishing, New York, NY, USA

Beckett S.T. (2006). The science of chocolate. The Royal Society of Chemistry, Cambridge, UK

Beckett S.T., Fowler M.S. and Ziegler G.R. (2017). Beckett's industrial chocolate manufacture and use. 5th edition, Wiley Blackwell, Chichester, UK, (the whole book)

Belgacem M.N. and Gandini A. (2008). Monomers, Polymers and Composites from Renewable Resources, Elsevier Science, 289-304

Hartel R.W., von Elbe J.H. and Hofberger R (2018). Confectionery science and technology. Springer International Publishing AG, Cham, Switzerland, (the whole book)

Kozłowski R.M. (2012). Handbook of natural fibres. Woodhead publishing limited, 11-23.

Kuddus M. and Aguilar C.N. (2022). Value-Addition in Food Products and Processing Through Enzyme Technology, Academic Press, 111-122

Fry S.C. (1988). The growing plant cell wall: chemical and metabolical analysis, John Wiley & Sons, New York, NY, USA

Sixta H. (2006). Handbook of pulp. Wiley – VCH Verlag GmbH & Co. KGaA, Weinheim, Germany, (the whole book)

Websites:

COMMISSION REGULATION (EU) No 231/2012 (retrieved on Aug. 31st 2022): https://www.legislation.gov.uk/eur/2012/231/introduction#:~:text=Commission%20Regulation%20%28EU%29%20No%20231%2F2012%20of%209%20March,of%20the%20European%20Parliament%20and%20of%20the%20Council

Definition of the official EU health claim 'high fibre' (retrieved on August 16th, 2022): https://food.ec.europa.eu/safety/labelling-and-nutrition/nutrition-and-health-claims/nutrition-claims_en

Error for natural logarithm of a function (retrieved on January 3rd, 2023):

https://physics.stackexchange.com/questions/95254/the-error-of-the-natural-logarithm

Molecular formula of lignosulfonic acid (retrieved August 26th, 2022):
https://pubchem.ncbi.nlm.nih.gov/compound/Lignosulfonic-acid

Sigma-Aldrich: Lignosulfonic acid, desulfonated sodium salt (retrieved August 20th, 2022):
https://www.sigmaaldrich.com/GB/en/product/aldrich/471046

6 Appendix

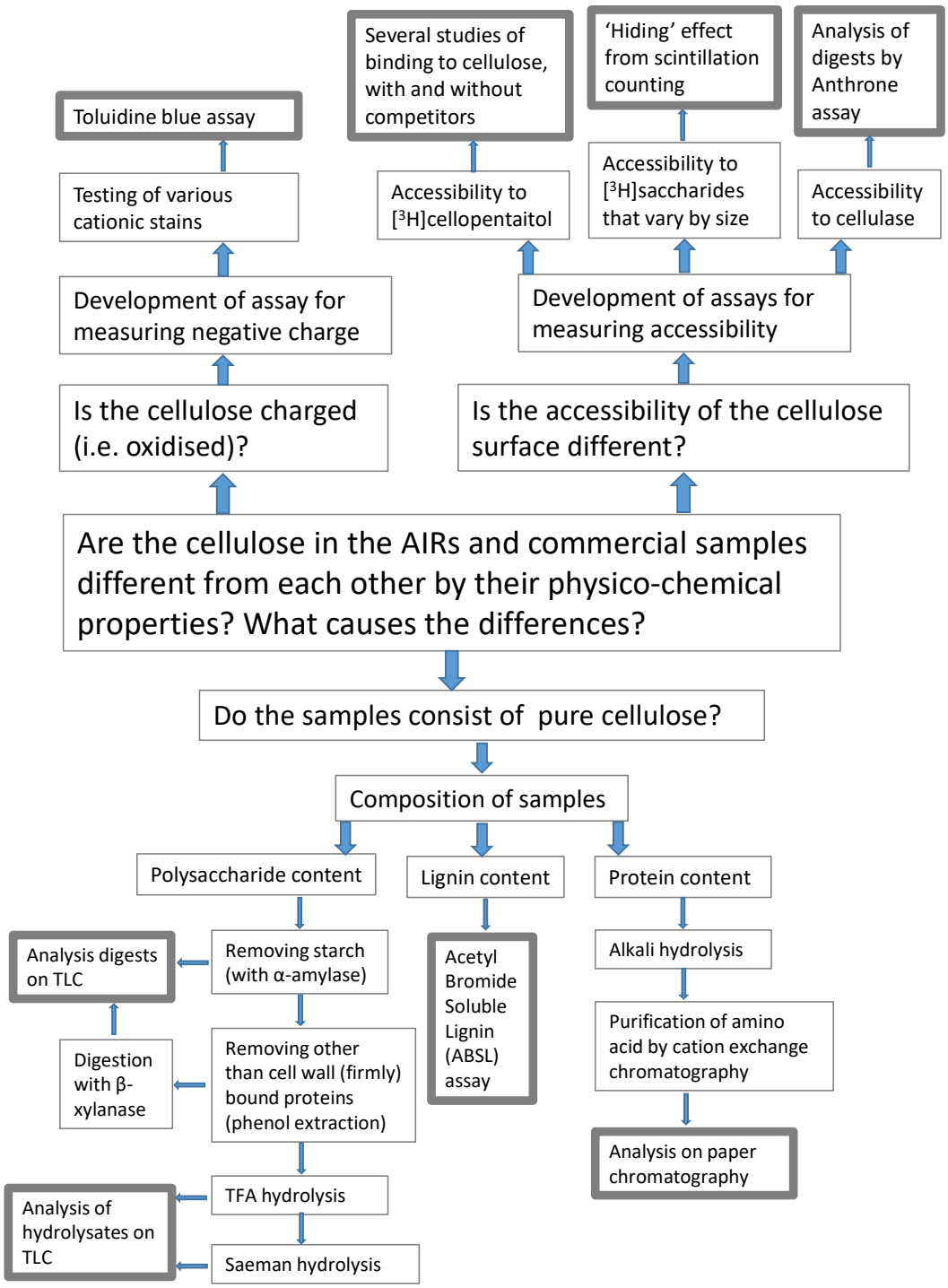

Figure 64. Summarising flow chart of the studies done and the methods used in this thesis.

The boxes with a bold frame relate to the figures shown in the Results chapter (for instance, figures of thin-layer chromatograms).